

THE INTERNATIONAL CONFERENCE



**SPIN PHYSICS,  
SPIN CHEMISTRY  
AND  
SPIN TECHNOLOGY**

ABSTRACTS

KAZAN 1-5 NOVEMBER 2011







SPIN PHYSICS,  
SPIN CHEMISTRY  
AND  
SPIN TECHNOLOGY

ABSTRACTS OF THE  
INTERNATIONAL CONFERENCE

Editor:  
KEV M. SALIKHOV

KAZAN, NOVEMBER 1–5, 2011

Prof. Kev M. Salikhov  
Zavoisky Physical-Technical Institute,  
Russian Academy of Sciences, Kazan, Russian Federation  
Phone: 7 (843) 2720503  
E-mail: salikhov@kfti.knc.ru

This work is subject to copyright.

All rights are reserved, whether the whole or part of the material is concerned, specifically those of translation, reprinting, re-use of illustrations, broadcasting, reproduction by photocopying machines or similar means, and storage in data banks.

© 2011 Zavoisky Physical-Technical Institute, Kazan

© 2011 Igor A. Aksenov, graphic design

Printed in the Russian Federation

Published by the Zavoisky Physical-Technical Institute, Kazan  
[www.kfti.knc.ru](http://www.kfti.knc.ru)

---

## FOREWORD

It is extremely exciting that the conference “Spin Physics, Spin Chemistry and Spin Technology” provides a forum for specialists from different fields of science: chemical physics, spintronics, photonics, electron processes in semiconductors, etc., and technology. Spin science is extensively and intensively developing. In many cases the state of electron spins determines the properties of materials and the processes in them. Therefore, the number of materials, the functional properties of which are determined by the behavior of spins, increases continuously. A remarkable example is the spin-dependent recombination of free radicals. The study of magnetic and spin effects in radical reactions led to the creation of a new field of science, spin chemistry. One can also note the spin-dependent recombination of electron-hole pairs in semiconductors, spin-dependent annihilation of triplet excitons in molecular crystals. Electron paramagnetic resonance (EPR) spectroscopy plays an important role in the development of spin science. EPR methods are extremely useful not only for monitoring the state of spin systems but also to control the state of electron spins and to change the spin functional properties of materials.

In parallel to the development of spin science, the number of promising suggestions for spin technology increases permanently: spintronics, molecular magnets, spin optoelectronics based on the resonance microwave field dependence of the electron-hole recombination luminescence, magnetic isotope effect in radical reactions, electron spin-based quantum computing, to name a few.

Following these speculations and consultations with the international scientific community, I initiated this conference. I hope that it will be a good start for a series of conferences to take place regularly in different places all over the world and to affect the further development of the spin science and spin technology.

This year our conference hosts the Zavoisky Award 2011 ceremony. Professor Seigo Yamauchi (Japan) is the Zavoisky Awardee. The Annual Workshop “Modern Development of Magnetic Resonance” and the Russian-German Workshop “Functional Spin Materials: From Fundamental Research towards Novel Applications” nicely complement the program of the conference.

I am grateful for the financial support to the Government of the Republic of Tatarstan, the Russian Academy of Sciences, the Russian Foundation for Basic Research, Bruker BioSpin, and ABAK.

Kev Salikhov

**PROGRAM COMMITTEE**

Büchner B. (Dresden, Germany), co-chairman  
Salikhov K.M. (Kazan, Russia), co-chairman  
Baskevich P.P. (Kazan, Russia)  
Fattakhov Ya.V. (Kazan, Russia)  
Freed J.H. (Ithaca, NY, USA)  
Garifullin I.A. (Kazan, Russia)  
Kataev V.E. (Dresden, Germany)  
Kusraev Yu.G. (St. Petersburg, Russia)  
Möbius K. (Berlin, Germany)  
Ohta H. (Kobe, Japan)  
Ovchinnikov I.V. (Kazan, Russia)  
Petukhov V.Yu. (Kazan, Russia)  
Ryazanov V.V. (Chernogolovka, Russia)  
Tagirov L.R. (Kazan, Russia)  
Tagirov M.S. (Kazan, Russia)  
Tarasov V.F. (Kazan, Russia)  
Teitelbaum G.B. (Kazan, Russia)  
Timofeev V.B. (Moscow, Russia)  
Ustinov V.V. (Ekaterinburg, Russia)  
Voronkova V.K. (Kazan, Russia)  
Vavilova E.L. (Kazan, Russia), coordinator of workshop

---

**LOCAL ORGANIZING COMMITTEE**

Tarasov V.F., chairman  
Adzhaliyev Yu.A.  
Akhmin S.M.  
Falyn M.L.  
Galeev R.T.  
Gavrilova T.P.  
Goleneva V.M.  
Gubaidulina A.Z.  
Guseva R.R.  
Kurkina N.G.  
Kupriyanova O.O.  
L'vov S.G.  
Mosina L.V.  
Petrushkin S.V.  
Voronkova V.K.  
Voronova L.V.  
Yanduganova O.B.  
Yatzik I.V.

**SECRETARIAT**

Voronkova V.K.  
Mosina L.V.  
Gerasimov K.I.  
Savostina L.I.  
Vavilova E.L.  
Yatzik I.V.

## **ADDRESS**

The International Conference  
“Spin physics, spin chemistry and spin technology”  
Zavoisky Physical-Technical Institute  
Sibirsky trakt 10/7, Kazan, 420029  
Russian Federation  
E-mail: [kazan.spin2011@gmail.com](mailto:kazan.spin2011@gmail.com)  
Phone: +7 (843) 231 90 86  
Fax: +7 (843) 272 50 75  
[www.kfti.knc.ru](http://www.kfti.knc.ru)

## **ORGANIZERS**

The Zavoisky Physical-Technical Institute of  
the Kazan Scientific Center of the Russian Academy of Sciences  
The Academy of Sciences of the Republic of Tatarstan

## **SUPPORTED BY**

The Russian Academy of Sciences  
The Russian Foundation for Basic Research  
Bruker BioSpin GmbH, Germany  
ABAK Ltd., Russia

## **CONFERENCE LOCATION**

The Academy of Sciences of the Republic of Tatarstan  
ul. Bauman 20, Kazan

---

## CONTENTS

### PLENARY LECTURES

<i>B. Büchner</i> : Intrinsic Inhomogeneities in Spin Correlated Solids as Revealed by Magnetic Resonance	2
<i>A. V. Dvurechenskii, A. F. Zinovieva, A. V. Nenashev</i> : Spins in Low-Dimensional Quantum Dot Semiconductor Nanostructures	3
<i>S. A. Dzuba</i> : EPR Probing of Nanoscale Dynamics in Molecular Disordered Systems	4
<i>I. A. Garifullin</i> : Spin-Polarized Electrons in Superconductor/Ferromagnets Hybrid Structures	6
<i>D. Gatteschi, M. Fittipaldi, C. Sangregorio, L. Sorace, L. Castelli</i> : EMR to Investigate the No Man's Land between Molecular Nanomagnets and Magnetic Nanoparticles	8
<i>D. Goldfarb</i> : Nanometer Scale Distance Measurements in Proteins and Nucleic Acids Using Gd <sup>3+</sup> Spin Labelling	10
<i>I. V. Koptug, K. V. Kovtunov, V. V. Zhivonitko, I. V. Skovpin, D. A. Barskiy, R. Z. Sagdeev</i> : Parahydrogen-Induced Polarization and Heterogeneous Catalysis	11
<i>Yu. G. Kusrayev</i> : Spin Relaxation in Semiconductors and Semiconductor Nanostructures	13
<i>W. Lubitz</i> : In Search of Renewable Energy Resources: Mechanisms of Light-Induced Water Splitting and Hydrogen Production in Nature Studied by Advanced EPR Techniques	15
<i>K. Möbius, A. A. Dubinskii, M. Flores, W. Lubitz, A. Savitsky</i> : Spin-Polarized Radical-Pair States in Photosynthesis: Characterization of Transient Conformational Changes by High-Field Dipolar EPR Spectroscopy	17
<i>T. F. Prisner</i> : Enhanced Sensitivity in EPR and NMR: New Experimental Developments and Biomolecular Applications	19

<i>V. V. Ryazanov</i> : Physics and Applications of Superconductor-Ferromagnet Phase Inverters in Superconducting Electronics and Spintronics	20
<i>V. V. Ustinov, M. A. Milyaev</i> : Spin Valves with Giant Magnetoresistance	22
<i>A. V. Vedyayev, N. V. Strelkov, N. V. Ryzhanova, M. Chshiev, B. Diény</i> : Spin as an Itinerant Carrier of Information	23
<i>S. Yamauchi</i> : Time-Resolved EPR in the Electronically Excited States	25
<i>J. H. Freed</i> : Molecular Dynamics in Proteins and Membranes by Multi-Frequency ESR	26
INVITED TALKS	
<i>B. Aktaş, R. Topkaya, M. Erkovan, M. Özdemir</i> : Magnetic Properties of Exchange-Coupled Py/Cr/Py Films	28
<i>V. A. Atsarkin, V. V. Demidov</i> : Electron Magnetic Resonance and Conductivity around the Curie Point	29
<i>E. Bagryanskaya, M. Fedin, S. Veber, V. Ovcharenko, H. Mazuoka, S. Yamauchi</i> : Thermal and Optical Switching of the Exchange Interactions in Nitroxide-Copper(II)-Nitroxide Clusters	30
<i>M. Belli, M. Fanciulli, N. V. Abrosimov</i> : Pulse Electron Spin Resonance Investigation of Bismuth-Doped Silicon	32
<i>M. K. Bowman, P. R. Vennam, M. Krzyaniak, A. G. Maryasov</i> : Dipolar Interactions for the Determination of Macromolecular Structure	34
<i>M. Brustolon, A. Collauto, A. Barbon</i> : Nitronyl Nitroxides as Spin Probes?	35
<i>A. Bukharaev, N. Nurgazizov, D. Biziaev, D. Lebedev, A. Chuklanov, I. Shakirov, T. Khanipov</i> : Fabrication of Magnetic Nanostructures for the Investigation of Spin-Dependent Transport Phenomena	36
<i>E. S. Demidov, E. D. Pavlova, A. I. Bobrov, V. V. Podolskii, V. P. Lesnikov, M. V. Sapozhnikov, B. A. Gribkov, S. N. Gusev, S. A. Levchuk, V. V. Karzanov</i> : Structure and Magnetotransport Properties of Deposited from Laser Plasma Nanosized Layers of the High-Temperature Diluted Magnetic Semiconductor Si:Mn	37

<i>B. Dzikovski, D. Tipikin, J. H. Freed</i> : Location, Conformation and Aggregation of PC Spin Labels in the Gel Phase Lipid Bilayers by Multifrequency ESR	39
<i>M. Fanciulli, A. Vellei, C. Canevali, D. Rotta, M. Basini, S. Paleari</i> : Electrically Detected Magnetic Resonance Characterization of Silicon Nanowires	41
<i>E. B. Fel'dman</i> : Quantum Entanglement and Quantum Discord in Multiple Quantum NMR in Solids	42
<i>A. J. Fielding, F. Brodhun, C. Koch, R. Pievo, V. Denysenkov, I. Feussner, M. Bennati</i> : Multifrequency Electron Paramagnetic Resonance Characterization of PpoA, a CYP450 Fusion Protein that Catalyses Fatty Acid Dioxygenation	45
<i>A. A. Fraerman</i> : Noncollinear Magnetic States and Transport Properties of Ferromagnetic Nanostructures	46
<i>Y. Kobori, M. Fuki</i> : Orientational Structures and Electronic Couplings of Photoinduced Charge-Separated States in Human Proteins	47
<i>G. Kothe, T. Yago, J.-U. Weidner, G. Link, M. Lukaschek, T.-S. Lin</i> : Nuclear Spin Polarization and Spin Entanglement in Photoexcited Triplet States	48
<i>T. V. Leshina, I. M. Magin, N. E. Polyakov, E. A. Khramtsova, A. I. Kruppa</i> : Spin Chemistry Investigation of Peculiarities of Photoinduced Electron Transfer in Donor-Acceptor Linked System	50
<i>G. I. Likhtenshtein</i> : Spin-Spin Interactions in Investigation of Structure and Dynamics Biological Molecules	51
<i>H. Matsuoka, J.-R. Shen, A. Kawamori, Y. Ohba, S. Yamauchi</i> : Multifrequency EPR on Single Crystals of Photosystem II	53
<i>A. S. Mel'nikov, A. I. Buzdin, N. G. Pugach</i> : Domain Walls and Long-Range Triplet Correlations in SFS Josephson Junctions	55
<i>S. Nakazawa, K. Sato, T. Yoshino, S. Nishida, R. Rahimi, T. Ise, N. Mori, Y. Morita, K. Toyota, D. Shiomi, K. Nakasuji, M. Kitagawa, H. Hara, P. Carl, P. Höfer, T. Takui</i> : Molecular-Spin Based Quantum Computing and Quantum Information Processing	56
<i>H. Ohta, S. Okubo, T. Kobayashi, T. Sakurai, A. Matsuo, K. Kindo, X. G. Zheng, S. Nishihara, M. Fujisawa, H. Kikuchi</i> : Application of THz High-Field EMR to Antiferromagnets with THz Spin Gaps	58

<i>A. K. Powell</i> : SPIN Mapping of Iron-Containing Coordination Clusters Using Mössbauer Spectroscopy	59
<i>A. V. Sekretenko, A. V. Larionov, A. I. Il'in</i> : Electron Spin Dynamics in a GaAs Quantum Well with a Controllable Lateral Confinement	60
<i>M. S. Tagirov</i> : Magnetic Properties of PrF <sub>3</sub> Nanoparticles and Microparticles at Low Temperatures	61
<i>S. A. Tarasenko</i> : Spin Dephasing of Conduction Electrons in High-Mobility Quantum Wells	63
<i>N. V. Volkov, E. V. Eremin, M. V. Rautskiy, D. A. Smolyakov</i> : Interplay between Spin-Polarized Current and Spin Dynamics in Magnetic Nanostructures: Microwave Detection	64
<i>L. Weiner</i> : Generation and Oxidation of Nitroxyl Radicals by Ruthenium Complexes: A Novel ESR Approach to the Study of Photoelectron Transfer	67
<i>A. V. Yurkovskaya, O. B. Morozova</i> : Time-Resolved CIDNP as a Tool To Study Inter- and Intramolecular Electron Transfer Reactions	69
ORAL TALKS	
<i>N. Akdoğan</i> : Studying Spintronics Materials with Synchrotron Radiation	72
<i>L. Arda, O. Cakiroglu, N. Dogan</i> : Structural and Magnetic Properties of Zn <sub>0.95-x</sub> Co <sub>0.05</sub> Cu <sub>x</sub> O Diluted Magnetic Semiconductors by Sol-Gel Process	74
<i>A. A. Bloshkin, A. I. Yakimov, A. V. Dvurechenskii</i> : Singlet-Triplet Energy Splitting and Entanglement of Two Holes in Double Ge/Si Quantum Dots	75
<i>K. A. Earle</i> : Quasioptical Techniques for High Field EPR: Opportunities, Perspectives, and Challenges	76
<i>U. Eichhoff, P. Höfer</i> : Recent Developments in MR- and EPR-Imaging	77
<i>O. L. Ermolaeva, B. A. Gribkov, S. A. Gusev, A. Yu. Klimov, V. L. Mironov, V. V. Rogov, O. G. Udalov, A. A. Fraerman</i> : Magnetic States in Cross-Like Nanomagnets	79

---

<i>V. R. Gorelik, V. F. Tarasov, Yu. A. Zakharova, E. G. Bagryanskaya:</i> Electron Spin Polarized Nitroxide Radicals as Alternative Spin Probes for Inhomogeneity of Molecular Aggregates	81
<i>Yu. Grishin, A. Savitsky, R. Rakhmatullin, E. Reijerse, W. Lubitz:</i> Improved Probehead for Pulse High Field / High Frequency EPR Spectroscopy	83
<i>I. Gromov, P. Höfer, D. Schmalbein:</i> Novel Millimeter Wave EPR System ELEXSYS E780 (Bruker): Design and Performance	84
<i>A. V. Klochkov, E. M. Alakshin, R. R. Gazizulin, V. V. Kuzmin, M. S. Tagirov, D. A. Tayurskii:</i> Spin Kinetics of $^3\text{He}$ in Porous Substrates	85
<i>A. I. Kokorin, E. A. Konstantinova:</i> Determining the Parameters of ESR Spectra by Computer Analysis of the Spectrum Lineshape	86
<i>G. Mazzeo, E. Prati, M. Belli, G. Leti, S. Cocco, M. Fanciulli, F. Guagliardo, G. Ferrari:</i> Charge and Spin Dynamics of a Single Donor Coupled to an SET in Silicon	88
<i>A. G. Maryasov, M. K. Bowman:</i> Spin Dynamics and Bloch Equations for Paramagnetic Centers with Spin 1/2 Having Anisotropic $g$ -Tensor	90
<i>S. Moiseev:</i> Quantum Memory on Electron Spins in Resonator	93
<i>V. A. Morozov, N. N. Lukzen:</i> Cooperative Spin Crossover Phenomena in Elastic Chains of Exchange Clusters. Transfer Matrix Approach	94
<i>V. A. Nadolnny, Yu. N. Palyanov, I. N. Kupriyanov, M. E. Newton, S. L. Veber:</i> EPR Data on the Transformation of As-Grown Phosphorus Centers in Synthetic Diamonds at the Hthp Treatment	96
<i>B. Rameev:</i> Magnetic Resonance Studies of Spintronic and Nanomagnetic Materials	97
<i>A. A. Soltamova, V. A. Soltamov, P. G. Baranov:</i> Competition between Two Spin Teams: Defects in Diamond vs. Defects in Carborundum	98
<i>S. S. Sosin, L. A. Prozorova, O. A. Petrenko, M. E. Zhitomirsky:</i> Spin Dynamics of Heisenberg and XY Pyrochlore Magnets Studied by ESR	100
<i>A. Talantsev, A. Dmitriev, S. Zaitsev, O. Koplak, R. Morgunov:</i> Effect of the Orientation of Substrate on $\delta$ -<Mn>-Layer Magnetization and Photoluminescence of Quantum Well in InGaAs/GaAs Heterostructures	103

<i>S. N. Vdovichev, A. A. Fraerman, B. A. Gribkov, S. A. Gusev, A. Yu. Klimov, V. L. Mironov, V. V. Rogov</i> : Tunnel Magnetoresistance and Peculiarity of Magnetization Process of Multilayer Ferromagnetic Nanoparticles	105
<i>R. V. Yusupov, I. N. Gracheva, A. A. Rodionov, P. P. Syrnikov, A. Dejneka, A. I. Gubaev, V. A. Trepakov, M. Kh. Salakhov</i> : Photo-EPR Studies of KTN-1.2: Evidences of the Nb <sup>4+</sup> -O-Polaronic Excitons	107
<i>A. M. Ziatdinov</i> : Conduction Electron Spin Resonance in Two-Dimensional Systems	109
 WORKSHOP	
INVITED TALKS	
<i>B. Büchner</i> : Ferromagnetism and Superconductivity in LiFeAs	112
<i>S.-L. Drechsler, S. Nishimoto, R. Kuzian, J. Malek, J. Richter, J. van den Brink, R. Klingeler, W. E. A. Lorenz, A. Wolter, B. Büchner, M. Schmitt, H. Rosner</i> : Topical Magnetic and Electronic Properties of Frustrated Edge-Shared Chain Cuprates	113
<i>M. Farle</i> : Visualization of Spin Dynamics and Magnetic Hysteresis in Single Nanosized Magnetic Elements	114
<i>V. Kataev</i> : High Field Sub-Terahertz ESR Spectroscopy on Molecular Magnets	115
<i>G. Khaliullin</i> : Spin-Orbit Entangled Ground States and Excitations in Iridium Oxides	116
<i>R. Klingeler, S. Nishimoto, S.-L. Drechsler, R. Kuzian, J. Malek, J. Richter, W. E. A. Lorenz, N. Wizent, J. van den Brink, Y. Skourski, B. Büchner</i> : The Frustrated Quasi-1D Quantum Antiferromagnet Li <sub>2</sub> CuO <sub>2</sub>	117
<i>K. I. Kugel, A. O. Sboychakov, A. L. Rakhmanov, D. I. Khomskii</i> : Magnetic Inhomogeneities in Doped Materials with Spin-State Transitions	118
<i>L. R. Tagirov, R. G. Deminov, O. V. Nedopekin, Ya. V. Fominov, M. Yu. Kupriyanov, T. Yu. Karminskaya, A. A. Golubov</i> : Superconducting Triplet Spin Valve Based on the Superconductor-Ferromagnet Proximity Effect	121

## WORKSHOP

## ORAL TALKS

- A. Alfonsov, R. Zahn, G. Lang, F. Lipps, V. Kataev, S. Aswartham, S. Wurmehl, J. S. Kim, J. Deisenhofer, H.-A. Krug von Nidda, A. Loidl, B. Büchner*: High Field ESR Spectroscopy on Fe-Based Superconductors 124
- I. A. Bezkishko, V. A. Milyukov, O. N. Kataeva, O. G. Sinyashin, P. Lonneck, E. Hey-Hawkins, Yu. Krupskaya, V. Kataev, R. Klingeler, B. Büchner*: Magneto-Structural Correlations of 1,2-Diphosphacyclopentadienide Transition Metal Complexes 125
- V. Bisogni, L. Braicovich, G. Ghiringhelli, M. Moretti Sala, N. B. Brookes, L. Simonelli, R. Kraus, C. Monnay, K. Zhou, T. Schmitt, J. van den Brink, B. Büchner, J. Geck*: Resonant Inelastic X-ray Scattering: a New Approach for Investigating Spin Excitations 127
- V. S. Iyudin, Yu. E. Kandrashkin, V. K. Voronkova, V. S. Tyurin, E. N. Kirichenko, Yu. P. Yaschuk*: Spin-Spin Interactions and Electron Spin Polarization in Systems Based on Metalloporphyrins 128
- N. Hlubek, P. Ribeiro, R. Saint-Martin, S. Singh, A. Revcolevschi, G. Roth, G. Behr, B. Büchner, C. Hess*: Magnetic Heat Transport in One-Dimensional Quantum Antiferromagnets 129
- Y. Krupskaya, F. Moro, V. Kataev, T. C. Stamatatos, G. Christou, A. J. Tasiopoulos, J. van Slageren, B. Büchner*: Classical versus Quantum Magnetism in Single Molecular Magnetic Complexes 131
- P. V. Leksin, N. N. Garif'yanov, I. A. Garifullin, J. Schumann, V. Kataev, O. G. Schmidt, B. Büchner*: Experimental Realization of the Spin Switch Effect for the Superconducting Current in a Superconductor/Ferromagnet Thin Film Heterostructure 132
- H. Maeter, A. A. Zvyagin, H. Luetkens, G. Pascua, Z. Shermadini, R. Saint-Martin, A. Revcolevschi, C. Hess, B. Büchner, H.-H. Klauss*: Low Temperature Ballistic Spin Transport in the  $S = 1/2$  Antiferromagnetic Heisenberg Chain Compound  $\text{SrCuO}_2$  135
- R. F. Mamin*: Charge Segregation and Phase Separation in Manganites and the Possibility of Multiferroic Behaviour 136

<i>T. Mühl, S. Vock, J. Körner, F. Wolny, V. Neu, A. Leonhardt, B. Büchner</i> : Monopole-Like Probes for Magnetic Force Microscopy	137
<i>L. Salakhutdinov, Yu. Talanov, G. Teitel'baum, T. Adachi, T. Noji, Y. Koike, R. Khasanov</i> : EPR Study of Local Magnetic Fields on the $\text{Bi}_2\text{Sr}_2\text{Ca}_{1-x}\text{Y}_x\text{Cu}_2\text{O}_{8+y}$ Single Crystal Surface above $T_c$	138
<i>A. Useinov</i> : Tunnel Magnetoresistance in Double-Barrier Planar Magnetic Tunnel Junctions	139
<i>T. Vasilchikova, T. Kuzmova, A. Kamenev, O. Volkova, A. Kaul, R. Klingeler, B. Büchner, A. Vasiliev</i> : The Interrelation of Various Temperature Dependent Contributions to Magnetization in $\text{Eu}_{1-x}\text{Ca}_x\text{CoO}_{3-\delta}$ Solid Solutions	140
<i>R. Zaripov, E. Vavilova, Y. Krupskaya, A. Parameswaran, V. Milyukov, I. Bezkishko, D. Krivolapov, O. Kataeva, O. Sinyashin, E. Hey-Hawkins, V. Voronkova, K. Salikhov, R. Klingeler, V. Kataev, B. Büchner</i> : Relaxation Study of Novel Binuclear Mn Molecular Complexes by Pulse EPR Techniques	143
<i>E. Zvereva, O. Savelieva, V. Nalbandyan, M. Evstigneeva, L. Medvedeva, A. Wolter, J.-Y. Lin, A. Vasiliev, R. Klingeler, B. Büchner</i> : Spin Dynamics in New Honeycomb-Layered Antimonates of Alkali and Transition Metals	144

## POSTERS

<i>M. M. Akhmetov, G. G. Gumarov, V. Yu. Petukhov, G. N. Konygin, D. S. Rybin, E. P. Zhiglov</i> : Influence of Admixtures on the Formation of Paramagnetic Centers in Calcium Gluconate at Mechanoactivation	148
<i>A. Alfonsov, C. G. F. Blum, O. Volkonskyi, S. Rodan, D. Bombor, C. Hess, A. Wolter, S. Wurmehl, B. Büchner</i> : Optimization of Heusler Compounds via Control of the Relations between Structure and Physical Properties	151
<i>T. S. Altshuler, Y. V. Goryunov, A. V. Levchenko, A. N. Nateprov</i> : Electron Spin Resonance in Eu-Based Antiferromagnetic Compounds	152
<i>O. Antonova</i> : Influence of UV Irradiation on EPR and Optical Spectra of Tetraphenylborate Salts	154
<i>M. Bakirov, K. Salikhov, B. Bales</i> : EPR Investigation of Heisenberg Spin Exchange and Dipole Dipole Interactions in Diluted Free Radicals	156

<i>A. A. Bayazitov, K. S. Saikin, Ya. V. Fattakhov</i> : Transceiver System for NMR Tomography, Sensor “Joint”	158
<i>O. Cakiroglu, N. Dogan, L. Arda</i> : Structure and Magnetic Properties of $\text{Ni}_x\text{Zn}_{1-x}\text{Fe}_2\text{O}_4$ Nanoparticles	159
<i>O. Cakiroglu, N. Dogan, L. Arda</i> : Preparation, Structure and Magnetic Characterization of $\text{Zn}_{1-x}\text{Ni}_x\text{O}$ Nanoparticles	160
<i>N. E. Domracheva, A. V. Pyataev, M. S. Gruzdev</i> : EMR Detection of Presumable Suhl’s Instability in Magnetic $\gamma\text{-Fe}_2\text{O}_3$ Nanoparticles Encapsulated into PPI Dendrimer	161
<i>R. M. Eremina, T. P. Gavrilova, D. V. Mamedov, I. V. Yatsyk, Ya. M. Mukovskii</i> : ESR Spectra in Monocrystal and Thin Film GdMnO	164
<i>M. L. Falin, V. A. Latypov</i> : Magnetic Resonance of the Rare-Earth Impurity Centers in $\text{CsCaF}_3$ Single Crystal	166
<i>M. L. Falin, K. I. Gerasimov, V. A. Latypov</i> : EPR and Optical Spectroscopy of the $\text{Tm}^{2+}$ Ion in the $\text{KMgF}_3$ Single Crystal	167
<i>B. Farrakhov, Ya. Fattakhov, M. Galyautdinov</i> : Dynamics of Recrystallization and Thermometry of a Implanted Semiconductor at Pulsed Light Irradiation Measured via Optical Diffraction Method	169
<i>Ya. V. Fattakhov, A. R. Fakhrutdinov, V. N. Anashkin, V. A. Shagalov, K. S. Saikin, M. K. Galyaltidinov, D. D. Gabidullin, N. M. Gafiyatullin, N. A. Krylatykh</i> : Low-Field Spectroscopic Studies of Magnetic Resonance Contrast Agents	171
<i>L. Gafiyatullin, L. Savostina, L. Mingalieva, T. Ivanova, O. Turanova, G. Ivanova, A. Turanov, I. Ovchinnikov</i> : EPR, UV, and DFT Study of Spin-Crossover Complexes Fe(III) and Their Photoisomerizable Ligands	172
<i>N. M. Gafiyatullin, Ya. V. Fattakhov, N. A. Krylatykh, D. D. Gabidullin</i> : Gradient System Control Unit for MRI System “Tmr-Kfti”	173
<i>R. T. Galeev</i> : EPR Line Shape of a System of Two Coupled Spins with Difference Rates of Transverse Relaxation	174
<i>E. R. Galiakberova, R. T. Galeev, A. R. Fakhrutdinov</i> : The Calculation of Correctional System for the Basic Field of Magnetic Resonance Imaging with a Permanent Magnet	175

<i>T. P. Gryaznova, S. A. Katsyuba, M. Yu. Filatov, I. A. Bezkishko, V. A. Milyukov, O. G. Sinyashin: Vibrational Spectroscopy and Quantum Chemical Computations as a Tool for Metal Spin State Diagnostics</i>	176
<i>M. I. Ibragimova, A. I. Chushnikov, V. N. Moiseev, V. Yu. Petukhov, E. P. Zheglov: Paramagnetic Proteins of Blood as Biomarkers of Malignant Neoplasm Anemia in Urogenital System</i>	178
<i>K. L. Ivanov, S. E. Korchak, A. S. Kiryutin, A. V. Yurkovskaya, T. Köchling, H.-M. Vieth: Coherent Transfer of Spin Hyperpolarization in Coupled Spin Systems at Variable Magnetic Field</i>	181
<i>Yu. E. Kandrashkin: Angular Dependence of ESEEM Signal in the Pair Spin Polarized Quartet–Radical</i>	182
<i>I. T. Khairuzhdinov, K. M. Salikhov: Computer Simulation of PELDOR Experiment for Three-Spin Systems</i>	183
<i>S. S. Khutshishvili, T. I. Vakulskaya, S. A. Korzhova, T. V. Kon'kova, A. S. Pozdnyakov, T. G. Ermakova, G. F. Prozorova: Determination of the Iron Oxides Nature in Polymeric Nanocomposites by EPR Spectroscopy</i>	184
<i>A. B. Konov, K. M. Salikhov: Manifestation of the Compensating Effect for the Self-Diffusion Coefficient of Molecules in Liquid Crystals</i>	187
<i>K. Konov, R. Zaripov: Improvement of Selective Hole-Burning Technique Using a Fast-Relaxing Paramagnetic Compound</i>	188
<i>S. Krivenko: Competition between the Crystal Field and Superexchange Interactions in the <math>t_{2g}</math> Orbital Mott Insulators</i>	190
<i>N. Krylatykh, A. Fakhrutdinov, R. Khabipov: Optimization of Device for Measuring of Magnetic Field Inhomogeneity</i>	192
<i>G. S. Kupriyanova, A. P. Popov, A. Y. Zyubin, A. Orlova, E. Prokhorenko, A. Goykhman, P. Ershov: The Problem of the Nano-Structures Diagnostics for the Needs of Spintronics by Magnetic Resonance Methods</i>	193
<i>V. N. Lisin, A. M. Shegeda: Zeeman-Switched Photon Echo in <math>\text{LuLiF}_4:\text{Er}^{3+}</math> and <math>\text{YLiF}_4:\text{Er}^{3+}</math></i>	194

---

<i>N. N. Lukzen, A. B. Doktorov, M. V. Petrova</i> : CPMG Echo Amplitudes with Arbitrary Refocusing Angle: Explicit Expressions, Asymptotic Behavior, Approximations	197
<i>S. Lvov, E. Kukovitsky</i> : ESR Study of Ternary Dilute Alloys Cu-Me-Er	198
<i>A. Lyubin, A. Zinovieva, A. Dvurechenckii</i> : Spin Properties of Electron in Two Dimensional Quantum Dot Arrays	200
<i>R. Mantovan, S. Vangelista, B. Kutrzeba-Kotowska, S. Cocco, A. Lamperti, G. Tallarida, D. Mameli, M. Fanciulli</i> : ALD/CVD Synthesis of Magnetic Tunnel Junctions	202
<i>L. V. Mingalieva, V. K. Voronkova, R. T. Galeev, A. A. Sukhanov, V. Chiornea, Gh. Novitchi</i> : EPR Investigation of Spin-Spin Interactions in $[\text{Fe}(\text{L})_3][\text{Cr}_2(\text{OH})(\text{Ac})(\text{nta})_2] \cdot n\text{H}_2\text{O}$ (L = phen, bpy)	204
<i>I. R. Mukhamedshin, H. Alloul</i> : NMR Evidence for Charge and Orbital Order of Cobalt Ions in $\text{Na}_{2/3}\text{CoO}_2$	206
<i>E. A. Nasibulov, K. L. Ivanov, L. V. Kulik</i> : Pulsed Reaction Yield Detected EPR of Radical Pairs. Theoretical Treatment	207
<i>I. A. Nurmamyatov</i> : Algorithm for Optimizing the Using of Contrast Agents in Low-Field MRI	208
<i>A. A. Obynochny, A. A. Sukhanov, V. R. Gorelik, V. F. Tarasov</i> : TR EPR Investigation of Excited State Anthraquinone/TEMPO Radical Complexes	210
<i>I. V. Ovchinnikov, T. A. Ivanova, O. A. Turanova, G. I. Ivanova</i> : Spin-Crossover Fe(III) Complexes with Light-Sensitive Properties	212
<i>I. V. Romanova, A. V. Egorov, S. L. Korableva, M. S. Tagirov</i> : $^{19}\text{F}$ NMR and Local Fields in Double Rare-Earth Fluoride $\text{LiTbF}_4$	213
<i>A. A. Ryadun, V. A. Nadolinny, A. A. Pavluk</i> : EPR and Luminescence of $\text{Li}_2\text{Zn}_2(\text{MoO}_4)_3$ Crystals Doped with Transition Metal Ions	214
<i>L. I. Savostina, G. M. Zhidomirov, M. Ya. Mel'nikov, I. D. Sorokin</i> : EPR Spectra and Quantum Chemistry Calculations of Structure and Magnetic Resonance Parameters of Methylsubstituted Radical Cations	216
<i>K. R. Sharipov, R. M. Eremina, L. V. Mingalieva, I. A. Fayzrahmanov, A. G. Badelin, A. V. Evseeva</i> : Investigations of $\text{La}_{1-x}\text{Sr}_x\text{Mn}_{0.925}\text{Zn}_{0.075}\text{O}_3$ ( $x = 0.075; 0.095; 0.115$ ) Ceramics	218

<i>A. Sukhanov, V. Voronkova, A. Baniodeh, G. Novitchi, A. K. Powell:</i> EPR Investigation of the Fe <sup>II</sup> Dy <sup>III</sup> Coordination Clusters	220
<i>V. Tarasov, D. Akhmetzyanov, A. Konovalov, E. Zhiteitceva,</i> <i>E. Zharikov:</i> Structure and Magnetic Properties of Chromium Impurity Ions as Studied by Multifrequency EPR	221
<i>V. A. Ulanov, I. M. Safarov, M. M. Zaripov, G. S. Shakurov:</i> Unambiguous Determination of Spin-Hamiltonian Parameters of Low Symmetry Paramagnetic Centers with $S_{\text{eff}} \geq 2$	222
<i>V. N. Verkhovlyuk, O. A. Anisimov:</i> Optically Detected ESR of Radical Ion Pairs Induced by Vacuum Ultraviolet	223
<i>M. Volkov, K. M. Salikhov:</i> Application to the Electron Spins of Pulse Sequences Designed for the Nuclear Spins	224
<i>B. G. Yavishev:</i> ESR of P-Containing Substances in Electrochemistry and Biology	226
<i>S. V. Yurtaeva, V. N. Efimov, V. S. Iydin, Kh. L. Gainutdinov,</i> <i>G. G. Jafarova:</i> Magnetic Resonance of Crystalline Nanoparticles in Nervous Tissue of Snail	227
<i>S. V. Yurtaeva, V. N. Efimov, N. I. Silkin, A. A. Rodionov,</i> <i>M. V. Burmistrov, A. V. Panov, A. A. Moroshek:</i> Magnetic Resonance of Ferritin in Tumor Tissue	230
<i>L. N. Zalyalyutdinova, D. A. Nasybullina, A. Y. Sabirova:</i> Development of a New Approach to NMR Diagnostics of Malignant Tumors Using the Metal Compounds with Antineoplastic Activity	233
<i>L. N. Zalyalyutdinova, R. G. Yakhin, N. A. Samigullina, A. Y. Sabirova:</i> Paramagnetic Centers of Blood Plasma and Their Prognostic Value for Tumor Innidiation	235
<i>R. Zaripov, L. Kulik, K. Salikhov:</i> New Aspects of the Nanoscale Distance Measurement Using Pulse EPR	237
<i>T. Zinkevich, K. Saalwachter, D. Reichert, B. Reif, A. Krushelnitsky:</i> Investigation of Millisecond to Second Motions in Proteins Using Exchange NMR-Spectroscopy	239
AUTHOR INDEX	241

---

## PLENARY LECTURES

## **Intrinsic Inhomogeneities in Spin Correlated Solids as Revealed by Magnetic Resonance**

*B. Büchner*

*Leibniz Institute for Solid State and Materials Research IFW Dresden, Dresden D-01069,  
Germany, [b.buechner@ifw-dresden.de](mailto:b.buechner@ifw-dresden.de)*

## Spins in Low-Dimensional Quantum Dot Semiconductor Nanostructures

*A. V. Dvurechenskij, A. F. Zinovieva, and A. V. Nenashev*

*Institute of Semiconductor Physics, Russian Academy of Science,  
Novosibirsk 630090, Russian Federation, dvurech@isp.nsc.ru*

Spin effects in nanostructures are considered to be attractive for realization of new semiconductor devices. Several device applications such as spin transistors, spin memory, and also the spin quantum computer have been proposed to utilize spin dependent effects in semiconductors. The electron spin is considered as a natural bit of quantum information and can provide an implementation of the ideas of quantum computation. The fabrication of some useful devices suggest the generation of a non-equilibrium spin density in semiconductor, manipulation of the spins by external fields and the detecting of the resulting spin state. For successive manipulation of spin it is necessary to know such fundamental spin properties as effective g-factor and spin relaxation time.

Strong electron confinement in low-dimensional structures such as quantum wells and quantum dots (QDs) should leads to a significant increase of spin lifetimes. A promising way for the producing of zero-dimensional structures is the strain epitaxy. Ge/Si QDs, grown by molecular beam epitaxy in Stranski-Krastanow growth mode, are characterized by the relative homogeneity in shape and size (inhomogeneity is about 10–15%), and high density, which can reach up to  $10^{12} \text{ cm}^{-2}$ . This type of QDs is currently considered as one of the best candidates for solid state implementation of spintronics and quantum computation schemes because of the expected long spin lifetime in silicon and developed technology to control the nanostructure growth.

The outline of present report is the following:

- Spin relaxation in single quantum dot.
- Spin relaxation at the electron resonant tunneling between coupled QDs.
- Spin relaxation in two-dimensional structures with asymmetrical quantum wells.
- Spin relaxation in zero-dimensional structures with asymmetrical tunnel-coupled QDs.
- Anisotropic exchange interaction in the structures with Ge/Si QDs.
- Double-occupancy probability and entanglement electronic states in Ge/Si QDs.

A spin coherence time of up to 20 us was obtained for electrons confined in Ge/Si QDs. The measurement of spin echo allows revealing the mechanism of spin relaxation.

## EPR Probing of Nanoscale Dynamics in Molecular Disordered Systems

*S. A. Dzuba*

*Institute of Chemical Kinetics and Combustion, Russian Academy of Sciences, Novosibirsk, Russian Federation, dzuba@kinetics.nsc.ru*

Three different types of EPR experiments are described which allows obtaining information on molecular dynamics at the nanometric scale of distances in molecular glasses, polymers and biological systems.

Continuous wave EPR spectra of triplet state of fullerene  $C_{70}$  were obtained under continuous light illumination in molecular glasses of *o*-terphenyl and *cis/trans*-decaline and in the glassy polymers polymethylmethacrylate (PMMA) and polystyrene (PS). Above  $\sim 100$  K, a distinct narrowing of the EPR lineshape of the triplet was observed, which was very similar for the all systems studied. EPR lineshape was simulated fairly well within a framework of a simple model of isotropic orientational motion by sudden jumps of arbitrary angles. The obtained results evidence that above 100 K nanostructure of glassy media is soft enough to allow fast reorientations of large  $C_{70}$  molecular probes.

Electron spin echo envelope modulation (ESEEM) induced by spin-spin interactions between radicals in the  $D^+Q^-$  radical pair has been investigated for bacterial reaction centers of *Rhodobacter sphaeroides* R26. An abrupt change of the ESEEM time-domain traces was observed in a narrow temperature range near 80 K. This change corresponds to a much broader lineshape of the Fourier-transformed, frequency-domain spectrum below 100 K. The lineshapes could be well simulated under the assumption that the distance between the two radicals, centering around 2.9 nm, at low temperatures is distributed within a range of about 0.4 nm.

The pulsed electron-electron double resonance (ELDOR) technique was employed to study nitroxide spin probes of three different sizes dissolved in glassy *o*-terphenyl. A microwave pulse applied to the central hyperfine structure (hfs) component of the nitroxide EPR spectrum was followed by two echo-detecting pulses of different microwave frequency to probe the magnetization transfer (MT) to another hfs component. MT between hfs components is readily related to flips in the nitrogen nuclear spin which in turn are induced by molecular motion. For a bulky nitroxide, it was found that MT rates approach dielectric  $\alpha$  (primary) relaxation frequencies reported for *o*-terphenyl in the

literature. For small nitroxides, MT rates were found to match the frequencies of dielectric  $\beta$  (secondary) Johari-Goldstein relaxation. The nature of the latter nowadays is heavily debated in literature. Presented results of MT studies provide evidence that Johari-Goldstein relaxation is induced by cooperative reorientations within a set of some fixed reorientations.

## Spin-Polarized Electrons in Superconductor/Ferromagnets Hybrid Structures

*I. A. Garifullin*

*Zavoisky Physical-Technical Institute, Russian Academy of Sciences, Kazan 420029,  
Russian Federation*

The mutual influence of magnetism and superconductivity in superconductor/ferromagnet (S/F) nanofabricated thin film heterostructures has been an exciting topic in Solid State Physics during the last 15 years. The antagonism of superconductivity and ferromagnetism consists of strong suppression of superconductivity by ferromagnetism because ferromagnetism requires parallel (P) and superconductivity requires antiparallel orientation of spins. The interaction between the magnetic and superconducting (SC) order parameters in these heterostructures is realized due to the so-called S/F proximity effect (PE). Recently an interest to the study of the hybrid S/F systems arose and the following interesting and important effects have been discovered in course of these studies.

1. It was shown that in an S/F structure the SC wave function which penetrates from a superconductor into a ferromagnet exhibits a damped oscillating behavior because of strong suppression of superconductivity by ferromagnetism and non-zero momentum of the Cooper pairs in the F layer. The characteristic depth of the decay of the pairing function in the F layer  $\xi_F = (4\hbar D_F/I)^{1/2}$  is determined by the diffusion coefficient  $D_F$  of conduction electrons and the exchange splitting of the conduction band in the F layer. This leads to a non-monotonic dependence of the SC critical temperature  $T_c$  on the thickness of the F layer  $d_F$ . What is more interesting that is the oscillatory behavior of the critical Josephson current in S/F/S junction and the negative critical current at certain  $d_F$ . This effect has been predicted long ago but observed only recently by Ryazanov et al. and Kontos et al. The Josephson junctions with negative critical current (the so called  $\pi$ -junctions) can be applied in future quantum computers.

2. Another interesting effect which was predicted and observed in S/F structures is related to a new type of superconducting correlations, the so-called odd triplet superconductivity, that can arise due to the PE in the F layer with a non-homogenous magnetization. In case of an uniform magnetization in the F layer the pair wave function in F consists of the singlet and triplet components with zero projection of the total spin of a Cooper pair. Both components oscillate in

space and decay on a short length  $\xi_F$ . The situation drastically changes if the magnetization in F is nonuniform. In this case not only the singlet component arises in the F layer but also a triplet component with a nonzero projection of the total spin. The penetration depth of the triplet component does not depend on  $I$  and is much longer than  $\xi_F$ . It may be comparable with the penetration depth of the SC condensate into the normal metal  $\xi_N = (4\hbar D_F / 2\pi T)^{1/2}$ . This component can be called the long-range triplet component.

3. There is another interesting theoretical prediction which was experimentally realized only recently. This is the spin valve switch based on the S/F proximity effect. The physical origin of this effect relies on the idea to control the pair-breaking, and hence the SC transition temperature  $T_c$ , by manipulating the mutual orientation of the magnetizations of the F layers in a heterostructure comprising, e.g., two F and one S layer in a certain combination. This is because the mean exchange field from two F layers acting on Cooper pairs in the S layer is smaller for the AP orientation of the magnetizations of these F layers compared to the P case. The detailed information concerning the first experimental realization of the full spin valve effect will be presented on this Conference by Leksin et al.

4. As it was shown theoretically [1], besides the ordinary PE (penetration of the condensate from the superconductor into the ferromagnet) the inverse PE (penetration of the magnetic moment from the ferromagnet into the superconductor) takes place in S/F structures. Qualitatively the physical origin of this effect can easily be understood. Let us consider an S/F bilayer with the F layer being thin compared to  $\xi_F$ . Due to the exchange field the conduction electron spins in the F layer are polarized in one direction predominantly. These electrons have their Cooper partners deep in the S layer on the distance  $\xi_S$  which is the SC coherence length. Thus, due to the SC correlations a spin polarization is induced in the S layer. The magnetic moment in the S layer should be oriented antiparallel to the magnetization of conduction electrons in the F layer. This phenomenon was observed recently using nuclear magnetic resonance (NMR) technique [2]. In NMR the inverse PE (the spin screening effect) manifests itself as a distortion of the NMR signal due to decrease of the Knight shift upon the transition to the SC state. The present talk will be devoted to the detailed presentation of the experimental observation of this phenomenon.

1. Bergeret F.S., Volkov A.F., Efetov K.B.: Europhys. Lett. **66**, 111 (2004); Phys. Rev. B **69**, 174504 (2004)
2. Salikhov R.I., Garifullin I.A., Tagirov L.R., Theis-Bröhl K., Westerholt K., Zabel H.: Phys. Rev. Lett. **102**, 087003 (2009); Phys. Rev. B **80**, 214523 (2009)

## EMR to Investigate the No Man's Land between Molecular Nanomagnets and Magnetic Nanoparticles

*D. Gatteschi, M. Fittipaldi, C. Sangregorio, L. Sorace, and L. Castellì*

*Chemistry Department, University of Florence, INSTM, Sesto Fiorentino 50019, Italy,  
dante.gatteschi@unifi.it*

Iron oxides are perhaps among the first functional materials used by humans taking advantage of their colour and of their magnetic properties. After a few millennia they are still of much interest, the nano revolution having provided new opportunities of investigation. In fact nanosize magnetic iron oxides have new properties which are exploited in so different areas as nanomedicine and information technology [1]. There is now a continuous transition from micro to nanoparticles which allows for separately investigating different size ranges and consequently different properties. Particles larger than 10 nm (corresponding to  $10^5$  iron ions) are usually considered as small parts of oxides and their magnetic properties interpreted using a top-down approach. On the contrary, when particles in the range of 1–5 nm, comprising 10–10.000 ions, are investigated a molecular bottom-up approach may be more useful. This size range is also particularly promising for observing new properties associated with the co-existence of classic and quantum behaviours [2–5]. In fact the explosive development of molecular nanomagnetism in the last few years has been ignited by the discovery that some molecules can behave as single molecule magnets, SMM, i.e. show a locked magnetization at low temperature and give origin to stepped magnetic hysteresis [6, 7] The latter is the proof of coexistence of quantum and classic effects. This breakthrough started a hunt to SMM with “improved” properties which produced some new molecules showing slow relaxation of the magnetization, and a large number of clusters which do not behave like that. All these complexes, referred to as molecular nanomagnets, MNM [8], offer however the opportunity to understand the transition between the behaviour of a single paramagnetic centre and that of a cluster of  $N$  ions, with  $N$  increasing to very large values. Appealing as it can be, the molecular approach has been able to produce iron-oxo based MNM with  $N = 30$  as a maximum. The next step would be that of  $N = 100$ – $1000$ , which currently is better covered by magnetic nanoparticles, MNP. Therefore efforts must be done to synthesize clusters with large and controlled  $N$  looking for emerging properties [9].

We will try to highlight the current understanding of the correlation among structural and magnetic properties of MNP of 1–5 nm and compare them with those of iron-oxo based molecules. We are not covering in detail all the reported

iron-oxo clusters but rather we focus on systems which can be considered as milestones in the ideal bottom-up approach, *i.e.* molecular systems which for structure and/or magnetic properties describe the transition from isolated ions to bulk. On the other side, we will discuss some examples of small ( $d < 4$  nm) MNP obtained by a top-down approach, looking for the possibility to observe quantum effects. In particular we will focus on small MNP which can be grown using solution chemistry techniques or taking advantage of natural nanolaboratories as those provided by oligomeric ferritin-like proteins as Dps (DNA binding proteins from starved cells) [10], which have an inner cavity of about 4 nm diameter, hosting up to 600 ions. Under specific conditions, in both Ferritin and Dps it is possible to synthesize uniform magnetite or maghemite cores [11, 12]

We will first briefly recall some aspects of nanomagnetism which are common to both MNP and MNM, followed by an overview of the structure and magnetic properties of selected examples of iron-oxo clusters, focusing on those sharing structural features with most common iron oxides. Finally we will briefly review the smallest iron oxide MNP synthesized to date showing how EMR can be a very useful tool to investigate the properties of such small systems

1. (a) Hyeon T.: Chem. Commun. 927 (2003); Nanomagnetism and Spintronics (Shinjo T., ed.) Elsevier, Amsterdam, 2009. (b) Magnetism in Medicine: A Handbook (Andra W., Nowak H., eds.) Wiley-VCH, Weinheim Germany, 2007. (c) Gupta A.K., Gupta M.: Biomaterials **26**, 3995 (2005). (d) Pankhurst Q.A., Connolly J., Jones S.K., Dobson J.: J. Phys. D **36**, R167 (2003)
2. Noginova N., Weaver T., Giannelis E.P., Bourlinos A.B., Atsarkin V.A., Demidov V.V.: Phys. Rev. B **77**, 014403 (2008)
3. Li H., Klem M.T., Seby K.B., Singel D.J., Young M., Douglas T., Idzerda Y.U.: J. Magn. Magn. Mater. **321**, 175 (2009)
4. Fittipaldi M., Innocenti C., Ceci P., Sangregorio C., Castelli L., Sorace L., Gatteschi D.: Phys. Rev. B **83**, 104409 (2011)
5. Tejada J., Zhang X.X., del Barco E., Hernandez J.M., Chudnovsky E.M.: Phys. Rev. Lett. **79**, 1754 (1997)
6. (a) Caneschi A., Gatteschi D., Sessoli R., Barra A.L., Brunel L.C., Guillot M.: J. Am. Chem. Soc. **113**, 5873 (1991). (b) Sessoli R., Gatteschi D., Caneschi A., Novak M.A.: Nature **365**, 141 (1993)
7. (a) Thomas L., Lioni F., Ballou R., Gatteschi D., Sessoli R., Barbara B.: Nature, **383**, 145 (1996). (b) Friedman J.R., Sarachik M.P., Tejada J., Ziolo R.: Phys. Rev. Lett. **76**, 3830 (1996)
8. Sessoli R., Villain J., Gatteschi D.: Molecular Nanomagnets. Oxford University Press, Oxford, 2006.
9. Fittipaldi M., Sorace L., Barra A. L., Sangregorio C., Sessoli R., Gatteschi D.: Phys. Chem. Chem. Phys. **11**, 6555 (2009)
10. Chiancone E., Ceci P., Ilari A., Ribacchi F., Stefanini S.: Biomaterials **17**, 197 (2004)
11. Ceci P., Chiancone E., Kasyutich O., Bellapadrona G., Castelli L., Fittipaldi M., Gatteschi D., Innocenti C., Sangregorio C.: Chem. Eur. J. **16**, 709 (2010)
12. Uchida M., Klem M.T., Allen M., Suci P., Flenniken M., Gillitzer E., Varpness Z., Liepold L.O., Young M., Douglas T.: Adv. Mater. **19**, 1025 (2007)

## Nanometer Scale Distance Measurements in Proteins and Nucleic Acids Using Gd<sup>3+</sup> Spin Labelling

*D. Goldfarb*

*Department of Chemical Physics, Weizmann Institute of Science, Rehovot 76100, Israel,  
Daniella.goldfarb@weizmann.ac.il.*

Methods for measuring nanometer scale distances between specific sites in biomolecules (proteins and nucleic acids) and their complexes are essential for analysis of their structure and function. In the last decade pulse EPR techniques, mainly pulse double-electron-electron resonance (DEER), have been shown to be a very effective for measuring distances between two spin labels attached to a biomolecule. DEER is routine for distances up to 5 nm and with some extra effort and favorable conditions distances as high as 8 nm can be accessed. So far such measurements have been applied mostly to biomolecules labeled with nitroxide stable radicals. The measurements are usually carried out at standard X-band frequencies (~9.5 GHz, 0.35 mT). Here we introduce a new family of spin labels that are based on Gd<sup>3+</sup> for DEER measurements at high frequencies, particularly W-band (95 GHz, ~3.5 T). The benefit such spin label offers is the considerable increase in sensitivity that reduces the amount of the biomolecule needed by more than an order of magnitude. Gd<sup>3+</sup> has a spin of 7/2 and its unique ERP spectral properties turn it into an excellent spin label for distance measurements at high fields and this will be discussed. Then, examples of Gd<sup>3+</sup>-Gd<sup>3+</sup> distance measurements in models compounds will be described followed by a presentation of a few applications distance measurements in peptides, proteins, protein complexes and DNA molecules. The Gd<sup>3+</sup> is attached to the biomolecule using a chelator that can be covalently attached at specific sites of the molecule, just like nitroxide spin labels. The chemical and physical requirement for the ultimate Gd<sup>3+</sup> will be discussed.

## Parahydrogen-Induced Polarization and Heterogeneous Catalysis

*I. V. Koptyug, K. V. Kovtunov, V. V. Zhivonitko, I. V. Skovpin, D. A. Barskiy,  
and R. Z. Sagdeev*

*International Tomography Center SB RAS, Novosibirsk 630090,  
Russian Federation, koptyug@tomo.nsc.ru*

Among the modern trends in NMR, there are two avenues of development that recently became a focus of significant attention of the magnetic resonance community. One is the development of a number of hyperpolarization techniques for the enhanced sensitivity and specificity of novel NMR applications. Another is the utilization of the peculiar properties of the long-lived nuclear spin states to extend the applicability of NMR techniques to the studies of slow physical and chemical processes by eliminating the restrictions imposed by the relaxation on the lifetime of nuclear spin coherences. Parahydrogen represents both an example of the long-lived spin state and the means to enhance an NMR signal by several orders of magnitude. Parahydrogen-induced polarization (PHIP) of nuclear spins is an established spectroscopic tool for the mechanistic studies of homogeneous hydrogenations catalyzed by transition metal complexes in solution. More recently, PHIP-based NMR signal enhancement was demonstrated to be a promising way to produce hyperpolarized species in solution for the advanced *in vivo* MRI applications such as molecular and cellular imaging.

The objective of our research is to significantly broaden the scope of the PHIP phenomenon applications by extending it to the heterogeneously (HET) catalyzed hydrogenation reactions and other heterogeneous processes that involve activation of molecular hydrogen. In fact, parahydrogen can be very useful for developing HET-PHIP as a hypersensitive NMR-based technique for the *in situ* and *operando* studies of heterogeneous catalytic processes. Furthermore, HET-PHIP can be useful for producing hyperpolarized gases as well as catalyst-free hyperpolarized liquids for various MRI applications including the advanced *in vivo* studies.

We have demonstrated that, similar to their homogeneous counterparts, heterogenized transition metal complexes are able to produce strong NMR signal enhancements when parahydrogen is used in the liquid-solid or in the gas-solid hydrogenation reactions [1]. This implies that the heterogenization of metal complexes does not alter the reaction mechanism which involves the formation of a metal dihydride. For supported metal catalysts (e.g., Pt/Al<sub>2</sub>O<sub>3</sub>),

dissociative hydrogen chemisorption and migration of H atoms on the metal surface were expected to make the pairwise hydrogen addition to a substrate impossible. Unexpectedly, our results demonstrate that PHIP can in fact be observed both in liquid-solid and in gas-solid heterogeneous hydrogenations catalyzed by supported metal catalysts [2]. The contribution of this pairwise addition route to the overall reaction mechanism was estimated and the structure-reactivity relationship was investigated. In particular, it was established that the NMR signal enhancement is sensitive to the metal nanoparticle size, the nature of the support, the type of the substrate, and that it also exhibits a correlation with the catalyst activity. Our results demonstrate that PHIP is likely to be a phenomenon common to many H<sub>2</sub>-activating heterogeneous catalysts [3–5]. While the signal enhancements achieved so far with HET-PHIP are much less than the maximum possible values, several MRI applications of HET-PHIP have been already demonstrated [6–8], including the MR imaging of gas flow in microfluidic devices and of the progress of a catalytic reaction in a model microreactor.

**Acknowledgments.** This work was supported by the grants from RAS (5.1.1), RFBR (11-03-00248-a, 11-03-93995-CSIC-a), SB RAS (integration grants 9, 67, 88), the program of support of leading scientific schools (NSh-7643.2010.3), Russian Ministry of Education and Science (02.740.11.0262) and the Council on Grants of the President of the Russian Federation (MK-1284.2010.3).

1. Koptyug I.V., Kovtunov K.V., Burt S.R., Anwar M.S., Hilty C., Han S., Pines A., Sagdeev R.Z.: *J. Amer. Chem. Soc.* **129**, 5580 (2007)
2. Kovtunov K.V., Beck I.E., Bukhtiyarov V.I., Koptyug I.V.: *Angew. Chem. Int. Ed.* **47**, 1492 (2008)
3. Kovtunov K.V., Zhivonitko V.V., Corma A., Koptyug I.V.: *J. Phys. Chem. Lett.* **1**, 1705 (2010)
4. Kovtunov K.V., Zhivonitko V.V., Kiwi-Minsker L., Koptyug I.V.: *Chem. Commun.* **46**, 5764 (2010)
5. Koptyug I.V., Zhivonitko V.V., Kovtunov K.V.: *Chem. Phys. Chem.* **11**, 3086 (2010)
6. Bouchard L.-S., Kovtunov K.V., Burt S.R., Anwar M.S., Koptyug I.V., Sagdeev R.Z., Pines A.: *Angew. Chem. Int. Ed.* **46**, 4064 (2007)
7. Bouchard L.-S., Burt S.R., Anwar M.S., Kovtunov K.V., Koptyug I.V., Pines A.: *Science* **319**, 442 (2008)
8. Telkki V.-V., Zhivonitko V.V., Ahola S., Kovtunov K.V., Jokisaari J., Koptyug I.V.: *Angew. Chem. Int. Ed.* **49**, 8363 (2010)

## Spin Relaxation in Semiconductors and Semiconductor Nanostructures

Yu. G. Kusrayev

*A. F. Ioffe Physical Technical Institute, St. Petersburg 194021, Russian Federation,  
kusrayev@orient.ioffe.ru*

During the last years there has been an intensive development of research in semiconductor spin physics. This research has yielded a large variety of interesting and spectacular phenomena [1]. At present the field of spin related phenomena is known as *spintronics* defined as “...spin-based electronics, where it is not the electron charge but the electron spin that carries information, and this offers opportunities for a new generation of devices combining standard microelectronics with spin-dependent effects...” [2]. Spintronics assumes the fabrication of some useful devices using i) creation of a non-equilibrium spin density in a semiconductor, ii) manipulation of the spins by external fields, and iii) detection of the resulting spin state. The listed possibilities are based on the knowledge of the spin related phenomena.

After the short review of spin physics we will focus on the one particular but important issue of spintronics – spin relaxation of electrons. The majority of spin relaxation data has been obtained in the experiments on optical orientation. The first experiment on optical spin orientation of electrons in a semiconductor (Si) was done by G. Lampel [3] in 1968, as a direct application of the ideas of optical pumping in atomic physics. This pioneering work was followed by extensive experimental and theoretical studies mostly performed by small research groups at Ecole Polytechnique in Paris and at Ioffe Institute in St Petersburg (Leningrad) in the 70ies and early 80ies [1].

Spin relaxation can be generally understood as a result of the action of fluctuating in time magnetic fields. These random “effective fields” originate from the spin-orbit, hyperfine or exchange interactions. It is the precession of spin in this random field which results in the spin relaxation. Different channels of spin relaxation can interfere both in constructive or destructive way.

For possible applications of the electron spin in the field of spintronics long spin relaxation lifetimes are required. Therefore, materials with weak spin-orbit or hyperfine interactions are attractive. On the other hand for manipulation of the spins by external electric field (that is most convenient) strong enough spin-orbit SO-interaction is necessary. To overcome these contradictory conditions it can be suggested the use of materials where two or more channels of spin relaxation interfere in destructive way. We discuss two examples of

such material systems: asymmetric quantum wells and p-type semiconductors doped with magnetic impurities. In asymmetric quantum wells Dresselhaus and Rashba terms can be tuned in such a way that they compensate each other. In p-type semiconductors dominant spin relaxation mechanism is an exchange scattering by holes. In p-GaAs doped with magnetic impurity Mn surprisingly long spin relaxation time of electrons has been found. Manganese in GaAs serves as an acceptor and magnetic impurity. The suppression of spin relaxation can be considered as a partial compensation of fluctuating fields, produced by manganese spin  $S = 5/2$  and hole magnetic moment  $J = 3/2$ . This compensation is a result of antiferromagnetic interaction of manganese with hole, leading to the enhanced spin memory.

Support by Russia Foundation for Basic Research and Academy of Sciences is acknowledged.

1. Optical Orientation (Maier F., Zakharchenya B.P., eds.). North-Holland, 1984.
2. Wolf S.A. *et al.*: Science **294**, 1488 (2001)
3. Lampel G.: Phys. Rev. Lett. **20**, 491 (1968)

## In Search of Renewable Energy Resources: Mechanisms of Light-Induced Water Splitting and Hydrogen Production in Nature Studied by Advanced EPR Techniques

*W. Lubitz*

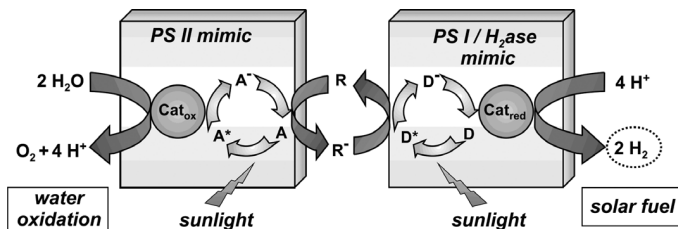
*Max-Planck-Institut für Bioanorganische Chemie, Mülheim an der Ruhr 45470, Germany,  
wolfgang.lubitz@mpi-mail.mpg.de*

Hydrogen is considered the fuel of the future if produced from sunlight-driven water splitting. A hydrogen economy based on genetically modified organisms or bioinspired synthetic catalysts (scheme) requires a profound knowledge of the structure and function of the respective enzymes in nature, namely water-oxidase and hydrogenase[1].

EPR in combination with quantum chemical calculations is the method of choice to elucidate the electronic structure of the (often paramagnetic) intermediates in these processes and thus understand the reaction mechanisms.

Light-induced water splitting and oxygen release ( $2\text{H}_2\text{O} \rightleftharpoons 4\text{H}^+ + \text{O}_2 \uparrow$ ) is performed by a  $\text{Mn}_4\text{O}_5\text{Ca}$  cluster located in photosystem (PS) II of all organisms performing oxygenic photosynthesis (for an X-ray crystallographic structure see [2]). CW/pulse EPR and  $^{55}\text{Mn}$  ENDOR experiments [3] are used to study the various paramagnetic “S” states of the enzymatic cycle. Together with theoretical approaches and additional experiments (e.g.  $\text{Ca}^{2+}/\text{Sr}^{2+}$  exchange [4]) a robust model for the geometric and electronic structure of the  $\text{Mn}_4\text{O}_5\text{Ca}$  cluster is obtained with important implications for the catalytic mechanism. Furthermore the binding of substrate water to the paramagnetic cluster is probed by  $\text{H}_2^{17}\text{O}$ .

[NiFe] and [FeFe] hydrogenases are the two main classes of this enzyme [5, 6]. They contain bridged binuclear transition metal cores in their active



sites, which are tuned by a special ligand environment (including CO, CN<sup>-</sup> ligands) to fulfill the task of efficient conversion of protons to hydrogen, or *vice versa*, via a heterolytic splitting mechanism. The intermediate states in the catalytic cycle are studied by various spectroscopic techniques (EPR/ENDOR, FTIR) combined with electrochemical and theoretical approaches (see e.g. [7]). The activation of the enzyme, the catalytic cycle and the inhibition, e.g. by molecular oxygen, have been investigated for both classes of enzymes. This led to proposals for the reaction mechanisms.

1. Lubitz W., Reijerse E.J., Messinger J.: *Energy Environ. Sci.* **1**, 15 (2008)
2. Umena Y., Kawakami K., Shen J.-R., Kamiya N.: *Nature* **473**, 55 (2011)
3. Kulik L., Epel B., Lubitz W., Messinger J.: *J. Am. Chem. Soc.* **129**, 13421 (2007)
4. Cox N., Rapatskiy L., Su J.H., Pantazis D.A., Sugiura M., Kulik L., Dorlet P., Rutherford A.W., Neese F., Boussac A., Lubitz W., Messinger J.: *J. Am. Chem. Soc.* **133**, 3635 (2011)
5. Fontecilla-Camps J.C., Volbeda A, Cavazza C., Nicolet Y.: *Chem. Rev.* **107**, 4273 (2007)
6. Lubitz W., Reijerse E.J., van Gestel M.: *Chem. Rev.* **107**, 4331 (2007)
7. Pandelia M.-E., Ogata H., Lubitz W.: *Chem. Phys. Chem.* **11**, 1127 (2010)

## Spin-Polarized Radical-Pair States in Photosynthesis: Characterization of Transient Conformational Changes by High-Field Dipolar EPR Spectroscopy

K. Möbius<sup>1,2</sup>, A. A. Dubinskii<sup>3</sup>, M. Flores<sup>4</sup>, W. Lubitz<sup>2</sup>, and A. Savitsky<sup>2</sup>

<sup>1</sup> Dept. of Physics, Free University Berlin, Berlin 14195, Germany,  
moebius@physik.fu-berlin.de

<sup>2</sup> MPI for Bioinorg. Chemistry, Mülheim 45470, Germany,  
savitsky / lubitz@mpi-muelheim.mpg.de

<sup>3</sup> Semenov Institute of Chemical Physics, Moscow 117977, Russian Federation,  
doubinsk@chph.ras.ru

<sup>4</sup> Dept. of Chemistry, Arizona State University, Tempe, AZ 85287, USA, mafloresr@asu.edu

To understand the primary, i.e., light-initiated steps of photosynthesis on the molecular level the spatial and electronic structures of the initial, intermediate and final cofactor states of the reaction center (RC) protein complex are of particular concern. Distance and relative orientation of functional groups within protein domains and their conformational changes during the reaction determine the efficiency of the light-driven electron-transfer (ET) process. The vectorial primary ET process from a dimeric bacteriochlorophyll donor (P) to a primary ubiquinone acceptor ( $Q_A$ ) has an extremely high quantum yield since subtle cofactor-protein interactions secure the charge-recombination ET reaction to be much slower than the charge-separation reaction. Such an essential “fine-tuning” of the electronic structure of the reactant states is achieved by transient intramolecular conformational changes and/or modifications of the weak intermolecular interactions between specific sites of the protein and its “solvent” matrix, e.g., hydrogen bonding. In a famous fast laser-spectroscopy experiment, Kleinfeld, Okamura and Feher (University of California, San Diego) observed significant differences in the ET charge-recombination kinetics of RCs from purple bacteria *Rb. sphaeroides*, when freezing them in the dark before light irradiation or freezing them under light irradiation [1]. Based on this observation, they suggested light-induced structural changes associated with the charge-separated state,  $P^+Q_A^-$ , probably at the binding site of  $Q_A$ , as an evolutionary means to secure high quantum efficiency of the first charge-separation ET step. By employing pulsed high-field EPR spectroscopy with its distinct advantages concerning orientational selectivity as well as spectral and temporal resolution, we have critically reexamined this suggestion by exploring the nature of the postulated conformational changes.

EPR at high magnetic fields/microwave frequencies, e.g., 3.3 T/95 GHz, and its extensions to 95 GHz ESE (electron spin echo), ENDOR (electron-nuclear double resonance) and PELDOR (pulsed electron-electron double resonance) are particularly powerful for in-depth studies of randomly oriented transient radical and radical-pair intermediates in frozen RC solutions by allowing for (i) 3D-structure determination of spin-polarized radical pairs and their potential light-induced conformational changes and for (ii) anisotropy resolution of  $T_2$  relaxation due to librational fluctuations of the cofactors in their binding sites.

We applied orientation resolving 95 GHz high-field EPR, ESE and PELDOR as well as 35 GHz ENDOR on RCs from *Rb. sphaeroides* at 90 K to explore the nature of the postulated structural changes. Happily, similar ET recombination kinetics data were measured as reported by Kleinfeld et al. [1], confirming that the “Kleinfeld effect” is of general nature. However, in contrast to the suggestion by Kleinfeld et al. [1], all our multi-frequency EPR experiments together with their ambitious data analysis consistently revealed that the distance and (relative) orientation of  $P^{+}$  and  $Q_A^{-}$ , do not change significantly under charge separation [2]. This is definitely in disagreement with the analysis of recent quantum-beat EPR experiments [3]. Besides solvation effects due to hydrogen bonding to residues of the RC protein, a substantial energetic contribution to stabilizing the primary charge-separated state may be expected from unbound or weakly hydrogen-bonded water molecules interacting with the quinone in the RC. The results will be discussed also in view of recent X-ray crystallographic data.

1. Kleinfeld D., Okamura M.Y., Feher G.: *Biochemistry* **23**, 57801 (1984)
2. Flores M., Savitsky A., Paddock M.L., Abresch E.C., Dubinskii A.A., Okamura M.Y., Lubitz W., Möbius K.: *J. Phys. Chem. B* **114**, 16894 (2010)
3. Heinen U., Utschig L.M., Poluektov O.G., Link G., Ohmes, E., Kothe G.: *J. Am. Chem. Soc.* **129**, 15935 (2007)

## Enhanced Sensitivity in EPR and NMR: New Experimental Developments and Biomolecular Applications

T. F. Prisner

*Institute of Physical and Theoretical Chemistry and Center of Biomolecular Magnetic Resonance, Goethe University Frankfurt, Germany*

Sensitivity is a major problem for the application of magnetic resonance methods to applications with low spin concentration or restricted sample size. EPR has in principle an increased sensitivity, compared to NMR, because of the at 660 times larger magnetic moment of the electron spin with respect to a proton spin, but is typically performed at lower magnetic fields. High-field pulsed EPR, ENDOR and PELDOR and DNP methods typically suffer from the low microwave excitation power available at high microwave frequencies [1]. Here we will show new approaches to improve the sensitivity at high magnetic fields by the application of new pulse schemes for EPR and the use of high power cw microwave gyrotrons for DNP [2] and discuss the potential of these methods for biomolecular applications *in-vitro* and *in-cell* [3].

1. Bennati M., Prisner T.F.: Reports on Progress in Physics, **68**, 411–448 (2005)
2. Denysenkov V., Prandolini M.J., Gafurov M., Sezer D., Endeward B., Prisner T.F.: Phys. Chem.Chem.Phys. **12**, 5786–5790 (2010)
3. Krstić I., Hänsel R., Romainczyk O., Engels J. W., Dötsch V., Prisner T.F.: Angewandte Chemie. Int. Ed. **50**, 5070–5074 (2011)

## Physics and Applications of Superconductor-Ferromagnet Phase Inverters in Superconducting Electronics and Spintronics

V. V. Ryazanov

*Institute of Solid State Physics, Russian Academy of Sciences, Chernogolovka 142432,  
Russian Federation, Ryazanov@issp.ac.ru*

The talk reviews recent fundamental and applied investigations of superconductor/ferromagnet structures carried out by Chernogolovka experimentalists in collaboration with different scientific groups. Nb/CuNi bilayers and Nb/CuNi/Nb Josephson sandwiches were investigated in detail to study different effects related to the superconducting order parameter spatial oscillations.

One of the exciting topics in studying the coexistence of superconductivity (S) and ferromagnetism (F) is the proximity-induced sign-reversal superconductivity in ferromagnets close to SF interfaces (see [1] as a review). The spatial variation of the superconducting order parameter in the ferromagnet arises as a response of the Cooper pair to the energy difference between the two electron spin directions. Due to the spatial oscillations of the superconducting pairing wavefunction, interference effects occur in SF layered structures similar to the optical case of light in a Fabry-Perot interferometer, yielding an oscillation of the critical temperature,  $T_c$ , with increasing thickness of the F layer [2, 3]. Another consequence of the sign-reversal superconductivity in ferromagnets close to SF interfaces is the  $\pi$ -state in Josephson SFS junctions [4]. Due to the spatial oscillations different signs of the order parameter can occur at the two banks of the Josephson SFS junction when the ferromagnetic layer thickness is of the order of half a period of the oscillations. The  $\pi$ -state corresponds to the inverse Josephson current-phase relation and a negative junction coupling energy. The  $\pi$ -junction presence results in the superconducting phase inversion [5, 6] and arising of spontaneous flux [7] in superconducting circuits. The Josephson phase inverters are considered as very promising elements for engineering superconducting circuits suitable for both the classical digital and quantum operation regimes [8].

Recently, the fabrication technology of the superconductor-ferromagnet-superconductor (SFS)  $\pi$ -junctions based on Nb/CuNi/Nb sandwiches has been substantially improved [9] and offered the basis for realization of integrated superconducting logic circuits including both conventional and  $\pi$ -type Nb-based Josephson junctions. The junctions are based on a classical niobium thin-film technology so they can be incorporated directly into existing architectures of

superconducting electronics. Successful integration of the SFS  $\pi$ -junction in the Toggle Flip-Flop (TFF) circuit was presented in ref. [10]. The SFS junction was used as a phase shifting element inserted in the storage loop of the TFF. A quantum Josephson circuit, a  $\pi$ -biased phase qubit, was also realized [8]. Coherent qubit operation (Rabi oscillation of the excited qubit state population probability) was demonstrated. We find no degradation of the measured coherence time compared to that of a reference qubit without a  $\pi$ -junction.

The work was supported by Russian Foundation for Basic Research.

1. Buzdin A.I.: *Rev. Mod. Phys.* **77**, 935 (2005)
2. Рязанов В.В., Обоэнов В.А., Прокофьев А.С., Дубонос С.В.: *Письма в ЖЭТФ* **77**, 43 (2003)
3. Zdravkov V.I., Kehrlé J., Obermeier G, Ullrich A., Gsell S., Lenk D., Müller C., Morari R, Sidorenko A.S., Ryazanov V.V., Tagirov L.R., Tidecks R., Horn S. *Superconductor Science and Technology* **24**, 095004 (2011)
4. Ryazanov V.V., Oboznov V.A., Rusanov A.Yu., Veretennikov A.V., Golubov A.A., Aarts J.: *Phys. Rev. Lett.* **86**, 2427 (2001)
5. Ryazanov V.V., Oboznov V.A., Veretennikov A.V., Rusanov A.Yu.: *Phys. Rev. B* **65**, 020501(R) (2002)
6. Frolov S.M., Van Harlingen D.J., Oboznov V.A., Bolginov V.V., Ryazanov V.V.: *Phys. Rev B* **70**, 144505 (2004)
7. Frolov S.M., Stoutimore M.J.A., Crane T.A., Van Harlingen D.J., Oboznov V.A., Ryazanov V.V., Ruosi A., Granata C., Russo M.: *Nature Physics* **4**, 32 (2008)
8. Feofanov A.K., Oboznov V.A., Bol'ginov V.V., Lisenfeld J., Poletto S., Ryazanov V.V., Ros-solenko A.N., Khabipov M., Balashov D., Zorin A.B., Dmitriev P.N., Koshelets V.P., Ustinov A.V.: *Nature Physics* **6**, 593 (2010)
9. Oboznov V.A., Bol'ginov V.V., Feofanov A. K., Ryazanov V.V., Buzdin A.I.: *Phys. Rev. Lett.* **96**, 197003 (2006)
10. Khabipov M.I., Balashov D.V., Maibaum F., Zorin A.B., Oboznov V.A., Bolginov V.V., Ros-solenko A.N., Ryazanov V.V.: *Superconductor Science and Technology* **23**, 045032 (2010)

## Spin Valves with Giant Magnetoresistance

V. V. Ustinov and M. A. Milyaev

*Institute of Metal Physics UB RAS, Ekaterinburg 620990, Russian Federation,  
milyaev@imp.uran.ru*

Spintronics is a new trend in microelectronics which exploits an electron spin along with its charge in order to provide new functionality of electronic devices. Recent advances in spintronics are related to a discovery of giant magnetoresistance (GMR) and tunnel magnetoresistance (TMR) effects observed in magnetic multilayers. One of extensively investigated and widely used spintronic devices are “spin valve” type nanostructures with GMR and TMR effects [1]. Spin valves have some advantages in their physical properties in comparison to magnetic multilayers. Metallic spin valves exhibit magnetoresistance ratio of tens percents in switching magnetic fields of several Oersteds, and their magnetoresistive sensitivity can be at least by one order of magnitude higher than in magnetic multilayers. In optimized TMR nanostructures the magnetoresistance ratio can achieve the value of up to one thousand percents [2]. Besides high sensitivity, a thermal stability and low field hysteresis are important characteristics for various applications as well. Spin valves with some hysteresis caused by a “free layer” magnetization reversal is typically used in digital devices – hard disc recording heads, magnetic memory (MRAM) and many others. For precise magnetic field measurements (magnetic field sensors, current sensors, angular dependent resistance measurements) one must have a magnetic field dependence of magnetoresistance with a very low or negligible hysteresis. In this case modifications of preparation methods and magnetoresistance measurements are used to reduce the spin valve hysteresis.

The comparison of magnetoresistive properties of GMR magnetic multilayers and different types of spin valves is given. Special attention is paid to experimental methods aimed to decrease the low field hysteresis of spin valves with FeMn and MnIr antiferromagnetic layers.

The work is supported by RFBR, project No. 10-02-00590, by the Program of Presidium RAS, project No. 09-P-2-1037, and OFI-UB RAS, project No. 11-2-23-NPO.

1. Tumanski S.: Thin Film Magnetoresistive Sensors, p. 229. IOP Publishing Ltd, 2001.
2. Jiang L., Naganuma H., Oogane M., Ando Y.: Appl. Phys. Express. **2**, no. 8, 083002 (2009)

## Spin as an Itinerant Carrier of Information

A. V. Vedyayev<sup>1,2</sup>, N. V. Strelkov<sup>1,2</sup>, N. V. Ryzhanova<sup>1,2</sup>, M. Chshiev<sup>2</sup>,  
and B. Dieny<sup>2</sup>

<sup>1</sup>Lomonosov Moscow State University, Moscow 119992, Russian Federation, vedy@magm.ru

<sup>2</sup>SPINTEC, UMR 8191 CEA-INAC/CNRS/ UJF-Grenoble 1, Grenoble 38054, France

Since the discovery of Giant Magnetoresistance (GMR), invention of Spin Valve structures and creation of the first prototype of MRAM the idea that spin gives an additional to charge degree of freedom for storage and transmission of information became very popular. Later a lot of attention attracted so called Spin Hall Effect (SHE) [1–4] which exists in paramagnetic metals due to spin-orbit interaction. All these phenomena became the foundation for new field of science – SPINTRONICS.

We will discuss some features of tunnel magnetoresistance in magnetic three layer and SHE in hybrid paramagnetic layer/ferromagnetic dot. First of all we will discuss the voltage dependence of spin torque and will show that field-like term of it may be written as  $T^{\text{field}} = \alpha_0 + \alpha_1 V + \alpha_2 V^2$  and real spin torque as  $T^{\text{S}} = \beta_1 V + \beta_2 V^2$ , where  $V$  is voltage and all the coefficients depend on the parameters of electronic structure of ferromagnetic electrodes and insulating barrier. It's important to notice that the coefficient  $\alpha_1 = 0$  for the case of identical ferromagnetic electrodes.

As well we will discuss the possibility of manipulation with magnetization of small ferromagnetic metal dots situated on the surface of the thin paramagnetic metal layer with large value of SHE conductivity.

To find spin accumulation we wrote expressions for charge and spin currents as follows:

$$\mathbf{j}_e = -\sigma_0 \text{grad } \varphi - \beta \frac{\sigma_0}{e\nu} \text{grad}(\mathbf{U}_M \mathbf{m}) + \sigma_H a_0^3 [\mathbf{m} \text{grad } \varphi], \quad (1)$$

$$\mathbf{j}_m = -\beta \sigma_0 \text{grad } \varphi \mathbf{U}_m - \frac{\sigma_0}{e\nu} \text{grad } m - \sigma_{\text{SH}} \mathbf{U}_m [\mathbf{U}_m \text{grad } \varphi], \quad (2)$$

where  $\sigma_0$  is the conductivity,  $\beta$  is the spin-asymmetry parameter of conductivity,  $\sigma_H$  – anomalous Hall conductivity in ferromagnetic metal,  $\sigma_{\text{SH}}$  is the spin Hall conductivity,  $\mathbf{U}_M = \mathbf{M}/M$ ,  $\mathbf{M}$  is magnetization vector in ferromagnetic,  $\mathbf{U}_m = \mathbf{m}/|m|$ ,  $\mathbf{m}$  is spin accumulation vector and  $\nu$  is density of states. Writing down the equation for divergence of these currents and solving them we have

found the coordinate dependence of spin accumulation and potential  $\phi$  for the case of  $\mathbf{M}$  parallel to  $y$  axis and current parallel to  $x$  axe:

$$m_1 = -\frac{Vev}{den} \frac{\sigma_H}{\sigma_1} \frac{l_{sf1}}{L_x} \left[ \text{sh} \frac{L_1}{2l_{sf1}} \text{sh} \frac{L_1 + 2z}{2l_{sf1}} + \frac{\sigma_2}{\sigma_1} \frac{l_{sf1}}{l_{sf2}} (1 - \beta^2) \text{th} \frac{L_2}{l_{sf2}} \text{sh} \frac{z}{l_{sf2}} \right];$$

$$m_2 = -\frac{Vev}{den} \frac{\sigma_H}{\sigma_1} \frac{l_{sf1}}{L_x} \text{ch} \frac{L_2 - z}{l_{sf2}} \text{sh}^2 \frac{L_1}{2l_{sf1}} / \text{ch} \frac{L_2}{l_{sf2}},$$

$$\phi_1 = \frac{V}{2} \left( 1 + \frac{x}{L_x} \right) - \frac{(Vev)^2}{2den} \left( \frac{\sigma_H}{\sigma_1} \frac{l_{sf1}}{L_x} \right)^2 \times \text{sh}^2 \frac{L_1}{2l_{sf1}} \left\{ 2 \text{sh} \frac{L_1}{2l_{sf1}} \text{ch} \frac{L_1 + 2z}{2l_{sf1}} + \frac{\sigma_2}{\sigma_1} \frac{l_{sf1}}{l_{sf2}} \text{th} \frac{L_2}{l_{sf2}} \frac{\text{ch} \frac{z}{l_{sf2}} - \text{ch} \frac{L_x}{l_{sf1}}}{1 - \text{ch} \frac{L_x}{l_{sf1}}} \right\},$$

$$\phi_2 = \frac{V}{2} \left( 1 + \frac{x}{L_x} \right) - \frac{(Vev)^2}{2den} \left( \frac{\sigma_H}{\sigma_1} \frac{l_{sf1}}{L_x} \right)^2 \text{sh}^2 \frac{L_1}{2l_{sf1}} \left\{ \text{sh} \frac{L_1}{l_{sf1}} + \frac{\sigma_2}{\sigma_1} \frac{l_{sf1}}{l_{sf2}} \text{th} \frac{L_2}{l_{sf2}} \right\} - \text{sign} M_1 \frac{V}{den} \beta \frac{\sigma_H}{\sigma_1} \frac{l_{sf1}}{L_x} \frac{\text{ch} \frac{L_2}{l_{sf2}} - \text{ch} \frac{L_2 - z}{l_{sf2}}}{\text{ch} \frac{L_2}{l_{sf2}}},$$

$$den \equiv \left[ \text{sh} \frac{L_1}{l_{sf1}} + \frac{\sigma_2}{\sigma_1} \frac{l_{sf1}}{l_{sf2}} (1 - \beta^2) \text{th} \frac{L_2}{l_{sf2}} \text{ch} \frac{L_1}{l_{sf1}} \right].$$

For the different orientations of magnetization the corresponding equations were solved numerically. As a result we found that torque created by spin accumulation due to influence of SHE has component similar to damping or antidumping spin torque in non-collinear magnetic multilayers.

1. Dyakonov M.I., Perel V.I.: JETF Lett. **13**, 467–469 (1971)
2. Hirsh J.E.: Phys. Rev. Lett. **83**, 1834 (1999)
3. Zhang S.: Phys. Rev. Lett. **85**, 393 (2000)
4. Fert A., Levy P.: Phys. Rev. Lett. **106**, 157208 (2011)

## Time-Resolved EPR in the Electronically Excited States

*S. Yamauchi*

*Institute of Multidisciplinary Research for Advanced Materials, Tohoku University,  
Sendai 980-8577, Japan, yamauchi@tagen.tohokuac.jp*

Electronically excited states of organic and metal complexes have been investigated by means of various time-domain EPR techniques, which include ODMR, time-resolved EPR (TR-EPR), TR-ENDOR, Fourier transform EPR (FT-EPR), 2D-nutation EPR, and high frequency high field EPR (HF-EPR). Studied states involve the excited triplet ( $T_1$ ) states and the excited high spin (doublet, triplet, quartet, and quintet) states, which are generated from interactions of  $T_1$  with the stable radical(s) [1].

The subjects of our research by TR-EPR started from non-phosphorescent organic molecules such as ortho-diazaaromatics and conjugated enones. As these molecules are distorted in the  $T_1$  states, I became interested in several distorted molecules which include acetone, benzil, and recently the Möbius molecule. I also found that the distorted molecules sometimes involve intramolecular charge transfer (TICT) states; we have two attractive such examples of nitrogen bridged fullerene-aromatic ring (benzene, naphthalene, and pyrene) systems and boron-anthracenes.

Dimers are also very stimulating groups partially because the special pair (dimer) is very important in the photosynthesis system. We have studied various dimers, aromatic ring-bridged porphyrin dimers, crowned or rare-earth metal bridged porphyrin and phthalocyanine dimers, carbazole dimers, and fullerene dimers. In some cases excitation electrons are delocalized over the two units and the other localized at one side.

Recently we have become very interested in metal complexes because of their complexity and functionality. We started various TR-EPR studies and have just published several papers [2, 3] in corporation with researchers of coordination chemistry. Although many excited states are relevant, anisotropic EPR parameters are so helpful as to analyze the interactions.

1. Yamauchi S.: Bull. Chem. Soc. Jpn. **77**, 1255 (2004)
2. Yamauchi S., Takahashi K., Ohba Y., Tarasov V.: J. Phys. Chem. B **114**, 14559 (2010)
3. Yamauchi S., Tanabe M., Takahashi K., Saiful I., Matsuoka H., Ohba Y.: Appl. Magn. Reson. **37**, 317 (2010)

## Molecular Dynamics in Proteins and Membranes by Multi-Frequency ESR

*J. H. Freed*

*Department of Chemistry and Chemical Biology and National Biomedical Center for Advanced ESR Technology (ACERT), Cornell University, Ithaca, NY 14853, USA jhf3@cornell.edu*

ESR studies of protein dynamics are less familiar than related NMR studies. The virtues of ESR include: It is more sensitive per spin. In time domain experiments, ESR's time-scale is nanoseconds, (NMR's is milliseconds). The spin-label spectrum is simple and can focus on a limited number of spins. ESR spectra change dramatically as the tumbling motion slows, thereby providing great sensitivity to local "fluidity"; in NMR nearly complete averaging occurs, so only residual rotational effects are observed by  $T_1$  and  $T_2$ . Multi-frequency (MF)-ESR permits one to take "fast-snapshots" with very high-frequencies and "slow-snapshots" using lower frequencies. For example, high frequency spectra "freeze out" the overall tumbling of proteins and are more sensitive to the faster internal modes. Also, the high-frequency ESR spectra provide orientational resolution of the dynamics [1]. Our MF-ESR studies at ACERT on spin-labeled mutants of T4 Lysozyme have shown this enhanced ability to discriminate the complex modes of protein dynamics. The ESR spectral line shapes are analyzed by a sophisticated theory, based on the stochastic Liouville equation (SLE). The "Slowly Relaxing Local Structure" (SRLS) model allows one to simultaneously fit the faster internal modes of motion and the slower overall tumbling modes. It has led to a systematic picture of the dynamics [2]. This approach is a mesoscopic one, so it is desirable to enhance it by comparison with the more atomistic viewpoint from Molecular Dynamics (MD). The prediction of ESR spectra by MD posed several challenges. They included: exact time-domain integrators for the quantal dynamics of the spins and for the classical motions of the protein; force field parameters for the nitroxide side chain; a procedure for estimating a Markov chain model from the MD trajectories, given the longer time scales needed. The successful solutions to these matters will be described, and their implications discussed [3].

1. Dzikovski B., Tipikin D., Livshits V., Earle K., Freed J.H.: *Phys. Chem. Chem. Phys.* **11**, 6676–6688 (2009)
2. Zhang Z., Fleissner M., Tipikin D., Liang Z., Moscicki J.K., Earle K.A., Hubbell W., Freed J.H.: *J. Phys. Chem. B* **114**, 5503–5521 (2010)
3. Sezer D., Freed J.H., Roux B.: *J. Am. Chem. Soc.* **131**, 2597–2605 (2009)

---

## INVITED TALKS

## Magnetic Properties of Exchange-Coupled Py/Cr/Py Films

*B. Aktas<sup>1</sup>, R. Topkaya<sup>1</sup>, M. Erkovan<sup>1</sup>, and M. Özdemir<sup>1</sup>*

<sup>1</sup> *Gebze Institute of Technology, Gebze-Kocaeli 41400, Turkey*

<sup>2</sup> *Marmara University, Göztepe / Istanbul 81040, Turkey*

Recently so-called spin electronics (or spintronics) have increasing attractions due to its possible applications in new generations of technological devices in different areas. Of these the Giant Magneto-Resistance (GMR) in the magnetic-nonmagnetic multi-layers have already found applications especially as magnetic sensors of the reading heads of computer hard discs and magnetic cards. For the applications, the most important magnetic properties in these types of structures are the saturation magnetization, magnetic anisotropy, exchange coupling parameters and the dynamic behavior of the magnetization. The physical size of the elements of the multilayered structure has to be reduced to even nanometer scale in ultra high density magnetic recording technology. However as the dimensions (thickness) of the films decrease the magnetic signal intensity weakens so much that its detection becomes one of the major issues. But still ferromagnetic resonance (FMR) can be powerful enough to study these multilayered magnetic structures.

In this work, we presents a theoretical model for analyzing FMR data and extracting relevant magnetic parameters. We have chosen NiFe (permalloy, Py) films as a model FMR system. The Py/Cr/Py multilayers with various Cr thicknesses were grown on Si substrate by conventional dc/rf-magnetron sputtering technique. We have used an X-band ESR spectrometer to record the FMR data at different temperatures. The experimental FMR data were taken at different orientations of the dc magnetic field with respect to the sample plane. The dc magnetization measurements are carried out as a function of temperature by using Quantum Design PPMS system.

We have observed two well-resolved, symmetrical and strong FMR peaks when the direction of the external dc field is close to the film normal. As the field is rotated from the film normal the minor peak weakens and almost completely disappeared when the field lies in film plane. The spectra deeply depend on the thickness of Cr layer as well. The relative positions of the strong and the weak modes are interchanged for particular thickness of Cr layer. We have applied the developed model and successfully simulated the experimental data. Thus we have deduced all relevant magnetic parameters. We observed the significant perpendicular anisotropy in very thin films. The relative phase and amplitudes of dynamic (excited by microwave) magnetization of individual layers have been calculated.

## Electron Magnetic Resonance and Conductivity around the Curie Point

*V. A. Atsarkin and V. V. Demidov*

*Kotel'nikov Institute of Radio Engineering and Electronics, Russian Academy of Sciences,  
Moscow 12509, Russian Federation, atsarkin@mail.cplire.ru*

Transformation from ferro- to paramagnetism occurring around the Curie point ( $T_C$ ) can be revealed as the corresponding change in the master equation which evolves from the Landau-Lifshits to Bloch type [1]. As a consequence, the saturation of the electron magnetic resonance (EMR) should lead to decreasing of the magnetization magnitude  $|\mathbf{M}|$  even in the ferromagnetic phase (below  $T_C$ ). In conducting ferromagnets exhibiting the colossal magnetoresistance effect (CMR), such as the doped rare-earth manganites, this decrease in  $|\mathbf{M}|$  should result in increasing of the electrical resistivity. This can be viewed as the electrically detected EMR and a way to transfer electron-spin properties to the charge ones.

An increment in electrical resistivity associated with the resonant microwave pumping under the EMR conditions has been detected experimentally [2] in the  $\text{La}_{0.67}\text{Sr}_{0.33}\text{MnO}_3$  thin films in the temperature range of 300–370 K, both in the ferro- and paramagnetic phases. To compare the observed effect with the model predictions, the quantitative estimations were performed using independent measurements of the CMR effect and magnetization. Theoretical calculations based on the combined Landau-Lifshits-Bloch equations [1] agree well with the experimental data, including the absolute values of the effect and its temperature dependence.

The results of this study can be considered as a further argument for the “paramagnetic-like” (quantum) description of ferromagnetic resonance in intermediate situations, such as superparamagnetic nanoparticles [3] and the vicinity of magnetic transition [1, 2].

The work was supported by Russian Foundation for Basic Research (Grant 11-02-00349-a) and International Science and Technology Center (Project 3743).

1. Garanin D.A.: Phys. Rev. B **55**, 3050 (1997)
2. Atsarkin V.A., Demidov V.V., Levkin L.V., Petrzhik A.M.: Phys. Rev. B **82**, 144414 (2010)
3. Noginova N., Chen F., Weaver T., Giannelis E.P., Bourlinos A.B., Atsarkin V.A.: J. Phys.: Condens. Matter **19**, 246208 (2007)

## Thermal and Optical Switching of the Exchange Interactions in Nitroxide-Copper(II)-Nitroxide Clusters

*E. Bagryanskaya*<sup>1</sup>, *M. Fedin*<sup>1</sup>, *S. Veber*<sup>1</sup>, *V. Ovcharenko*<sup>1</sup>, *H. Mazuoka*<sup>2</sup>,  
and *S. Yamauchi*<sup>2</sup>

<sup>1</sup> *International Tomography Center SB RAS, Novosibirsk 630090, Russian Federation, elena@tomo.nsc.ru*

<sup>2</sup> *Institute of Multidisciplinary Research for Advanced Materials, Tohoku University, Sendai, Japan, yamauchi@tagen.tohoku.ac.jp*

The light-induced spin state conversion and light-induced excited spin state trapping (LIESST) are well known for spin-crossover complexes of iron(II) as promising effects for potential applications in light-operated magnetic nanodevices. Recently we have found LIESST-like effects to occur in family of polymer-chain complexes  $\text{Cu}(\text{hfac})_2\text{L}^{\text{R}}$  as well [1]. These compounds represent an interesting type of molecular magnets exhibiting thermally magnetic switching [2]. During rearrangements the exchange interaction in nitroxide-copper(II)-nitroxide clusters changes by 1-2 orders of magnitude. This results in a change of the magnetic moment, since at high temperatures the spins are weakly coupled referred to as weakly-coupled spin state (WS), whereas at low temperatures strong antiferromagnetic exchange effectively couples two of the three spins and thus the spin triad converts to the strongly-coupled spin state (SS). We have found recently that EPR study of molecular magnets  $\text{Cu}(\text{hfac})_2\text{LR}$  allow to monitor the spin transitions between WS and SS states and to measure the exchange interactions [3].

In this report we discuss the general trends, characteristics and mechanism of light-induced spin state switching and following relaxation to the ground state using several polymer-chain complexes  $\text{Cu}(\text{hfac})_2\text{LR}$  studied by steady state X and Q-band and time-resolved W-band EPR. It was found that after the photoswitching to WS state, the spin triad relaxes back to the SS state on a time scale of hours at low temperature (5–12 K). The observed kinetics had self decelerating character and can be described by exponent with time dependent decay parameter. The obtained kinetics was simulated using theoretical models based on proposal that light effect is determined by the changes in internal pressure of crystal.

We performed Time-Resolved EPR study at W-band for the  $\text{Cu}(\text{hfac})_2\text{L}^{\text{Pr}}$ /glycerol mixture in the temperature range 5–30 K. It is known that TR EPR in most cases can be detected on spin-polarized radical intermediates only. A

heating for a few degrees leads to an appearance of intensive TR EPR signal due to quite strong Boltzmann polarization for the sample with high magnetic concentration. At 5–12 K, the increase of the temperature leads to a decrease of the EPR signal according to the factor  $gH/kT$ . The observed TR EPR spectrum contains the lines of both one- and three-spin units, while spin transition occurs in three spin units only. Thus the kinetics detected on the isolated copper (one spin units) reflects temperature changes of the sample and was used as a reference. The kinetics of WS decay and SS rise were obtained and found to be exponential with the same parameter of exponent  $1/k_{\text{obs}}$ . The possible mechanisms of relaxation are under discussion.

This work was supported by the Russian Foundation for Basic Research (№11-03-00158), the Council at the RF president (MK-4268.2010.3), Russian Scientific School-7643.2010.3, Division of Chemistry and Material Science (5.1.1).

1. Fedin M. *et al.*: *Angew. Chem. Ed.* **47**, 6897 (2008)
2. Fedin M. *et al.*: *J. Phys. Chem. A* **111**, 4449 (2007)
3. Fedin M. *et al.*: *Inorg. Chem.* **46**, 11405 (2007)
4. Fedin M. *et al.*: *J. Amer. Chem. Soc.* **132**, 13886–13891 (2010)
5. Fedin M. *et al.*: *Phys. Chem. Chem. Phys.* **11**, 6654–6663 (2009)
6. Veber S. *et al.*: *J. Amer. Chem. Soc.* **130**, 2444 (2008)

## Pulse Electron Spin Resonance Investigation of Bismuth-Doped Silicon

*M. Belli<sup>1</sup>, M. Fanciulli<sup>1,2</sup>, and N. V. Abrosimov<sup>3</sup>*

<sup>1</sup>Laboratorio MDM, IMM-CNR, Agrate Brianza I-20864, Italy,

<sup>2</sup>Università di Milano-Bicocca, Milano I-20126, Italy, [Marco.Fanciulli@unimib.it](mailto:Marco.Fanciulli@unimib.it)

<sup>3</sup>Institute for Crystal Growth, Berlin D-12489, Germany

The development of quantum-devices based on the single charge/spin manipulation and detection suitable for the implementation of quantum bits and quantum logic gates requires systems displaying long relaxation times, possibly at room temperature. The present work reports on a pulse-EPR study of spin-spin and spin-lattice relaxation times, and ESEEM spectroscopy on bismuth donors in silicon. [1]

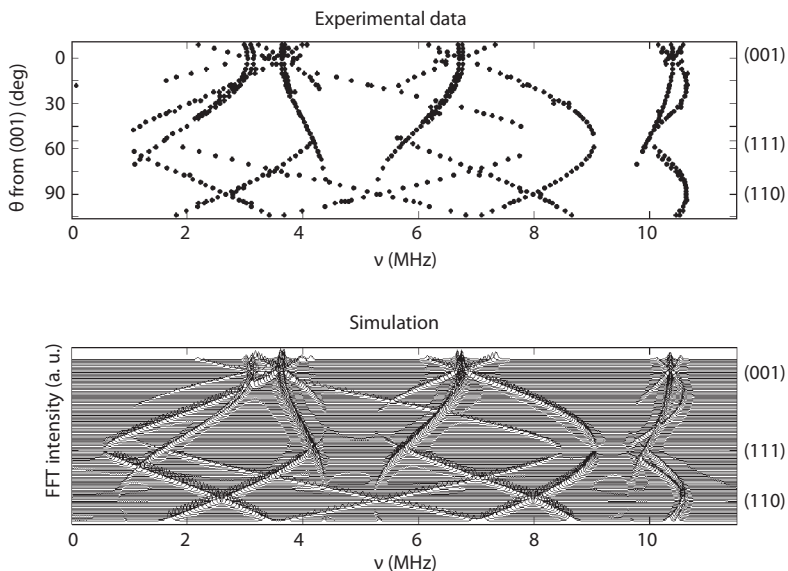


**Fig. 1.** Peak frequencies in modulus of the two-pulse ESEEM spectra recorded at 12 K at different orientations for a sample of Si:Bi with  $\text{Bi} = 4.0 \cdot 10^{15} \text{ cm}^{-3}$ , along with the corresponding Easyspin simulation 4.

The choice of silicon is based not only on the technological advantages delivered by decades of continuous industrial progress in micro/nanoelectronics, but also on specific physical properties such as low spin-orbit interaction, relatively low natural abundance of nuclei with spin. Bismuth presents several advantages on standard technological donors such as P and As [2]: it is deeper, hence its relaxation times are expected to be longer; it is characterized by a large spin ( $I = 9/2$ ), which yields a large Hilbert space; it displays also a zero-field splitting in the GHz range, opening the possibility for fast zero-magnetic field operation. The system was studied in the bulk form [3], which represents a starting point for further investigation on low-dimensional nanostructures. We infer the high localization of the electron wavefunction from shell E superhyperfine parameters (measured by the angular variation of ESEEM spectra, Fig. 1) and shell E relative contribution to the lineshape. However, despite the comparable or longer relaxation times in the Si:Bi system than e.g. Si:P, we find evidence that silicon optical phonons matching the  $1s(A_1) - 2p_0$  energy separation dominate Orbach spin-lattice relaxation at relatively high temperatures, reducing other advantages introduced by the Si:Bi system. We conclude that the Si:Bi system is a good candidate system for spin-operation in nanostructured devices, though even deeper donors may yield longer spin-spin and spin-lattice relaxation times.

The financial support of the CARIPLO Foundation in the framework of the ELIOS national project is gratefully acknowledged.

1. Belli M., Fanciulli M., Abrosimov N.V.: Phys. Rev. B **83**, 235204 (2011)
2. Ferretti A., Fanciulli M., Ponti A., Schweiger A.: Phys. Rev. B **72**, 235201 (2005)
3. Riemann H., Abrosimov N.V., Noetzel N.: ECS Transactions **3**, 53 (2006)
4. Stoll S., Britt R.D.: Phys. Chem. Chem. Phys. **11**, 6614 (2009)

## Dipolar Interactions for the Determination of Macromolecular Structure

*M. K. Bowman<sup>1</sup>, P. R. Vennam<sup>1</sup>, M. Krzyaniak<sup>1</sup>, and A. G. Maryasov<sup>2</sup>*

*<sup>1</sup>Department of Chemistry, The University of Alabama, Tuscaloosa, Alabama 35487, USA, mkbowman@as.ua.edu*

*<sup>2</sup>Institute of Chemical Kinetics and Combustion, Novosibirsk 630090, Russian Federation, maryasov@ns.kinetics.nsc.ru*

Anisotropic dipolar interactions between spins are an important source of detailed structural information about macromolecules even, for example, in non-crystalline forms such as frozen solutions, glasses and on surfaces. Measurement of dipolar interactions by DEER or PELDOR between nitroxide spin labels attached to proteins or nucleic acids to determine interspin distances which reveal structure of the macromolecules and transitions between different conformations. Dipolar interactions can be measured between a paramagnetic metal center and a free radical or another metal center although large  $g$ -factor anisotropy can introduce several novel features. 1) Strong orientation selection can greatly reduce the intensity of the DEER or PELDOR signal but this can be overcome by using spin-lattice relaxation to modulate the dipolar interaction rather than applied microwave pulses. 2) Large  $g$ -factor anisotropy modifies the simple dipolar interaction between isotropic species and the shape of the spectrum of dipolar splittings. An example of determining the distance between a quinone free radical and a heme using dipole induced phase memory relaxation will be presented.

Dipolar interactions of an electron spin with nuclear spins reveals the distance between them and the spatial direction to the nucleus. ESEEM spectra, and particularly HYSCORE, allow separation of isotropic hyperfine from anisotropic dipolar interactions. Recent advances in HYSCORE spectral resolution will be described with illustrations showing conformational changes resulting from mutations in proteins and illustrations of different modes of binding of ligands and inhibitors within the active sites of enzymes.

This work was supported by the National Institutes of Health: GM61409 and HL95820.

## Nitronyl Nitroxides as Spin Probes?

*M. Brustolon, A. Collauto, and A. Barbon*

*Department of Chemical Sciences, University of Padova, Padova 35131, Italy*

Nitronyl nitroxides are well known stable radicals with interesting properties as their nature of bidentate ligands and a strong  $\pi$  spin polarization, making them suitable as building blocks in designing magnetic materials. Many examples of materials containing these radicals are reported in literature, for example a molecular crystal of a nitronyl nitroxide was the first example of an organic ferromagnet [1]. These radicals could have also a potential use as spin probes, in particular for their long spin relaxation times. However, they are much less popular than nitroxide radicals for their more complex ESR spectra. A recently implemented method to calculate the CW-ESR spectral profiles, the *ab initio* Integrated Computational Approach (ICA) [2] have shown the possibility of extracting dynamical and structural information from their spectra [3, 4].

In this communication I will present an extended characterization by cw and pulsed ESR on phenylnitronyl nitroxide monoradicals in isotropic and nematic solutions and in solid composite phases. The excellent agreement between calculated and experimental spectra in different dynamical regimes, and the long relaxation times will show that the use of nitronyl nitroxide radicals as spin probes might be considered feasible and extremely interesting in the future.

1. Tamura M., Nakazawa Y., Shiomi D., Nozawa K., Hosokashi Y., Ishikawa M., Takahashi M., Kinoshita M.: *Chem. Phys. Lett.* **186**, 401 (1991)
2. Barone V., Polimeno A.: *Phys. Chem. Chem. Phys.* **8**, 4609 (2006)
3. Barone V., Brustolon M., Cimino P., Polimeno A., Zerbetto M., Zoleo A.: *J. Am. Chem. Soc.* **128**, 15865 (2006)
4. Collauto A., Zerbetto M., Brustolon M., Polimeno A., Gatteschi D., Sorace L., to be published.

## Fabrication of Magnetic Nanostructures for the Investigation of Spin-Dependent Transport Phenomena

*A. Bukharaev<sup>1,2</sup>, N. Nurgazizov<sup>1</sup>, D. Biziaev<sup>1</sup>, D. Lebedev<sup>1</sup>, A. Chuklanov<sup>1</sup>, I. Shakirov<sup>2</sup>, and T. Khanipov<sup>2</sup>*

<sup>1</sup>*Zavoisky Physical-Technical Institute, Russian Academy of Sciences, Kazan 420029, Russian Federation, a\_bukharaev@kfti.knc.ru*

<sup>2</sup>*Kazan Federal University, Kazan 420008, Russian Federation*

The magnetization switching of nanostructures by the spin-polarized (SP) current is of great interest from the theoretical and applied points of view. The individual nanoparticle is expected to change the magnetization orientation under the injection of the SP current through the point contact. Two types of the structures consisting of different metals of the transition group may be used for the investigation of spin-dependent transport phenomena.

In the first type of the structures the magnetic nanoparticle acting as conducting bridge are placed in the nanogap between two thin contact ferromagnetic pads formed on the dielectric substrate. In this work the nanogap in the magnetic nanowires was obtained using the electromigration technique. The single ferromagnetic Co or Ni nanowires connecting two contact pads on the silicon oxide surface were fabricated using the scanning probe nanolithography technique based on the nanoscratching of PMMA and lift-off process. The change in magnetic structure of nanowires after the nanogap formation was visualized by magnetic force microscopy.

The second type of the structures for the investigation of spin-dependent transport phenomena are the ferromagnetic nanoparticles separately placed on the conductive substrate. In this case the injection of the electrons to the nanoparticle is implemented through the point contact between the particle and the conductive magnetic probe of the atomic force microscope (AFM) or magnetic tip of the scanning tunneling microscope (STM). In this work the Co particles with the dimensions from 5 to 50 nm separately placed on the HOPG substrate were fabricated in the ultrahigh vacuum preparation chamber of the Omicron Multiprobe P setup. The conductive AFM with the magnetic coating or STM magnetic tips were homebuilt in the Multiprobe P setup and then were used for the subsequent measurements of the current-voltage characteristics of the tip-nanoparticle-substrate structures without contact with air.

This work was supported partly by the Russian Foundation of Basic Research (project 09-02-00568) and by the Programs of RAS.

## Structure and Magnetotransport Properties of Deposited from Laser Plasma Nanosized Layers of the High-Temperature Diluted Magnetic Semiconductor Si:Mn

*E. S. Demidov<sup>1</sup>, E. D. Pavlova<sup>1</sup>, A. I. Bobrov<sup>1</sup>, V. V. Podolskii<sup>1</sup>, V. P. Lesnikov<sup>1</sup>,  
M. V. Sapozhnikov<sup>2</sup>, B. A. Gribkov<sup>2</sup>, S. N. Gusev<sup>1</sup>, S. A. Levchuk<sup>1</sup>,  
and V. V. Karzanov<sup>1</sup>*

<sup>1</sup> *Nizhni Novgorod State University, Nizhni Novgorod 603950, Russian Federation,  
author@phys.phys.com*

<sup>2</sup> *Institute for Physics of Microstructures, RAS, Nizhni Novgorod 603950, Russian Federation*

Coexistence of magnetism and semiconducting properties in diluted magnetic semiconductors (DMS) increases functionalities of spin-electronics [1, 2]. The most high-temperature DMSs based both on III–V compounds or Ge and Si semiconductors were synthesized by deposition from the laser-plasma onto single crystal substrates. Previous our publications papers [3] demonstrated a possibility to use such method for synthesis of thin (30–200 nm) GaSb:Mn and InSb:Mn layers with the Curie temperature,  $T_c$ , above 500 K and Ge:Mn, Si:Mn, Si:Fe layers with  $T_c$  up to 400, 500, 250 K, respectively, on GaAs, Si and sapphire ( $\text{Al}_2\text{O}_3$ ) substrates. Ultra-fast crystallization and quenching inherent in laser technology are responsible for the supersaturating of solid solution with a 3d-impurity. DMSs based on elementary Si semiconductor doped with 3d-impurities are of particular interest for spintronics due to their compatibility with wide-spread silicon integrated technology. It is important to notice, that according to the data [4], among all the binary silicides prepared by the usual

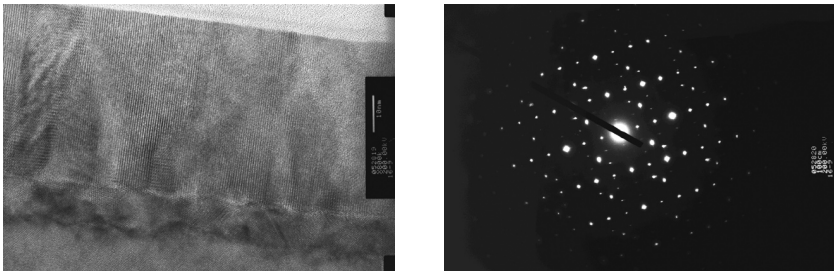


**Fig. 1.** Cross-sectional high-resolution transmission electron microscopy lattice image of Si:Mn layer along the  $\langle 100 \rangle$  direction of the GaAs substrate (left) and the selected area electron diffraction pattern Si:Mn layer (right).

technology of the growth of bulk single crystals from a melt under almost equilibrium conditions, only iron and silicon form alloys with spin ferromagnetic ordering above room temperature. This report represents results of structural research of magnetic Si:Mn layers with 10–15% Mn grown at temperature range  $T_g = 20\text{--}550$  °C. The variants of random and digital alloys, ion beam introduction of additional “not magnetic” shallow acceptor boron impurity and influence of the additional subsequent pulse laser annealing were studied. The ferromagnetism of layers was controlled by results of ferromagnetic resonance (FMR), magneto-optical Kerr effect, anomalous Hall effect, negative magnetoresistance measurements. The surface profile and distribution of magnetization were determined by atomic and magnetic force microscopies. We used the laser deposition by pulse Nd-YAG laser (0.53  $\mu\text{m}$ , 0.3 J, 12 ns) on the equipment LQ 529 of Byelorussian firm SOLAR LS to fabricate our samples of thin layers. The plates of single crystal GaAs, Si or sapphire  $\text{Al}_2\text{O}_3$  were used as substrates. The thickness of the layers was ranged from 30 to 100 nm. The X-ray spectral analysis with electronic excitation was applied for definition of the contents of a 3d-impurity. For observations of FMR measurements of 9.3 GHz microwave absorption were carried out by the Bruker EMX EPR-spectrometer at temperatures from 77 up to 500 K at various orientations of a magnetic field till 1.5 T. The high-resolution transmission electron microscopy (HRTEM) and the selected area electron diffraction (SAED) were made on JEM-2100F of JEOL. Comparison structural and magnetotransport properties of the layers Si:Mn which have been grown up under various conditions, various influences on them, shows that layers represent a magnetic homogeneous material. Structural uniformity proves to be true data of HRTEM and SAED on Fig. 1. In the report crystal structure synthesized high-temperature Si:Mn is discussed.

Supported by RFBR (08-02-01222-a, 11-02-00855-a), the Ministry of Education of Russian Federation (projects 2.1.1/2833 and 2.1.1/12029) and the State contract № 02.740.11.0672 of the Federal purpose program “Scientific and scientific-pedagogical cadre of innovative Russia” 2009-2013 is acknowledged.

1. Furdyna J.K.: *J. Appl. Phys.* **64**, R29 (1988)
2. Wolf S.A. *et al.*: *Science* **294**, 1488 (2001)
3. Demidov E.S., Podolskii V.V., Lesnikov V.P. *et al.*: *JETP* **106**, 110 (2008)
4. Chikazumi S.: *The Physics of Ferromagnetism*. Syokabo, Tokyo, 1980; Mir, -M., 1983.

## Location, Conformation and Aggregation of PC Spin Labels in the Gel Phase Lipid Bilayers by Multifrequency ESR

*B. Dzиковski, D. Tipikin, and J. H. Freed*

*ACERT Research Center Department of Chemistry and Chemical Biology, Baker Laboratory, Cornell University, Ithaca, NY 14853, USA, bd55@cornell.edu*

*n*-PC spin labels (*n* = 5, 7, 10, 12, 14, 16) in DMPC, DPPC and EYL bilayers with and without cholesterol were studied by multifrequency ESR at 9–240 MHz and CW-saturation techniques at 77 K. In the presence of cholesterol, the hyperfine splitting component  $A_{zz}$  determined at 9 GHz and the relaxation enhancement induced by nickel ions absorbed at the membrane surface change regularly with an increase in the *n*-PC number. High field ESR at 240 GHz for all spin labeling positions *n* > 7 clearly shows well-resolved spectra with two distinct components corresponding to hydrogen-bonded and non-bonded forms of the nitroxide, with the non-bonded form prevailing. On the contrary, in DMPC without cholesterol rigid limit X-band spectra shows little trend in the  $A_{zz}$  value which remains ~34.5 G through the *n*-PC series. Relaxation enhancement by nickel ions at 19 °C ( $P_{\beta}$  phase) is also similar for all studied spin labeling positions. Rigid limit X-band spectra in DPPC are more complex with signs of aggregation, which are most pronounced for 7–12 PC positions. High Field ESR shows significant spin label aggregation in both DMPC and DPPC in the absence of cholesterol. Similar to phospholipid/cholesterol systems, two components are discernible in the spectrum. However, (1) in the absence of cholesterol the fraction of the hydrogen-bonded component is higher for all *n*-PC positions; (2) the hydrogen-bonded component is always broadened by aggregation of spin labels. This broadening dramatically depends on the sample treatment routine, the rate of cooling in particular, which determines whether one observes a singlet or a resolved rigid limit spectrum.

Our results can be explained by multiple conformations of PC spin labels in the membrane bilayer. While in the presence of cholesterol the distribution of conformations (erected, bent or stretched along the membrane surface) seems to be random for all phase states, the gel phase of pure-lipid membranes ( $P_{\beta}$ ,  $L_{\beta}'$  or  $L_c'$  = rippled gel, gel, or pseudo-crystalline phase) tends to partially exclude the nitroxide fragments from the membrane interior to the surface. This effect is similar to the exclusion of solutes from crystallizing liquid in the 3-dimensional case. Moreover, the spin-labeled lipid molecules with the nitroxides at the membrane surface slowly undergo lateral aggregation, within

minutes or hours, in the  $L'_\beta$  or  $L'_c$ . This aggregation manifests itself in broad features of the ESR spectra and in a gradual decrease in saturation factors ( $P = g_e^2 T_1 T_2^{\text{eff}}$ ) of *n*-PC spin labels in the lipid bilayer stored below pretransition/subtransition temperatures.

Our results provide a good explanation for previous observations ([1], [2]; etc.) and demonstrate the conformational flexibility of PC spin labels, which should be taken into account in all studies where they are used. This work also illustrates the superior resolution of High Field ESR and its advantages in membrane studies.

1. Earle K.A., Moscicki J.K., Ge M., Budil D.E., Freed J.H.: *Biophys. J.* **66**, 1213 (1994)
2. Kurad D., Jeschke G., Marsh D.: *Biophys. J.* **85**, 1025 (2003)

## Electrically Detected Magnetic Resonance Characterization of Silicon Nanowires

*M. Fanciulli<sup>1,2</sup>, A. Velle<sup>2</sup>, C. Canevali<sup>1</sup>, D. Rotta<sup>1</sup>, M. Basini<sup>1</sup>, and S. Paleari<sup>1</sup>*

<sup>1</sup> *Università di Milano-Bicocca, Milano I-20126, Italy*

<sup>2</sup> *Laboratorio MDM, IMM-CNR, Agrate Brianza I-20864, Italy,  
marco.fanciulli@unimib.it*

Silicon nanowires (SiNWs) have been extensively investigated in the last decades [1]. The interest in these nanostructures stems from both fundamental and applied research motivations. The functional properties of one- and zero-dimensional silicon structures are significantly different, at least below a certain critical dimension, from those well known in the bulk. The key and peculiar functional properties of SiNWs find applications in nanoelectronics, classical and quantum information processing and storage, optoelectronics, photovoltaics, thermoelectric, battery technology, nano-biotechnology, and neuroelectronics. We report our work [2, 3] on the characterization by electrically detected magnetic resonance (EDMR) measurements of silicon nanowires (SiNWs) produced by different top-down processes. SiNWs were fabricated starting from SOI wafers using standard e-beam lithography and anisotropic wet etching or by metal-assisted chemical etching. Further oxidation was used to reduce the wire cross section. Different EDMR implementations were used to address the electronic wave function of donors (P) and to characterize point defects at the SiNWs/SiO<sub>2</sub> interface. The EDMR spectra of as produced SiNWs with high donor concentration ( $[P] = 10^{18} \text{ cm}^{-3}$ ) show a single line related to delocalized electrons. SiNWs produced on substrates with lower donor concentration ( $[P] < 10^{16} \text{ cm}^{-3}$ ) reveal the doublet related to substitutional P in Si, as well as lines related to interfacial defects such as Pb<sub>0</sub>, Pb, E', and E'-like. The EDMR spectra of samples produced by metal-assisted chemical etching exposed to post production oxidation reveal a disordered and defective interface and the disappearance of the P related signal. Forming gas annealing, on the other hand, reduces the contribution of interfacial defects and allows a better resolution of the P related doublet. EDMR spectra of SiNWs having different sizes and doping (P, As) will be presented and discussed.

1. Koshida N. (ed.): *Device Applications of Silicon Nanocrystals and Nanostructures*. Springer, 2009.
2. Fanciulli M., Vellei A., Canevali C., Baldovino S., Pennelli G., Longo M.: *Nanoscience and Nanotechnology Letters*, to be published.
3. Fanciulli M., Molle A., Baldovino S., Vellei A.: *Microelectronic Engineering* **88**, 1482 (2011)

## Quantum Entanglement and Quantum Discord in Multiple Quantum NMR in Solids

*E. B. Fel'dman*

*Theoretical Department, Institute of Problems of Chemical Physics, Chernogolovka 142432, Russian Federation, efeldman@icp.ac.ru*

Entanglement [1] is the key concept in quantum information theory. It has played a crucial role in experiments on quantum computing and quantum teleportation. This resulted in intensive interest in the physics of entanglement from both theorists and experimentalists [2]. Effective manipulations with quantum correlations result in significant advantages in quantum devices (in particular quantum computers) in comparison with their classical counterparts. Till recently, entanglement has been used as a measure of quantum correlations. However, it was shown both theoretically [3] and experimentally [4] that some mixed separable states (i.e., states with zero entanglement) allow one to realize advantages of quantum algorithms in comparison with their classical counterparts. Moreover, quantum nonlocality can be observed in systems without entanglement [5]. Such observations suggest that entanglement does not involve all quantum correlations responsible for the advantages of quantum algorithms in comparison with the classical ones.

The concept of quantum discord which is developing intensively in recent years [6] is based on the separation of the quantum part out of the total mutual information encoded in a bipartite system. The discord is completely defined by quantum properties of the system and becomes zero for classical systems.

Entanglement is detected with the help of a so called entanglement witness (EW). By definition, EW is an observable, which has a positive expectation value for separable states and a negative value for some entangled states [7]. In particular, the internal energy and magnetic susceptibility were used as EWs in some cases. In our report, we propose a new type of entanglement witness, the intensity of multiple quantum coherences in spin systems. This quantity is accessible in NMR experiments and, thus, opens a new approach to probing entanglement with highly advanced NMR techniques.

We focus on the simplest relevant system, a pair of spins  $S = 1/2$  coupled by the dipole–dipole interaction in the conditions of the MQ NMR experiment [8]. Here, the initial thermodynamic density matrix describing the interaction

of the spins with a strong external magnetic field is subjected to the irradiation by a specially tailored sequence of resonant rf pulses. The anisotropic dipolar Hamiltonian oscillates rapidly when the period of the sequence is less than the inverse dipolar frequency. The spin dynamics of the system is described by an averaged Hamiltonian, which is responsible for the emergence of the MQ coherences of the zeroth and plus/minus second orders [9]. It is evident that the initial state of the system is separable. However, we show with the Wootters criterion [10] that the entangled state emerges when the intensity of the MQ coherence of order 2 ( $-2$ ) exceeds the exactly calculated threshold depending on the external magnetic field and the temperature. Thus, the intensity of the MQ coherence of the second order which is the observable in MQ NMR experiments serves as EW for the spin systems.

We consider also an analogous model taking into account the effect of spin-lattice relaxation. We have found that the entangled states emerge at temperatures  $T$  below the temperature  $T_E$  which is [11, 12]

$$T < T_E = \frac{\hbar\omega_0}{k \ln\left(\frac{\sqrt{2+a}}{2-\sqrt{2+a}}\right)}, \quad (1)$$

where  $a = \exp(\tau/T_1) - 1$ ,  $k$  is the Boltzman constant,  $\omega_0$  is the Larmour frequency,  $\tau$  is the time of the preparation period of the MQ NMR experiment [8] and  $T_1$  is the spin-lattice relaxation time. According to Eq. (1), entangled states emerge at  $\ln 3 > \tau/T_1$ . The temperature  $T_E$  decreases with the decrease in the spin-lattice relaxation time. We have found a simple relationship between the intensities of MQ NMR coherences of the second order and the concurrence  $C$  which determines [10] entanglement in the system:

$$C = \sqrt{\tanh \frac{\beta}{2} (J_2(\tau) + J_{-2}(\tau)) - \frac{\exp(-\tau/T_1)}{2 \cosh^2 \beta/2} - \frac{1 - \exp(-\tau/T_1)}{2}}, \quad (2)$$

where  $\beta = \hbar\omega_0/kT$  and  $J_{\pm 2}(\tau)$  is the intensity of MQ NMR coherence of the second (minus second) order [11].

We calculate also the quantum discord in the considered system and demonstrate that it is different from zero at temperatures  $T > T_E$ . This means that quantum correlations are significant when there is no entanglement in the system.

This work was supported by the Program of the Presidium of Russian Academy of Sciences No. 7 (the program “Development of the methods for obtaining chemical substances and creating new materials”).

1. Nielsen M.A., Chuang I.L.: Quantum Computation and Quantum Information. Univ. Press, Cambridge, 2000.
2. Amico L., Fazio R., Osterloh A., Vedral V.: Rev. Mod. Phys. **80**, 517 (2008)
3. Meyer D.A.: Phys. Rev. Lett. **85**, 2014 (2000)
4. Lanyon B.P., Barbieri M., Almeida M.P., White A.G.: Phys. Rev. Lett. **101**, 200501 (2008)
5. Bennet C.H., DiVincenzo D.P., Fuchs *et al.*: Phys. Rev A **59**, 1070 (1999)
6. Ollivier H., Zurek W.H.: Phys. Rev. Lett. **19**, 017901 (2002)
7. Horodeski M., Horodeski P., Horodeski R.: Phys.Lett. A **223**, 1 (1996)
8. Baum J., Munowitz M., Garroway A.N., Pines A.: J. Chem. Phys. **83**, 2015 (1985)
9. Fel'dman E.B., Lacelle S.: J. Chem. Phys. **107**, 7067 (1997)
10. Wootters W.K.: Phys. Rev. Lett. **80**, 2245 (1998)
11. Fel'dman E.B., Pyrkov A.N.: JETP Letters **88**, 398 (2008)
12. Fel'dman E.B., Pyrkov A.N.: Chem. Phys. Lett. (in press)

## Multifrequency Electron Paramagnetic Resonance Characterization of PpoA, a CYP450 Fusion Protein that Catalyses Fatty Acid Dioxygenation

A. J. Fielding<sup>1</sup>, F. Brodhun<sup>2</sup>, C. Koch<sup>2</sup>, R. Pievo<sup>1</sup>, V. Denysenkov<sup>3</sup>,  
I. Feussner<sup>2</sup>, and M. Bennati<sup>1,4</sup>

<sup>1</sup>Max-Planck Institute for Biophysical Chemistry, Göttingen, Germany, [afieldi@gwdg.de](mailto:afieldi@gwdg.de)

<sup>2</sup>Department of Plant Biochemistry, Georg-August-University, Göttingen, Germany

<sup>3</sup>J. W. Goethe University, Frankfurt, Germany

<sup>4</sup>Institute for Organic and Biomolecular Chemistry, Georg-August-University, Germany

PpoA is a fungal dioxygenase that produces hydroxylated fatty acids involved in the regulation of the life cycle and secondary metabolism of *Aspergillus nidulans*. It was recently proposed that this novel enzyme employs two different heme domains to catalyze two separate reactions: within a heme peroxidase domain, linoleic acid is oxidized to (8*R*)-hydroperoxyoctadecadienoic acid [(8*R*)-HPODE]; in the second reaction step (8*R*)-HPODE is isomerized within a P450 heme thiolate domain to 5,8-dihydroxyoctadecadienoic acid [1]. In the present study, pulsed EPR methods were applied to find spectroscopic evidence for the reaction mechanism, thought to involve paramagnetic intermediates. We observe EPR resonances of two distinct heme centres with *g*-values typical for Fe(III) *S* = 5/2 high-spin and Fe(III) *S* = 1/2 low-spin hemes. <sup>14</sup>N ENDOR spectroscopy on the *S* = 5/2 signal reveals resonances consistent with an axial histidine ligation. Reaction of PpoA with the substrate leads to the formation of an amino acid radical on the early ms time scale concomitant to a substantial reduction of the *S* = 5/2 heme signal. High-frequency EPR (95- and 180-GHz) unambiguously identifies the new radical as a tyrosyl, based on *g*-values and hyperfine couplings from spectral simulations. Further, EPR distance measurements revealed that the radical is distributed among the monomeric subunits of the tetrameric enzyme at a distance of approx. 5 nm [2].

1. Brodhun F., Gobel C., Hornung E., Feussner I.: J. Biol. Chem. **284**, 11792 (2009)
2. Fielding A.J., Brodhun F., Koch C., Pievo R., Denysenkov V., Feussner I., Bennati M.: J. Am. Chem. Soc. **133**, 9052–9062 (2011)

## Noncollinear Magnetic States and Transport Properties of Ferromagnetic Nanostructures

*A. A. Fraerman*

*Institute of Physics of Microstructures, Russian Academy of Sciences,  
Nizhni Novgorod 603950, Russian Federation, andr@ipm.sci-nnov.ru*

Investigations of spin and spatial degrees of freedom for electrons and their interplay in conducting ferromagnets are of great interest from both theoretical and practical points of view. For collinear distribution of magnetization, spatial and spin degrees of freedom for current carriers are independent. But for non-collinear distribution, the motions of electron in real and spin spaces are coupling. This can lead to the peculiarities of physical properties for noncollinear magnetic systems. In general case, distribution of magnetization in laterally-confined magnetic nanostructures is noncollinear and, what is more, – non coplanar. In the report I am going to demonstrate some examples of magnetic nanostructures with chiral distribution of magnetization and discuss connection between magnetic states and physical properties of such systems. Namely

- control of vorticity for triangle magnetic nanoparticles [1],
- antivortex state in magnetic cross-like nanostructure [2],
- spiral state in laterally confined magnetic multilayer [3].

1. Yakata S. *et al.*: Appl. Phys. Let. **97**, 222503 (2010)
2. Mironov V.L. *et al.*: Phys. Rev. B **81**, 094436 (2010)
3. Fraerman A. A. *et al.*: J. Appl. Phys. **103**, 073916 (2008)

## Oriental Structures and Electronic Couplings of Photoinduced Charge-Separated States in Human Proteins

*Y. Kobori*<sup>1,2</sup> and *M. Fuki*<sup>2</sup>

<sup>1</sup> *Department of Chemistry, Faculty of Science, Shizuoka University, Shizuoka 422-8529, Japan*

<sup>2</sup> *PRESTO, Japan Science and Technology Agency (JST), Saitama 332-0012, Japan,  
sykobor@ipc.shizuoka.ac.jp*

Analysis of radical-pair (RP) interaction between a ligand and its target protein is important to directly understand how the protein structures play key roles on several biological processes. The protein-ligand structure of the photoinduced charge-separated (CS) state should be essential to design the useful functions for the biological solar-energy conversion and for the bio-photocatalysis using proteins. Also, understanding the geometry effects on the electronic interactions between ligands and their neighboring residues are quite important to analyze the underlying biological functions for the tunneling and for the transport of the holes in proteins. Despite the quite importance of the RP interactions, no study has experimentally clarified both the 3D structure and the electronic coupling of the photoinduced CS states in the protein-ligand systems. The time-resolved EPR (TREPR) observations of the correlated RP polarization have been powerful to investigate the orientational structures and the exchange couplings ( $2J$ ) of the photoinduced CS state in the photosynthetic reaction centers and in the electron donor-acceptor [1, 2] linked systems. Concerning the correlated RP polarization generated by the triplet-precursor reaction systems, we have recently proposed a model of triplet-triplet electron spin polarization transfer (ESPT) by which the anisotropic magnetic properties of the excited triplet states are transferred to the quantum levels of the spin correlated RP (SCRIP) [1].

In the present study, by the light-excitations of 9,10-anthraquinone-1-sulfonate (AQ1S<sup>-</sup>) as a ligand bound to human serum albumin (HSA), we have characterized the protein-ligand geometries of the photoinduced CS states in which the energy-wasting charge-recombination (CR) is electronically prohibited even at contact amino acid-ligand separations.

1. Kobori Y. *et al.*: *J. Phys. Chem. B* **114**, 14621–14630 (2010)

2. Kobori Y. *et al.*: *J. Am. Chem. Soc.* **131**, 1624–1625 (2009)

## Nuclear Spin Polarization and Spin Entanglement in Photoexcited Triplet States

G. Kothe<sup>1</sup>, T. Yago<sup>1</sup>, J.-U. Weidner<sup>1</sup>, G. Link<sup>1</sup>, M. Lukaschek<sup>1</sup>, and T.-S. Lin<sup>2</sup>

<sup>1</sup> Department of Physical Chemistry, University of Freiburg, Freiburg 79104, Germany, [gerd.kothe@physchem.uni-freiburg.de](mailto:gerd.kothe@physchem.uni-freiburg.de)

<sup>2</sup> Department of Chemistry, Washington University, St. Louis MO 63130, USA

Recently, *nuclear quantum oscillations* have been detected in an organic triplet state subject to an external magnetic field [1]. The observed quantum coherences can be rationalized using an analytical theory. Analysis suggests that the nuclear spins are actively involved in the intersystem crossing process. The novel mechanism also acts as a source of *oscillatory nuclear spin polarization*. In the present study we report magnetic field dependent NMR experiments indicating large signal enhancement factors even at very high magnetic fields. This opens new perspectives for the analysis of CIDNP in mechanistic studies of photo-active proteins.

In general, photochemistry in these proteins proceeds via spin-correlated radical pairs formed either in a singlet or in a triplet state [2, 3]. The resulting spin configuration depends on the photophysical properties of the excited cofactor. If, initially a singlet radical pair is formed, the observed photo-CIDNP can be analyzed using a radical pair mechanism [2–5]. In case of a triplet radical pair, however, the spin dynamics in the precursor state should also be considered. This requires a more comprehensive analysis involving the triplet mechanism outlined in the present study [1].

At level anti-crossing (LAC) conditions of excited triplet states, *entanglement* is created between a highly polarized electron spin and several hyperfine coupled nuclear spins. In case of a single proton, this gives rise to four *entangled quantum states* composed of one electron spin and one nuclear spin qubit. Due to the abrupt change of the spin quantization axis after the intersystem crossing, the triplet starts out in a *coherent superposition of entangled eigenstates* which manifests itself as quantum oscillations in the longitudinal electron and nuclear spin magnetization (see Fig. 1). We report first low-field NMR experiments which probe these oscillations in the longitudinal nuclear magnetization. Thus, the quantum oscillations can be used for the detection and manipulation of entangled states which is a basic requisite in quantum information processing.

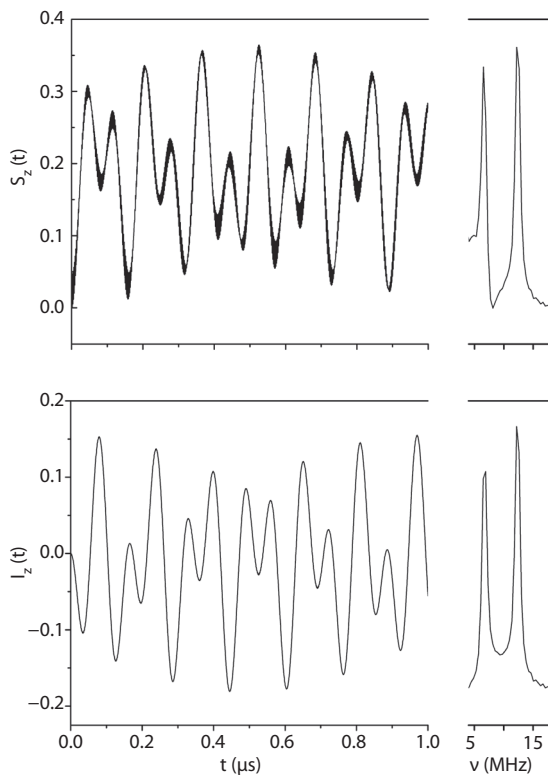


**Fig. 1.** Quantum oscillations between entangled spin states at triplet level anti-crossing conditions.

1. Kothe G., Yago T., Weidner J.-U., Link G., Lukaschek M., Lin T.-S.: *J. Phys. Chem B* **114**, 14755, (2010)
2. Kaptein R., Dijkstra K., Nicolay K.: *Nature* **274**, 293 (1978)
3. Hore P.J., Broadhurst R.W.: *Prog. Nucl. Magn. Reson. Spectrosc.* **25**, 345 (1993)
4. Polenova T., McDermott A.E.: *J. Phys. Chem. B* **103**, 535 (1999)
5. Jeschke G., Matysik J.: *Chem. Phys.* **294**, 239 (2003)

## Spin Chemistry Investigation of Peculiarities of Photoinduced Electron Transfer in Donor-Acceptor Linked System

*T. V. Leshina, I. M. Magin, N. E. Polyakov, E. A. Khramtsova, and A. I. Kruppa*

*Institute of Chemical Kinetics and Combustion RAS, Novosibirsk 630090,  
Russian Federation, leshina@kinetics.nsc.ru*

Photoinduced intramolecular electron transfer (PET) in linked systems, (*R,S*)- and (*S,S*)-naproxen-*N*-methylpyrrolidine dyads, has been studied by means of spin chemistry methods (magnetic field effect and chemically induced dynamic nuclear polarization, CIDNP). The relative yield of the triplet state of the dyads in different magnetic field has been measured, and dependencies of the high field CIDNP of *N*-methylpyrrolidine fragment on solvent polarity have been investigated. It has been demonstrated that the main peculiarities of photoprocesses in this linked system are connected with the participation of singlet exciplex alongside with PET in chromophore excited state quenching. As for the nature of the influence of chiral centers on chemical reactivity of NPX-Pyr dyads, described in [1], spin chemistry study allows us to make some suggestions. At first we were under the impression that the most plausible reason of the difference between the rates of quenching of the excitation of the chromophore of the (*R,S*)- and (*S,S*)-NPX-Pyr dyads could be the difference of the energy of electron exchange interaction in the biradical ions of (*R,S*)- and (*S,S*)-enantiomers. In this case the stereoselectivity might be the result of different rates of back electron transfer in biradical ions of the isomers. The way of the possible influence of back electron transfer rates on fluorescence quenching, connected with existence of fast equilibrium between the exciplex and the biradical ion. However, the small intensity of CIDNP for the dyads detected in solvents with high polarity, the identity of the CIDNP effects for the stereoisomers, and the absence of the influence of external MF on triplet yield of the dyads make us conclude that processes in the biradical ions are not the main source of the stereo selectivity. Then it might be reasonable to consider the possibility of processes in the exciplex of the dyads to influence the rate of fluorescence quenching. The internal singlet-triplet conversion of exciplex has to be highly sensitive to both energetic and steric effects.

This work was supported by the grants 08-03-00372 and 11-03-01104 of Russian Foundation of Basic Research, and the grant of Priority Programs of RAS, No 5.1.5.

1. Jim'enez M.C., Pischel U., Miranda M.A.: J. Photochem. Photobiol. C: Photochemistry Reviews **8**, 128–42 (2007)

## Spin-Spin Interactions in Investigation of Structure and Dynamics Biological Moltecules

*G. I. Likhtenshtein*

*Department of Chemistry, Ben-Gurion University, Beer-Sheva 84105, Israel,  
gertz@bgu.ac.il*

First studies on application spin-spin dipole-dipole and exchange interactions in biophysics were reported in late 1960-th and early 1970-th [1–6]. Within this period, methods of double spin labels (DSLML) [1–3] and spin label-spin probe methods (SLSPM) [4, 6] were proposed, developed and implemented. In the frame of DSLML, it was demonstrated that the label ESR spectra are sensitive to static spin-spin interactions between spin labels on proteins, such as Cu(II) complexes and nitroxides, that allowed to estimate distances between the labels up to 30 Å, [1–4, 6, 7]. Later, by employing effects of static spin-spin dipole-dipole interactions on the nitroxide labels spin lattice relaxation time, the DSLML method sensitivity was expanded to about 50–55 Å [5, 6]. In parallel, strong static exchange spin-spin interactions were demonstrated on the ESR spectra of nitroxide labels attached to proteins at close proximity to each other [6].

SLSPM are based on the facts that dynamic spin-spin and spin lattice relaxation times of two molecules bearing spin are affected by microviscosity, steric hindrances, local charges in the vicinity of spin of interest and its immersion depth. The following four versions of SLSPM have been developed and implemented [4, 7–11 and references therein]: 1. Nitroxide spin label, attached to a macromolecule and paramagnetic transition complex freely diffused in solution; 2. Paramagnetic complex on a macromolecule and nitroxide freely diffused in solution; 3. A radical or triplet molecule immersed in object of interest and nitroxide; 4. Molecules bearing proton and nitroxide, both freely diffused in solution. The use of the DSLML and SLSPM [4, 6–11] allowed us to solve a number experimental tasks including: investigation of structure of  $Fe_nS_m$  clusters in proteins, structure of photosynthetic reaction center, establishing microviscosity profile around proteins; estimating local charges in the vicinity of the myoglobin and cytochrome heam groups; investigation of distribution of the electrostatic potential around biologically important molecules; measurements of active encounters in wide range of characteristic time between molecules in membranes using novel spin cascade system and .estimating depth of immersion of nitroxides and fluorophors in biological membranes.

Initial idea of combining a chromophore and a nitroxide in one molecule that could be used for studying molecular dynamics, intramolecular fluorescence quenching and the nitroxide fragment reduction has been suggested in the 1980-th [12]. In such a super molecule the nitroxide strongly quenches the fluorescence from the chromophore fragment by the intersystem crossing mechanism [9–14 and references therein]. Then any chemical or photo-reactions of nitroxide fragment would result in a decrease of ESR signal that accompanied by a drastic increase in fluorescence. These properties of the new probes were intensively exploited for several practical applications including a real time analysis of antioxidants, nitric oxide and superoxide [9–14]. Owing high sensitivity, simplicity, availability of fluorescence and ESR techniques, these methods can be widely employed in chemistry, biotechnology and biomedicine using the standard techniques and are potentially adaptable to fibroptic sensing and focal microscopy.

1. Likhtenshtein G.I.: *Mol. Biol.* **2**, 234–240 (1968)
2. Medzhidov A.A., Likhtenshtein G.I., Kirichenko L.A.: *Bull. Acad. Sci. USSR (Chemistry)* **3**, 698–902 (1969)
3. Kulikov A.I., Likhtenshtein G.I., Rozantzev E.G., Suskina V.I., Shapiro A.V.: *Biofizika*, **17**, 42–49 (1969)
4. Likhtenstein G.I., Grebentchikov Yu.B., Bobodzhanov P.Kh., Rosantev E.G., Kokhanov Yu.I.: *Mol. Biol.* **4**, 682–691 (1972)
5. Kulikov A.V., Likhtenstein G.I.: *Biofizika* **19**, 420–424 (1974)
6. Likhtenshtein G.I.: *Spin Labeling Method in Molecular Biology*. Wiley Interscience, N.Y., 1976.
7. Likhtenshtein G.I.: *Biophysical Labeling Methods in Molecular Biology*. Cambridge University Press, Cambridge, N.Y., 1993.
8. Likhtenshtein G.I. in: *Magnetic Resonance in Biology* (Berliner L., Eaton S., Eaton G., eds.), pp. 1–36. Kluwer Academic Publishers, Dordrecht, 2000.
9. Likhtenstein G.I., Ishii K., Nakatsuji S.: *Photochem. and Photobiol.* **83**, 871–881 (2007)
10. Likhtenshtein G.I., Yamauchi J., Nakatsuji S., Smirnov A., Tamura R.: *Nitroxides: Application in Chemistry, Biomedicine, and Materials Science*. WILEY-VCH, Weinheim, 2008.
11. Likhtenshtein G.I., Kulikov A.V., Kotelnikov A.I., Bogatyrenko V.R.: *Photobiochem. Photobiol.* **3**, 178–182 (1982)
12. Bystryak I.M., Likhtenshtein G.I., Kotelnikov A.I., Hankovsky O.H., Hideg K.: *Russ. J. Phys. Chem.* **60**, 1679–1983 (1986)
13. Likhtenshtein G.I.: *Applied Biochemistry and Biotechnology* **152**(1), 135–155 (2009)
14. Likhtenshtein G.I. *Proceeding of International Conference on Biochemistry and Medical Chemistry*, pp. 49–57. Cambridge, Uk. February 23–25, 2011.

## Multifrequency EPR on Single Crystals of Photosystem II

*H. Matsuoka<sup>1</sup>, J.-R. Shen<sup>2</sup>, A. Kawamori<sup>3</sup>, Y. Ohba<sup>1</sup>, and S. Yamauchi<sup>1</sup>*

<sup>1</sup> *Institute of Multidisciplinary Research for Advanced Materials, Tohoku University, Sendai 980-8577, Japan, hmatsu@tagen.tohoku.ac.jp*

<sup>2</sup> *Department of Biology, Okayama University, Okayama 700-8530, Japan*

<sup>3</sup> *Agape-Kabutoyama Institute of Medicine, Nishinomiya 662-0001, Japan*

Molecular oxygen is produced from water by the water-oxidizing complex (WOC) in photosystem II (PSII), which is composed of four exchange-coupled manganese (Mn) atoms and one calcium (Ca) atom. Very recently, one of the authors (J.-R. Shen) and his collaborators have succeeded in solving the crystal structure of photosystem II at 1.9 Å, which yielded a detailed picture of the WOC for the first time [1]. High-frequency electron paramagnetic resonance (EPR) studies have also provided detailed information on the electronic and molecular structures of redox-active molecules in PSII. We precisely determined the  $g$ -tensors and their orientation relative to the crystal axes for WOC by W-band EPR studies on single crystals of PSII [2]. We also investigated the  $g$ -anisotropy of the tyrosine radical  $Y_Z'$  to provide insight into the mechanism of  $Y_Z'$  proton-coupled electron transfer in Mn-depleted PSII. The anisotropy was highly resolved by W-band EPR using PSII single crystals. The  $g_x$ -component

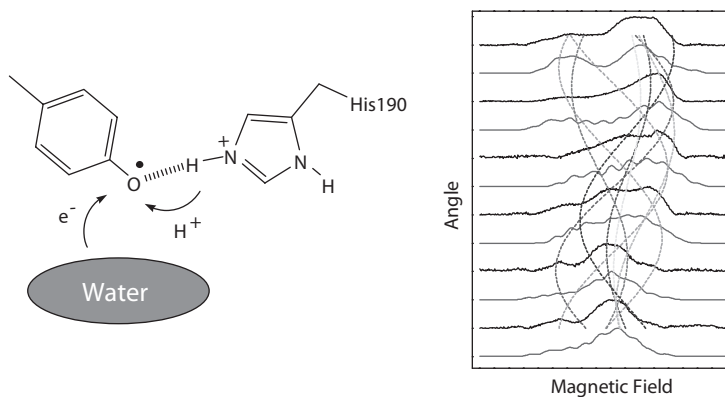


**Fig. 1.** Schematic presentation of  $YZ'$  proton-coupled electron transfer and W-band EPR Spectra of  $YZ'$  in single crystals of PSII.

along the phenolic C-O bond of  $Y_z^{\cdot-}$  was calculated by density functional theory (DFT). It was concluded from the highly resolved  $g$ -anisotropy that  $Y_z$  loses a phenol proton to D1-His<sub>190</sub> upon tyrosine oxidation, and D1-His<sub>190</sub> redonates the same proton back to  $Y_z^{\cdot-}$  upon reduction.

1. Umena Y., Kawakami K., Shen J.-R., Kamiya N.: *Nature* **473**, 55 (2011)
2. Matsuoka H., Furukawa K., Kato T., Mino H., Shen J.-R., Kawamori A.: *J. Phys. Chem. B* **110**, 13242 (2006)
3. Matsuoka H., Shen J.-R., Kawamori A., Nishiyama K., Ohba Y., Yamauchi S.: *J. Am. Chem. Soc.* **133**, 4655 (2011)

## Domain Walls and Long-Range Triplet Correlations in SFS Josephson Junctions

*A. S. Mel'nikov, A. I. Buzdin, and N. G. Pugach*

*Institute for Physics of Microstructures RAS, Nizhny Novgorod, Russian Federation,  
melnikov@ipm.sci-nnov.ru*

We study the contribution of domain walls to the Josephson current through a ferromagnetic metal both in clean and diffusive limits. Our consideration of these limits is based on the quasiclassical version of the Bogolubov-de Gennes equations and Usadel theory, correspondingly. In the clean limit the domain walls connecting superconducting leads are shown to be responsible for strong enhancement of Josephson current even for domain structure with collinear magnetic moments. In the dirty limit a noticeable increase in the critical current appears only for a system with noncollinear magnetic moments. We demonstrate that a thin domain wall in this case may serve as an efficient source of the long-range triplet proximity effect.

## Molecular-Spin Based Quantum Computing and Quantum Information Processing

S. Nakazawa<sup>1,7</sup>, K. Sato<sup>1,7</sup>, T. Yoshino<sup>1</sup>, S. Nishida<sup>1,7</sup>, R. Rahimi<sup>1</sup>, T. Ise<sup>1,7</sup>, N. Mori<sup>1</sup>, Y. Morita<sup>2,7</sup>, K. Toyota<sup>1,7</sup>, D. Shiomi<sup>1,7</sup>, K. Nakasuji<sup>3</sup>, M. Kitagawa<sup>4,7</sup>, H. Hara<sup>5</sup>, P. Carl<sup>6</sup>, P. Höfer<sup>6</sup>, and T. Takui<sup>1,7</sup>

<sup>1</sup> Graduate School of Science, Osaka City University, Osaka 558-8585, Japan

<sup>2</sup> Graduate School of Science, Osaka University, Toyonaka 560-0043, Japan

<sup>3</sup> Fukui University of Technology, Fukui 910-8505, Japan

<sup>4</sup> Graduate School of Engineering Science, Osaka University, Toyonaka 560-8531, Japan

<sup>5</sup> Bruker Biospin K. K., Japan

<sup>6</sup> Bruker Biospin GmbH, Germany

<sup>7</sup> FIRST-JSPS, Japan, takui@sci.osaka-cu.ac.jp

The past decade has witnessed that quantum computers (QCs) and quantum information processing (QIP) have rapidly emerged in pure and applied sciences. Applications of quantum computing to quantum chemistry are the focus of current topics in the fields [1, 2]. Photon-qubit based QIP was practically utilized in Swiss Federal Election in October, 2007 and the relevant field work was tested in October, 2010 in Tokyo. Scalable implementation of qubits is the most intractable issue to be solved for any physical systems pursuing realistic practical QCs/QIP. Building-up of scalable matter qubits is now a materials challenge for scientists from the experimental side. Among matter qubits, molecular electron spin-qubits are the latest arrival, but can afford the promise in implementing scalable QCs/QIP [3–5], as relevant to an electron version of the Lloyd model [6].

In this presentation, we illustrate how to design and implement electron spin-qubits and nuclear spin-qubits in organic molecular frames. They are all synthetic qubits, as well defined in terms of matter spin-qubits. The synthetic spin-qubit systems in ensemble allow us to generate quantum entanglements between the electron spin and proton nuclear spins and to carry out super dense coding. For molecular spin-qubits, we have synthesised weakly exchange-coupled open-shell entities based on stable nitroxides. We have shown that both pulse-based ENDOR/Multiple and ELDOR techniques serve as the most useful spin-state manipulation technology for QCs/QIP.

1. Abrams D.S., Lloyd S.: Phys. Rev. Lett. **83**, 5162–5165 (1999)
2. (a) Aspuru-Guzik A. *et al.*: Science **309**, 1704–1707 (2005). (b) Lanyon B.P. *et al.*: Nature Chem. **2**, 106–111 (2010)

3. (a) Mehring M. *et al.*: Phys. Rev. Lett. **90**, 153001-4 (2003). (b) Mehring M. *et al.*: Phys. Rev. Lett. **73**, 052303/1–12 (2006)
4. (a) Rahimi. D.R. *et al.*: Int. J. Quant. Info. **3**, 197–204 (2005). (b) Sato K. *et al.*: J. Mater. Chem. **19**, 3739–3754 (2009)
5. Morton J.J.L. *et al.*: Nature Physics **2**, 40–43(2006)
6. Lloyd S: Sci. Am. **273**, 140–145 (1995)

## Application of THz High-Field EMR to Antiferromagnets with THz Spin Gaps

*H. Ohta*<sup>1,2</sup>, *S. Okubo*<sup>1</sup>, *T. Kobayashi*<sup>2</sup>, *T. Sakurai*<sup>3</sup>, *A. Matsuo*<sup>4</sup>, *K. Kindo*<sup>4</sup>,  
*X. G. Zheng*<sup>5</sup>, *S. Nishihara*<sup>6</sup>, *M. Fujisawa*<sup>7</sup>, and *H. Kikuchi*<sup>7</sup>

<sup>1</sup> *Molecular Photoscience Research Center, Kobe University, Kobe 657-8501, Japan, hohta@kobe-u.ac.jp*

<sup>2</sup> *Graduate School of Science, Kobe University, Kobe 657-8501, Japan*

<sup>3</sup> *Center for Supports to Research and Education Activities, Kobe University, Kobe 657-8501, Japan*

<sup>4</sup> *ISSP, University of Tokyo, Kashiwa 277-8581, Japan*

<sup>5</sup> *Faculty of Science and Engineering, Saga University, Saga 840-8502, Japan*

<sup>6</sup> *Graduate School of Science, Hiroshima University, Higashihiroshima 739-8511, Japan*

<sup>7</sup> *Department of Applied Physics, University of Fukui, Fukui 910-8507, Japan*

Firstly, recent developments of our multi-extreme THz EMR, which covers the frequency region between 0.03 and 7 THz and the temperature region between 1.8 and 300 K [1] together with the pulsed magnetic field up to 55 T [2] and the high pressure up to 1.4 GPa [3], will be presented. Our micro-cantilever EMR also enables the measurement of micrometer size single crystal [4]. Our system is applied to study the antiferromagnetic state of multiferroic material CuO at 4.2 K. We have succeeded in observing the antiferromagnetic gap of 1.6 THz for the first time, and the magnetic anisotropy of CuO will be discussed.

1. Ohta H., Okubo S., Kawakami K., Fukuoka D., Inagaki Y., Kunimoto T., Hiroi Z.: *J. Phys. Soc. Jpn.* **72**, Supplement B 26–35 (2003). Ohta H., Tomoo M., Okubo S., Sakurai T., Fujisawa M., Tomita T., Kimata M., Yamamoto T., Kawauchi M., Kindo K.: *J. Phys.: Conf. Series* **51**, 611–614 (2006)
2. Ohta H., Okubo S., Souda N., Tomoo M., Sakurai T., Yoshida T., Ohmichi E., Fujisawa M., Tanaka H., Kato R.: *Appl. Magn. Reson.* **35**, 399–410 (2009)
3. Sakurai T., Taketani A., Tomita T., Okubo S., Ohta H., Uwatoko Y.: *Rev. Sci. Instr.* **78**, 065107/1-6 (2007). Sakurai T., Horie T., Tomoo M., Kondo K., Matsumi N., Okubo S., Ohta H., Uwatoko Y., Kudo K., Koike Y., Tanaka H.: *J. Phys.: Conf. Series* **215**, 012184/1-4 (2010)
4. Ohta H., Kimata M., Okubo S., Ohmichi E., Osada T.: *AIP Conference Proceedings* **850**, 1643–1644 (2006). Ohmichi E., Mizuno N., Kimata M., Ohta H.: *Rev. Sci. Instrum.* **79**, 103903/1-5 (2008). Ohmichi E., Mizuno N., Kimata M., Ohta H., Osada T.: *Rev. Sci. Instrum.* **80**, 013904/1-5 (2008). Ohta H., Ohmichi E.: *Appl. Magn. Reson.* **37**, 881–891 (2010). Ohmichi E., Mizuno N., Hirano S., Ohta H.: *J. Low Temp. Phys.* **159**, 276–279 (2010)

## SPIN Mapping of Iron-Containing Coordination Clusters Using Mössbauer Spectroscopy

A. K. Powell

*Karlsruhe Institute of Technology, Institute of Inorganic Chemistry,  
Karlsruhe D-76131, Germany, annie.powell@kit.edu*

Molecules are attractive as units for storing or processing information as a result of their small dimensions and the fact that they can be manipulated using chemical principles. The hope is that this will allow for miniaturisation of devices, thereby saving materials and energy. However, gaining insights into the magnetic couplings in such molecules is challenging for large collections of individual spins. We have recently been developing methods to use Mössbauer spectroscopy in order to gain information about the nature of coupling pathways in iron-containing clusters. Furthermore, we can also use the Mössbauer technique to sense anisotropy by following the changes in the spectra of the iron nuclei. This is particularly useful in investigating Fe/4f coordination clusters.

## Electron Spin Dynamics in a GaAs Quantum Well with a Controllable Lateral Confinement

*A. V. Sekretenko<sup>1</sup>, A. V. Larionov<sup>1</sup>, and A. I. Il'in<sup>2</sup>*

<sup>1</sup>*Institute of Solid State Physics, Russian Academy of Sciences, Chernogolovka 142432, Russian Federation, asekretenko@gmail.com*

<sup>2</sup>*Institute of Microelectronic Technology and Ultra-High-Purity Materials, Russian Academy of Sciences, Chernogolovka 142432, Russian Federation*

In this work the spin dynamics of electrons in an ensemble of specific potential wells in the plane of a GaAs quantum well has been investigated by means of time-resolved magneto-optical Kerr rotation technique. Lateral confinement for electrons was induced by a gold electrode with a regular array of micrometer-sized round orifices created onto the sample surface by means of electron lift-off lithography. Comparative measurements with a semitransparent electrode have been simultaneously carried out to distinguish changes in electron spin dynamics due to the band bending from those due to the lateral confinement controlled by applying an external bias. The electron spin lifetime in the mosaic electrode structure has been found to increase by an order of magnitude relatively to the semitransparent electrode structure. The measured values of the electron  $g$ -factor in the quantum well plane and the magnetic field dependence of the electron spin lifetimes indicate an emergence of a strong three dimensional confinement under an orifice in the mosaic electrode. The observed electron spin relaxation anisotropy is possibly caused by the anisotropy of the confining lateral potential.

The work was supported by Foundation for Basic Research.

1. Larionov A.V., Sekretenko A.V., Il'in A.I.: Pis'ma v JETP **93**, 299 (2011); JETP letters **93**, 269 (2011)
2. Cherbunin R.V., Kuznetsova M.S., Gerlovin I.Ya. *et al.*: Fiz. Tverd. Tela **51**, 791 (2009); Phys. Solid State **51**, 837 (2009)
3. Larionov A.V., Golub L.E.: Phys. Rev. B **78**, 033302 (2008)

## Magnetic Properties of PrF<sub>3</sub> Nanoparticles and Microparticles at Low Temperatures

*M. S. Tagirov*

*Kazan Federal University, Kazan 420008, Russian Federation, murat.tagirov@ksu.ru*

The “PrF<sub>3</sub>–liquid <sup>3</sup>He” system is of interest because of the possibility of using the magnetic coupling between the nuclei of the two spin systems for the dynamic nuclear polarization of liquid <sup>3</sup>He. The dielectric Van-Vleck paramagnets are known to have high anisotropy of the effective nuclear magnetogyric ratio and for <sup>141</sup>Pr in PrF<sub>3</sub>,  $\gamma_x/2\pi = 3.322$  kHz/Oe,  $\gamma_y/2\pi = 3.242$  kHz/Oe, while for <sup>3</sup>He  $\gamma/2\pi = 3.243$  kHz/Oe. As a result, a direct interaction between magnetic moments of equal magnitude at the liquid <sup>3</sup>He–solid state substrate interface becomes possible.

The resonance magnetic coupling between liquid <sup>3</sup>He nuclei and the <sup>141</sup>Pr nuclei of microsized (45  $\mu$ m) van Vleck paramagnet PrF<sub>3</sub> powder has been discovered by authors [1]. Using nanosized PrF<sub>3</sub> powder would create a highly-coupled <sup>3</sup>He-<sup>141</sup>Pr spin system and could show new aspects of effects discovered earlier. From the other hand the low temperature magnetism of nanosized PrF<sub>3</sub> powders could exhibit a new features, compare to the magnetism of bulk van Vleck paramagnet PrF<sub>3</sub> due to the great impact of huge surface area of a sample. Besides, the influence of quantum confinement in the case of nanoscopic samples also could give some additional effects. Thus, synthesis of nanosized PrF<sub>3</sub> powders and study of their low temperature magnetism is very interesting goal.

The method of synthesis of nanosized powders of crystalline trifluoride rare earths compounds and further its size modification by means of hydro-thermal reaction was tested. As a result, a series of nanoscopic samples (size 10–50 nm) of van Vleck paramagnet PrF<sub>3</sub> were synthesized. X-ray analysis established a high crystallinity of the synthesized samples. According to the results of HRTEM during hydro-thermal reaction PrF<sub>3</sub> particles transfer from polycrystalline to single crystal structure [2].

NMR spectra of <sup>141</sup>Pr in the synthesized PrF<sub>3</sub> powders were investigated. The spectra of nanosized samples are wider than that of microsized PrF<sub>3</sub> sample, investigated earlier [1]. The simulations of <sup>141</sup>Pr NMR spectra are in good agreement with experimental data.

At the first time, nuclear pseudoquadrupole resonance was observed on  $\text{PrF}_3$  samples (including nanosized crystals) on a homebuilt pulsed NMR spectrometer. The influence of huge surface to volume ratio of nanosized powders is sensed in NMR spectroscopy parameters, as well as in nuclear magnetic relaxation rates, compared to those of microscopic and single crystal samples.

This work is partially supported by the Ministry of Education and Science of the Russian Federation (FTP “Scientific and scientific – pedagogical personnel of the innovative Russia” GK-P900).

1. Egorov A.V. *et al.*: JETP Lett. **86**, 416 (2007)
2. Tagirov M.S. *et al.*: J. Low. Temp. Phys. **162**, 645 (2011)
3. Alashin E.M. *et al.*: JETP Lett. **94**, 259 (2011)

## Spin Dephasing of Conduction Electrons in High-Mobility Quantum Wells

*S. A. Tarasenko*

*A. F. Ioffe Physical-Technical Institute, St. Petersburg 194021, Russian Federation,  
tarasenko@coherent.ioffe.ru*

An overview of recent theoretical and experimental studies of optical orientation and spin dephasing of conduction electrons in  $n$ -type quantum well (QW) structures is presented. It is shown that electron spin dynamics in high-mobility QWs drastically differs from that in low-mobility structures and is determined by the QW crystallographic orientation.

In QWs grown from III-V semiconductors along the axis [001], the electron spin relaxation in the wide range of temperature and carrier density is determined by the Dyakonov-Perel mechanism, which is based on the precession of individual electron spins in the spin-orbit Dresselhaus and Rashba magnetic fields. The time evolution of spin polarization in high-mobility structures is, therefore, damping oscillations [1, 2] rather than an exponential decay in low-mobility samples. The oscillatory regime of spin dynamics leads to a drastic change in the Hanle effect, the depolarization of optically oriented electrons in a perpendicular magnetic field. In contrast to the Lorentz function in low-mobility QWs, the Hanle curve in high-mobility samples is nonmonotonic: The spin polarization rises with the magnetic field at small fields, reaches maximum and then decreases [3]. We show that the position of the Hanle curve maximum can be used for a direct measurement of the Rashba/Dresselhaus field.

In (110)-oriented QWs, the Dyakonov-Perel mechanism is suppressed and the spin lifetime can be as long as tens of nanoseconds [4]. It is shown that, in asymmetric structures, the in-plane and out-of plane spin components are coupled and the relaxation of electron spin initially oriented along the QW normal leads to the emergence of an in-plane component [5]. We also show that optically created holes in the valence band drastically decreases the electron spin lifetime and modify the spin diffusion [6].

1. Leyland W.J.H., Harley R.T., Henini M. *et al.*: Phys. Rev. B **76**, 195305 (2007)
2. Griesbeck M., Glazov M.M., Korn T. *et al.*: Phys. Rev. B **80**, 241314 (2009)
3. Poshakinskiy A.V., Tarasenko S.A.: Phys. Rev. B (2011), arXiv:1104.2701
4. Müller G.M., Römer M., Schuh D. *et al.*: Phys. Rev. Lett. **101**, 206601 (2008)
5. Tarasenko S.A.: Phys. Rev. B **80**, 165317 (2009)
6. Völkl R., Griesbeck M., Tarasenko S.A. *et al.*: arXiv:1105.2739

## Interplay between Spin-Polarized Current and Spin Dynamics in Magnetic Nanostructures: Microwave Detection

*N. V. Volkov<sup>1,2</sup>, E. V. Eremin<sup>1,2</sup>, M. V. Rautskiy<sup>1</sup>, and D. A. Smolyakov<sup>1</sup>*

<sup>1</sup>*Kirensky Institute of Physics, Russian Academy of Sciences, Siberian branch, Krasnoyarsk 660036, Russian Federation, volk@iph.krasn.ru*

<sup>2</sup>*Siberian State Aerospace University, Krasnoyarsk 660014, Russian Federation*

In recent years, the interplay between the spin-polarized current and spin dynamics in magnetic nanostructures has attracted great interest [1]. Such interplay makes these materials promising for application in microwave signal processing and is interesting for fundamental study of spin dynamics in the nanostructures. Here we discuss the phenomenon of microwave detection in some classes of the magnetic nanostructures where both the dynamics of magnetization and the spin-polarized current play a key role.

The first class is a cooperative assembly of magnetic tunnel junctions (MTJs). A ramified network of MTJs is formed, for example, in granular manganese materials: ferromagnetic conducting grains serve as electrodes of the junctions and insulator boundaries of the grains represent potential barriers. Such materials exhibit a great value of magnetoresistance and the magnetic-

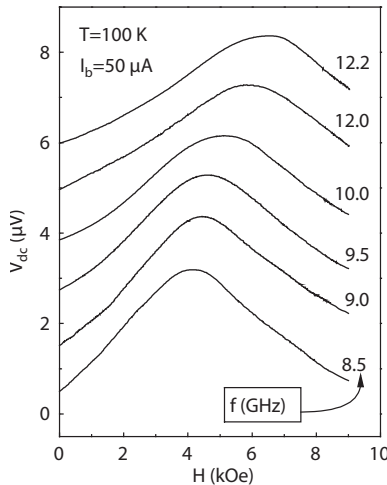


**Fig. 1.** Detected dc voltage as a function of a magnetic field in granular  $La_{0.7}Ca_{0.3}MnO_3$ .

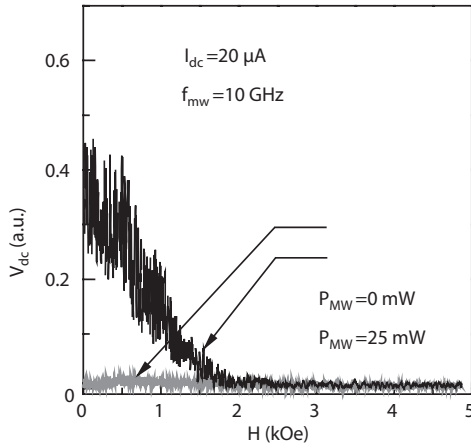


**Fig. 2.** Detected dc voltage as a function of a magnetic field in the LSMO/LSM<sub>1-g</sub>MnSi magnetic tunnel structure.

field-driven microwave detection effect (Fig. 1) [2, 3]. The magnetoresistance is caused by the magnetic tunnel mechanism, while the rectification effect is based on the interplay between the spin-polarized rf current through the tunnel junctions and magnetic resonance inside the grains forming the junctions.

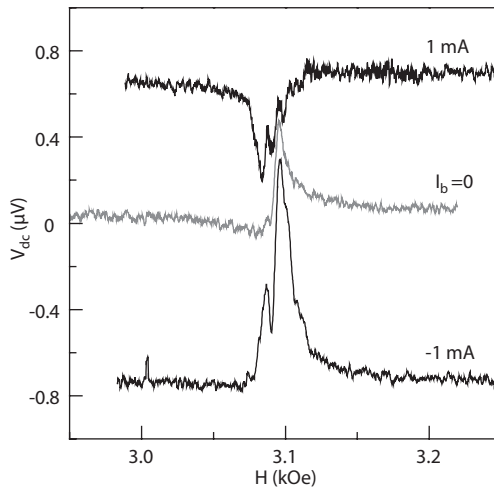


**Fig. 3.** Detected dc voltage as a function of a magnetic field in the Co/YIG magnetic bilayer.

Both rf current and resonance precession are induced by a microwave magnetic field. A rectified voltage on the sample is a total response of a set of the tunnel junctions formed in a granular system.

The second class is manganese-based magnetic tunnel structures in the current-in-plane (CIP) geometry. Current-channel switching between conducting layers determines the main peculiarities of the transport properties of the structures. The process of switching depends on resistance of MTJs between the layers and, consequently, can be driven by a bias current and a magnetic field [4, 5]. We demonstrate that a significant voltage signal can be generated by the structure irradiated by microwaves due to the rectification effect (Fig. 2). The value of the microwave-induced voltage strongly depends on a bias current and can be driven by a magnetic field. The rectification effect is caused by a classical mechanism related to nonlinearity of the current-voltage characteristic and by a mechanism involving the interplay between the spin-polarized current and dynamics of magnetization in the layers of a magnetic tunnel structure.

The third class of the magnetic nanostructures that can effectively detect microwaves is *ferromagnetic metal/ferromagnetic insulator* bilayers. As was shown for a Co/YIG structure, dc voltage is induced across the cobalt layer when resonance precession is excited in the YIG ( $\text{Y}_3\text{Fe}_5\text{O}_{12}$ ) layer (Fig. 3). In this case, the value and sign of the effect strongly depend on a bias current through the Co layer. Voltage generation is based on combination of spin pumping from a ferromagnetic insulator to a ferromagnetic metal, which induces precession of magnetization and transformation of a spin current into a charge current in the ferromagnetic film.

This work was supported by the Russian Foundation for Basic Research, project no. 11-02-00367-a; Presidium of the Russian Academy of Sciences, program Fundamentals for Basic Research of Nanotechnology and Nanomaterials (project no. 21.1); the Division of Physical Sciences of the Russian Academy of Sciences, program Spin-Dependent Effects in Solids and Spintronics (project no. 2.4.4.1); and the Federal program (St. contract no. NK-556P\_15).

1. Pribiag V.S., Krivorotov I.N. *et al.*: Nature Physics **3**, 498 (2007)
2. Volkov N.V., Eremin E.V. *et al.*: J. Phys. D: Appl. Phys. **41**, 015004 (2008)
3. Volkov N.V., Eremin E.V. *et al.*: J. Magn. Magn. Mater. **323**, 1001 (2011)
4. Volkov N.V., Eremin E.V. *et al.*: J. Phys. D: Appl. Phys. **42**, 065005 (2009)
5. Volkov N.V., Eremin E.V. *et al.*: Tech. Phys. Lett. **35**, 990 (2009)

## Generation and Oxidation of Nitroxyl Radicals by Ruthenium Complexes: A Novel ESR Approach to the Study of Photoelectron Transfer

L. Weiner

Weizmann Institute of Science, Rehovot 76 100, Israel, [lev.weiner@weizmann.ac.il](mailto:lev.weiner@weizmann.ac.il)

Novel ruthenium complexes with three bipyridyl ligands were synthesized, in which one of the bipyridyl moieties was modified by attachment of one or two hydroxamic acids groups. Photoexcitation of these Ru(II) complexes with blue light ( $\lambda_{\text{max}} = 477 \text{ nm}$ ) results in conversion of the hydroxamate to a long-lived nitroxyl radical that could be detected and characterized by ESR. Quenching of the excited state of these complexes by oxygen can generate either singlet oxygen,  $^1\text{O}_2$ , via energy transfer, or the superoxide radical,  $\text{O}_2^-$ , via electron transfer (ET). In the latter case, the  $\text{O}_2^-$  is confined within a cage complex (*vide infra*).  $^1\text{O}_2$  is the reactive species responsible for oxidation of the hydroxamate group to its corresponding nitroxyl radical. This was confirmed by use of a specific quencher,  $\text{NaN}_3$ , and by following the kinetics of nitroxyl radical formation in deuterated solvents. By use of either spin traps or superoxide dismutase we were able to remove the  $\text{O}_2^-$  radicals from the cage complex with concomitant generation of the Ru(III) which is a very powerful oxidant. Thus, the yield of nitroxyl radical formation in the novel ruthenium complexes can be increased by almost 30-fold relative to the level generated by  $^1\text{O}_2$ .

To study ET in biological systems, the donor/acceptor pair needs to be incorporated at specific loci. Stable nitroxyl radicals, SNR, and photoactive Ru(II) complexes are a good candidate pair. Site-directed mutagenesis now permits routine substitution of a Cys residue for any amino acid residue in a protein. The Cys can then be labelled with the SNR (site-directed spin labelling, SDSL). The Ru-complex is introduced at another desired site, thus allowing study of ET by both CW and time-resolved ESR. To establish the method, we first followed the kinetics of oxidation in different solvents and at different temperatures of a stable radical in solution after photo-transformation of Ru(II) to Ru(III), as described above, using time-resolved ESR with time resolution as high as  $10^{-5} \text{ s}$ . A kinetic scheme of ET in solution was proposed, and quantitative characteristics of the ET reactions, according to the Marcus theory, were obtained.

To demonstrate the applicability of the proposed ESR approach to biological systems, where both components of redox pair are fixed and spatially separated, the protein bacteriorhodopsin, BR, was selected. We used site-directed spin-labelled mutants of BR, *viz.*, BR74C, BR103C, BR163C. A spin-labelled analogue of BR retinal was synthesized and then incorporated into the active site of the apo-enzyme (BR<sub>art</sub>). The Ru(II)-bipyridyl complex was also attached at a well-defined locus of BR. Time-resolved ESR show that rates of photo-stimulated ET were significantly lower for the buried retinal analogue in BR<sub>art</sub> than for mutants in which the spin label was located at an external sites. The crystal structure of BR was used to interpret the rates of ET observed. The data obtained validate the use of the novel ESR methodology developed for investigation of photo-stimulated ET in proteins, nucleic acids and biological membrane systems.

## Time-Resolved CIDNP as a Tool To Study Inter- and Intramolecular Electron Transfer Reactions

*A. V. Yurkovskaya and O. B. Morozova*

*International Tomography Center SB RAS, Novosibirsk 630090, Russian Federation,  
yurk@tomo.nsc.ru*

Charge migration is one of the important processes in the oxidized form of biologically important molecules. Detection of the radicals resulting from oxidation using transient optical spectroscopy is not always applicable for that since not all the radicals are good chromophores. CIDNP offers a good alternative: enhancements are observed for NMR signals of nuclei that have non-zero HFI constants in transient radicals. The essence of TR-CIDNP method in investigation of the reductive electron transfer reactions is in the following. Photoinduced oxidation of the dye molecule by the quencher – biologically important molecule – is used to generate the radicals the reduction of which is a subject of study. At the geminate stage of the reaction, nuclear-spin dependent inter-system crossing and spin-selective recombination give rise to the geminate CIDNP. This stage is not resolved in CIDNP experiment, and geminate polarization is detected as NMR enhancements with no delay after the laser pulse. According to the spin-sorting nature of S-T<sub>0</sub> mechanism of CIDNP formation, radicals that escape geminate termination are “marked” by nuclear polarization that is opposite in sign to the geminate one. When the reductive electron transfer takes place, this CIDNP superimposes the geminate polarization leading to CIDNP decay (so-called CIDNP cancellation effect). The observed CIDNP kinetics is very much sensitive to the rate of the reductive electron transfer, that opens the possibility to study this reaction quantitatively by analyzing CIDNP kinetics.

One of the applications of time-resolved CIDNP is the investigation of the reduction of guanoyl radicals by different reducing agents, the reactions that models so-called “chemical way” of DNA repair. Oxidative damage of DNA is known to cause different life-degrading phenomena. Guanine is the most easily oxidized DNA component, and electron deficiency in DNA migrating over a long distance eventually ends on a guanine base. There are several enzymatic DNA repair pathways evolved in nature to prevent accumulation of damages that block a number of critical processes. Besides the relatively slow enzymatic processes of DNA repair for protecting genetic information, the electronic vacancies in DNA may be refilled rather fast via electron transfer from

the surrounding protein pool. This “chemical way” of DNA repair efficiently competes with the formation of modified sites that are targets for enzymatic repair. Our TR-CIDNP measurements were applied to reversible photocycle that includes the formation of guanosyl radicals in the quenching reaction of triplet excited dye, 2,2'-dipyridyl (DP), by guanosine-5'-monophosphate (GMP), and subsequent radical termination with the restoration of the initial compounds. CIDNP formed in the photoreactions of DP with GMP serves as a reference, and is compared to that formed in the photoreaction of DP, GMP, and reducing agent (N-acetyl derivatives of tyrosine and tryptophan, L-cysteine, L-cysteine-L-glycine and other peptides). Quantitative analysis of CIDNP kinetics allowed to obtain the rate constant of the repair of guanosyl radical in different protonation states by the above mentioned species.

Another example of time-resolved CIDNP application is spin density migration from histidyl radical to tyrosine. The long-range electron-transfer (ET) reaction involving tyrosyl radicals is known to be of great importance in proteins. Transient absorption measurements restrict observation to the tyrosyl radical, whereas TR-CIDNP technique allows one to follow the reactions of transient histidyl radicals as well using NMR detection of histidine signals. We have demonstrated that the oxidized peptides Tyr-His and His-Tyr with the radical center at the His residue undergo intramolecular ET (with the rate constant  $k_e$ ), which leads to the formation of peptide radicals with the radical center at the Tyr residue. This process was shown unambiguously by the decay of CIDNP kinetics detected for the His residue in both peptides. The influence of protonated state of amino group on  $k_e$  was explicitly shown for both peptides.

Another example of the reactions of reductive electron transfer that was studied using TR-CIDNP is intramolecular electron transfer from tyrosine residue to oxidized tryptophanyl residue in peptides and proteins.

Financial support by the Russian Fund for Basic Research (projects No. 09-03-91006-FWF, 09-03-00837-a, and 11-03-00296-a), the program of the President of Russia for support of leading scientific schools (NSh-7643.2010.3), the Program of the Division of Chemistry and Material Science RAS (project 5.1.1), and the SB RAS (projects No. 28) is gratefully acknowledged.

---

## ORAL TALKS

## Studying Spintronics Materials with Synchrotron Radiation

*N. Akdoğan*

*Department of Physics, Gebze Institute of Technology, Kocaeli 41400, Turkey,  
akdogan@gyte.edu.tr*

Spintronics, short notation for spin-based electronics, is a new research area which seeks to exploit the spin of electrons in addition to their charge in semiconductors [1]. The basic idea is to combine the characteristics of existing magnetic devices with semiconductor devices in order to realize a new generation of devices that are much smaller, more energy efficient, non-volatile, and much faster than presently available.

Diluted magnetic semiconductors (DMS) are promising candidates for spintronics applications at ambient temperatures, provided that their Curie temperature ( $T_c$ ) is far enough above room temperature. Therefore, a number of different semiconductor hosts have been investigated to test their magnetic properties. Actually, some of these studies indeed claim ferromagnetic signals above room temperature. However, the origin of ferromagnetism in this system is still under debate.

In this talk, the structural, magnetic and electronic properties of Co-implanted n-type ZnO films grown on sapphire substrates will be presented. In an attempt to fabricate ferromagnetic semiconductors, ZnO films are exposed to magnetic cobalt ions for varying implantation doses. Then the structural and magnetic properties have been investigated using synchrotron radiation.

The X-ray diffraction and transmission electron microscopy results show the presence of a (10-10)-oriented hexagonal Co phase in the sapphire substrate, but not in the ZnO film. The diameter of the Co clusters are about 5–6 nm, forming a Co rich layer in the substrate close to the ZnO/Al<sub>2</sub>O<sub>3</sub> interface [4].

However, the multiplet structure of the X-ray absorption spectra around the Co  $L_3$  edge indicates that the implanted cobalt ions are in the Co<sup>2+</sup> state in the ZnO film. Magnetization measurements show that there are two magnetic phases in the implanted region. One is the intrinsic room temperature ferromagnetism due to the Co substitution on Zn sites in the ZnO layer and the second magnetic phase originates from Co clusters in the sapphire substrate. The magnetic moment per substituted cobalt is found about 2.81  $\mu_B$  which is very close to the theoretical expected value of 3  $\mu_B$ /Co for Co<sup>2+</sup> in its high spin state [4]. Magnetic dichroism at the 0 K edge and the AHE are also observed

---

in Co-implanted ZnO films, supporting the intrinsic nature of the observed ferromagnetism.

1. Prinz G.A.: *Science* **282**, 1660 (1998)
2. Akdogan N., Zabel H., Nefedov A., Westerholt K., Becker H.W., Gök S., Khaibullin R., Tagirov L.: *J. Appl. Phys.* **105**, 043907 (2009)
3. Akdogan N., Nefedov A., Zabel H., Westerholt K., Becker H.W., Somsen C., Gök S., Bashir A., Khaibullin R., Tagirov L.: *J. Phys. D Appl. Phys.* **42**, 115005 (2009)
4. Akdogan N., Nefedov A., Westerholt K., Zabel H., Becker H.W., Somsen C., Khaibullin R., Tagirov L.: *J. Phys. D, Appl. Phys.* **41**, 165001 (2008)
5. Kobayashi M., Ishida Y., Hwang J.I., Mizokawa T., Fugimori A., Mamiya K., Okamoto J., Takeda Y., Okane T., Saitoh Y., Muramatsu Y., Tanaka A., Saeki H., Tabata H., Kawai T.: *Phys. Rev. B* **72**, 201201(R) (2005)
6. Akdoğan N., Rameev B., Güler S., Öztürk O., Aktaş B., Zabel H., Khaibullin R., Tagirov L.: *Appl. Phys. Lett.* **95**, 102502 (2009)

## Structural and Magnetic Properties of $\text{Zn}_{0.95-x}\text{Co}_{0.05}\text{Cu}_x\text{O}$ Diluted Magnetic Semiconductors by Sol-Gel Process

L. Arda<sup>1</sup>, O. Cakiroglu<sup>2</sup>, and N. Dogan<sup>3</sup>

<sup>1</sup> Department of Sciences, Bahcesehir University, Istanbul 34100, Turkey

<sup>2</sup> Istanbul University, Hasan Ali Yucel Education Faculty, Istanbul 34452, Turkey

<sup>3</sup> Gebze Institute of Technology, Department of Physics, Gebze/Kocaeli 41400, Turkey

$\text{Zn}_{0.95-x}\text{Co}_{0.05}\text{Cu}_x\text{O}$  ( $x = 0.00, 0.01, 0.02, 0.03, 0.04$  and  $0.05$ ) solutions were prepared by sol-gel synthesis using 2, 4-pentanedionate and acetate precursors which were dissolved into solvent and chelating agent [1–2].  $\text{Zn}_{0.95-x}\text{Cu}_x\text{Co}_{0.05}\text{O}$  thin films with different thickness and temperature were grown on glass and Si substrates using sol-gel deep coating. The nanoparticles and thin films were then annealed at various temperatures and times, were tried to observe the doping ratio, temperature, and thin films effect on structural and magnetic properties. The particle size, crystal structure, surface morphology and film thickness were characterized by X-ray diffraction, Scanning Electron Microscope and Atomic Force Microscope. Magnetic properties of nanoparticles and thin films were investigated by Quantum design PPMS measurement system. The temperature and applied field dependences of magnetization of nanoparticles and thin films were recorded by using a Vibrating Sample Magnetometer (VSM). Zero-field cooling (ZFC) and field-cooling (FC) conditions for magnetization as a function of temperature were performed at magnetic field of 0.5 kOe. The structure, particle size, surface morphology, film thickness, and magnetic properties of nanoparticles and the thin films with different doping ratio, thickness (number of dipping), temperature and time of annealing process are presented.

1. Heiba Z.K., Arda L.: Cryst. Res. Technol. **44**, 845–850 (2009)

2. Heiba Z.K., Arda L.: Journal of Molecular Structure, submitted for publication.

## Singlet-Triplet Energy Splitting and Entanglement of Two Holes in Double Ge/Si Quantum Dots

*A. A. Bloshkin, A. I. Yakimov, and A. V. Dvurechenskii*

*Rzhanov Institute of Semiconductors Physics, Novosibirsk 630090, Russian Federation,  
bloshkin@isp.nsc.ru*

We theoretically investigate the energy spectrum and electronic structure of two vertically stacked Ge/Si quantum dots loaded with a pair of interacting holes, and study the dependence of basic physical characteristics on dot size and interdot separation. In particular, we focus on the splitting of the lowest spin singlet and triplet states and spatial correlations between holes. Here the term “spin” is rather an index for two Kramers degenerate states. The two holes are treated by six-band  $\mathbf{k} \cdot \mathbf{p}$  calculations combined with the configuration-interaction model taking into account the realistic situation when both Si matrix and Ge nanoclusters are inhomogeneously strained. It is shown that asymmetry of strain distribution and spin-orbit coupling of the valence band introduce characteristic features in both single- and many-particle hole states, which are not captured by the usual one-band heavy-hole approximation. We find a level anticrossing between the lowest singlet and triplet states with a zero anticrossing energy gap as a function of interdot spacing. It is demonstrated that the level anticrossing between many-particle states is accompanied by a level crossing between single-particle bonding and antibonding molecular orbitals. We argue that both phenomena of level crossing and anticrossing originate from the asymmetry-induced localization of single-particle hole wave functions on different dots. Above a certain dot separation, the Mott-type delocalized-to-localized transition for the many-particle hole states is observed. We show that the transition is caused by the combined action of correlations and strain asymmetry.

We have calculated the exchange energy, double occupation probability of the lowest singlet state, and degree of entanglement of two holes in vertically coupled double Ge/Si quantum dots. We determined the conditions on which the exchange coupling is large enough for a fast swap operation in quantum computation and the double-occupancy probability is still low, thus maximizing the entanglement for a small computation error. We found that both the degree of entanglement and double-occupancy probability for quantum dots with different dot size collapse onto universal, size independent curves when plotted as a function of singlet-triplet splitting.

## **Quasioptical Techniques for High Field EPR: Opportunities, Perspectives, and Challenges**

*K. A. Earle*

*University at Albany (SUNY), Albany, USA, kearle@albany.edu*

## Recent Developments in MR- and EPR-Imaging

*U. Eichhoff and P. Höfer*

*Bruker BioSpin GmbH, Rheinstetten D76287, Germany, uwe.eichhoff@bruker-biospin.de*

Many analytical methods can be extended to image the spatial distribution of components in an inhomogeneous sample. For this purpose a space-selective excitation has to be performed and space-selective spectra have to be measured. The amplitude of any line in the spectrum may then be selected and its spatial distribution can be mapped resulting in a chemical image. The most simple method, used in FT-IR- and Raman-Microscopy, X-ray- and MALDI-TOF-imaging, employs a point-selective excitation and scans the excitation point over the sample. Today focal plane array detectors allow the registration of the complete spatial/spectral information in one shot. This is the preferred technique in FT-IR- and Raman-imaging. NMR- and EPR-imaging use a different principle. The spatial information is first encoded by orthogonal field gradients and then extracted from the NMR signal using multiple Fourier transform or projection/reconstruction techniques.

MR imaging (MRI) has unsurpassed tissue contrast and is therefore the most powerful medical imaging method. Brain areas can be correlated with various neuronal activities by non-invasive functional MRI, connectivities of neuronal fibres can be visualized by Diffusion Tensor Imaging. Applications of MRI range from clinical diagnostics to imaging of the gene expression on a cellular level. No other imaging technique offers such a broad range of medical and biological applications. In material science rocks, porous media like, polymers and rheological processes can be studied.

As compared to MRI EPR-imaging has yet limited applications in life science and material science. **First** the size of the investigated object must fit into the resonator, the dimension of which cannot exceed the line width. Therefore biomedical imaging on living objects is restricted to L- and S-band, where a mouse body and rat head can be placed in resonator. Material imaging is performed mostly on small samples in X-band and Q-band. **Secondly** the EPR signals are too fast to be registered with sufficient sensitivity in a free induction decay or spin echo, as it is done in MRI, especially if the applied gradients broadens the lines and shortens the time domain signals. Therefore EPR-Imaging (EPRI) is performed in continuous wave mode with stepped gradients. To obtain a concentration profile the signals have to be deconvoluted with the spectral line form obtained in the absence of a gradient.

Despite these limitations EPRI finds its applications. In life science tissue oximetry is probably the most important application. In material science the distribution of radicals induced by ionizing radiation and distribution of EPR-active crystal defects can be investigated. To achieve the necessary gradients a new gradient assembly and slim line resonator had to be developed. The necessary hardware and some applications will be discussed.

## Magnetic States in Cross-Like Nanomagnets

O. L. Ermolaeva, B. A. Gribkov, S. A. Gusev, A. Yu. Klimov, V. L. Mironov,  
V. V. Rogov, O. G. Udalov, and A. A. Fraerman

*Institute for Physics of Microstructures RAS, Nizhny Novgorod, Russian Federation,  
bg@ipm.sci-nnov.ru*

We report on results of computer micromodelling of anti-vortex states in cross-like ferromagnetic nanoparticles and their practical realization. Besides being a remarkable magnetic structure, the anti-vortex is expected to show unusual transport properties in an applied external magnetic field: namely, a spectacular new phenomenon, the so-called “topological” Hall effect [1].

As micromagnetic modeling and experimental results showed, that realization of anti-vortex magnetic state in symmetrical cross-like structures was very unlikely because of the high energy (=the sum of exchange and magnetostatic energies) of this magnetic configuration. Magnetic structure of symmetrical crosses depended on their aspect ratio, as expected. Crosses with relatively small aspect ratio (with lateral size of branch  $600 \times 100$  nm) showed spontaneous quasi-uniform states. The crosses with larger aspect ratio (with lateral size of branch  $600 \times 200$  nm) could go into vortex states.

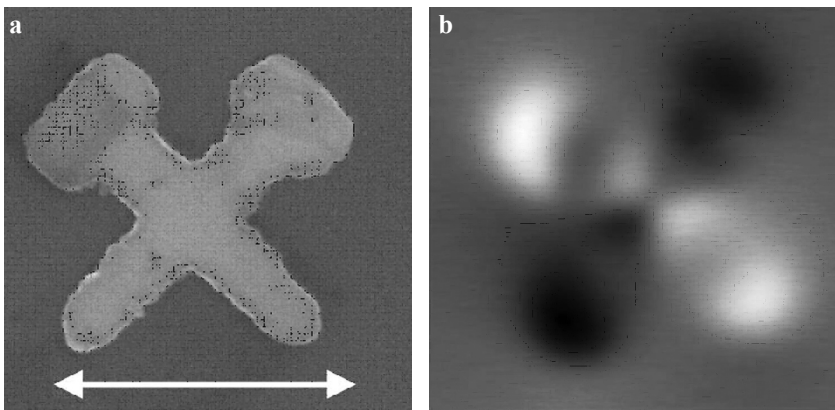


**Fig. 1.** **a** SEM image of asymmetrical cross-like Co nanoparticle. White arrows indicate the magnetization directions. The scan size is  $1.7 \times 1.7$   $\mu\text{m}$ . **b** MFM image of anti-vortex state in Co asymmetrical cross-like structure. The scan size is  $1.7 \times 1.7$   $\mu\text{m}$ .

Another situation was observed in asymmetrical cross-like ferromagnetic structures. Each branch of the cross was tapered at one end and bulbous at the other (Fig. 1a). Using the micromagnetic modeling we have demonstrated that the magnetic structure in the asymmetrical cross can be manipulated by an external magnetic field directed along one of the diagonals of the cross as follows (Fig. 1a). After magnetization in a sufficiently strong ( $\sim 1$  kOe) magnetic field we obtained a quasi uniform distribution of magnetization and after the action of reversed magnetic field  $H_1 < H < H_2$  ( $H_1$  and  $H_2$  are the coercivity of bulbous and tapered ends respectively) we obtained the anti-vortex distribution. The arrays of cobalt crosses with  $1 \mu\text{m}$  branches,  $100 \text{ nm}$  widths of the branches and  $30 \text{ nm}$  thicknesses, were fabricated using e-beam lithography and ion etching. The stable formation of anti-vortex magnetic states in these nanostructures during magnetization reversal was demonstrated experimentally using magnetic force microscopy (Fig. 1b).

The work was supported by the RFBR.

1. Neubauer A., Pfleiderer C., Binz B. *et al.*: Phys. Rev. Lett. **102**, 186602 (2009)

## Electron Spin Polarized Nitroxide Radicals as Alternative Spin Probes for Inhomogeneity of Molecular Aggregates

*V. R. Gorelik<sup>1</sup>, V. F. Tarasov<sup>2</sup>, Yu. A. Zakharova<sup>2</sup>, and E. G. Bagryanskaya<sup>1</sup>*

*<sup>1</sup> International Tomography Center SB RAS, Novosibirsk 630090, Russian Federation, vit@tomo.nsc.ru*

*<sup>2</sup> Semenov's Institute of Chemical Physics, RAS, Moscow 119991, Russian Federation, valery742@gmail.com*

It is well known that polyelectrolytes in aqueous micellar solutions of oppositely charged ionic detergents generate self-assembling molecular aggregates whose structure is still poorly understood [1]. At the same time the chemical structure of polyelectrolyte and detergent, their concentrations, pH of solution, and etc. are well established to effect on the aggregates' properties, such as molecular weight, solubility, amount of charged groups, conformation of polymer chains and etc. The EPR spectroscopy of the spin probe has been proved to be capable for securing valuable information on the molecular mobility of a environment where the spin probe is presumably located. Unfortunately, interpretation of this information is heavily based on intuitive expectations concerning the localization of the probe. Moreover, there are examples [2] when EPR spectra of the probe are the same as in the micellar and micelle-polymer aggregate aqueous solutions.

To gain insight the characteristics of the clusters' interior, we apply the time resolved EPR of the electron spin polarized probe. The new experimental approach is based upon the Electron Spin Polarization Transfer (ESPT) from the spin polarized electronically excited molecular triplet (benzil) to the stable nitroxide radical (TEMPO). The systems under investigation were the aqueous micellar solutions of the anionic (SDS) or cationic (Tetradecyltrimethylammonium Bromide) surfactants in the presence of polycation (quaternized poly-(N-ethyl-4-vinyl-pyridine bromide with 50% and 90% quaternization degree) or the polyanion (polymethacrylic acid), respectively.

Whereas the "Polarized Spin Probe" was found to be sensitive to the quaternization degree of PEVP, the CW EPR spectra of TEMPO do not reveal any difference. The advantage of new approach is provided by that the fact that two probes were involved into operation. This essentially restricts an ambiguity in conclusions on the location sites since the other probe (molecular triplet) were chosen to possess different hydrophilic characteristics.

Acknowledgments: Russian Scientific School-7643.2010.3, Division of Chemistry and Material Science (5.1.1), Russian Federal Agency for Education (P1144) are acknowledged for the financial support.

1. Hayakawa K., Kwak J. in: Cationic Surfactants: Physical Chemistry; Surfactant Sci. Ser. (Rubingh D., Holland P.M., eds.), p. 189. 1991.
2. Wasserman A.M., Motyakin M.V., Yasina L.L. *et al.*: J. Appl. Magn. Reson. **38**, 117–135 (2010)

## Improved Probehead for Pulse High Field / High Frequency EPR Spectroscopy

Yu. Grishin<sup>1,3</sup>, A. Savitsky<sup>1</sup>, R. Rakhmatullin<sup>2</sup>, E. Reijerse<sup>1</sup>, and W. Lubitz<sup>1</sup>

<sup>1</sup>Max-Planck-Institut für Bioanorganische Chemie, Mülheim an der Ruhr 45470, Germany

<sup>2</sup>Kazan Federal University, Kazan 420008, Russian Federation

<sup>3</sup>Institute of Chemical Kinetics & Combustion, Novosibirsk 630090, Russian Federation, grishin@kinetics.nsc.ru

The sensitivity and time resolution (bandwidth) of pulsed EPR spectrometer are defined by the characteristics of the resonator. The performance of the resonator is characterized by the value  $\eta \cdot Q$ , where  $Q$  is a figure of merit ( $Q$ -factor) of the resonator, and  $\eta$  is the filling factor [1]. The resonator is connected to the transmission line with the coupling device and resulting loaded  $Q_L$  – “Loaded  $Q$ -factor” is related to the bandwidth  $\Delta\omega$  of the resonator by  $\Delta\omega = \omega_0/Q_L$ ,  $Q_L = I_0/(1 + \beta)$ , where  $Q_0$  is the unloaded quality factor and  $\beta$  is the coupling parameter. The advanced pulsed techniques require wide range of the loaded quality change that can be done with the appropriate coupling device.

In present work we suggest a coupler construction with the circular coupling hole and a spherical movable element similar to one, used by Prof. Möbius and co. and described in [2], but in a different geometry. The combination of “sphere – circular hole” acts as a broadband impedance transformer, which greatly facilitates its use. This device has less number of degrees of freedom in choosing of the device dimensions as compared to used in commercial instruments (two parameters of change – sphere diameter and distance to “iris hole” only), greatly facilitates its manufacture and reproducibility, and, finally, enables us to obtain the fine adjustment of  $\beta$  from undercoupling ( $\beta \ll 1$ ) to strong overcoupling ( $\beta \gg 1$ ).

We present in the report the probehead design for Q- and W-band EPR as well as results of electromagnetic simulation and measurements.

This work was supported by RFBR (project No.09-03-91335-NNIO\_a).

1. Poole C.P.: Electron Spin Resonance: A Comprehensive Treatise on Experimental Techniques. 2nd Edition, Dover Publications, 1997.
2. Burghaus O., Rohrer M., Gotzinger T., Plato M., Möbius K.: Meas. Sci. Technol. **3**, 765 (1992)

## Novel Millimeter Wave EPR System ELEXSYS E780 (Bruker): Design and Performance

*I. Gromov<sup>1</sup>, P. Höfer<sup>2</sup>, and D. Schmalbein<sup>2</sup>*

<sup>1</sup> Bruker Biospin, Rheinstetten D-76287, Germany, Igor.Gromov@Bruker-Biospin.de

<sup>2</sup> Bruker Biospin, Rheinstetten D-76287, Germany

A novel ELEXSYS E700/E780 EPR spectrometer has recently been developed by Bruker Biospin. The spectrometer utilizes the latest achievements of millimeter wave technology in combination with the well-proven Bruker intermediate frequency (IF) concept. The IF bridge operates at X-band frequencies for excitation and detection in both CW and pulse EPR modes. The quasi-optical front-end converts the IF bridge frequencies up to 263 GHz for excitation and down converts the resulting reflection mode or induction mode signal to X-band frequencies for quadrature detection.

An innovative cryogen-free sweepable 12 T magnet has been specifically designed. Its main and high-resolution  $\pm 0.15$  T sweep coils provide ultimate and fast control over magnetic field. The cryogen-free approach simplifies magnet maintenance considerably and eliminates the extra helium boil off during main coil sweeps. The spectrometer is controlled via the Xepr software package.

ELEXSYS E700/E780 features two detection modes: reflection and induction. In reflection mode, the response signal co-polarized to the excitation wave is recorded while in induction mode, the cross-polarized wave is observed. In both detection modes, the signal is detected in quadrature providing absorption/dispersion signals in CW operation and real/imaginary signals in pulse operation.

The E780 wide sample space probe head is based on a tapered corrugated transmission line and works in a non-resonant and resonant configuration. The cylindrical sample area is up to 5 mm of diameter. The samples are mounted in a Teflon cylinder which is then attached to a sample holder for vertical positioning of the sample. The TE<sub>011</sub> ENDOR probe head has similar transmission line ended with taper to rectangular waveguide. It has variable frequency tuning and coupling. Moreover, the probe incorporates both ENDOR and CW modulation coils and, optionally, optical access for sample illumination. Both probeheads are suitable for helium temperature operation.

## Spin Kinetics of $^3\text{He}$ in Porous Substrates

*A. V. Klochkov, E. M. Alakshin, R. R. Gazizulin, V. V. Kuzmin, M. S. Tagirov,  
and D. A. Tayurskii*

*Kazan Federal University, Kazan 420008, Russian Federation, klochkov@gmail.com*

The study of spin kinetics of  $^3\text{He}$  in porous substrates at low temperatures is in the matter of interest due to two research directions. One is the study of direct magnetic coupling between  $^3\text{He}$  and solid state substrate. The second – is the obtaining information about properties of porous media. The main subject of the present work is the study of spin kinetics of  $^3\text{He}$  in contact with different types of silica aerogels, clay minerals and nanosized crystal powders of van Vleck paramagnet  $\text{PrF}_3$ .

The spin kinetics of  $^3\text{He}$  in the silica aerogel was studied in temperature range 1.5–4.2 K. The magnetic relaxation times  $T_1$  and  $T_2$  for adsorbed, gaseous, and liquid  $^3\text{He}$  in the 95%-porosity aerogel at a temperature of 1.5 K were obtained by NMR technique. It was shown that the intrinsic relaxation mechanisms in the liquid and gas phases are much weaker than the relaxation through the adsorbed surface layer. Also, the influence on the magnetic relaxation of thermalization processes in the system “ $^3\text{He}$ -aerogel” has been studied [1, 2].

In the case of clay minerals, new method of obtaining of integral porosity of porous sample by the means of  $^3\text{He}$  NMR was proposed and tested. Also, using inverse Laplace transform algorithm, the distribution of nuclear magnetic relaxation times of  $^3\text{He}$  was obtained [3].

Spin kinetics of  $^3\text{He}$  in the system “nanosized  $\text{PrF}_3$ - $^3\text{He}$ ” was investigated. The model of longitudinal magnetization relaxation of  $^3\text{He}$  nuclei was proposed. According to this model the longitudinal relaxation of  $^3\text{He}$  is carried out both by the  $^3\text{He}$  adsorbed film on the surface and due to the modulation of dipole-dipole interaction in strongly inhomogeneous magnetic field, caused by nanosized  $\text{PrF}_3$  particles [4].

This work was supported partly by the Russian Foundation for Basic Research (project 09-02-01253).

1. Klochkov A.V. *et al.*: JETP Lett. **88**, 823 (2008)
2. Alakshin E.M. *et al.*: JETP Lett. **93**, 223 (2011)
3. Gazizulin R.R. *et al.*: Appl. Magn. Resonance. **38**, 271 (2010)
4. Tagirov M.S. *et al.*: J. Low. Temp. Phys. **162**, 645 (2011)

## Determining the Parameters of ESR Spectra by Computer Analysis of the Spectrum Lineshape

*A. I. Kokorin<sup>1</sup> and E. A. Konstantinova<sup>2</sup>*

<sup>1</sup> *Department of Kinetics and Catalysis, N. Semenov Institute of Chemical Physics RAS, Moscow 119991, Russian Federation, alex-kokorin@yandex.ru*

<sup>2</sup> *Physics Department, Lomonosov Moscow State University, Moscow 119991, Russian Federation*

Nitrogen doped titanium dioxide (N-TiO<sub>2</sub>) photocatalysts, effective in different oxidation reactions under illumination with visible light ( $400 < \lambda < 1000$  nm), were prepared according to [1]. Electron paramagnetic resonance (EPR) X-band spectra were recorded at 298 and 77 K. Two types of paramagnetic centers involved into photocatalytic process were revealed (Fig. 1). Dynamic concentrations of N<sup>•</sup> and NO depended strongly on temperature and irradiation of the samples with visible or UV light.

The simulation of the spectra gave the following parameters of spin-Hamiltonian:  $g_1 = 2.0028$ ,  $g_2 = 2.0001$ ,  $g_3 = 1.9280$ ;  $A_1 = 0.1$  G,  $A_2 = 31.0$  G,  $A_3 = 7.0$  G, and  $\Delta H_1 = 5.0$  G,  $\Delta H_2 = 6.2$  G,  $\Delta H_3 = 21.0$  G, where  $\Delta H_k$  are the appropriate line widths. Parameters are in a good agreement with those published in [2]:  $g_1 = 2.000$ ,  $g_2 = 1.996$ ,  $g_3 = 1.9248$ ;  $A_1 = 0$ ,  $A_2 = 32.2$  G,  $A_3 = 3.6$  G, and  $\Delta H_1 = 4.5$  G,  $\Delta H_2 = 3.9$  G,  $\Delta H_3 = 20.1$  G, which were ascribed to the nitric oxide NO molecule, the unpaired electron in which is located in  $2\pi$ -antibonding orbital.

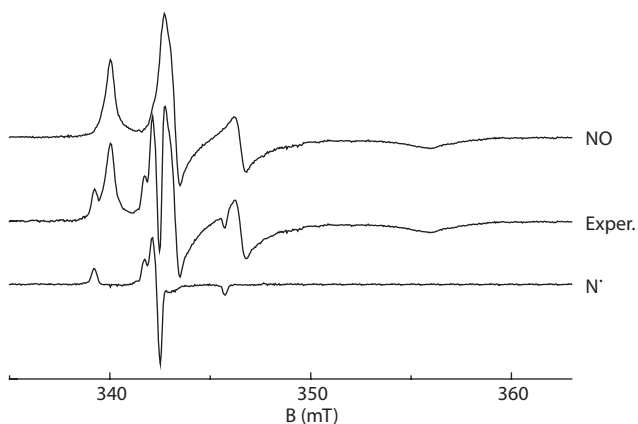


**Fig. 1.** EPR spectra of N-TiO<sub>2</sub> at 77 K: experimental (Exper.) and divided to NO and N<sup>•</sup>.

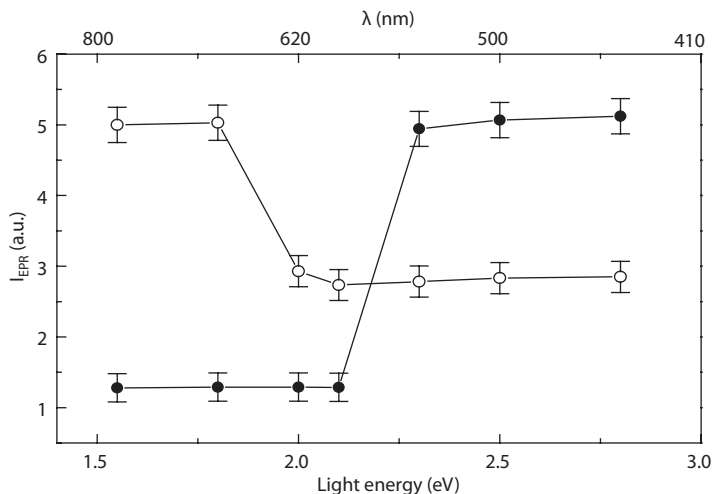


**Fig. 2.** Dependence of the integral intensity of EPR spectra on the laser wavelength after 10 min of irradiation at 298 (●) and 120 K (○).

Simulation of the second spectrum gave:  $g_1 = 2.009$ ,  $g_2 = 2.0054$ ,  $g_3 = 2.00408$ ;  $A_1 = 2.3$  G,  $A_2 = 3.1$  G,  $A_3 = 32.75$  G, and  $\Delta H_1 = 3.5$  G,  $\Delta H_2 = 3.0$  G,  $\Delta H_3 = 3.2$  G, which are close to:  $g_1 = 2.0044$ ,  $g_2 = 2.003$ ,  $g_3 = 2.002$ ;  $A_1 = 2$  G,  $A_2 = 3.2$  G,  $A_3 = 32.3$  G, and  $\Delta H_1 = 3.9$  G,  $\Delta H_2 = 2$  G,  $\Delta H_3 = 2.8$  G. These signals are attributed to N' atoms embedded in a solid matrix [3], which can be either substitutional ones (Ti–N'–Ti) or interstitial ones (O–N'–Ti).

Energy levels, equal to 2.3 and 2.0 eV correspondingly to N' and NO centers, were measured in the band gap of N-TiO<sub>2</sub> (Fig. 2). *In-situ* EPR studies at 298 K were carried out for dry and wet samples in dark and under illumination. Probable photochemical and chemical reactions in which NO and N' radicals are involved, will be discussed.

The authors are thankful to Prof. H. Kisch (Erlangen-Nurnberg University, Germany) and Prof. N. Alonso-Vante (University of Poitiers, France), kindly provided a few samples for this work. EPR measurements were partially done with the equipment of the MSU Center of the Collective Usage.

1. Sakthivel S., Kisch H.: *ChemPhysChem* **4**, 487 (2003)
2. Konstantinova E.A., Kokorin A.I., Lips K., Sakthivel S., Kisch H.: *Appl. Magn. Reson.* **35**, 421 (2009)
3. Livraghi S., Paganini M.C., Giamello E., Selloni A., Valentin C.D., Pacchioni G.: *J. Am. Chem. Soc.* **128**, 32 (2006)

## Charge and Spin Dynamics of a Single Donor Coupled to an SET in Silicon

*G. Mazzeo<sup>1,2</sup>, E. Prati<sup>2</sup>, M. Belli<sup>2</sup>, G. Leti<sup>2</sup>, S. Cocco<sup>2</sup>, M. Fanciulli<sup>1,2</sup>,  
F. Guagliardo<sup>3</sup>, and G. Ferrari<sup>3</sup>*

<sup>1</sup> *Material Science Department, Bicocca University, Milano, Italy*

<sup>2</sup> *Laboratorio MDM, IMM-CNR, Agrate Brianza, Milano, Italy*

<sup>3</sup> *Dipartimento di elettronica e informazione – Politecnico di Milano, Milano, Italy*

Achieving control of the charge of a single donor and of the spin of the electron bound to it represents the first building block for donor based quantum computing. A Silicon SET has been recently used with success to measure the charge and spin of a single donor [1]. Using a similar system we studied the statistics of the charge transfer dynamics between the SET and the donor and the influence of the magnetic field on it. The sample consists of an MOS transistor with a gate of 300 nm length and 30 nm width. Electrostatics and quantum effects reduce the charge density below the gate, where a quantum dots is formed. Two lateral gates, on both sides of the main gate, are used to modify

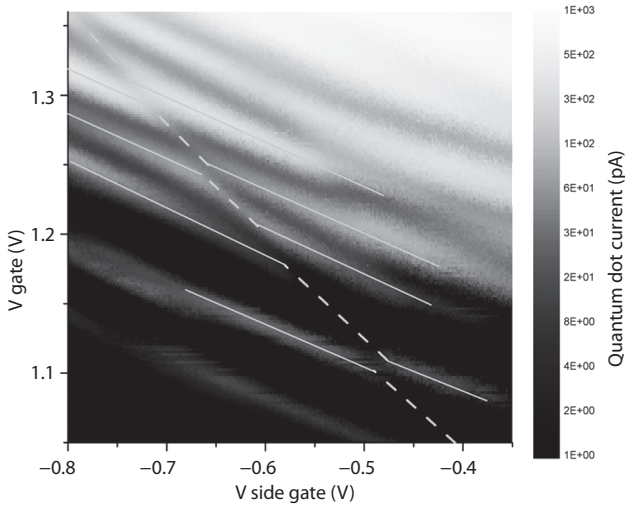


**Fig. 1.** Coulomb blockade peaks controlled by the gate and the side gates of the transistor. A shift in the pattern is observed when the QD energy levels (gray line) cross the donor energy (dashed line).

the energy profile around the quantum dot. The device is realized on a phosphorous doped substrate with a doping concentration of  $1\text{--}5 \cdot 10^{15} \text{ cm}^{-3}$  such that only few donors are expected to be in the vicinity of the quantum dot therefore not contributing to the conduction. Coulomb blockade is observed at cryogenic temperature as conductance peaks vs. gate voltage, while the lateral gates determine a rigid translation of the energy spectrum. We associate a spin state to each conductance peak by observing their Zeeman shift up to 12 T. Ionization/deionization of single donors, observed as sudden shifts of the Coulomb blockade pattern, can be controlled applying proper voltages on the gates. Due to the capacitive coupling between the quantum dot and the donor the addition of a single electron to the donor shifts the Coulomb blockade peaks leading to a measurable change of the conduction current through the SET.

Using a custom cryogenic amplifier realized in standard 3.3V CMOS technology 0.35  $\mu\text{m}$ , operating at 1.5 K and mounted close to the device we detect random telegraph signal with a bandwidth of 30 kHz and large signal to noise ratio, when the quantum dot and donor levels are aligned in energy. The statistics of this noise can contain information on the energy levels involved in the process [3, 4]. A study of the full statistics as a function of the temperature, down to 300 mK, and the magnetic field, up to 6 T, has been performed in order to investigate the charge and spin dynamics of this system.

1. Morello A. *et al.*: Nature **467**, 687–691 (2010), doi:10.1038/nature09392
2. Prati E., Belli M., Cocco S., Petretto G., Fanciulli M.: Appl. Phys. Letters **98**, 5, 053109 (2011)
3. Prati E., Belli M., Fanciulli M., Ferrari G.: Appl. Phys. Letters **96**, 113109 (2010)
4. Zhang X.C., Mazzeo G., Brataas A., Xiao M., Yablonovitch E., Jiang H.W.: Phys. Rev. B **80**, 035321 (2009)

## Spin Dynamics and Bloch Equations for Paramagnetic Centers with Spin 1/2 Having Anisotropic $g$ -Tensor

*A. G. Maryasov<sup>1</sup> and M. K. Bowman<sup>2</sup>*

<sup>1</sup> *Institute of Chemical Kinetics & Combustion SB RAS, Novosibirsk 630090, Russian Federation, maryasov@kinetics.nsc.ru*

<sup>2</sup> *Department of Chemistry, University of Alabama, Tuscaloosa 35487, USA, mkbowman@as.ua.edu*

Paramagnetic centers (PCs) with anisotropic  $g$  tensor possess some unique features compared to isotropic PCs because their magnetic moment is not coincident with direction of their mean spin vector, and because the length of the magnetic moment varies with the orientation of spin. Their spins are not quantized along the external magnetic field. The manifestation of such anisotropy in continuous wave (CW) EPR experiments has been described [1]. Here we examine features of the spin dynamics of PCs having significant anisotropy of  $g$ -tensors ( $\delta g \sim g$ ) during the course of pulsed EPR experiments.

The magnetic moment operator,  $\hat{\mu}$ , of the PC is proportional to its spin operator,  $\hat{S}$ , via

$$\hat{\mu} = -\beta g \hat{S}. \quad (1)$$

Here  $\beta$  is the Bohr magneton, the minus sign is due to the negative charge of the electron, and  $g$  is the  $g$ -tensor. The Zeeman interaction of the anisotropic PC with an external magnetic field  $\mathbf{B}_0 = B_0 \mathbf{b}$  is described by the Hamiltonian  $\mathcal{H} = -\mathbf{B}_0 \cdot \hat{\mu} = \beta \mathbf{B}_0^T g \hat{S}$ . The latter may be presented as  $\mathcal{H} = -\beta B_0 g_{\text{eff}} \mathbf{k} \cdot \hat{S}$  using the unit vector  $\mathbf{k}$  defining the quantization axis for the PC's spin,  $\mathbf{k} = \mathbf{g}^T \mathbf{b} / g_{\text{eff}}$ , with  $g_{\text{eff}}$  being the effective value of  $g$ -tensor defined by  $g_{\text{eff}} = (\mathbf{b}^T \mathbf{G} \mathbf{b})^{1/2}$ , where  $\mathbf{G}$  is the symmetric tensor [1],  $\mathbf{G} = \mathbf{g} \mathbf{g}^T$ . The spin dynamics of a PC governed by the above Hamiltonian with an arbitrary magnetic field  $B_0(t)$  is precession of spin around the instantaneous direction of the quantization axis with an instantaneous angular Zeeman frequency  $\omega_0 = \beta B_0 g_{\text{eff}} / \hbar$ . The Bloch equation for the mean value of spin vector  $\mathbf{s}$  in the absence of relaxation is

$$\partial \mathbf{s} / \partial t = (\beta / \hbar) = \{ \mathbf{s} \times \mathbf{g}^T \mathbf{B}_0 \}. \quad (2)$$

The quantity to measure experimentally is magnetic moment  $\mathbf{M} = \langle \hat{\mu} \rangle$ , making use of (1) it is easy to get  $\partial \mathbf{M} / \partial t = (\beta / \hbar) \mathbf{g} \{ \mathbf{g}^{-1} \mathbf{M} \times \mathbf{g}^T \mathbf{B}_0 \}$ , see also [2]. After some algebra

$$\partial \mathbf{M} / \partial t = (\beta / \hbar) \text{Det}(\mathbf{g}) \{ \mathbf{G}^{-1} \mathbf{M} \times \mathbf{B}_0 \} = s(\beta / \hbar) \sqrt{\text{Det}(\mathbf{g})} \{ \mathbf{G}^{-1} \mathbf{M} \times \mathbf{B}_0 \}, \quad (3)$$

where  $\text{Det}(X)$  is the determinant of matrix  $X$ ,  $s$  is the  $g$ -tensor signature,  $s = \text{sign}(\text{Det}(g))$ . It should be noted that eigenvectors  $\mathbf{M}_j$  of Eq. (3) are not “directly” orthogonal, the proper relation is  $\mathbf{M}_i^T \mathbf{G}^{-1} \mathbf{M}_j \propto \delta_{ij}$ .

The easier way to calculate signal in pulse EPR experiments is to use rather simple Eq. (2) for spin dynamics calculation taking account of (1) at the latest stage of the signal detection during free precession period. The oscillating magnetic moment components in the laboratory frame may be presented as

$$\begin{aligned} M_x(t) &= A g_1 \sin(\Psi - \omega_0 t), \\ M_y(t) &= A \{ g_0 \cos(\Psi - \omega_0 t) + g_2 \sin(\Psi - \omega_0 t) \}. \end{aligned} \quad (4)$$

Here the time  $t$  is counted after the end of the last pulse, the amplitude  $A$  is proportional to equilibrium magnetization, and altogether with the phase  $\Psi$  depends on the parameters of sequence of microwave pulses during preparing period, and on  $g$ -tensor anisotropy, and

$$\begin{aligned} g_0 &= \sqrt{\text{Det}(\mathbf{G})} / g_1 g_{\text{eff}}, \\ g_1 &= \sqrt{G_{xx} - G_{xz}^2 / G_{zz}} \quad [1], \\ g_2 &= (G_{yx} G_{zz} - G_{yz} G_{zx}) / (g_1 G_{zz}). \end{aligned} \quad (5)$$

Magnetization (4) is elliptically polarized. In the standard rotating frame the signal may be presented as

$$M_+(t) = \iota A' \exp[\iota(\Delta t - \Psi)] \{ (g_1 + s g_0) + \iota g_2 \}, \quad (6)$$

where  $\Delta$  is the mw frequency offset.

The main difference between isotropic and anisotropic case is appearance of the factor which is linear combination of  $g_i$ .

The most important consequences of  $g$ -tensor anisotropy are the following, a) the spectrum of free induction decay (FID) is different compared to CW EPR spectrum, b) the two pulse spin echo signal does not coincide with two back-to-back FID signals.

This research is supported by the National Institutes of Health through GM069104 and HL095820.

1. Abragam A., Bleaney B.: Electron Paramagnetic Resonance of Transition Ions, chapters 3, 15. Dover Publications, N.Y., 1986.
2. Pryce M.H.L.: Phys. Rev. Letters **3**, 375 (1959)

## Quantum Memory on Electron Spins in Resonator

S. Moiseev

*Zavoisky Physical-Technical Institute, Russian Academy of Sciences, Kazan 420029,  
Russian Federation, samoi@yandex.ru*

## Cooperative Spin Crossover Phenomena in Elastic Chains of Exchange Clusters. Transfer Matrix Approach

*V. A. Morozov and N. N. Lukzen*

*International Tomography Center SB RAS, Novosibirsk, Russian Federation,  
Novosibirsk 630090, Russian Federation, moroz@tomo.nsc.ru*

Last years a considerable interest is attracted to polymer-chain heterospin complexes of  $\text{Cu}(\text{hfac})_2$  with nitronyl nitroxide radicals [1]. These compounds display unusual cooperative spin crossover phenomena at low temperature. The effective magnetic moment of these complexes as well as exchange integral of paramagnetic clusters can very sharply change in a narrow temperature range that is typical for solid state phase transitions. The cooperative phenomena can occur both in chains of two- and three-spin exchange  $\text{Cu}(\text{II})$  clusters with different motifs of polymer chain. It was proved [2] that quasi one-dimensional molecular structure of these complexes is essential for the phenomena to take place since it was established that analogous compounds with 2D and 3D structures display no phase transitions.

In the contribution presented we suggest a new theoretical approach [3] to describe such a magnetic structural transitions in chains of exchange clusters. The approach is based on the **exact solution** for partition function of infinite elastic chain of exchange clusters developed with a transfer matrix technique [4]. Including elastic parameters of chain and distant dependent exchange integral our model describes smooth spin crossover as well as experimentally observable cooperative spin crossover of spin-Peierls type that results in duplication of chain constant. The temperature of possible phase transition and its magnetic effect are analytically estimated. Temperature dependences of effective magnetic moment, averaged exchange integrals of clusters and heat capacities are also obtained. We considered both cases of two-spin polymer chains with “head-to-tail” motif and three-spin polymer chains with “head-to-head” motif. In practice a mixtures of exchange clusters of different metals can be prepared. Within our model we also have calculated how such a mixture of  $\text{Cu}(\text{II})$  exchange clusters with exchange clusters of different metal can shift cooperative properties of pure compounds.

The work was supported by Russian Foundation for Basic Research (Project 10-03-00075 and Project 09-03-00091).

1. Ovcharenko V.I., Fokin S.V., Romanenko G.V., Ikorskii V.N., Tretyakov E.V., Vasilevsky S.F., Sagdeev R.Z.: *Mol. Phys.* **100**, 1107 (2002); Ovcharenko V.I., Romanenko G.V., Maryunina K. Yu., Bogomyakov A.S., Gorelik E.V.: *Inorg. Chem.* **47**, 9537 (2008)
2. Tretyakov E.V., Fokin S.V., Romanenko G.V., Ikorskii V.N., Vasilevsky S.F., Ovcharenko V.I.: *Inorg. Chem.* **45**, 3671 (2006)
3. Morozov V.A., Lukzen N.N., Ovcharenko V.I.: *Phys.Chem.Chem.Phys.* **12**, 13667 (2010)
4. Stanley H.E.: *Introduction to Phase Transitions and Critical Phenomena*. Clarendon Press, Oxford, 1971.

## EPR Data on the Transformation of As-Grown Phosphorus Centers in Synthetic Diamonds at the Hthp Treatment

*V. A. Nadolinniy<sup>1</sup>, Yu. N. Palyanov<sup>2</sup>, I. N. Kupriyanov<sup>2</sup>, M. E. Newton<sup>3</sup>,  
and S. L. Veber<sup>3</sup>*

<sup>1</sup> *A. V. Nikolaev's Institute of Inorganic Chemistry, SB RAS, Novosibirsk 630090,  
Russian Federation, [spectr@niic.nsc.ru](mailto:spectr@niic.nsc.ru)*

<sup>2</sup> *Institute of Geology and Mineralogy, SB RAS, Novosibirsk 630090,  
Russian Federation, [palyanov@uiggm.nsc.ru](mailto:palyanov@uiggm.nsc.ru)*

<sup>3</sup> *University of Warwick, Physics, Warwick, UK, [m.e.newton@warwick.ac.uk](mailto:m.e.newton@warwick.ac.uk)*

This communication presents new data on phosphorus – containing centers in synthetic diamonds grown in P-C system by HTHP method and annealed in the temperature range 2073–2573 K. EPR study have shown that as-grown at 1873 K diamonds contain single substitutional nitrogen (P1) and single substitutional phosphorus (MA1) centers. The main part of the spin density in the MA1 center locates on the carbon atom  $C_1$  separated from phosphorus by one carbon atom. HPHT annealing (7 GPa, 2073–2273 K) results in aggregating substitutional nitrogen and phosphorus atoms. On the first step of annealing (2073 K) of as-grown diamonds nitrogen- phosphorus NIRIM8 (NP1) centers are created. There is supposed that nitrogen and phosphorus atoms in this center are separated by two carbons. Further temperature increasing shifts nitrogen atom towards phosphorus and creates two new nitrogen-phosphorus centers NP2, NP3 with the supposed structures  $C_1-N-C-P$  and  $N-P-C_1$  respectively. The main part of the spin density in MA1, NIRIM8 (NP1), NP2 and NP3 is located on the carbon atom  $C_1$ . Annealing these samples in the temperature range 2073–2273 shown a vanishing of NIRIM8 and an increasing of NP2 and NP3 centers. HPHT annealing of diamonds at 2573 K significantly changes EPR spectra: all previous nitrogen–phosphorus centers disappeared and two new phosphorus centers NP4 and NP5 are created. Features of these centers are  $g \approx 2.001$  and the high spin density located on the phosphorus atoms. The NP5 center is sensitive to X-ray irradiation and low temperature annealing. EPR spectra of both these centers are due to hyperfine structure of one phosphorus atom. The structures of all phosphorus containing centers are discussed.

## Magnetic Resonance Studies of Spintronic and Nanomagnetic Materials

B. Rameev<sup>1,2</sup>

<sup>1</sup> *Zavoisky Physical-Technical Institute, Russian Academy of Sciences, Kazan 420029, Russian Federation*

<sup>2</sup> *Department of Physics, Gebze Institute of Technology, Gebze-Kocaeli 41400, Turkey*

Magnetic resonance has been proven as unsurpassed method to probe various properties of magnetic materials, such as the local magnetic anisotropy and exchange energies, structural properties, dynamic damping parameters, *etc.* One of the most fascinating fields of nanoscience is study of spintronic (magneto-electronic) materials, which are very important for both fundamental science and technology applications.

In this work we review an application of magnetic resonance to study the magnetic properties of various thin films, including half metallic ferromagnets (e.g., as chromium dioxide and Heusler alloys) and magnetic oxides (TiO<sub>2</sub>, ZnO, double perovskites and others). It is demonstrated that this technique is very effective technique to study the magnetic anisotropies. For instance, the effect of magnetocrystalline anisotropies, including the strain anisotropies, have been studied by ferromagnetic resonance (FMR) in half metallic films. Besides, the room-temperature anisotropic ferromagnetism in the oxides, implanted by transition metal ions (Co, Fe), have been observed. We have also shown that the anisotropy in the magnetic properties of the TiO<sub>2</sub> and ZnO thin films/plates, implanted by Co<sup>+</sup> or Fe<sup>+</sup> ions, may appear both as result of an intrinsic (substitutional ions) and extrinsic (magnetic nanoparticles) ferromagnetism.

The author acknowledges the support of DPT (State Planning Organization of Turkey) by the project No. 2009K120730 and RFBI/TUBITAK Programme under the grant 10-02-91225\_CT / 209T061.

## Competition between Two Spin Teams: Defects in Diamond vs. Defects in Carborundum

A. A. Soltamova, V. A. Soltamov, and P. G. Baranov

*Department of the Solid State Physics, Ioffe Physical-Technical Institute,  
St. Petersburg 194021, Russian Federation, pavel.baranov@mail.ioffe.ru*

Day after day, year after year the era of the computers that deals with spin states instead of charge states of electrons – the era of quantum information processing – is becoming closer. Many single-spin systems appropriate for these purposes were proposed during the past years that can be generally separated into two big groups, namely, quantum dots and atoms. The latter group, among others, includes the most promising center – nitrogen-vacancy defect (NV) in diamond. To date it is the only system that can be initialized, manipulated and measured under ambient conditions due to the specific excitation-emission cycle that leads to more than 90% spin alignment between electron spin levels and the very strong dependence of the fluorescence intensity on the spin state of the system [1].

The systematic theoretical approach towards the search of the systems that would possess properties similar to those of the NV defects has been recently launched by Weber and co-workers [2]. The comprehensive list of criteria that should be satisfied by the host material and the defect itself so that the whole system can be operated likewise NV center was suggested. So now the question is: can we find defects in other hosts that overcome the properties of NV center in diamond and become more appropriate as qubits? And the answer is – it's quite probable. We suggest a silicon vacancy ( $V_{\text{Si}}$ ) in silicon carbide (carborundum) to be the one.

The SiC perfectly complies with a specification postulated in [2, 3] for the lattice, i.e. it has wide band gap, small spin-orbit coupling, the production of SiC has been for a long time available technology and it is possible to isotopically engineer the SiC crystals.

As distinct from the known NV defect in diamond, the silicon vacancy is an intrinsic defect. The presence of any other impurity is not required to produce this center in contrast to the NV center. To produce the latter one needs a single nitrogen atom, which, if not coupled with the vacancy, strongly constrain the coherence times of the system.

Silicon vacancies in SiC also are attractive because they exhibit a multitude ZPLs in the region of 850–920 nm, depending on their position in the crystal lattice, while the NV center in diamond exhibit only one ZPL at 632 nm. The emission wavelength of  $V_{Si}$  coincides with the spectral window of silica glass optical fiber, while at the emission wavelength of the NV center it exhibit very strong attenuation of about 7 dB/km.

Two opposite schemes were observed for the optical alignment of the populations of the spin sublevels in the ground state of a Si vacancy in SiC upon illumination with unpolarized light. In the first scheme the  $M_S = 0$  level is predominantly populated upon optical pumping. This case correspond to the optical spin alignment of the NV center in diamond. In the second scheme  $M_S = \pm 1$  sublevels are predominantly populated and this type of the optically induced inverse population of the spin sublevels in the zero magnetic field opening the possibility of obtainment of the maser effect on such systems.

The electron spin of the Si vacancy can be manipulated by low-energy radio wave quanta in the range 20–150 MHz, which is two orders of magnitude lower than the corresponding energy for the NV defect in diamond.

All abovementioned facts together with a change of a factor 2-3 that was observed in the luminescence intensity of the zero-phonon lines in zero magnetic field upon absorption of radio waves with energy equal to the fine-structure splitting of spin sublevels of the vacancy ground state, not only opens the possibility for magnetic-resonance detection of a single vacancy but makes them very favorable candidate for quantum computing.

This work has been supported by Ministry of Education and Science, Russia, under the Contracts No. 14.740.11.0048 and No. 16.513.12.3007; the Programs of the Russian Academy of Sciences: “Spin-Dependent Effects in Solids and Spintronics”; “Basic Researches of Nanotechnologies and Nanomaterials” and by the Russian Foundation for Basic Research under Grants No. 09-02-01409 and No. 09-02-00730

1. Jelezko F., Wrachtrup J.: Phys. Stat. Sol. (a) **13**, 3207–3225 (2006)
2. Weber J.R., Koehl W.F., Varley J.B., Janotti A., Buckley B.B., Van de Walle C.G., Awschalom D.D.: Proc.Natl. Acad. Sci. **107**, 8513 (2010)
3. DiVincenzo D.: Nat. Mater. **9**, 468 (2010)
4. Baranov P.G., Bundakova A.P., Soltamova A.A., Orlinskii S.B., Borovykh I.V., Zondervan R., Verberk R., Schmidt J.: Phys. Rev. B **83**, 125203 (2010)

## Spin Dynamics of Heisenberg and XY Pyrochlore Magnets Studied by ESR

*S. S. Sosin<sup>1</sup>, L. A. Prozorova<sup>1</sup>, O. A. Petrenko<sup>2</sup>, and M. E. Zhitomirsky<sup>3</sup>*

<sup>1</sup>*P. Kapitza Institute for Physical Problems, RAS, Moscow 119334, Russian Federation*

<sup>2</sup>*Department of Physics, University of Warwick, Coventry CV4 7AL, UK*

<sup>3</sup>*SPSMS/INAC/CEA, Grenoble 38054, France*

The strong frustration of a nearest-neighbor (NN) exchange interaction in spin systems on a pyrochlore crystal lattice is known to result in a macroscopic degeneracy of the magnetic ground state enhancing the role of other interactions and fluctuations in magnetic ordering. Various combinations of these forces can produce a large variety of disordered or ordered states, which sometimes are indeed observed in various pyrochlore materials. The study of spin dynamics in such systems is one of conclusive methods to choose between different ordering scenarios. Using the electron spin resonance spectroscopy (ESR) we compare the low energy spin dynamics of two compounds:  $\text{Gd}_2\text{Sn}_2\text{O}_7$  and

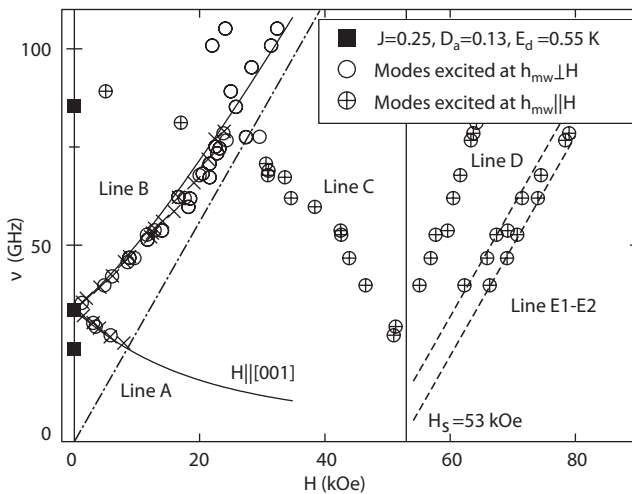


**Fig. 1.** Frequency-field diagram of  $\text{Gd}_2\text{Sn}_2\text{O}_7$  at  $T = 0.45$  K, closed squares are gaps calculated from the spin-wave theory. Solid lines is the theory for a “rigid” planar structure at  $H \ll H_s$ .

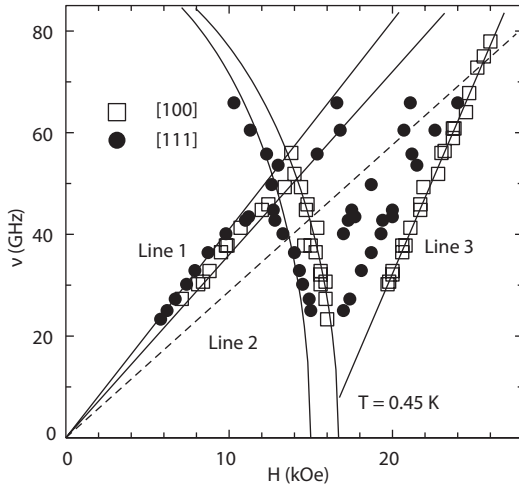


**Fig. 2.** Three branches of the resonance spectrum of  $\text{Er}_2\text{Ti}_2\text{O}_7$ , measured in the ordered phase in two directions of applied magnetic field. Solid lines are guide-to-eyes.

$\text{Er}_2\text{Ti}_2\text{O}_7$ . The first system with large  $S = 7/2$  and relatively weak single-ion anisotropy of magnetic  $\text{Gd}^{3+}$  ion, known as the best realization of a classical Heisenberg pyrochlore system orders below  $T_N = 1$  K in a “plane cross” structure [1]. Three gapped resonance modes were detected in the ordered phase (Fig. 1). Zero field gap values are well described by the spin-wave theory with the parameters for the NN exchange, dipolar interaction and single ion anisotropy determined from other measurements. The field evolution of two of these branches (lines A, B) at low fields is peculiar to acoustic modes of a planar magnetic structure with an isotropic susceptibility. The third mode (Line C) softens in the vicinity of the saturation field  $H_s \approx 53$  kOe as should be expected for an exchange branch. The theory also predicts a lowest gap (lying below our experimental frequency range), which determines the exponential decrease in the specific heat at low temperature. In the saturated phase ( $H > H_s$ ), two resonance modes with linear field dependence were detected [2]. This observation is the first direct evidence of the existence of quasi-local soft modes (intrinsic to strongly frustrated Heisenberg magnets), which are in particular responsible for an enhanced magnetocaloric effect in these systems.

The second compound is characterized by a strong splitting of  $\text{Er}^{3+}$  orbital momentum in the crystal field producing at low temperatures an effective  $S = 1/2$  spin system with the strong local XY-anisotropy of magnetic moments.

The non-planar ordering observed in this system below  $T_N \approx 1.2$  K is supposed to result mainly from the effect of fluctuations (order by disorder effect) [3]. The crucial argument in favor of this suggestion can be obtained by comparing the resonance spectra experimentally observed in various field directions with the results of a spin-wave theory either in the simplest XY-model or taking into account also dipolar interaction. Our measurements performed in the ordered phase of  $\text{Er}_2\text{Ti}_2\text{O}_7$  at  $H \parallel [100]$ ,  $[110]$  and  $[111]$  axes reveal the existence of a Goldstone mode acquiring an isotropic “Zeeman” gap under field (line 1 on Fig. 2). The second mode (line 2) has a gap softening near  $H_c \approx 15\text{--}16.5$  kOe which is a II order field induced transition into a state with spin canting from local easy planes. The approximately linear in field branch (line 3) is observed above  $H_c$  in qualitative agreement with previous inelastic neutron scattering data [4]. The theoretical calculations of the spectra are upcoming soon.

1. Wills A.S. *et al.*: J. Phys.: Condens. Matter **18**, L37 (2006)
2. Sosin S.S. *et al.*: Phys. Rev. B **79**, 014419 (2009)
3. Champion J.D.M. *et al.*: Phys. Rev. B **68**, 020401(R) (2003)
4. Ruff J.P.C. *et al.*: Phys. Rev. Lett. **101**, 147205 (2008)

## Effect of the Orientation of Substrate on $\delta$ -<Mn>-Layer Magnetization and Photoluminescence of Quantum Well in InGaAs/GaAs Heterostructures

*A. Talantsev<sup>1</sup>, A. Dmitriev<sup>1</sup>, S. Zaitsev<sup>2</sup>, O. Koplak<sup>3</sup>, and R. Morgunov<sup>1</sup>*

<sup>1</sup> *ICPCP RAS, Chernogolovka, Russian Federation, artgtx32@mail.ru*

<sup>2</sup> *ISSP RAS, Chernogolovka, Russian Federation*

<sup>3</sup> *Kyiv National University, Kiev, Ukraine*

The influence of orientation of surfaces GaAs on magnetic properties, spin dynamics and photo-luminescence of heterostructures with quantum well InGaAs/GaAs and  $\delta$ -<Mn>-layer was observed [1]. The temperature dependencies of magnetic momentum, ESR-spectra, and temperature dependencies

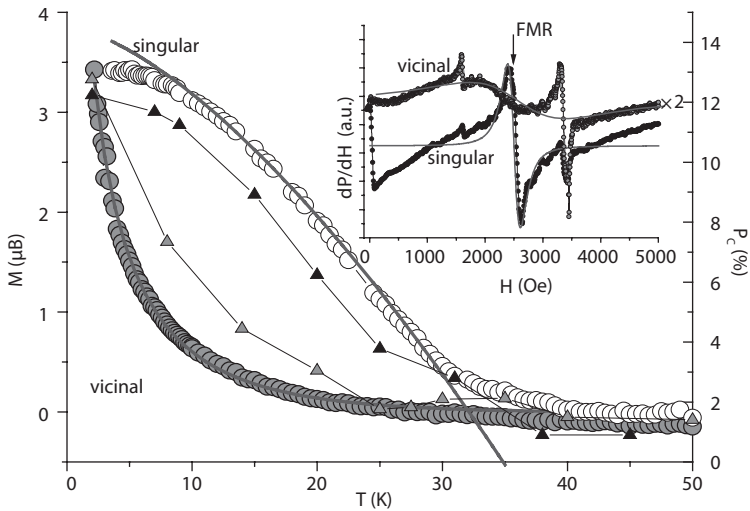


**Fig. 1.** Temperature dependencies of magnetization  $M$  of  $\delta$ -Mn-layer ( $\mu_B$  – Bohr’s magneton) and circular polarization  $P_c$  of photoluminescence of quantum well in singular and vicinal samples. Open symbols mark temperature dependencies of magnetization  $M$  of singular and vicinal samples in magnetic field of 1 kOe (solid lines depict the approximation by Bloch law and percolation formula). Solid (triangular) symbols mark dependencies of the degree of circular polarization  $P_c$  in singular and vicinal samples on temperature in magnetic field of 2 and 5 kOe, respectively (lines are guides for eyes). The inset depicts the electron spin resonance spectra of singular and vicinal samples at the temperature  $T=4$  K. Line FMR corresponds to magnetic resonance in  $\delta$ -Mn-layer 2.

of photo-luminescence polarization of quantum well for singular and vicinal heterostructures InGaAs/GaAs/ $\delta$ -Mn are qualitatively different (Fig. 1).

In singular InGaAs/GaAs/ $\delta$ -Mn heterostructures temperature dependence of magnetization follows the Bloch's "3/2" law, as in ordered bulk ferromagnets.

In vicinal InGaAs/GaAs/ $\delta$ -Mn heterostructures temperature dependence of magnetization follows the predictions of percolation theory in disordered ferromagnets. Despite the fact that in the investigated heterostructures, carriers in the quantum well and paramagnetic manganese ions in the delta-manganese layer are separated from each other, temperature dependence of circular polarization  $P_c$  of photoluminescence for the singular and vicinal samples qualitatively follows the dependence of magnetic moment on the temperature. This means that magnetic field of  $\delta$ -Mn-layer induces spin polarization of charge carriers in quantum well.

The work is supported by the Grant of the President of Russia MK-1764.2011.3.

1. Dmitriev A.I., Talantsev A.D. *et al.*: JETP **112** (2011) article in press.
2. Dmitriev A.I., Morgunov R.B. *et al.*: JETP **112**, 317 (2011)

## Tunnel Magnetoresistance and Peculiarity of Magnetization Process of Multilayer Ferromagnetic Nanoparticles

*S. N. Vdovichev, A. A. Fraerman, B. A. Gribkov, S. A. Gusev, A. Yu. Klimov, V. L. Mironov, and V. V. Rogov*

*Institute for Physics of Microstructures, Russian Academy of Sciences, Nizhny Novgorod 603950, Russian Federation, vdovichev@ipm.sci-nnov.ru*

The interest to multilayer system consists from ferromagnetic layers is due to possibility of fabrication of new type of data storage [1]. In general case, distribution of magnetization in laterally-confined magnetic multilayer is noncollinear and strongly depends on number of magnetic layers due to their magnetostatic interaction [2]. It is possible to form new magnetic states in a multilayer magnetic particle [2]. Magnetic anisotropy ( $K$ ) of the system is determined by eccentricity of the particles. Interaction between magnetic layers due to magnetostatic interaction leads to their “antiferromagnetic” coupling with strength  $J$ . Behavior of the system in external magnetic field is determined by interplay of the two factors. If  $J > K$ , noncollinear phase is possible. In opposite case ( $J < K$ ), only collinear states exist.

In the report the connection between magnetic states and transport properties of such systems is discussed. We observed the tunnel magnetoresistance in CPP geometry of the particle  $\text{CoFe}/\text{TaO}_x/\text{CoFe}$  and  $\text{CoFe}/\text{AlO}_x/\text{CoFe}$  with different lateral sizes fabricated by electron lithography. The transport measurement of tunnel magnetoresistance and magnetic force microscopy measurements of two layer magnetic particle can give more information about the magnetization process of such particle. Such information can be interested both for application and fundamental interest [3, 4]. “Flip-flop” switching between magnetic states of two layer magnetic particle (magnetic tunnel junction) is demonstrated. Dependence of switching process from later size of particle and magnetoresistance of multilayer ferromagnetic nanoparticles are discussed.

The transport measurement of tunnel magnetoresistance of  $\text{Co}/\text{AlO}_x/\text{Co}/\text{AlO}_x/\text{Co}$  junctions of different lateral size and numerical simulation of magnetization process of 3 magnetic layer particles will be presented also.

The work was supported by the RFBR (№11-02-97077 and others), by Russian Federal Educational Agency (contract № P 417).

1. Zhu J.-G.: Proceedings of IEEE **96**, no.11, 1786 (2008)
2. Fraerman A. A. *et al.*: J. of Appl. Phys. **103**, 073916 (2008)
3. Worledge D.C.: Appl. Phys. Lett. **84**, 4559 (2004)
4. Forrester D.M., Kürten K.E., Kusmartsev F.V.: Phys. Rev. B. **76**, 134404 (2007)

## Photo-EPR Studies of KTN-1.2: Evidences of the Nb<sup>4+</sup>-O–Polaronic Excitons

*R. V. Yusupov<sup>1</sup>, I. N. Gracheva<sup>1</sup>, A. A. Rodionov<sup>1</sup>, P. P. Syrnikov<sup>2</sup>, A. Dejneka<sup>3</sup>,  
A. I. Gubaev<sup>4</sup>, V. A. Trepakov<sup>2,3</sup>, and M. Kh. Salakhov<sup>1</sup>*

<sup>1</sup> *Kazan Federal University, Kazan 420008, Russian Federation, Roman.Yusupov@ksu.ru*

<sup>2</sup> *Ioffe Physical-Technical Institute, St.-Petersburg 194021, Russian Federation*

<sup>3</sup> *Institute of Physics, ASCR, Prague 182 21, Czech Republic*

<sup>4</sup> *Institute for Physical Chemistry, Münster University, Münster, Germany*

Behaviour of the systems close to the quantum mechanical limit is of great interest. Recently an observation of a giant photodielectric effect and photoconductivity at low temperatures was reported in perovskite-like quantum paraelectrics SrTiO<sub>3</sub> and KTaO<sub>3</sub> [1–4]. Although the phenomena were qualitatively related to the inhomogeneous polar state induced by the photo-generated charge carriers, the understanding of the microscopic structure of both the state and the photo-carriers was not achieved.

We report here on the results of the photoinduced electron paramagnetic resonance (photo-EPR) studies of the KTN crystal with  $x = 0.012$  (KTN-1.2,

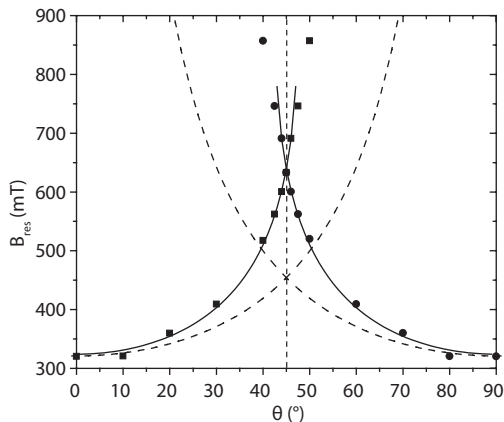


**Fig. 1.** Angular dependence of the resonance field  $B_{\text{res}}$  for the anisotropic photo-EPR signal in the KTN-1.2. Dashed curves are the angular dependencies  $B_{\text{res}} = B_{\text{res}}^0 / \cos\theta$  with  $B_{\text{res}}^0 = 312.4$  mT (limit case for a spin doublet with  $g_{\perp} = 0$ ). Solid lines – result of the angular dependence fit to the model of  $S = 1$ .

$T_c = 16$  K for a transition from cubic to trigonal phase [5]) which is a logical continuation of our previous work [6]. In particular, it is shown that the idea about the “simple”  $\text{Nb}^{4+}$  photo-polaron formation in KTN is in fact simplified; our studies indicate the creation of a more complex object – the  $\text{Nb}^{4+}\text{-O}^-$  polaronic exciton.

The X-band EPR spectrum induced by a broadband ( $\lambda < 450$  nm, xenon arc lamp) UV illumination of KTN-1.2 crystal is observed only below 10 K and consists of two main components: narrow nearly isotropic at  $g \sim 2$  and strongly anisotropic one. Nearly isotropic signal with emerging hyperfine structure most probably originates from the single trapped photo-carriers – electrons and/or holes. Anisotropic spectrum is caused by the magnetically non-equivalent centers oriented along the  $C_4$  principal axes of the crystal. Strong angular dependence of the resonance field presented in Fig. 1 evidences that this spectrum cannot originate from the transitions within any isolated spin doublet [7, 8], but can be fit well within the model of an axial center with  $S = 1$  with the  $g$  factors of  $g_{\parallel} = 0.82$ ,  $g_{\perp} = 0.52$  and fine structure constant  $D = 0.44 \text{ cm}^{-1}$ . Analysis shows that most probably these centers with  $S = 1$  are the  $\text{Nb}^{4+}\text{-O}^-$  excitons in the triplet state.

Temperature dependence of the anisotropic component is characterized by two activation energies:  $E_{a1} = 3.7 \pm 0.5$  meV for the internal dynamics (it makes the center unobserved in the EPR above 10 K), and  $E_{a2} = 52 \pm 4$  meV – for the center destruction.

It should be pointed out that centers of a similar electronic structure had been considered earlier in [9] as the origin of the photoinduced optical absorption and visible wideband “green” luminescence of  $\text{KTaO}_3$  and  $\text{SrTiO}_3$ . In particular, the spin triplet was predicted to be the ground state of such object. Our experiments reveal the strong evidence of the polaronic exciton creation under UV illumination of KTN crystals and extend our knowledge about the structure of these photoexcited electronic complexes.

1. Hasegawa T., Moury S., Yamanaka Y., Tanaka K.: *J. Phys. Soc. Jpn.* **72**, 41 (2003)
2. Katayama I., Ichikawa Y., Tanaka K.: *Phys. Rev. B* **67**, 100102(R) (2003)
3. Uchida K., Tsuneyuki S., Schimitsu T.: *Phys. Rev. B* **68**, 174107 (2003)
4. Takesada M., Yagi T., Itoh M., Ishikawa T., Koshihara S.: *Ferroelectrics* **298**, 317 (2004)
5. Boatner L.A., Höchli U.T., Weibel H.: *Helv. Phys. Acta* **50**, 620 (1977)
6. Gubaev A.I., Kapphan S.E., Jastabik L., Trepakov V.A., Syrnikov P.P.: *J. Appl. Phys.* **100**, 023106 (2006)
7. Laguta V.V., Zaritskii M.I., Glinchuk M.D., Bykov I.P., Rosa J., Jastrabik L.: *Phys. Rev. B* **58**, 156 (1998)
8. Maiwald M., Schirmer O.F.: *Europhys. Lett.* **64**, 776 (2003)
9. Vikhnin V.S., Eglitis R.I., Kapphan S.E., Borstel G., Kotomin E.A.: *Phys. Rev. B* **65**, 104304 (2002)

## Conduction Electron Spin Resonance in Two-Dimensional Systems

*A. M. Ziatdinov*

*Institute of Chemistry, Far Eastern Branch of the RAS, Vladivostok 690022,  
Russian Federation, ziatdinov@ich.dvo.ru*

The possibilities of conduction ESR (CESR) method in the study of graphite and its intercalation compounds are considered. The next questions are discussed in detail.

*1. Spins of conduction electrons as a probe of physical transformations in graphite intercalation compounds.* The effect of temperature on CESR spectra of 2-nd stage graphite intercalation compounds with nitric acid ( $C_{10}HNO_3$ ) were studied. In the liquid phase of intercalate ( $T > T_c = 250$  K) the CESR linewidth does not depend on temperature. In the solid incommensurate phase of intercalate ( $T < T_c$ ) the temperature dependence of CESR linewidth has a multibroken character with a global temperature dependence. Independently, on a temperature change direction, the “breaks” take place near the same values of the CESR linewidth. The found features of the CESR linewidth temperature dependence point out the change of intercalate density modulation vector in a mode of “devil’s staircase”. It also shows the presence of interaction between amplitude and phase of density modulation wave vector in temperature intervals between “breaks”. Apparently, this interaction is the reason for stepwise change of density modulation vector in a basal plane.

*2. Spins of conduction electrons as a probe of chemical transformations in graphite and its intercalation compounds.* At the intercalation of  $HNO_3$  molecules into a narrow highly oriented pyrolytic graphite slab the changes in the graphite CESR signal line shape, intensity and linewidth and the step-wise changes both of intensity and linewidth of CESR signal from intercalated sample have been clearly detected. Under the assumption that the graphite CESR signal evolution is caused by the advance of a boundary separating the intercalated and non-intercalated graphite, the average probability value of spin reorientation during the collision of current carriers with this interface and the constant of two-dimensional diffusion of nitric acid molecules into graphite have been extracted from experimental data. Using the dependence of chemical potential on exposure time of graphite in  $HNO_3$  atmosphere offered by the authors for the experimental conditions, the step-wise evolution of CESR signal intensity from intercalated graphite have been calculated theoretically.

The changes in the graphite CESR signal parameters and the step-wise change of intensity of CESR signal from intercalated part have been clearly detected during the intercalation of graphite by  $\text{SbF}_5$ . Under the assumption that the graphite signal evolution is caused by the advance of a boundary separating the intercalated and non-intercalated graphite, the average value of spin reorientation probability during the collision of current carriers with this interface and the constant of two-dimensional diffusion of  $\text{SbF}_5$  molecules into graphite have been extracted from experiment. The step-wise change of the CESR signal intensity points to the repeated-batch introduction of intercalate into graphite. The assumption is made that the reasons for such step-wise introduction of intercalate are the presence of upper threshold intercalation potential (intercalation into sample is permitted above this value) and lower threshold (intercalation is near impossible below it), and the periodical impoverishing of intercalate molecule layers adsorbed on graphite.

At the intercalation of  $\text{MoF}_5$ , the changes in the graphite CESR signal parameters are similar to the corresponding dependences observed at graphite intercalation by  $\text{SbF}_5$ . But in this case, on the basic graphite signal, the additional narrow signal is observed. At the advance of the intercalation front into the graphite slab, the intensities of this and basic signals decrease together, up to their complete disappearance. The assumption was made that the narrow signal corresponds to the localized spins, which appear on the intercalation front due to the strong distortion of graphite layers.

3. *Control of layer and interlayer conductivities in graphite and its intercalation compounds using the CESR data.* The electrical conductivities for graphite and its intercalation compounds with nitric acid  $\text{C}_{5n}\text{HNO}_3$  ( $n = 2, 3$ ) have been determined by the CESR method. In the incommensurate phase of second stage compounds ( $210 < T < 250$  K) absence of temperature of the  $c$ -axis conductivity, but preservation of the “metallic” temperature dependence of the basal plane conductivity, has been found. In the third stage compounds the similar “plateau” is less marked one. In both stages of compounds under investigation at the incommensurate crystallization of intercalate subsystem, the CESR linewidth undergoes a stepwise increase. It was shown that in compounds studied the  $c$ -axis conductivity is realized by means of a non-bond mechanism, which might be the mechanism of transport of free charge carriers along the  $c$ -axis through the defect-mediated narrow high-conductivity paths (channels).

The investigations were partially supported by the Russian Foundation for Basic Research (grant # 08-03-00211) and the Presidium of the FEB RAS (grant # 09-I-1118-07).

---

WORKSHOP  
INVITED TALKS

## **Ferromagnetism and Superconductivity in LiFeAs**

*B. Büchner*

*Leibniz Institute for Solid State and Materials Research IFW Dresden, Dresden D-01069,  
Germany, [b.buechner@ifw-dresden.de](mailto:b.buechner@ifw-dresden.de)*

## Topical Magnetic and Electronic Properties of Frustrated Edge-Shared Chain Cuprates

*S.-L. Drechsler<sup>1</sup>, S. Nishimoto<sup>2</sup>, R. Kuzian<sup>1</sup>, J. Malek<sup>1</sup>, J. Richter<sup>2</sup>,  
J. van den Brink<sup>1</sup>, R. Klingeler<sup>1</sup>, W. E. A. Lorenz<sup>1</sup>, A. Wolter<sup>1</sup>,  
B. Büchner<sup>1</sup>, M. Schmitt<sup>3</sup>, and H. Rosner<sup>3</sup>*

<sup>1</sup>Leibniz Institute IFW-Dresden, Dresden D-01171, Germany, *s.l.drechsler@ifw-dresden.de*

<sup>2</sup>Institut f. Theoretische Physik, Universität Magdeburg, Magdeburg D39016, Germany

<sup>3</sup>Max-Planck-Institut f. Chemische Physik Fester Stoffe, Dresden, Germany

We present an overview on the present theoretical understanding of strongly frustrated spin-chain compounds from the view point of the multi-band Hubbard model, the isotropic and the anisotropic J1-J2-Heisenberg models supplemented with interchain couplings, and L(S)DA+U based calculations for various magnetic structures with the aim to predict the dominant exchange integrals. The results are compared with available experimental data for thermodynamic and dynamic properties as observed by inelastic neutron scattering, saturation field and susceptibility measurements. We focus on  $\text{Li}_2\text{CuO}_2$  [1],  $\text{Ca}_2\text{Y}_2\text{Cu}_5\text{O}_{10}$ ,  $\text{LiVCuO}_4$  [2]  $\text{CuGeO}_3$ , linarite and other related compounds and discuss briefly the most outstanding puzzles such as the possible existence of multipolar phases worth to be attacked in near future both theoretically and by experiments.

The work was supported by the Deutsche Forschungsgemeinschaft (grants DR269/3-1 and RI/615-1 )

1. Nishimoto H. *et al.*: Phys. Rev. Lett. **107**, 097201 (2011)
2. Drechsler S-L. *et al.*: Phys. Rev. Lett. **106**, 219701 (2011)

## Visualization of Spin Dynamics and Magnetic Hysteresis in Single Nanosized Magnetic Elements

*M. Farle*

*Fakultät für Physik and Center for Nanointegration Duisburg-Essen,  
University of Duisburg-Essen, Duisburg 47048, Germany, farle@uni-due.de*

The design of future spintronic devices [1] requires a quantitative understanding of the microscopic static and dynamic magnetic response in nanometer-scale ferromagnetic systems. Ferromagnetic resonance (FMR) is the method of choice for a quantitative analysis of relaxation rates, magnetic anisotropy and susceptibility in a single experiment. X-ray magnetic circular dichroism with spatial resolution on the 20 nm scale is a newly developed method to record magnetic hysteresis loops of single nanoparticles. Different approaches [2, 3] to detect ferromagnetic resonance with sufficient sensitivity for the analysis of nanoscale particles will be discussed, and first single particle hysteresis loops [4] will be presented.

In the first example, we analyze the different excitation modes in a single nanometer-sized ferromagnetic stripe. Measurements are performed using a microresonator set-up which offers a sensitivity to quantitatively analyze the dynamic and static magnetic properties of single nanomagnets with volumes of  $(100 \text{ nm})^3$ . Uniform as well as non-uniform volume modes of the spin wave excitation spectrum are identified and found to be in excellent agreement with the results of micromagnetic simulations which allow the visualization of the spatial distribution of these modes in the nanostructures.

In the second example, results on the correlation of single particle magnetic hysteresis loops with their morphology and shape measured by transmission electron tomography with nm resolution will be presented.

The fruitful collaboration with the members of my research team and the colleagues from the Technical University Dortmund, the national Physical Laboratory London and BESSY is gratefully acknowledged. The work was supported by Deutsche Forschungsgemeinschaft, SFB 445 and European Network “SyntOrbMag”.

1. Reckers N. *et al.*: Phys. Rev. B **83** (2011) 184427
2. Rod I., Kazakova O., Cox D.C., Spasova M., Farle M.: Nanotechnology **20**, 335301 (2009)
3. Banholzer A. *et al.*: Nanotechnology **22**, 295713 (2011)
4. Kronast F. *et al.*: Nano Lett. **11**, 1710–1715 (2011)

## High Field Sub-Terahertz ESR Spectroscopy on Molecular Magnets

*V. Kataev*

*Leibniz Institute for Solid State and Materials Research IFW Dresden, Dresden D-01069,  
Germany, v.kataev@ifw-dresden.de*

Magnetically active metal-organic molecules that comprise in their cores interacting paramagnetic transition metal ions currently attract a significant interdisciplinary attention due to their unprecedented properties. Such molecular-based materials provide a unique playground to study fundamental aspects of quantum magnetism on the macroscopic level. Furthermore, some of them provide a realization on a molecular level of a superparamagnetic particle (single molecule magnet – SMM) characterized by a big and anisotropic magnetic moment, hysteresis behavior and metastable magnetic states. New techniques of tunable sub-Terahertz electron spin resonance spectroscopy in high magnetic fields (HF-ESR) enable detailed insights into the energy spectrum of the spin states, exchange interactions and anisotropy effects in such kind of systems.

In this talk several examples of the application of the HF-ESR method to studies of magnetic properties of Ni- and Mn-based polynuclear supramolecular complexes will be presented. A relationship between the chemical structure, bonding topology and magnetism with regard to the rational design of SMMs will be discussed.

## Spin-Orbit Entangled Ground States and Excitations in Iridium Oxides

*G. Khaliullin*

*Max Planck Institute for Solid State Research, Stuttgart, Germany*

A relativistic spin-orbit coupling may drive unusual interactions and orderings in Mott insulators. This coupling entangles the spin and orbital subspaces leading to a rich variety of effective Hamiltonians and exotic phases depending on the lattice geometry and orbital structure. Particular examples to be discussed are: (i) Iridium perovskite  $\text{Sr}_2\text{IrO}_4$  with an anomalously large spin canting [1]; (ii) The honeycomb lattice  $\text{Na}_2\text{IrO}_3$  where the celebrated Kitaev model with spin liquid ground state might be at work; (iii) Vanadate  $\text{Sr}_2\text{VO}_4$  which is predicted to exhibit a magnetically hidden octupolar order [3].

1. Jackeli G., Khaliullin G.: Phys. Rev. Lett. **102**, 017205 (2009)
2. Chaloupka J., Jackeli G., Khaliullin G.: Phys. Rev. Lett. **105**, 027204 (2010)
3. Jackeli G., Khaliullin G.: Phys. Rev. Lett. **103**, 067205 (2009)

## The Frustrated Quasi-1D Quantum Antiferromagnet $\text{Li}_2\text{CuO}_2$

R. Klingeler<sup>1</sup>, S. Nishimoto<sup>2</sup>, S.-L. Drechsler<sup>2</sup>, R. Kuzian<sup>2,5</sup>, J. Malek<sup>2,3</sup>,  
J. Richter<sup>4</sup>, W. E. A. Lorenz<sup>2</sup>, N. Wizen<sup>1,2</sup>, J. van den Brink<sup>2</sup>,  
Y. Skourski<sup>6</sup>, and B. Büchner<sup>2</sup>

<sup>1</sup>Kirchhoff Institute for Physics, University of Heidelberg, Germany

<sup>2</sup>Leibniz-Institut für Festkörper- und Werkstofforschung (IFW) Dresden, Germany

<sup>3</sup>Institute for Problems of Materials Science, Kiev, Ukraine

<sup>4</sup>University of Magdeburg, Inst. of Theoretical Physics, Chemistry Department, Germany

<sup>5</sup>Institute of Physics, ASCR-Prague, Czech Republic

<sup>6</sup>Hochfeld-Magnettlabor Dresden, Helmholtz-Zentrum Dresden-Rossendorf, Germany

$\text{Li}_2\text{CuO}_2$  is the first and most frequently studied compound of the growing class of edgeshared spin-chain cuprates. Being a model quasi-one-dimensional (quasi-1D) frustrated quantum spin magnet, we have explored in detail its magnetic and thermodynamic properties. Detailed studies of the thermal expansion, specific heat and magnetostriction allow to determine the resulting complex phase diagram and reflect signatures of critical fluctuations and the close vicinity to a critical point. Inelastic neutron diffraction studies detect long-sought quasi-1D magnetic excitations with a large dispersion along the  $\text{CuO}_2$ -chains. The total dispersion is governed by a surprisingly large ferromagnetic (FM) nearest neighbor exchange integral  $J_1 = -228$  K. An anomalous quartic dispersion near the zone center and a pronounced minimum near  $(0, 0.11, 0.5)$  r.l.u. point to the vicinity of a 3D FM-spiral critical point. Interchain coupling turns out to be the essential parameter governing the magnetic phase diagram. Remarkably, for a wide range of frustrated spin-chains the saturation field is completely independent of intra-chain interactions. We show that in the isotropic approximation the inter-chain coupling can be read off directly from the saturation field determined by pulsed field studies which hence represents a novel sensitive and attractive method to determine even weak inter-chain interactions of the order of few K. Support by DFG via KL1824/2 is gratefully acknowledged.

1. Lorenz W. *et al.*: EPL **88**, 37002 (2009)
2. Drechsler S.-L. *et al.*: JPCS **200**, 12028 (2010)
3. Nishimoto S. *et al.*: PRL, in print; arXiv:1004.3300

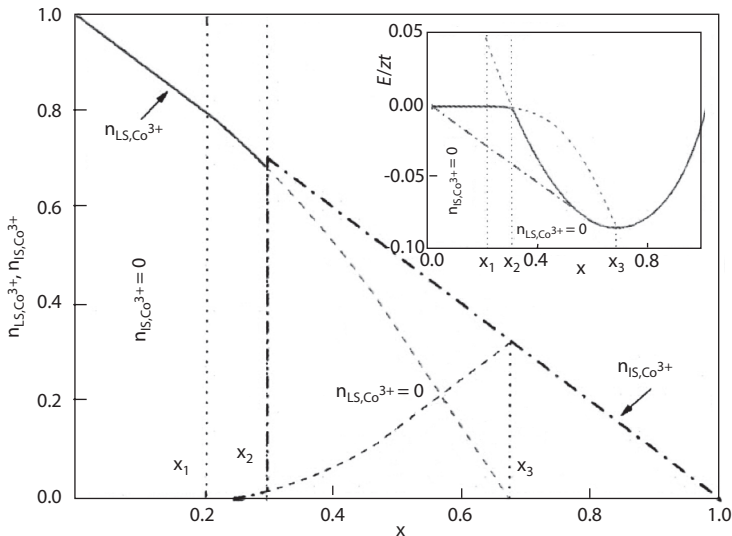
## Magnetic Inhomogeneities in Doped Materials with Spin-State Transitions

*K. I. Kugel<sup>1</sup>, A. O. Sboychakov<sup>1</sup>, A. L. Rakhmanov<sup>1</sup>, and D. I. Khomskii<sup>2</sup>*

<sup>1</sup>*Institute for Theoretical and Applied Electrodynamics, Russian Academy of Sciences, Moscow 125412, Russian Federation, kugel@orc.ru*

<sup>2</sup>*II. Physikalisches Institut, Universität zu Köln, Köln 50937, Germany*

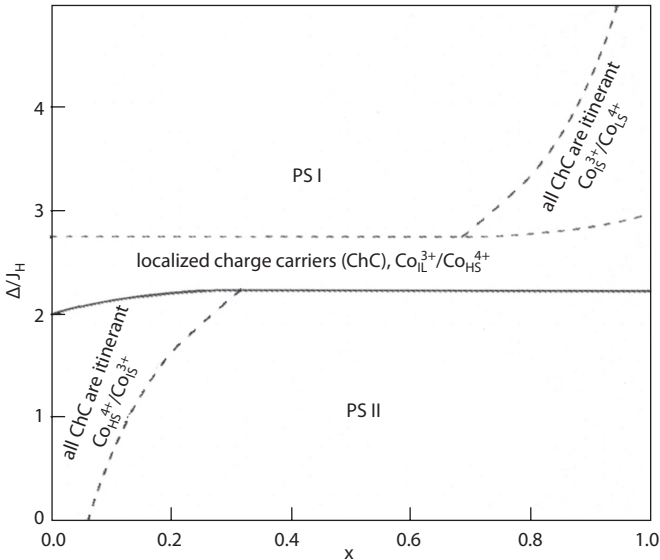
Complex cobalt-based oxides with perovskite structure (cobaltites), such as  $\text{La}_{1-x}\text{Sr}_x\text{CoO}_3$ , can undergo the transitions between different spin states of cobalt ions (spin-state transitions – SST), which can occur with the change of temperature, pressure, and doping  $x$ . They are often accompanied by the metal-insulator transition. The  $\text{Co}^{3+}$  ion having six electrons at the 3d shell can exist in three different spin states: low-spin (LS) state with  $S = 0$  ( $t_{2g}^6 e_g^0$ ), intermediate-spin (IS) state  $S = 1$  ( $t_{2g}^5 e_g^1$ ), and high-spin (HS) state ( $t_{2g}^4 e_g^2$ ) with  $S = 2$ . Thus, cobaltites, in addition to quite common charge, orbital, and spin degrees of freedom with the possibility of respective orderings, have an “extra dimension”: the possibility of spin-state (or, in other words, multiplet) transi-



tions. Correspondingly, if doping of materials like manganites can cause phase separation due to interplay of the motion (kinetic energy) of doped holes with the underlying magnetic and orbital structure, in systems with SST one can expect similar phenomena due to interplay with the spin state of the matrix.

Let  $\Delta$  be the energy difference between  $t_{2g}$  and  $e_g$  levels in  $\text{Co}^{3+}$  and  $\text{Co}^{4+}$  ions. Then, the energies of IS and HS states will differ from the energy of LS  $\text{Co}^{3+}$  by  $(\Delta - J_H)$  and  $2(\Delta - 2J_H)$ , respectively, where  $J_H$  is the Hund's rule coupling constant. The corresponding energies for  $\text{Co}^{4+}$  are  $(\Delta - 2J_H)$  and  $2(\Delta - 3J_H)$ . For  $\Delta > 3J_H$  and  $\Delta < 2J_H$ , the ground state of both  $\text{Co}^{3+}$  and  $\text{Co}^{4+}$  is LS and HS, respectively. At  $2J_H < \Delta < 3J_H$ , we have LS  $\text{Co}^{3+}$  and HS  $\text{Co}^{4+}$ . Thus, for isolated Co ions, the IS state is always unfavorable in energy. The situation becomes more complicated if there exists a charge transfer between cobalt ions. In this case, the IS state becomes possible due to the gain in kinetic energy related to the intersite hopping of electrons promoted from the  $t_{2g}$  to  $e_g$  level. Two hopping processes turn out to be most probable: the transitions of electrons between the IS  $\text{Co}^{3+}$  and LS  $\text{Co}^{4+}$  ( $\Delta > 3J_H$ ) and transitions between the HS  $\text{Co}^{3+}$  and IS  $\text{Co}^{4+}$  ( $\Delta < 2J_H$ ). The hopping integral  $t$  should be comparable to  $\Delta$ .

We describe such a situation in the framework of a simple model similar to that used for doped manganites [1], where the competition between the localized and band states of charge carriers can lead to a nanoscale phase separation.



In the case of cobaltites, the role of a localized level is played by the ground state of cobalt ions, LS  $\text{Co}^{3+}$  ( $\Delta > 3J_H$ ) or HS  $\text{Co}^{4+}$  ( $\Delta < 2J_H$ ), whereas the itinerant charge carriers correspond to electrons or holes promoted to  $e_g$  levels in the intermediate spin state. However, here, in contrast to manganites, a possibility of a jump-like transition to the state, where all charge carriers are itinerant, appears at a certain doping level, i.e. we have LS to IS transition for all  $\text{Co}^{3+}$  ions (at  $\Delta > 3J_H$ ) [2]. The variation of the relative number of  $\text{Co}^{3+}$  ions in LS (solid curve) and IS (dashed curve) states as function of doping  $x$  is illustrated in Fig. 1, where  $(\Delta - J_H)/zt = 0.2$ ,  $z$  is the number of nearest neighbors. At  $x_1 < x < x_2$ , both LS and IS states of  $\text{Co}^{3+}$  coexist, whereas at  $x = x_2$ , a jump-like transition to the purely IS state of  $\text{Co}^{3+}$  ions occurs. Thin dashed lines illustrate the corresponding behavior for the metastable state, for which the number of LS  $\text{Co}^{3+}$  gradually changes with doping. In the inset, the dependence of the system energy on  $x$  is shown by solid curve. The Maxwell construction (dot-and-dash line) shows the range where the phase separation is possible.

In the wide doping range, the formation of the inhomogeneous phase-separated state turns out to be favorable in energy. The phase diagram of the system with SST including the phase-separated states is shown in Fig. 2. PS I is the phase-separated state including regions without itinerant charge carriers, corresponding to LS  $\text{Co}^{3+}$ , and those with completely delocalized charge carriers promoted to IS  $\text{Co}^{3+}$ . PS II is the similar phase-separated state where regions with and without itinerant charge carriers correspond to IS  $\text{Co}^{4+}$  and HS  $\text{Co}^{4+}$ , respectively ( $t/J_H = 1$ ).

The work was supported by the Russian Foundation for Basic Research (projects 11-02-00708 and 11-02-91335-NNIO), the Deutsche Forschungsgemeinschaft via SFB 608 and the German-Russian projects 436 RUS 113/942/0 and No.GR1484/2-1, and the European project SOPRANO. A.O.S. acknowledges support from the Dynasty Foundation.

1. Kugel K.I., Rakhmanov A.L., Sboychakov A.O.: Phys. Rev. Lett. **95**, 267210 (2005)
2. Sboychakov A.O., Kugel K.I., Rakhmanov A.L., Khomskii D.I.: Phys. Rev. B **80**, 0244230 (2009)

## Superconducting Triplet Spin Valve Based on the Superconductor-Ferromagnet Proximity Effect

*L. R. Tagirov<sup>1,2</sup>, R. G. Deminov<sup>1</sup>, O. V. Nedopekin<sup>1</sup>, Ya. V. Fominov<sup>3</sup>,  
M. Yu. Kupriyanov<sup>4</sup>, T. Yu. Karminskaya<sup>4</sup>, and A. A. Golubov<sup>5</sup>*

<sup>1</sup>*Institute of Physics, Kazan Federal University, Kazan 420008, Russian Federation*

<sup>2</sup>*Institute of Physics, Augsburg University, Augsburg D-86135, Germany*

<sup>3</sup>*L. D. Landau Institute for Theoretical Physics RAS, Moscow 119334, Russian Federation*

<sup>4</sup>*Skobel'syn Institute of Nuclear Physics, Moscow State University, Moscow 119992, Russian Federation*

<sup>5</sup>*Faculty of Science and Technology and MESA+ Institute of Nanotechnology, University of Twente, Enschede 7500 AE, The Netherlands*

We study theoretically the critical temperature  $T_c$  of S/F1/N/F2 and S/F1/F2 core structures, where the magnetization direction of the outer F2 is kept fixed by exchange bias or another source of magnetic anisotropy. The F1/N/F2 spin-valve actuator is attached to the singlet superconductor layer S to control superconducting  $T_c$  of the latter. We have taken into account the long-range triplet component of the superconducting pairing, which can be generated at noncollinear magnetizations of the F layers [1]. Our calculations have shown that  $T_c$  can be a nonmonotonic function of the angle  $\alpha$  between magnetizations of the two F layers. The minimum is achieved at an intermediate  $\alpha$ , lying between the parallel (P,  $\alpha = 0$ ) and antiparallel (AP,  $\alpha = \pi$ ) cases, we coined it as triplet spin-valve effect (see ref. [2]). At the same time, considering only the P and AP orientations, we find that both, the “normal”  $T_c^{\text{AP}} > T_c^{\text{P}}$ , and the “inverse”  $T_c^{\text{AP}} < T_c^{\text{P}}$  switching effects are possible depending on the choice of material properties and thickness of the layers (see refs. [2–4]).

This work was supported by RFBR (projects No. 11-02-00077-a, 11-02-00848-a, and 10-02-90014-Bel\_a), DFG (project No. GZ: HO 955/6-1), the Russian Ministry of Education and Science (contract No. P799), and the program “Quantum physics of condensed matter” of the RAS.

1. Bergeret F.S., Volkov A.F., Efetov K.B.: *Rev. Mod. Phys.* **77**, 1321 (2005)
2. Fominov Ya.V., Golubov A.A., Karminskaya T.Yu. *et al.*: *JETP Lett.* **91**, 308 (2010)
3. Leksin P.V., Garif'yanov N.N., Garifullin I.A. *et al.*: *Phys. Rev. Lett.* **106**, 067005 (2011)
4. Deminov R.G., Tagirov L.R., Nedopekin O.V. *et al.*: *Phys. Rev. B*, submitted.



---

WORKSHOP

ORAL TALKS

## High Field ESR Spectroscopy on Fe-Based Superconductors

*A. Alfonsov<sup>1</sup>, R. Zahn<sup>2</sup>, G. Lang<sup>1</sup>, F. Lipps<sup>1</sup>, V. Kataev<sup>1</sup>, S. Aswartham<sup>1</sup>,  
S. Wurmehl<sup>1</sup>, J. S. Kim<sup>3</sup>, J. Deisenhofer<sup>4</sup>, H.-A. Krug von Nidda<sup>4</sup>,  
A. Loidl<sup>4</sup>, and B. Büchner<sup>1</sup>*

<sup>1</sup>*IFW Dresden, Dresden 01069, Germany*

<sup>2</sup>*HLD, FZ Dresden-Rossendorf, Dresden 01314, Germany*

<sup>3</sup>*Pohang University of Science and Technology, Pohang, Korea*

<sup>4</sup>*Center for Electronic Correlations and Magnetism, Augsburg University,  
Augsburg D-86135, Germany*

In the present work we study single-crystal samples of  $(\text{EuBa})(\text{FeCo})_2\text{As}_2$  by means of electron spin resonance (ESR) spectroscopy. At high temperatures, the linewidth of the spectra is dominated by the Korringa relaxation process, as shown at low and high frequencies by the decrease of the linewidth on cooling. The corresponding slope, related to the electronic density of states at the Fermi energy, shows a non-monotonous evolution with doping. This situation may reflect the multiorbital character of the compound. In addition, the high-frequency and high-field ESR measurements provide results qualitatively similar to those obtained in Gd-based 1111 pnictides [1]. Indeed, the line broadening seen in the undoped compound at the onset of the spin-density wave appears to be still present in doped superconducting samples with no long-range magnetic order, strongly suggesting the presence of quasi-static short-range magnetic correlations. This result casts a new light on the important issue of coexistence of superconductivity and static magnetism in these materials. We discuss the doping dependence of the density of states at the Fermi energy as well as that of static magnetism, especially with regard to a mixed local/itinerant character.

1. Alfonsov A. *et al.*: Phys. Rev. B **83**, 094526 (2011)

## Magneto-Structural Correlations of 1,2-Diphosphacyclopentadienide Transition Metal Complexes

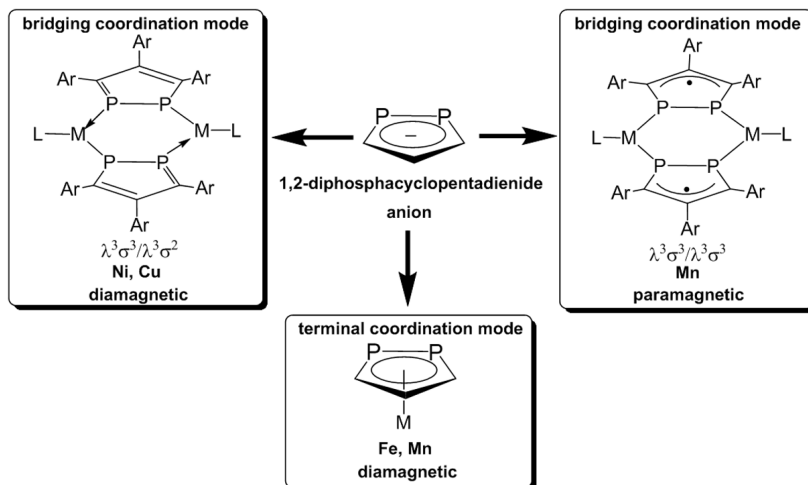
*I. A. Bezkishko<sup>1</sup>, V. A. Milyukov<sup>1</sup>, O. N. Kataeva<sup>1</sup>, O. G. Sinyashin<sup>1</sup>,  
P. Lonnecké<sup>2</sup>, E. Hey-Hawkins<sup>2</sup>, Yu. Krupskaya<sup>3</sup>, V. Kataev<sup>3</sup>, R. Klingeler<sup>3</sup>,  
and B. Büchner<sup>3</sup>*

<sup>1</sup>Arbuzov Institute of Organic and Physical Chemistry, Russian Academy of Sciences,  
Kazan 420088, Russian Federation, bezkishko@mail.ru

<sup>2</sup>Leipzig University, Institute of Inorganic Chemistry, Leipzig, Germany,  
hey@rz.uni-leipzig.de

<sup>3</sup>IFW Dresden, Dresden D-01171, Germany, V.Kataev@ifw-dresden.de

The 1,2-diphosphacyclopentadienide anions have significant interest due to possibility to form transition metal complexes with different coordination modes to metal. Recently we have found that bridging coordination mode of 1,2-diphosphacyclopentadienide ligand in manganese (I) carbonyl complexes results in the metal-to-ligand charge transfer (MLCT) with formation of low-spin Mn(II) species.



Analysis of crystal structure of some binuclear 1,2-diphosphacyclopentadienide transition metal complexes using X-ray single crystal diffraction allows us to find a significant redistribution of electronic density for paramagnetic manganese complexes resulting in the equivalent phosphorus atoms in contrast to diamagnetic complexes of copper and nickel in which phosphorus atoms are non-equivalent.

The authors are grateful to the Ministry of education and science of Russian Federation (grant of the President RF MK-954.2011.3)

## Resonant Inelastic X-ray Scattering: a New Approach for Investigating Spin Excitations

V. Bisogni<sup>1</sup>, L. Braicovich<sup>2</sup>, G. Ghiringhelli<sup>2</sup>, M. Moretti Sala<sup>3</sup>, N. B. Brookes<sup>3</sup>,  
L. Simonelli<sup>3</sup>, R. Kraus<sup>1</sup>, C. Monnay<sup>4</sup>, K. Zhou<sup>4</sup>, T. Schmitt<sup>4</sup>,  
J. van den Brink<sup>1</sup>, B. Büchner<sup>1</sup>, and J. Geck<sup>1</sup>

<sup>1</sup>IFW Dresden, Dresden 01069, Germany

<sup>2</sup>Politecnico di Milano, Milano 20133, Italy

<sup>3</sup>ESRF, Grenoble 38043, France

<sup>4</sup>PSI-SLS, Villigen 5232, Switzerland

Resonant Inelastic X-ray Scattering (RIXS) is emerging as a new method for investigating spin excitations. It has recently been demonstrated that Cu-L<sub>3</sub> RIXS is a new powerful experimental tool to map magnon dispersions in the high- $T_c$  cuprates and their parent compounds [1, 2]. Therefore RIXS is a complementary technique to inelastic neutron scattering (INS), especially since it can be used for small sample volumes [3] or even for thin films. Moreover, the resonant aspect of RIXS is an interesting degree of freedom which allows for a deep insight into the magnon density of states. The general characteristics of RIXS and its advantages will be discussed through the presentation of test cases. We will show recent results on 2D cuprates as well as on 1D spin chain cuprates, investigated with RIXS at the Cu-L<sub>3</sub> edge, at the O-K and at the Cu-K edges.

1. Braicovich L., van den Brink J., Bisogni V., Moretti Sala M., Ament L.J.P., Brookes N.B., De Luca G.M., Salluzzo M., Schmitt T., Strocov V.N., Ghiringhelli G.: Phys. Rev. Lett. **104**, 077002 (2010)
2. Schlappa J., Schmitt T., Vernay F., Strocov V.N., Ilakovac V., Thielemann B., Rønnow H.M., Vanishri S., Piazzalunga A., Wang X., Braicovich L., Ghiringhelli G., Marin C., Mesot J., Delle B., Patthey L.: Phys. Rev. Lett. **103**, 047401 (2009)
3. Guarise M., Dalla Piazza B., Moretti Sala M., Ghiringhelli G., Braicovich L., Berger H., Hancock J.N., van der Marel D., Schmitt T., Strocov V.N., Ament L.J.P., van den Brink J., Lin P.-H., Xu P., Rønnow H.M., Grioni M.: Phys. Rev. Lett. **105**, 157006 (2010)

## Spin-Spin Interactions and Electron Spin Polarization in Systems Based on Metalloporphyrins

*V. S. Iyudin<sup>1</sup>, Yu. E. Kandrashkin<sup>1</sup>, V. K. Voronkova<sup>1</sup>, V. S. Tyurin<sup>2</sup>,  
E. N. Kirichenko<sup>2</sup>, and Yu. P. Yashchuk<sup>2</sup>*

*<sup>1</sup>Zavoisky Physical-Technical Institute, Russian Academy of Sciences, Kazan 420029,  
Russian Federation, vasilus@yandex.ru*

*<sup>2</sup>A. N. Frumkin Institute of Physical Chemistry and Electrochemistry, Moscow 119991,  
Russian Federation*

Porphyrins and their derivatives play essential roles in nature, mostly due to their ability to bind a wide variety of metals and to become chemically active upon light excitation. This combination of properties could lead to the creation of materials with controllable magnetic properties. For example this could be used for spin-dependent electric transport through biomolecular devices, such as optical switches, information storage, molecular magnets [1, 2].

The study of the exchange interaction between the porphyrin molecule in the excited triplet state and paramagnetic ions may be crucial for search of new classes of the light-controlling magnetic molecular systems. The time-resolved EPR (TREPR) is a powerful tool to study the spin-involved processes initiated by the light irradiation.

We report here spin-polarized TREPR spectra of several copper porphyrins (CuP), zinc porphyrins connected by copper complexes and cluster CuP-ZnP-CuP. The investigated complexes demonstrate remarkable changes of the TREPR spectrum. Some of the copper porphyrins demonstrate the photo-excited high spin state (excited spin polarized quartet state). The photo-excited high spin state is also observed in the cluster CuP-ZnP-CuP. The effect of the spin delocalization in the porphyrin ring and the possible spin polarization mechanisms on the observation of photoexcited high spin states is discussed.

1. Khadis K.M., Smith K.M., Guillard R: *The Porphyrin Handbook*, vol. 1–10 (1999) and vol. 11–20 (2003). Academic Press.
2. Kahn O., Martinez C. J.: *Science* **279**, 44–48 (1998)

## Magnetic Heat Transport in One-Dimensional Quantum Antiferromagnets

*N. Hlubek<sup>1</sup>, P. Ribeiro<sup>1</sup>, R. Saint-Martin<sup>2</sup>, S. Singh<sup>2</sup>, A. Revcolevsch<sup>2</sup>, G. Roth<sup>3</sup>,  
G. Behr<sup>1</sup>, B. Büchner<sup>1</sup>, and C. Hess<sup>1</sup>*

<sup>1</sup>IFW-Dresden, Institute for Solid State Research, Dresden D-01171, Germany,  
*c.hess@ifw-dresden.de*

<sup>2</sup>Laboratoire de Physico-Chimie de L'Etat Solide, Université Paris-Sud, Orsay 91405, France

<sup>3</sup>Institut für Kristallographie der RWTH, Aachen D-52056, Germany

Fundamental conservation laws predict ballistic transport behavior in one-dimensional quantum magnets. This suggests anomalously large life times and mean free paths of the quantum spin excitations. Despite this rigorous prediction, in any real system, the transport is dissipative, due to the interaction of spinons with defects and phonons. Nevertheless, not very long ago, a promis-

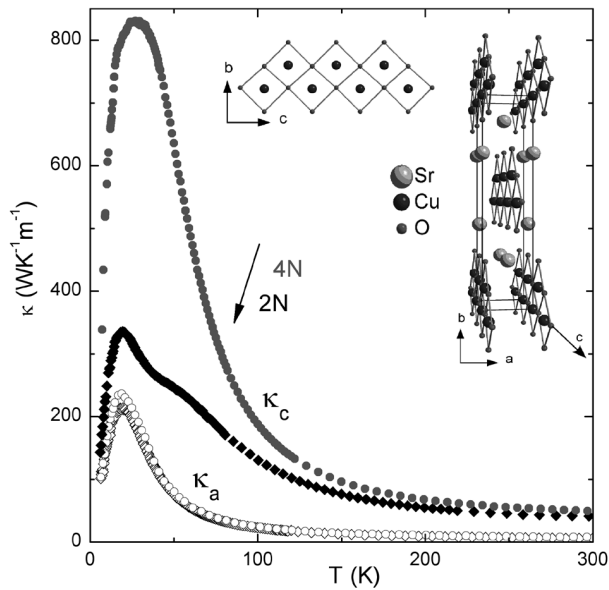


**Fig. 1.** Thermal conductivity of SrCuO<sub>2</sub> for two different purities.

ing large magnetic thermal conductivity  $\kappa_{\text{mag}}$  has been found in a number of spin chain materials with large exchange interaction  $J$ . Especially the single chain compound  $\text{Sr}_2\text{CuO}_3$  and the double chain  $\text{SrCuO}_2$  are good model systems for this new kind of transport mechanism. In high purity samples huge magnetic heat conductivities (confer to Fig. 1 and ref. [1]) and concomitantly, extremely large spinon mean free paths of  $>0.5 \mu\text{m}$  for  $\text{Sr}_2\text{CuO}_3$  and  $>1\mu\text{m}$  for  $\text{SrCuO}_2$  are observed. This demonstrates that  $\kappa_{\text{mag}}$  is only limited by extrinsic scattering processes, which is a clear signature of ballistic transport in the underlying spin model. Additionally, various subtle modifications of the spin chain are studied. Due to the large mean free path a pristine picture of the intrinsic incidents is expected. In particular, bond disorder by doping  $\text{SrCuO}_2$  with Ca on the Sr site has a surprisingly strong effect on  $\kappa_{\text{mag}}$ . Furthermore, the influence of site disorder is studied by substitution of Cu with magnetic Ni and non-magnetic Mg in  $\text{SrCuO}_2$ .

1. Hlubek N., Ribeiro P., Saint-Martin R., Revcolevschi A., Roth G., Behr G., Büchner B., Hess C.: Phys. Rev. B **81**, 020405R (2010)

## Classical versus Quantum Magnetism in Single Molecular Magnetic Complexes

Y. Krupskaya<sup>1,2</sup>, F. Moro<sup>3</sup>, V. Kataev<sup>1</sup>, T. C. Stamatatos<sup>4</sup>, G. Christou<sup>4</sup>,  
A. J. Tasiopoulos<sup>5</sup>, J. van Slageren<sup>6</sup>, and B. Büchner<sup>1</sup>

<sup>1</sup> Leibniz Institute for Solid State and Materials Research (IFW) Dresden, Dresden D-01171, Germany, [y.krupskaya@ifw-dresden.de](mailto:y.krupskaya@ifw-dresden.de)

<sup>2</sup> Zavoisky Physical-Technical Institute, Russian Academy of Sciences, Kazan 420029, Russian Federation

<sup>3</sup> School of Chemistry, University of Nottingham, Nottingham NG7 2RD, UK

<sup>4</sup> Department of Chemistry, University of Florida, Florida 32611-7200, USA

<sup>5</sup> Department of Chemistry, University of Cyprus, Nicosia 1678, Cyprus

<sup>6</sup> Institut fuer Physikalische Chemie, Universitaet Stuttgart, Stuttgart D-70569, Germany

We present a detailed magnetic study of Mn-based single molecular magnetic complexes by means of the static (DC) magnetization measurements and the high-field/frequency electron spin resonance (HF-ESR) spectroscopy. Our measurement results reveal different properties of the studied complexes; some of them can be understood from the classical point of view, however there are distinct features which can be explained only with the help of the quantum mechanics. And finally we discuss the interplay between the molecular structures of the complexes and their quantum mechanical and classical magnetic properties.

## Experimental Realization of the Spin Switch Effect for the Superconducting Current in a Superconductor/Ferromagnet Thin Film Heterostructure

*P. V. Leksin<sup>1</sup>, N. N. Garif'yanov<sup>1</sup>, I. A. Garifullin<sup>1</sup>, J. Schumann<sup>2</sup>, V. Kataev<sup>2</sup>, O. G. Schmidt<sup>2</sup>, and B. Büchner<sup>2</sup>*

<sup>1</sup>*Zavoisky Physical-Technical Institute, Russian Academy of Sciences, Kazan 420029, Russian Federation, ancientfear@mail.ru*

<sup>2</sup>*Leibniz Institute for Solid State and Material Research (IFW Dresden), Dresden D-01171, Germany*

The antagonism of superconductivity (S) and ferromagnetism (F) consists of strong suppression of S by F because F requires parallel (P) and S requires antiparallel (AP) orientation of spins. The significant interest in recent investigations of S and F interplay is focused on heterostructures where S and F are spatially separated (see, for example, review [1]). The effects observed in such multilayered systems are called S/F proximity effect. One of the theoretical predictions waiting for experimental confirmation is the so called spin valve effect for the superconducting (SC) current. Its physical origin relies on idea to control pair breaking, and hence SC transition temperature  $T_c$ , by manipulating the mutual orientation of the magnetizations of the F-layers in a heterostructure comprising, e.g., two F- and one S-layer (see Fig. 1). This is because the mean exchange field from two F-layers acting on Cooper pairs in the S-layer is smaller for AP orientation compared to the P case.

The possibility to develop a spin switch based on the on the S/F proximity effect has been theoretically substantiated in 1997 by Oh *et al.* [2]. They

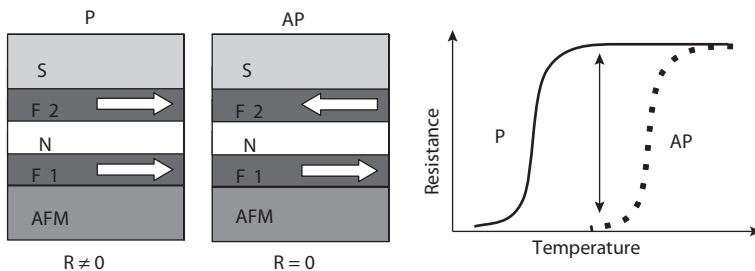


**Fig. 1.** Design of the SC spin valve sample.

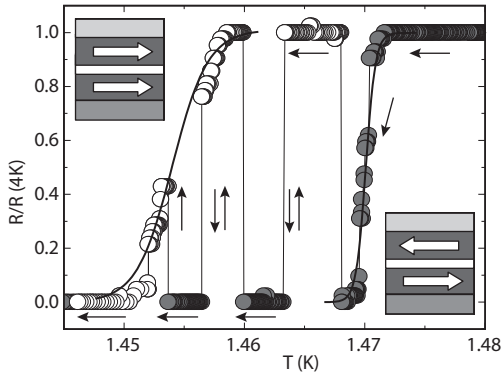


**Fig. 2.** Switching between normal and SC states for the spin valve sample during slow temperature sweep.  $\circ$  – P state,  $\bullet$  – AP state.

proposed the F1/F2/S layer scheme (Fig. 1) where an S-film is deposited on top of two F-layers.

In this scheme Cooper pairs penetrate inside the space between F1 and F2 layers where they are affected by the mean exchange field. Two years later a different construction based on an F/S/F trilayer was proposed theoretically by Tagirov [3] and Buzdin [4]. Several experimental works confirmed the predicted influence of the F layers on  $T_c$  (cf. e.g., ref [5]). However the difference in  $T_c$  between AP- and P-orientation  $\Delta T_c = T_c^{\text{AP}} - T_c^{\text{P}}$  turns out to be smaller than the SC width  $\delta T_c$ . Hence a full switching between the normal and the SC state was not achieved. Implementation of a design similar to the F1/N/F2/S trilayer scheme by Oh et al. [2] with a  $[\text{Fe}/\text{V}]_n$  antiferromagnetically coupled superlattice instead of a single F1/N/F2 [6] trilayer is not actually the spin switch device because the system cannot be switched from the AP to P state instantaneously. At the same time the analysis of the critical field has shown that the implicitly  $\Delta T_c$  of this system can reach up to 200 mK at  $\delta T_c \sim 100$  mK. Comparison of the results obtained for both proposed constructions of the spin switches gives grounds to suppose that the scheme by Oh et al. [2] may be more promising for the realization of the full spin switch effect. We have fabricated a set of samples  $\text{MgO}/\text{CoO}_x/\text{Fe1}/\text{Cu}/\text{Fe2}/\text{In}$  which show a full switching [7]. The value  $\Delta T_c$  was about 20 mK. It is not the largest among published before (cf. e.g., ref [5], where  $\Delta T_c = 41$  mK at  $\delta T_c \sim 100$  mK). However, very important is that it is larger than  $\delta T_c$  which is about 7 mK in our case. This opens a possibility to switch off and on the superconducting current flowing through our sample

*completely* within the temperature range corresponding to the  $\Delta T_c$  by changing the mutual orientation of magnetization of F1 and F2 layers (see Fig. 2). Our further investigations of this system revealed the sign changing oscillating behavior of the spin valve effect  $\Delta T_c$  with a varied F2-layer thickness which is correlated with the quantum interference of the Cooper pair wave functions on the F2/S interface [8].

This work was supported by the RFBR (Grants № 08-02-00098, № 08-02-91952-NNIO) and the DFG (Grant Nos. 436 RUS 113/936/0-1 and BU 887/13–1).

1. Garifullin I.A.: J.M.M.M. **240**, 571 (2002)
2. Oh S. *et al.*: Appl. Phys. Lett. **71**, 2376 (1997)
3. Tagirov L.R.: Phys. Rev. Lett. **83**, 2058 (1999)
4. Buzdin A.I. *et al.*: Europhys. Lett. **48**, 686 (1999)
5. Moraru I.C. *et al.*: Phys. Rev. Lett. **101**, 137001 (2008)
6. Nowak G. *et al.*: Phys. Rev. B **78**, 134520 (2008)
7. Leksin P.V. *et al.*: Appl. Phys. Lett. **97**, 102505 (2010)
8. Leksin P.V. *et al.*: Phys. Rev. Lett. **106**, 067005 (2011)

## Low Temperature Ballistic Spin Transport in the $S = 1/2$ Antiferromagnetic Heisenberg Chain Compound $\text{SrCuO}_2$

*H. Maeter*<sup>1</sup>, *A. A. Zvyagin*<sup>1,2</sup>, *H. Luetkens*<sup>3</sup>, *G. Pasqua*<sup>3</sup>, *Z. Shermadini*<sup>3</sup>,  
*R. Saint-Martin*<sup>4</sup>, *A. Revcolevschi*<sup>4</sup>, *C. Hess*<sup>5</sup>, *B. Büchner*<sup>5</sup>,  
and *H.-H. Klaus*<sup>1</sup>

<sup>1</sup> *Institute of Solid State Physics, TU Dresden, Dresden 01069, Germany,  
h.maeter@physik.tu-dresden.de*

<sup>2</sup> *Institute for Low Temperature Physics and Engineering of the NAS of Ukraine,  
Kharkov 61103, Ukraine*

<sup>3</sup> *Laboratory for Muon-Spin Spectroscopy, Paul Scherrer Institut, Villigen 5232, Switzerland*

<sup>4</sup> *Laboratoire de Physico-Chimie de L'Etat Solide, Universite Paris-Sud,  
Orsay 91405, France*

<sup>5</sup> *Leibniz Institute for Solid State and Materials Research Dresden, Dresden 01171, Germany*

For one-dimensional quantum spin chain systems recent experimental and theoretical studies indicate unexpectedly large, in some cases diverging spin and heat transport coefficients. Local probes, like e.g. muon spin relaxation ( $\mu\text{SR}$ ) can indirectly characterize the spin transport properties of low dimensional systems via the magnetic field dependence of the spin lattice relaxation rate  $\lambda(B)$ . For diffusive spin transport  $\lambda \propto B^{-0.5}$  is expected. For the ground state of the isotropic spin-1/2 antiferromagnetic Heisenberg chain the eigenstates of the Heisenberg Hamiltonian determine the spin transport, which is then *ballistic*. Using the Müller ansatz  $\lambda \propto B^{-1}$  is expected in this case. For  $\text{SrCuO}_2$  we find  $\lambda \propto B^{-0.9(3)}$ . This result is temperature independent for  $5 \text{ K} \leq T \leq 300 \text{ K}$ . Within conformal field theory and using the Müller ansatz we conclude ballistic spin transport in  $\text{SrCuO}_2$ .

## Charge Segregation and Phase Separation in Manganites and the Possibility of Multiferroic Behaviour

*R. F. Mamin*

*Zavoisky Physical-Technical Institute, Russian Academy of Sciences, Kazan 420029,  
Russian Federation, mamin@kfti.knc.ru*

The search for materials with the multiferroic behaviour had mainly been focused on insulating materials. The complicated interplay among charge, spin and lattice degrees of freedom in doped manganites lead to the unexpected phenomena such as phase separation with charge segregation [1]. The problem of spatially inhomogeneous states in the charged systems frustrated by the Coulomb interactions is constantly under debate for different systems. In this work we discuss the possibility of multiferroic-like behaviour due to magnetic phase separation with charge segregation phenomenon in pre-percolation regime.

Localized charged states and phase segregation are described in the framework of the phenomenological Ginzburg-Landau theory of phase transitions. The Coulomb interaction determines charge distributions and characteristic length of the phase separated states. The phase separation with charge segregation becomes possible because large dielectric constant and small density of extra charge in the range of charge localization. The phase diagram is calculated and the energy gain of the phase separated state is estimated. The role of the Coulomb interaction is elucidated. The influence of magnetic field on that states in the pre-percolation regime is investigated and the possibilities of polar states due Jan-Teller effect and of polar states induced by external electric field are discussed.

The colossal magnetocapacitance effect at  $\text{La}_{1-x}\text{Sr}_x\text{MnO}_3$  single crystals [2] is discussed in framework of that approach. It is also shown that the properties of the local states induced by electric field in  $\text{La}_{0.9}\text{Sr}_{0.1}\text{MnO}_3$  single crystals [3] can be associated with this phenomenon.

1. Dagotto E., Hotta T., Moreo A.: *Physics Report* **344**, 1 (2001)
2. Mamin R.F., Egami T., Marton Z., Migachev S.A.: *Phys. Rev. B* **75**, 115129 (2007)
3. Mamin R. F., Bdikin I. K., Kholkin A. L.: *Appl. Phys. Lett.* **94**, 222901 (2009)

## Monopole-Like Probes for Magnetic Force Microscopy

*T. Mühl, S. Vock, J. Körner, F. Wolny, V. Neu, A. Leonhardt, and B. Büchner*

*Leibniz Institute for Solid State and Materials Research Dresden,  
Dresden D-01069, Germany*

Magnetic force microscopy (MFM) is a powerful method dedicated to map stray-field distributions, or more precisely, derivatives in space of magnetic field components. Recently we developed a sensor for quantitative MFM based on an iron-filled carbon nanotube (FeCNT) [1, 2]. The long Fe nanowire contained in the carbon nanotube can be regarded as an arrangement of two well-separated magnetic monopoles of which only the monopole nearest to the sample surface is involved in the imaging process. The monopole-like character of FeCNT MFM probes allows easy calibration and thus quantitative evaluation of the MFM data. Moreover, as compared to conventional coated MFM probes, FeCNT sensors show remarkable magnetic stability in external in-plane fields [3].

Recently, we developed an improved MFM sensor design again employing FeCNTs. By using higher order flexural vibration modes of the cantilever the new sensor provides both in-plane and perpendicular sensitivity for quantitative MFM measurements. We discuss sensitivity issues related to the dynamic spring constants of the sensor.

1. Wolny F., Mühl T., Weissker U., Lipert K., Schumann J., Leonhardt A., Büchner B.: *Nanotechnology* **21**, 435501 (2010)
2. Vock S., Wolny F., Mühl T., Kaltofen R., Schultz L., Büchner B., Hassel C., Lindner J., Neu V.: *Appl. Phys. Lett.* **97**, 252505 (2010)
3. Wolny F., Mühl T., Weissker U., Leonhardt A., Wolff U., Givord D., Büchner B.: *J. Appl. Phys.* **108**, 01398 (2010)

## EPR Study of Local Magnetic Fields on the $\text{Bi}_2\text{Sr}_2\text{Ca}_{1-x}\text{Y}_x\text{Cu}_2\text{O}_{8+y}$ Single Crystal Surface above $T_c$

*L. Salakhutdinov<sup>1</sup>, Yu. Talanov<sup>1</sup>, G. Teitel'baum<sup>1</sup>, T. Adachi<sup>2</sup>, T. Noji<sup>2</sup>,  
Y. Koike<sup>2</sup>, and R. Khasanov<sup>3</sup>*

<sup>1</sup> *Zavoisky Physical-Technical Institute, Russian Academy of Sciences, Kazan 420029,  
Russian Federation, L\_Salakhutdinov@kfti.knc.ru*

<sup>2</sup> *Department of Applied Physics, Tohoku University, Sendai, Japan*

<sup>3</sup> *Paul Scherrer Institut, Villigen 5232, Switzerland*

Recently a rich variety of interesting and in most cases unexplained phenomena were discovered in cuprate high- $T_c$  superconductors (HTSC) near and above the critical temperature. All of them are connected with the pseudogap state (PGS). Here we present the HTSC study results obtained by EPR technique. We have investigated the  $\text{Bi}_2\text{Sr}_2\text{Ca}_{1-x}\text{Y}_x\text{Cu}_2\text{O}_{8+y}$  single crystals with different contents of yttrium. The spatial distribution of the internal magnetic field was studied with the surface paramagnetic probe. The thin layer of diphenylpicrylhydrazyl (DPPH) is used as a sensitive probe. The analysis of the temperature dependence of the ESR signal parameters, such as the resonance field and the line width, indicates the existence of the magnetic field inhomogeneity on the sample surface in PGS. We reason that it is due to the phase separation with the formation of areas of two types, magnetic and metallic, and the last ones may be in the vortex-type state.

## Tunnel Magnetoresistance in Double-Barrier Planar Magnetic Tunnel Junctions

*A. Useinov*

## The Interrelation of Various Temperature Dependent Contributions to Magnetization in $\text{Eu}_{1-x}\text{Ca}_x\text{CoO}_{3-\delta}$ Solid Solutions

*T. Vasilchikova<sup>1</sup>, T. Kuzmova<sup>1</sup>, A. Kamenev<sup>1</sup>, O. Volkova<sup>1</sup>, A. Kaul<sup>1</sup>, R. Klingeler<sup>3</sup>, B. Büchner<sup>2</sup>, and A. Vasiliev<sup>1</sup>*

<sup>1</sup> *Moscow State University, Moscow 119991, Russian Federation*

<sup>2</sup> *Leibniz Institute for Solid State and Materials Research, IFW Dresden, Dresden 01171, Germany*

<sup>3</sup> *Kirchhoff Institut for Physics, University of Heidelberg, Heidelberg 69120, Germany*

In the present work, we have investigated the magnetic susceptibility in  $\text{Eu}_{1-x}\text{Ca}_x\text{CoO}_{3-\delta}$  in order to evaluate trends in the spin-state transitions upon doping. The choice of  $\text{Eu}^{3+}$  ions among rare earths metals was motivated by the fact that these ions exhibit a half-filled f-shell and hence a vanishing total magnetic moment, i.e. the rather small contribution of the transition metal subsystem is not masked. The  $\text{Ca}^{2+}$  ions among alkaline earths metals were chosen because

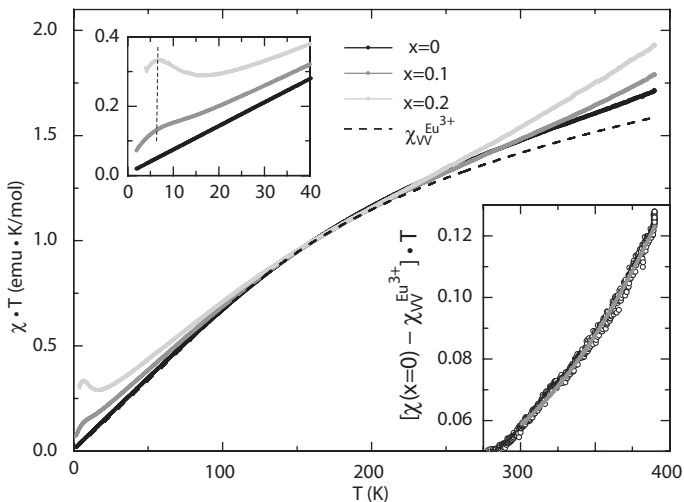


**Fig. 1.** The temperature dependences of the product  $\chi \cdot T$  for the  $\text{Eu}_{1-x}\text{Ca}_x\text{CoO}_{3-\delta}$  family of compounds. Lower inset represents the difference between the data for  $x = 0$  and the  $\text{Eu}^{3+}$  van Vleck contribution. The upper inset highlights the low temperature behavior.

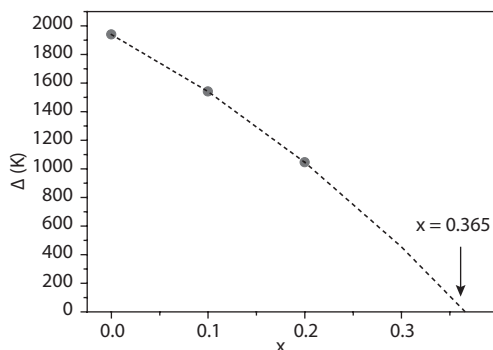


**Fig. 2.** The concentration dependence of the gap  $\Delta$  between low spin and high spin states in the  $\text{Eu}_{1-x}\text{Ca}_x\text{CoO}_{3-\delta}$  family of compounds.

the difference in ionic radii with the  $\text{Eu}^{3+}$  ions was expected to shift the spin-state transitions to lower temperatures.

The magnetization in  $\text{Eu}_{1-x}\text{Ca}_x\text{CoO}_{3-\delta}$  ( $0 < x < 0.2$ ) solid solutions is investigated in the temperature range 2–390 K. In accordance with the synthesis procedure, the partial substitution of  $\text{Eu}^{3+}$  ions by  $\text{Ca}^{2+}$  ions does not increase the mean valence state of cobalt but is accompanied by appearance of oxygen vacancies in the ratio  $\delta = x/2$ . Each oxygen vacancy reduces the local coordination of two neighboring  $\text{Co}^{3+}$  ions to pyramidal thereby locally creating magnetically active sites which couple to magnetic dimers. These dimers evolve on the background of the intrinsically non-magnetic lattice of octahedral coordinated low-spin  $\text{Co}^{3+}$  ions in  $\text{EuCoO}_3$ .

Generally, the expression for the magnetic susceptibility in  $\text{Eu}_{1-x}\text{Ca}_x\text{CoO}_{3-\delta}$  family of compounds can be written as a sum of virtually independent terms:  $\chi = \chi_0 + \chi_{\text{Eu}} + \chi_{\text{Co-pyr}} + \chi_{\text{Co-oct}}$  ( $\chi_0$  – the temperature-independent diamagnetic and Co van Vleck contribution,  $\chi_{\text{Eu}}$  – the van Vleck contribution of the  $\text{Eu}^{3+}$  ions,  $\chi_{\text{Co-pyr}}$  – the contribution of magnetically active  $\text{Co}^{3+}$  ions in pyramidal coordination,  $\chi_{\text{Co-oct}}$  – the  $\text{Co}^{3+}$  ions contribution dependent on their spin state in octahedral coordination). The analysis of the product  $\chi \cdot T$  allows revealing the major trends in behavior of the systems experiencing the transition between different spin states (Fig. 1). At lowest temperatures, the dimers dominate the magnetic response for  $x \neq 0$ . contrast, the  $\text{Eu}^{3+}$  van Vleck contribution is relevant in the whole temperature range for all samples. It is rather temperature independent at low temperatures and diminishes at intermediate temperatures.

At high temperatures, there is a temperature-induced spin-state transition of the octahedral  $\text{Co}^{3+}$  ions which causes an additional contribution to the magnetization. The temperature dependence of the magnetic susceptibility  $\chi_{\text{Co-oct}}$  can be approximated by the expression for two-level system [1]. An estimation of the gap  $\Delta$  can be made directly from this expression by analyzing the high temperature magnetic susceptibility. In Fig. 1 the product  $\chi \cdot T$  in the parent compound  $\text{EuCoO}_3$  is compared to the  $\text{Eu}^{3+}$  van Vleck contribution. The difference of these curves (the lower inset of Fig. 1) can be approximated by the magnetic susceptibility of two-level system multiplied by temperature. Fitting the data yields the energy gap  $\Delta$  between the low-lying  $t_{2g}$  orbitals and the high-lying  $e_g$  orbitals in  $\text{EuCoO}_3$  of  $\Delta = 1940$  K. Upon doping, the magnetization at high temperatures increases which already qualitatively indicates that the energy gap  $\Delta$  becomes smaller. Indeed, calculations similar to that for the parent compound allow to establish the concentration dependence of the energy gap  $\Delta$  in the  $\text{Eu}_{1-x}\text{Ca}_x\text{CoO}_{3-\delta}$  family of compounds (Fig. 2). Evidently, the gap decreases rapidly in the range doping  $0 < x < 0.2$  reaching  $\Delta = 1050$  K in  $\text{Eu}_{0.8}\text{Ca}_{0.2}\text{CoO}_{2.9}$ .

1. Baier J., Jodlauk S., Kriener M., Reichl A., Zobel C., Kierspel H., Freimuth A., Lorenz T.: Phys. Rev. B **71**, 014443 (2005)

## Relaxation Study of Novel Binuclear Mn Molecular Complexes by Pulse EPR Techniques

*R. Zaripov<sup>1</sup>, E. Vavilova<sup>1,2</sup>, Y. Krupskaya<sup>2</sup>, A. Parameswaran<sup>2</sup>, V. Milyukov<sup>3</sup>, I. Bezkishko<sup>3</sup>, D. Krivolapov<sup>3</sup>, O. Kataeva<sup>3</sup>, O. Sinyashin<sup>3</sup>, E. Hey-Hawkins<sup>4</sup>, V. Voronkova<sup>1</sup>, K. Salikhov<sup>1</sup>, R. Klingeler<sup>2</sup>, V. Kataev<sup>2</sup>, and B. Büchner<sup>2</sup>*

<sup>1</sup> *Zavoisky Physical-Technical Institute, Russian Academy of Sciences, Kazan 420029, Russian Federation, zaripov.ruslan@gmail.com*

<sup>2</sup> *IFW Dresden, Dresden, Germany*

<sup>3</sup> *Arbuzov Institute of Organic and Physical Chemistry, Russian Academy of Sciences, Kazan 420088, Russian Federation*

<sup>4</sup> *Institute of Inorganic Chemistry, Leipzig University, Leipzig 04109, Germany*

At present molecular clusters are actively studied as perspective systems for quantum informatics. In this work we report a study of binuclear Mn molecular complexes by pulse EPR methods. It should be noted that magnetic properties of this complex systematically depend on a ligand type. The transverse relaxation times of Mn spins at different temperatures in these complexes in the solid phase and in frozen solution (TGF) were determined. We observe a simple exponential decay in the latter samples and a non-exponential relaxation process in the former ones. Two pulse ESEEM (electron spin echo envelope modulation) data reveal the hyperfine coupling to the protons. This fact is very important in the electron spin decoherence processes. The data also suggest an important role of the intermolecular spin-spin coupling for the phase relaxation. The influence of both mechanisms is the real impediment to coherent spin manipulating of molecular magnets with regard to their possible application for quantum computing.

The work was supported by the DFG through grants FOR-1154 and BU 887/13-1, and by the RFBR through grant 08-02-91952-NNIO.

## Spin Dynamics in New Honeycomb-Layered Antimonates of Alkali and Transition Metals

*E. Zvereva*<sup>1</sup>, *O. Savelieva*<sup>1</sup>, *V. Nalbandyan*<sup>2</sup>, *M. Evstigneeva*<sup>2</sup>, *L. Medvedeva*<sup>2</sup>,  
*A. Wolter*<sup>3</sup>, *J.-Y. Lin*<sup>4</sup>, *A. Vasiliev*<sup>1</sup>, *R. Klingeler*<sup>5</sup>, and *B. Büchner*<sup>3</sup>

<sup>1</sup> Faculty of Physics, M. V. Lomonosov Moscow State University, Moscow 119992,  
Russian Federation, zvereva@mig.phys.msu.ru

<sup>2</sup> Chemistry Faculty, Rostov State University, Rostov-on-Don 344090, Russia

<sup>3</sup> Leibniz Institute for Solid State and Materials Research IFW, Dresden D-01171, Germany

<sup>4</sup> National Chiao Tung University, Hsinchu, Taiwan

<sup>5</sup> Kirchhoff Institute for Physics, University of Heidelberg, Heidelberg D-69120, Germany

Layered alkali and transition metal oxides are of great interest due to their high  $\text{Na}^+$  or  $\text{Li}^+$  ion conductivity and, as a consequence, their potential applications as electrode materials for Li-ion batteries. We report here on static (SQUID measurements:  $T = 2 \div 300$  K,  $B \leq 5$  T) and dynamic (X-band ESR:  $T = 6\text{--}470$

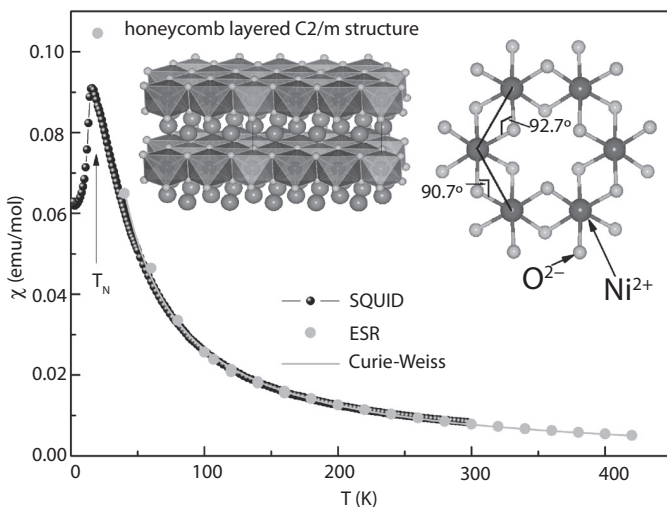


**Fig. 1.** Temperature dependence of magnetic susceptibility at  $B \approx 0.1$  T (black circles) and integral ESR intensity (gray circles) for  $\text{Li}_3\text{Ni}_2\text{SbO}_6$ , the solid curve represent an approximation in accordance with the Curie-Weiss law. Insets: Polyhedral view of the C2/m structure and its fragment in the  $ab$  plane, showing an organization of Ni-O-Ni bonds within the mixed-cation layer. Nickel, lithium and oxygen ions are shown by green, blue and red spheres, respectively.

K,  $B \leq 0.7$  T) magnetic properties of new layered compounds  $\text{Li}_3\text{Ni}_2\text{SbO}_6$ ,  $\text{Na}_3\text{Ni}_2\text{SbO}_6$ ,  $\text{Li}_4\text{FeSbO}_6$ , which represent superlattices of the  $\alpha\text{-NaFeO}_2$  type (rock-salt type) with  $\text{M}^{2+}/\text{Sb}^{5+}$  ordering on  $\text{Fe}^{3+}$  sites in a “honeycomb” fashion.

All antimonite systems under study demonstrate common features of magnetic behavior and order antiferromagnetically at  $T_N \sim 3.6, 15$  and  $17$  K for  $\text{Li}_4\text{FeSbO}_6$ ,  $\text{Li}_3\text{Ni}_2\text{SbO}_6$  and  $\text{Na}_3\text{Ni}_2\text{SbO}_6$  respectively (Fig. 1). At high temperatures, the magnetic susceptibility follows the Curie-Weiss law, however the Weiss temperature takes negative value  $\sim -17$  K for  $\text{Li}_4\text{FeSbO}_6$  compound, while it takes positive values  $\sim 8$  K for  $\text{Li}_3\text{Ni}_2\text{SbO}_6$  and  $\sim 15$  K for  $\text{Na}_3\text{Ni}_2\text{SbO}_6$  indicating predominance of ferromagnetic interactions in both later compounds. The effective magnetic moments are  $5.9 \mu_B$  per Fe atom and  $2.15 \mu_B$  per Ni atom respectively, which satisfactorily agree with theoretical estimations assuming high-spin configuration of  $\text{Fe}^{3+}$  ( $S = 5/2$ ) and  $\text{Ni}^{2+}$  ( $S = 1$ ). The  $M(H)$  isotherms at  $T < T_N$  show no hysteresis and no saturation in magnetic fields up to 5 T. However, the magnetization curve has a slight upward curvature suggesting the possible presence of a magnetic field induced spin-flop transition.

Electron spin resonance (ESR) spectra show single Lorentzian shape line attributed to transition metal ions to be in octahedral coordination. In the paramagnetic phase the absorption is characterized by isotropic temperature independent effective  $g$ -factor  $g = 1.99 \pm 0.01$  for iron antimonite and  $g = 2.150 \pm 0.005$  for nickel antimonite, correspondingly. The ESR linewidth, which is a measure of spin relaxation rate, anomalously increases when the temperature decreases up to  $T_N$ . Temperature dependence of  $g$ -value also demonstrates sharp anomaly in the vicinity of  $T_N$ . An analysis of line broadening at low temperature has been performed in the framework of theory developed for canonical antiferromagnetic and spin-glass systems and satisfactory agreement has been achieved.

The magnetic exchange pathways have been rationalized in accordance with the Goodenough-Kanamori rules. An analysis of the layered honeycomb crystal structure (see insets in Fig. 1) has shown that the dominant superexchange interaction within mixed-cation layers appears to be ferromagnetic, while the coupling between magnetically-active layers is obviously antiferromagnetic providing an antiferromagnetic ground state of the compounds.



---

## POSTERS

## Influence of Admixtures on the Formation of Paramagnetic Centers in Calcium Gluconate at Mechanoactivation

*M. M. Akhmetov<sup>1</sup>, G. G. Gumarov<sup>1,3</sup>, V. Yu. Petukhov<sup>1,3</sup>, G. N. Konygin<sup>2</sup>,  
D. S. Rybin<sup>2</sup>, and E. P. Zheglov<sup>1</sup>*

<sup>1</sup> *Zavoisky Physical-Technical Institute, Russian Academy of Sciences, Kazan 420029,  
Russian Federation, mansik86@mail.ru*

<sup>2</sup> *Physical-Technical Institute, Izhevsk 42600, Russian Federation*

<sup>3</sup> *Kazan Federal University, Kazan 420008, Russian Federation*

Earlier [1], it has been shown that mechanochemical treatment of calcium gluconate (CG) leads to sufficient increase of its therapeutic efficiency. At the same time the formation of paramagnetic centers responsible for appearance of an EPR signal with  $g = 2.005$  and line width  $\sim 8.5$  Oe was also observed in calcium gluconate subjected to mechanochemical treatment [2]. An assumption was made that therapeutic efficiency of the medical product may be connected with the formation of polymorphic molecular modifications and stereoisomerization of the CG molecule which are associated with formation of free radicals. Therefore it is extremely important to study the mechanism of their emergence and accumulation. Also it is known that interaction of radicals

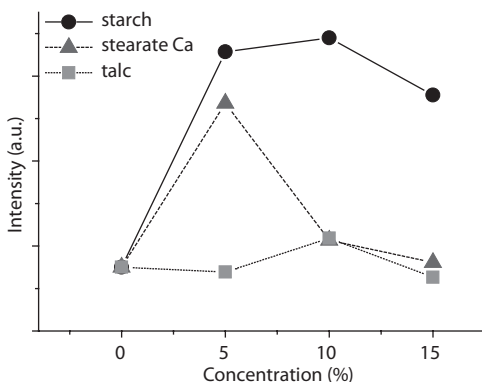


**Fig. 1.** EPR intensity vs. concentrations for different admixtures (line connecting the data points serves as an eye-guide)

emerging during mechanical activation with environmental components can significantly influence the radical emergence and stabilization [3].

The goal of the present work is to study the influence of admixtures (excipients) present in official calcium gluconate on formation and accumulation of paramagnetic centers upon mechanical activation of calcium gluconate.

Mechanochemical treatment of calcium gluconate with excipients (talc, starch and calcium stearate) was made using ball grinder Pulverizette-7, the grinding time being from 10 min to 1 hour. EPR spectra were recorded on Varian E-12 spectrometer at a frequency of ca. 9.5 GHz at room temperature.

The performed experiments showed that concentration of paramagnetic centers emerging in CG as a result of its mechanical treatment significantly depends on type and amount of introduced admixtures. As can be seen in Fig. 1, adding starch and calcium stearate in amount up to 5 wt% significantly increases the intensity of the EPR signal with respect to the signal of mechanically activated calcium gluconate without excipients (fourfold at  $t = 1$  h). Further increase of the starch content up to 15 wt% only slightly influences the amplitude of the EPR signal. The line intensity sharply changes with increasing content of calcium stearate, while adding talc up to 15 wt% has almost no impact on the EPR line intensity regardless of the duration of mechanical treatment.

To find out the direct influence of input admixtures on changes in registered spectra, EPR spectra of powders of initial excipients and those after mechanical activation were recorded separately. Starch is a paramagnet and mechanical treatment results in emergence of additional paramagnetic centers. However, the parameters of these EPR spectra significantly differ from those of a free radical emerging upon mechanical treatment of calcium gluconate. In particular, the  $g$ -factors and line widths of initial and mechanically activated (for  $t = 10$  min) powders of starch are  $g_s = 2.162$ ,  $\delta H_s \sim 265$  Oe and  $g_{MAS} = 2.51$ ,  $\delta H_{MAS} \sim 2000$  Oe, respectively. EPR spectra of initial and mechanically activated samples of calcium stearate and talc also have principal differences from those for both pure mechanically activated CG and pelleted.

Thus, it has been established that an intensive line with  $g \sim 2.005$  and width of ca. 8 Oe, observed in the EPR spectrum of mechanically activated binary compounds, originates from calcium gluconate and is not a superposition of lines from excipients present in the composition. At the same time, an amplitude of the line from mechanically activated calcium gluconate (and, consequently, the concentration of paramagnetic centers therein) significantly depends on the excipient type and its concentration. Apparently, excipients

play role in weakening of the processes of radical recombination and their stabilization immediately after their emergence.

1. Konygin G.N. *et al.*: Patent of the Russian Federation №2268053, 2004.
2. Gumarov G.G., Petuhov V.Yu., Konygin G.N., Rybin D.S., Zheglov E.P.: Almanac of Clinical Medicine, vol. XVII, part I, p. 47. MONIKI, -M., 2008.
3. Baramboim N.K. Mechano-Chemistry of Macromolecular Compounds. -2-nd ed. Himiya, -M., 1971. 363 p.

## Optimization of Heusler Compounds via Control of the Relations between Structure and Physical Properties

*A. Alfonsov, C. G. F. Blum, O. Volkonskyi, S. Rodan, D. Bombor, C. Hess, A. Wolter, S. Wurmehl, and B. Büchner*

*IFW Dresden, Dresden 01069, Germany*

Spintronics combines the use of both the charge and the spin of an electron as information carriers, which promises distinct advantages over the conventional electronics which make only use of the charge of electrons. Particularly, half-metallic ferromagnets are a hot topic of many research groups, as they are predicted to be 100% spin polarized, e.g. having electrons at the Fermi level with one single spin direction.

Heusler compounds are ternary intermetallic  $X_2YZ$ -compounds, crystallizing in the  $L2_1$  structure. Among them are many ferromagnets which are predicted to be half-metallic. This is the reason why Heusler compounds are an interesting research topic in the field of spintronic materials.

A successful application of spin-polarized materials in spintronic devices requires a detailed knowledge of the interplay between the structure and the magnetic and electronic properties. This is achieved by gaining knowledge of the local structure by means of Nuclear Magnetic Resonance (NMR). NMR probes the direct local environments of the active atoms and is thus able to resolve neighboring shells providing a unique tool to study the (local) structural properties of spin polarized materials [1–4].

Recent results of structural characterization of various spin polarized Heusler compound (such as bulk samples of  $\text{Co}_2\text{FeAl}$ , the substitutional series  $\text{Co}_2\text{Mn}_{(1-x)}\text{Fe}_x\text{Si}$ , thin films of  $\text{Co}_2\text{FeSi}$ , and Co-Fe-Al CPP-GMR spin valves) will be discussed. In particular, the local structure, as revealed by NMR, will be discussed with respect to their impact for spintronics.

1. Wurmehl S., *et al.*: Appl. Phys. Lett. **91**, 052506 (2007)
2. Wurmehl S., J. T. Kohlhepp: Topical review in J. Phys. D: Appl. Phys. **41**, 173002 (2008)
3. Wurmehl S., *et al.*: J. Phys. D: Appl. Phys. **42**, 084017 (2009)
4. Wurmehl S. *et al.*: Appl. Phys. Lett. **98**, 012506 (2011)

## Electron Spin Resonance in Eu-Based Antiferromagnetic Compounds

T. S. Altshuler<sup>1</sup>, Y. V. Goryunov<sup>1</sup>, A. V. Levchenko<sup>2</sup>, and A. N. Nateprov<sup>3</sup>

<sup>1</sup> Zavoisky Physical-Technical Institute, Russian Academy of Sciences, Kazan 420029, Russian Federation, goryunov@kfti.knc.ru

<sup>2</sup> Institute of the Material Science Problems, Kiev 03680, Ukraine

<sup>3</sup> Institute of Applied Physics, Kishinev 2028, Moldova

Recent years the considerable attention of researchers attracted to the phenomena occurring during phase transitions, the causes of phase transitions and order-parameter fluctuations, the quantum phase transitions. We investigated a number of europium-containing antiferromagnets and we found several common features of the temperature behavior of magnetic susceptibility and the Curie Weiss law. The peculiarity of this behavior is typical for temperature dependence of magnetic susceptibility of antiferromagnetic (see Fig. 1) and at the same time it is typical for a the temperature dependence of inverse susceptibility of ferromagnet. Another feature of the behavior of the investigated compounds are strong fluctuations of the magnetization that occur in a wide temperature range.

$\text{EuCd}_2\text{Sb}_2$  and  $\text{EuZn}_2\text{As}_2$  (space group P-3m1) are anti-ferromagnetic with  $\theta_p \sim -6.5$  and  $-16.5$  K and their electrical resistances  $R(T)$  are metal-like and semiconductor-like [1], respectively.  $\text{EuB}_6\text{C}_x$  (space group Pm-3m) is ferro-

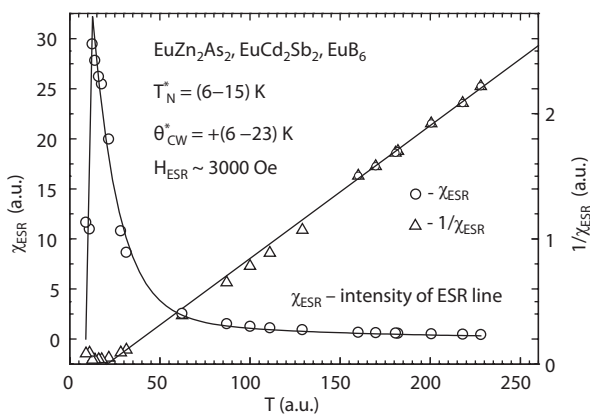


Fig. 1. The magnetic susceptibility of antiferromagnetic Eu-based compounds.

magnetic or anti-ferromagnetic ( $\theta_p \sim \pm 18$  K), semi-metal or semiconductor depending on content carbon impurities. The electron spin resonance (ESR) measurements were performed on frequency 9.3 GHz in TE<sub>102</sub> rectangular cavity in the temperature range from 4.2 to 300 K. At room temperature in all cases, we observed the resonance lines Eu<sup>2+</sup> with a Lorentzian lineshape and with linewidths 500–1300 Oe. At the temperature decreasing to  $T \sim \theta_p$  we observed sharp decreasing of resonance fields and sharp increasing of linewidths. Intensity of ESR signal is proportional magnetic susceptibility.

In general case, the magnetic susceptibility is a tensor. In this regard, the components of magnetization can have not a proportional relation with the components of the external magnetic field and the Curie-Weiss's law can be different for different directions. Paramagnetic Curie temperatures  $\theta_p$  were estimated by measuring the temperature dependences of inverse intensity of ESR signal.

Surprising, but it is quite explainable by suppression of an AFM order in EuZn<sub>2</sub>As<sub>2</sub> by the used magnetic fields, then that the paramagnetic temperature  $\theta_p$ , obtained from the temperature dependence of the ESR signal intensity, has the opposite sign. For EuB<sub>6</sub>C<sub>x</sub>,  $\theta_p$  was about 8 K in case an external magnetic field parallel to [111] axis and it is negative temperature  $-7$  K for the magnetic field along the [100] axis. Larger deviation ( $\Delta g \sim 0.03$ ) of the  $g$ -factor from 2.0 ( $g$ -factor of free electron) indicates on the more stronger hybridization of the europium f-electron states with the p- s-states of the band electrons. The obtained data are interpreted in terms of indirect exchange interaction between localized magnetic moments of europium through the electrons of the valence band (Bloembergen-Rowland's modified RKKY interaction [3]), the hybridization of the europium f-electrons with the valence band electrons and formation of Kondo-like bound states. In this interpretation, the indirect exchange interaction of europium ions through the anionic complexes leads to the breaking of the symmetry of the anionic complex (the Jahn-Teller effect) and, possibly, to a quantum phase transition in a magnetic field.

1. Nateprov A. *et al.*: Abstracts of Int. Conf. ICM-2009. 26–31 July 2009, Karlsruhe, p. 342 (2009)
2. Altshuler T.S., Goryunov Yu.V. *et al.*: JETP Lett. **88**, 779 (2008)
3. Bloembergen N., Rowland T.J.: Phys. Rev. **97**, 1679 (1955)

## Influence of UV Irradiation on EPR and Optical Spectra of Tetraphenylborate Salts

*O. Antonova*

*Nikolaev Institute of Inorganic Chemistry SB RAS, Novosibirsk 630090, Russian Federation, antonovaov1987@yandex.ru*

Tetraphenylborate anion  $[\text{BPh}_4]^-$ , (TPhB) is widely used for analytical purposes and as a counter-ion that allows one to stabilize cationic complexes of metals. TPhB salts are important model systems in studies of  $\text{X-H}\cdots\pi$  bonds with a strong ionic contribution, that play a leading role in the structural chemistry and structural biology. TPhB is used as a counter-ion in materials designed for optronics and nonlinear optics, and in high fluorescent compounds suited for studies in biology and biochemistry. Nevertheless, there is a little information about the fluorescent properties of the TPhB salts in a solid state. We revealed [1] for  $\text{NH}_4\text{BPh}_4$  (TPhBA) at  $T = 77$  K a self-excitation luminescence with wavelength max at  $\lambda = 460$  nm and long relaxation times:  $t_1 = 0.33$  s and  $t_2 = 0.053$  s. Further phenomenon investigation has showed that photoexcitation at 77 K resulted in a set of levels appearing in the band gap, which are responsible for the appearance of intensive luminescence. Experiments showed that UV irradiation leads to the capture of the excited electrons on the phenyl rings or on the cation of neighboring molecules, thereby forming electron-hole pairs with different distance between an electron and a hole. For practical applications electron-hole pairs with large distance between an electron and a hole must be removed, therefore we used mesoporous frameworks to limit the sample size.

Without photoexcitation TPhBA no EPR spectra both at 77 and 300 K are observed. UV irradiation of a TPhBA sample at room temperature also did not lead to an EPR spectrum observation, whereas irradiation at 77 K for one minute resulted in a complex EPR spectrum (Fig. 1). The spectrum is a superposition of a system of narrow lines. Irradiation at 77 K for 20 minutes resulted in a complex EPR spectrum consisting of the superposition of a system of narrow lines and a broad singlet. After the line decomposition, it was determined, that the line appears due to EPR spectra of the phenyl rings and excited states with different distance between an electron and a hole. The processes observed in the polycrystalline samples are mainly determined and restricted to the stage of electron transfer from anion to the electron traps. In Fig. 1c the EPR spectrum at 77 K for TPhBA in mesoporous structures is shown. There are two centers in this spectrum. The first is connected to the single broad

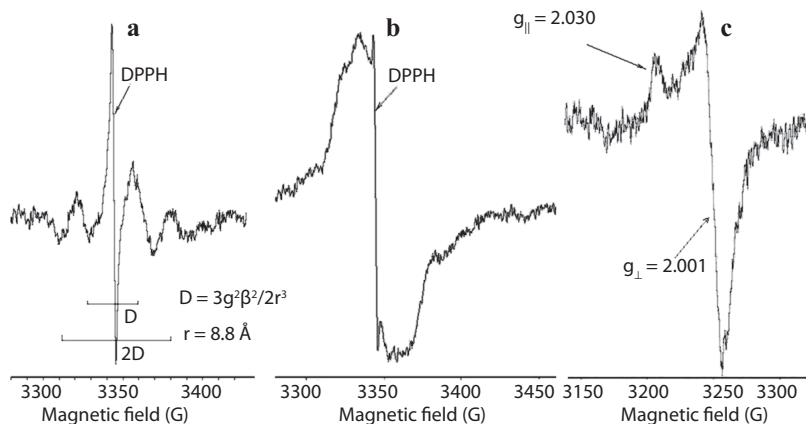


**Fig. 1.** EPR spectra: **a** irradiation of TPhBA bulk sample for 1 min; **b** irradiation of TPhBA bulk sample for 30 min; **c** irradiation of TPhBA in mesoporous structure with 3 nm pore size.

line and the second is attributed to the center with anisotropic  $g$ -factor, their principal values being as  $g_{\parallel} = 2.030$  and  $g_{\perp} = 2.001$ . The spectrum for TPhBA in mesoporous structure with 3 nm pore size is more intensive, than spectrum for TPhBA in mesoporous structure with 6 nm pore size. Analysis of the available data allowed attributing this  $g$ -factor to the ion-radical  $O_2^-$ . No such EPR spectra were observed for the bulk sample.

The principal feature of mesoporous thin films is an extensive surface which can absorb oxygen from atmosphere. Therefore the origin of ion-radical  $O_2^-$  can be connected to the capture of electron on oxygen molecule adsorbed on the surface of TPhBA nanoparticles.

An influence of photoexcitation on  $KBPh_4$  (TPhBK),  $[N(CH_3)_4]BPh_4$  (TMATPhB) bulk samples were studied by EPR. EPR spectra of TPhBK and TMATPhB are identical to EPR spectra of TPhBA. The thermoluminescence observed at the heat of irradiated bulk samples and the nanoparticles of TPhBA have confirmed the features of electron-hole pair recombination.

1. Nadolinny V.A., Antonova O.V., Il'inchik E.A.: *Physics of the Solid State* **53**, 284–291 (2011)

## EPR Investigation of Heisenberg Spin Exchange and Dipole Dipole Interactions in Diluted Free Radicals

*M. Bakirov<sup>1</sup>, K. Salikhov<sup>1</sup>, and B. Bales<sup>2</sup>*

<sup>1</sup> *Zavoisky Physical-Technical Institute, Russian Academy of Sciences, Kazan 420029, Russian Federation, pinas1@yandex.ru*

<sup>2</sup> *Department of Physics and Astronomy and the Center for Supramolecular Studies, California State University, Los Angeles CA 91330, USA*

Applications of nitroxide free radicals are important in biology, for example using them like spin probes in lipid membranes, investigation of micelles. Heisenberg spin exchange and dipole-dipole interactions in the shape of EPR of nitroxide free radical solutions have been investigated for a long time. These interactions broaden and shift the position of lines in the EPR spectrum at low spin concentrations and collapse the EPR spectrum into one broadened line by increasing spin concentrations. Separately both kind of this interactions are studied in detail. But, usually, interpreting experimental observations truncated algorithm was used ,

Which does not take into account all details arising from exchange interaction and the dipole-dipole interaction. Goal of our work is to use Salikhov's algorithm [1] to separate exchange and dipole-dipole interactions in common case.

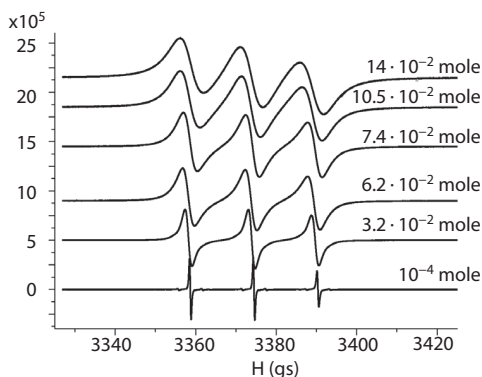


**Fig. 1.** Concentration dependence of EPR spectrum of tempone of X-band.

We analyzed concentration and temperature dependence EPR of 60 wt% glycerol diluted tempone radical solution. Samples were investigated on a Bruker EMX plus spectrometer equipped with an ER4102ST universal X-band resonator in the temperature range of 293–328 K. EPR spectra of tempone in perpendicular mode of X-band are shown on Fig. 1.

1. Salikhov K.M.: *Appl. Magn. Reson.* **38**, 237 (2010)
2. Peric M., Bales B.: *J. Phys. Chem. A* **113**, 4930 (2009)

## Transceiver System for NMR Tomography, Sensor “Joint”

*A. A. Bayazitov<sup>1,2</sup>, K. S. Saikin<sup>2</sup>, and Ya. V. Fattakhov<sup>2</sup>*

<sup>1</sup> *Kazan Federal University, Kazan 420008, Russian Federation, bajazitv.alf@rambler.ru*

<sup>2</sup> *Zavoisky Physical-Technical Institute, Russian Academy of Sciences, Kazan 420029, Russian Federation*

Transceiver system plays an important role in NMR tomography. This system consists of transmitting and receiving oscillating circuits. Sizes of system and radio data are chosen to reflect the designation. Transmission system generates a field in the researching area, so the size of the transmission system is much larger than the sizes of the receiving system. Receiving sensor “Joint” is intended to receive the signal in the knee, wrist and elbow joints.

Purpose and objectives of work is justify the choice of the design of high-frequency receiver sensor for the best sensitivity and signal-noise relation, which should be considered in the coordinate positions of the elements of the source and direction of linear polarization components of its field.

Transmission system must meet the following requirement. The  $Q$ -factor of the transmission system may be smaller then the receiving system’s  $Q$ -factor. The restrictions imposed on the transmission system are due to the size of power pulses and transverse relaxation time in due to the inhomogeneous broadening ( $T_2^*$ ). The forming field of the transmission system should be with the magnitude of the inhomogeneity of the order of  $10^{-1}$ , and the inhomogeneity of the polarizing field should be of the order of  $10^{-5}$ . The receiving system (sensor “joint”) must meet the following requirements: a field  $B_1$ , formed by the sensor must be directed perpendicular to the main field  $B_0$  of transmission system. Operating frequency  $f = 17$  MHz, the inductance of the order of  $0.23 \mu\text{H}$ ,  $Q$ -factor of the system should be about 200–300. The higher the  $Q$ -factor of the circuit, the higher the signal amplitude.

## Structure and Magnetic Properties of $\text{Ni}_x\text{Zn}_{1-x}\text{Fe}_2\text{O}_4$ Nanoparticles

O. Cakiroglu<sup>1</sup>, N. Dogan<sup>2</sup>, and L. Arda<sup>3</sup>

<sup>1</sup> Istanbul University, Hasan Ali Yucel Education Faculty, Istanbul 34452, Turkey

<sup>2</sup> Gebze Institute of Technology, Department of Physics, Gebze/Kocaeli 41400, Turkey

<sup>3</sup> Bahcesehir University, Faculty of Arts and Sciences, Besiktas/Istanbul 34349, Turkey, [lutfi.arda@bahcesehir.edu.tr](mailto:lutfi.arda@bahcesehir.edu.tr)

$\text{Ni}_x\text{Zn}_{1-x}\text{Fe}_2\text{O}_4$  precursor solutions with different ratio ( $x = 0, 0.05$  and  $0.1$ ) were prepared by sol-gel synthesis using Ni, Zn, and Fe based alkoxide which were dissolved into solvent and chelating agent.  $\text{Ni}_x\text{Zn}_{1-x}\text{Fe}_2\text{O}_4$  nanoparticles, annealed at various temperatures, were tried to observe the doping ratio and temperature effects on magnetic and structural properties. The particle size and crystal structure of nanoparticles were characterized by X-ray diffraction. Magnetic properties of  $\text{Ni}_x\text{Zn}_{1-x}\text{Fe}_2\text{O}_4$  nanoparticles were investigated by Quantum design PPMS measurement system. The magnetization and structure of the  $\text{Ni}_x\text{Zn}_{1-x}\text{Fe}_2\text{O}_4$  nanoparticles with different dopant ratio and temperature are presented.

## Preparation, Structure and Magnetic Characterization of $\text{Zn}_{1-x}\text{Ni}_x\text{O}$ Nanoparticles

O. Cakiroglu<sup>1</sup>, N. Dogan<sup>2</sup>, and L. Arda<sup>3</sup>

<sup>1</sup> *Istanbul University, Hasan Ali Yucel Education Faculty, Istanbul 34452, Turkey*

<sup>2</sup> *Gebze Institute of Technology, Department of Physics, Gebze/Kocaeli 41400, Turkey*

<sup>3</sup> *Bahcesehir University, Faculty of Arts and Sciences, Besiktas/Istanbul 34349, Turkey, [lutfi.arda@bahcesehir.edu.tr](mailto:lutfi.arda@bahcesehir.edu.tr)*

$\text{Zn}_{1-x}\text{Ni}_x\text{O}$  solutions with different ( $x = 0.0, 0.01, 0.02, 0.05, \text{ and } 0.1$ ) compositions were synthesized by the sol-gel technique using Zn and Ni based alkoxide. ZnNiO solutions were rotated to remove the solvent at room temperature using magnetic stirrer. After that the powders were ground, they were annealed at various temperatures (550–900 °C for 30 min) under air in a box furnace. The effects of doping ratio and annealing temperature on structure and magnetic properties were investigated systematically. The phase and the crystal structure of the  $\text{Zn}_{1-x}\text{Ni}_x\text{O}$  nanoparticles were characterized using X-ray diffraction. The size and microstructure of samples were characterized by Scanning Electron Microscope and X-ray diffraction. The particle sizes of nanoparticles were observed ~90 nm range Magnetic measurements were performed with a Quantum Design PPMS.

## EMR Detection of Presumable Suhl's Instability in Magnetic $\gamma\text{-Fe}_2\text{O}_3$ Nanoparticles Encapsulated into PPI Dendrimer

*N. E. Domracheva*<sup>1</sup>, *A. V. Pyataev*<sup>2</sup>, and *M. S. Gruzdev*<sup>3</sup>

<sup>1</sup> *Zavoisky Physical-Technical Institute, Russian Academy of Sciences, Kazan 420029, Russian Federation, domracheva@mail.knc.ru*

<sup>2</sup> *Kazan Federal University, Kazan 420008, Russian Federation*

<sup>3</sup> *Institute of Solution Chemistry, Ivanovo 153045, Russian Federation*

Physicists have well known that the isochronism of a harmonic oscillator, such as a Galileo's pendulum, is broken and results to bistability and foldover effects in the nonlinear regime when taking the nonlinear restoring force into account [1]. These nonlinear regimes are ubiquitous in nature, as found in mechanical [1] and magnetic [2, 3] systems.

The main goal of this report is to reveal such nonlinear instability in new magnetic system:  $\gamma\text{-Fe}_2\text{O}_3$  nanoparticles (NPs) encapsulated into poly(propylene imine) (PPI) dendrimer. The superparamagnetic and ferrimagnetic behaviour

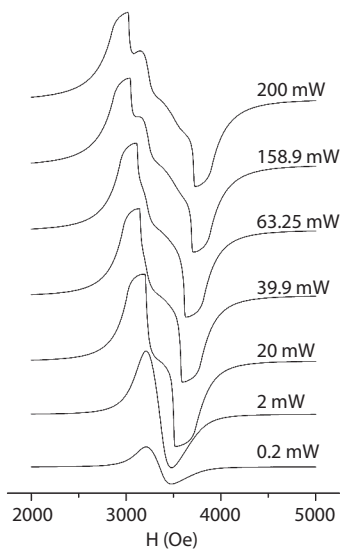


**Fig. 1.** EMR spectra of the sample at different levels of the microwave power at  $T = 300$  K.

of these single-domain NPs with mean diameter of about 2.5 nm and individual magnetic moment  $\sim 350$  Bohr magnetons have been studied by electron magnetic resonance (EMR) previously [4]. Note that the bulk maghemite ( $\gamma\text{-Fe}_2\text{O}_3$ ) shows ferrimagnetic ordering that arises due to two uncompensated spin sublattices aligned in the opposite directions. The Curie temperature of bulk maghemite is 860 K, so NPs at room temperature are formally in the ferrimagnetic single-domain state. The EMR spectrum of dendrimeric  $\gamma\text{-Fe}_2\text{O}_3$  NPs at low microwave power (0.2–2 mW) displays a single Lorentzian line centred at  $H_0 = \omega/\gamma + M_0$ , where  $\omega$  is the microwave frequency,  $\gamma$  is the gyromagnetic ratio and  $M_0$  – magnetization of the sample. Increasing the microwave power in the range 20–200 mW leads to the dramatic change in EMR spectra (Fig. 1).

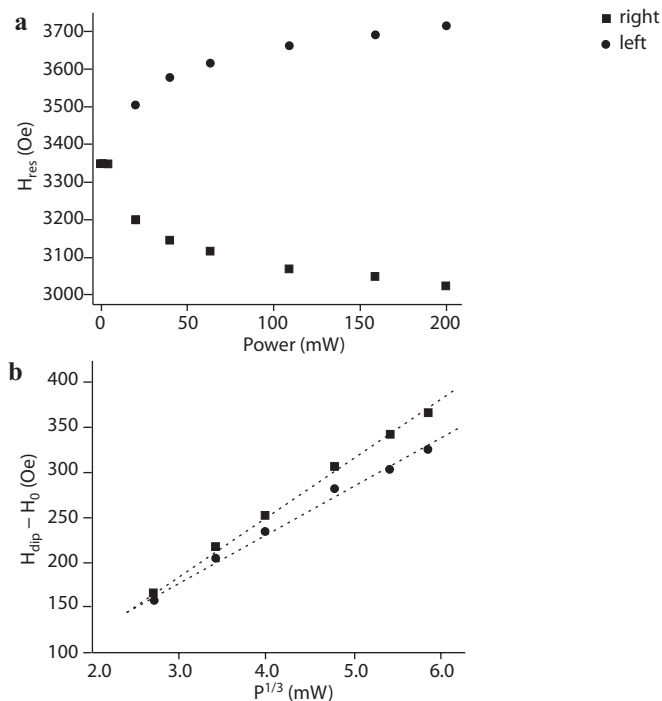


**Fig. 2.** **a** Dependence of the resonance field of the left and right maximums on the microwave power. **b** Power dependence of the resonance line shifts of the left and right maximums.

At high microwave power (above critical  $P_{\text{th}} = 20$  mW) we observe the appearance of the line with an irregular shape the left and right maximums of which shift away from  $H_0$  in the opposite directions (Fig. 1 and Fig. 2a).

The resonance field of the left and right maximum was defined as a position of a sharp dip line ( $H_{\text{dip}}$ ). The existence of a threshold microwave power ( $\sim 20$  mW), above which the dramatic change in ferromagnetic resonance occurred was reported in ref. [5, 6]. It was shown [5, 6] that a significant change in the spectrum was generally caused by development of a Suhl's instability [7]. The resonance line shift ( $H_{\text{dip}} - H_0$ ) above the threshold ( $P_{\text{th}}$ ) with increased power reflects the nonlinear magnetization dynamics: by increasing  $P$ , the cone angle  $\theta$  of the magnetization precession increases, so that the magnetization reduces from the value  $M_0$  to  $M_0(1 - \theta^2/2)$ , which shifts the resonance field from  $H_0 = \omega/\gamma + M_0$  to  $H_R = H_0 - M_0\theta^2/2$ . At high power ( $P > P_{\text{th}}$ ),  $\theta^2 \propto P^{1/3}$ , so the resonance line shift ( $H_{\text{dip}} - H_0$ ) should be proportional to  $P^{1/3}$ . The linear dependence ( $H_{\text{dip}} - H_0$ ) vs  $P^{1/3}$  was experimentally observed for dendrimeric  $\gamma\text{-Fe}_2\text{O}_3$  NPs (Fig. 2b). This proves applicability of the model discussed above.

Acknowledgements – grants № RFBR 11-03-01028, President of RF № MK-893.2011.3.

1. Landau L.D., Lifshitz E.M.: Mechanics, 2<sup>nd</sup> ed. Pergamon Press, Oxford, 1969.
2. Anderson P.W., Suhl H.: Phys. Rev. **100**, 1788 (1955)
3. Bertotti G., Mayergoyz I.D., Serpico C.: Phys. Rev. Lett. **87**, 217203 (2001)
4. Domracheva N.E., Pyataev A.V., Manapov R.A., Gruzdev M.S.: Book of Abstracts of the International conference Resonances in Condensed Matter. 21–25 June 2011, Kazan. p. 74.
5. Morgunov R.B., Mushenok F.B., Kazakova O.: Phys. Rev. B. **82**, 134439 (2010)
6. Gui Y.S., Wirthmann A., Mecking N., Hu C.-M.: Phys. Rev. B. **80**, 060402(R) (2009)
7. Suhl H.: J. Phys. Chem. Solids **1**, 209 (1957)

## ESR Spectra in Monocrystal and Thin Film GdMnO

*R. M. Eremina<sup>1</sup>, T. P. Gavrilova<sup>1</sup>, D. V. Mamedov<sup>1</sup>, I. V. Yatsyk<sup>1</sup>,  
and Ya. M. Mukovskii<sup>2</sup>*

<sup>1</sup> *Zavoisky Physical-Technical Institute, Russian Academy of Sciences, Kazan 420029,  
Russian Federation, REremina@yandex.ru*

<sup>2</sup> *Moscow State Institute of Steel and Alloys (Technological University), Moscow 119049,  
Russian Federation*

Recently there has been an increasingly growing interest in the substances, where the magnetic and electric degrees of freedom are linked (multiferroics). This is due not only to new physical properties of these substances, but also the ability to control their condition with the help of external magnetic or electric fields, which opens up good prospects for the creation of new functional materials and devices based on them. The literature discusses several models to explain the coexistence of magnetic and ferroelectric orderings. One of them is a change of symmetry. Distortion in the substance of spatial inversion leads to the formation of modulated spin structures, but it is possible the opposite

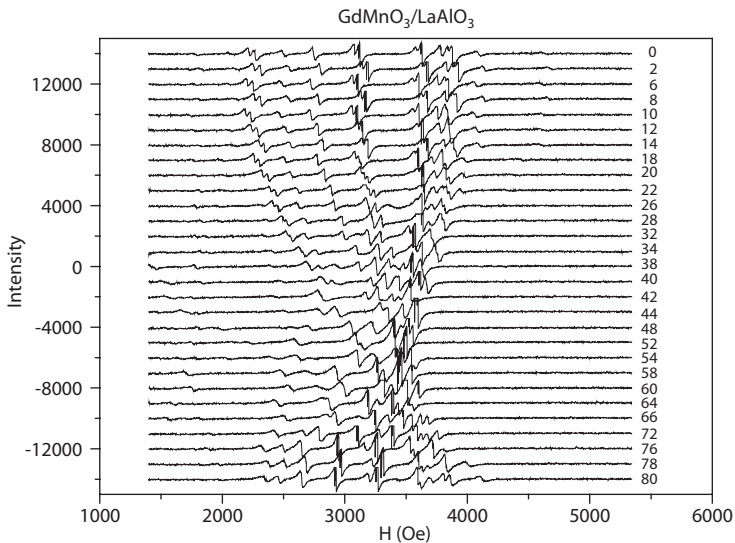


**Fig. 1.** Angular dependence of ESR linewidth in monocrystal GdMnO<sub>3</sub> (Q-band).

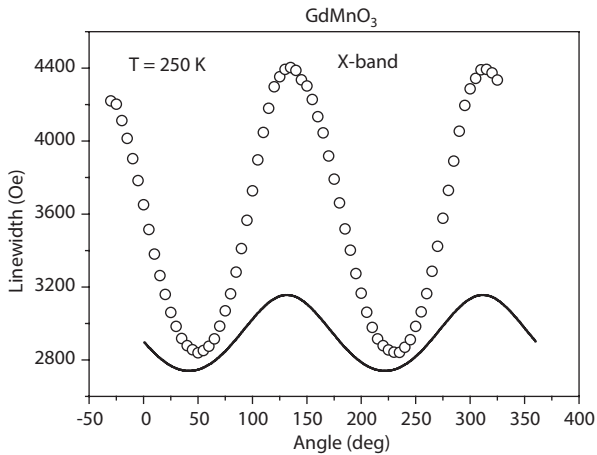


**Fig. 2.** Angular dependence of ESR line in thin film monocrystal  $\text{GdMnO}_3/\text{LaAlO}_3$  at 300 K.

effect: spatial modulation of spin can lead to the disappearance of the center of symmetry from among the elements of crystal symmetry and the appearance of electric polarization. Such a mechanism is believed to determine the appearance of electric polarization in orthorhombic manganites [1] and explains the control of electric polarization by a magnetic field [2].

The main goal of this work is to study the magnetic properties of multiferroics  $\text{GdMnO}_3$  by ESR methods. ESR measurements of  $\text{GdMnO}_3$  were performed in a Bruker ELEXSYS E500 CW-spectrometer at X-band (9.47 GHz) and Q-band (34 GHz) frequencies equipped with continuous He-gas-flow cryostats (Oxford Instruments) in the temperature range  $4.2 \leq T \leq 300$  K. The observed ESR absorption in monocrystal  $\text{GdMnO}_3$  is well described by a single exchange-narrowed Lorentzian line in all temperature regimes. Figure 1 shows the full angular dependence of the linewidth in the crystallographic plane at 250 K. The largest variation of the linewidth appears in the plane where it monotonously increases from 2800 Oe up to 4400 Oe on rotating the magnetic field in the plane. We calculated the Dzyaloshinski-Moria part of the linewidth for manganese ions (the solid line).

The ESR absorption observed in thin film  $\text{GdMnO}_3/\text{LaAlO}_3$ . Temperature dependencies of EPR lines are presented in Fig. 2. The spectra connect the group of lines with strange angular dependence.

1. Kadomtseva A.M., Popov Yu.F., Vorob'ev G.P., Ivanov V.Yu., Mukhin A.A., Balbashov A.M.: JETP Letters **82**, 590 (2005)
2. Kimura T., Goto T., Shintani H., Ishizaka K., Arima T., Tokura Y.: Nature **426**, 55 (2003)

## Magnetic Resonance of the Rare-Earth Impurity Centers in CsCaF<sub>3</sub> Single Crystal

*M. L. Falin and V. A. Latypov*

*Zavoisky Physical-Technical Institute, Russian Academy of Sciences Kazan, 420029, Russian Federation, vlad@kfti.knc.ru*

Double fluoride crystals with perovskite structure ABF<sub>3</sub> are very interesting because they are convenient model systems for studying the magneto-optical properties of impurity dopant ions. In principle, in these matrices it is possible to substitute two various cations being inequivalent positions. This enables one to carry out investigations of impurity dopant ions in sixfold or uncommon twelfold coordinations. The physical properties of rare-earth ions in these compounds are not sufficiently studied. The introduction of three-charge rare-earth ions is hampered because of heterovalent substitution and the essential difference in the ionic radii of rare-earth ions and lattice cations. Previously we presented results on the study of Nd<sup>3+</sup>, Ce<sup>3+</sup>, Nd<sup>3+</sup>, Sm<sup>3+</sup> and Yb<sup>3+</sup> in KMgF<sub>3</sub> and KZnF<sub>3</sub> and Yb<sup>3+</sup> in CsCaF<sub>3</sub> crystals [1–6]. This report is concerned with the further investigation of impurity paramagnetic centers (IPC) formed by Ce<sup>3+</sup>, Nd<sup>3+</sup>, and Dy<sup>3+</sup> ions in CsCaF<sub>3</sub> single crystals.

The crystals were grown using the Bridgman-Stockbarger method. The concentration of the impurity ions was 0.1–1.0 wt%. A wide variety of IPC is the characteristic feature of the studied crystals. In dopant crystals different types of IPC are discovered. The parameters of the corresponding spin Hamiltonians, the ground states and their wave functions were determined. Structural models of the observed complexes were proposed. The analysis of the obtained results as compared to those obtained for the same paramagnetic ions in other hosts was carried out.

1. Ibragimov I.R., Fazlizhanov I.I., Falin M.L. *et al.*: Phys. Solid State **34**, 1745 (1993)
2. Abdulsabirov R.Yu., Korableva L.S., Falin M.L.: Phys. Solid State **35**, 563 (1993)
3. Abdulsabirov R.Yu., Falin M.L. *et al.*: Appl. Magn. Reson. **5**, 377 (1993)
4. Bespalov V.F., Falin M.L., Kazakov B.N. *et al.*: Appl. Magn. Reson. **11**, 125 (1996)
5. Falin M.L., Latypov V.A., Kazakov B.N. *et al.*: Phys. Rev. B **61**, 9441 (2000)
6. Falin M.L., Anikeenok O.A., Latypov V.A. *et al.*: Phys. Rev. B **80**, 174110 (2009)

## EPR and Optical Spectroscopy of the $\text{Tm}^{2+}$ Ion in the $\text{KMgF}_3$ Single Crystal

*M. L. Falin, K. I. Gerasimov, and V. A. Latypov*

*Zavoisky Physical-Technical Institute, Russian Academy of Sciences, Kazan 420029,  
Russian Federation, gerasimov@kfti.knc.ru*

The rare-earth ions with the  $f^n$ -electron configuration are of great importance in connection with the development of solid-state devices such as lasers, scintillators and displays. The most common valence state of lanthanides in solids is the trivalent state. Some rare-earth ions may be stabilized in the divalent valence state and their properties are studied insufficiently. This work presents preliminary results of EPR and optical spectroscopy investigations of the  $\text{Tm}^{2+}$  ion in the  $\text{KMgF}_3$  single crystal. Moreover, to the best of our knowledge the optical data for cubic  $\text{Tm}^{2+}$  ion in the sixfold coordination are presented for the first time.

EPR results show the presence of two types of  $\text{Tm}^{2+}$  paramagnetic centers of different symmetry: cubic and rhombic (Fig. 1). The intensity of the EPR lines of the rhombic  $\text{Tm}^{2+}$  paramagnetic centers is much less than that of cubic ones. Luminescence spectra in the characteristic spectral range for  $\text{Tm}^{2+}$  are presented in Fig. 2. They consist of the lines of the two types with different

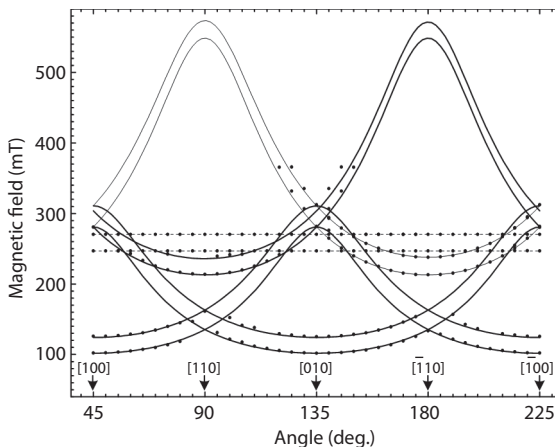


**Fig. 1.** Experimental and theoretical angular dependences of the EPR lines of  $\text{Tm}^{2+}$  in  $\text{KMgF}_3$  in the (001) plane. ● – experiment, line – theory.

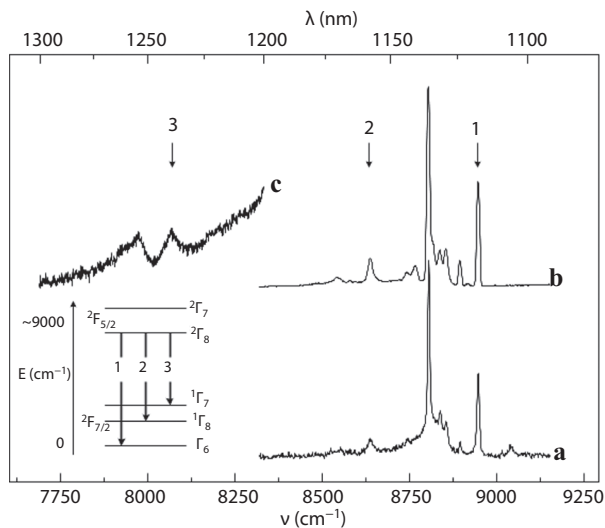


Fig. 2. Luminescence spectra of  $\text{Tm}^{2+}$  in  $\text{KMgF}_3$ .  $T = 77$  K (a),  $T = 2$  K (b, c).

the luminescence persistence:  $\tau = 1.7 \pm 0.17$  ms for  $8803 \text{ cm}^{-1}$  line and  $21.3 \pm 4.5$  ms for other lines. It is highly probable that the lines of the first type correspond to rhombic centers and the lines of the second type to cubic ones. The Stark level energies of the cubic  $\text{Tm}^{2+}$  multiplets were determined from luminescence spectra. These data and the  $g$ -factor of the ground state were used for the interpretation of the optical data within the crystal field theory. Information about the phonon spectra of the  $\text{KMgF}_3$  crystal was obtained from the electron-vibrational structure of the optical spectra. The obtained results were compared with the data for the cubic  $\text{Tm}^{2+}$  ion in fluorite-type crystals [1] and those for the isoelectronic  $\text{Yb}^{3+}$  ion in eight- and six-coordination complexes [2–7].

1. Anderson C.H. in: Crystal with Fluorite Structure (W. Hayes, ed.), p. 281. Clarendon, Oxford, 1974.
2. Falin M.L., Gerasimov K.I., Latypov V.A., Leushin A.M.: J. Phys.: Condens. Matter **15**, 2833 (2003)
3. Gerasimov K.I., Falin M.L.: Phys. Solid State **51**, 718 (2009)
4. Bepalov V.F., Falin M.L., Kazakov B.N., Leushin A.M., Ibragimov I.R., Safiullin G.M.: Appl. Magn. Reson. **11**, 125 (1996)
5. Bepalov V.F., Kazakov B.N., Leushin A.M., Safiullin G.M.: Phys. Solid State **39**, 925 (1997)
6. Kazakov B.N., Leushin A.M., Safiullin G.M., Bepalov V.F.: Phys. Solid State **40**, 1836 (1998)
7. Falin M.L., Gerasimov K.I., Leushin A.M., N.M. Khaidukov N.M.: J. Luminescence **128**, 1103 (2008)

## Dynamics of Recrystallization and Thermometry of a Implanted Semiconductor at Pulsed Light Irradiation Measured via Optical Diffraction Method

*B. Farrakhov, Ya. Fattakhov, and M. Galyautdinov*

*Zavoisky Physical-Technical Institute, Russian Academy of Sciences, Kazan 420029, Russian Federation, farrakhov@kfti.knc.ru, fattakhov@kfti.knc.ru*

The optical diffraction method for fast measurement of current temperature and dynamic of recrystallization on the surface of implanted silicon at light pulse irradiation was suggest and realized. This method is based on the application of the Fraunhofer diffraction and is implemented for silicon samples heated to melting temperatures  $T_{\text{melt}} = 1412 \text{ }^{\circ}\text{C}$  by a high-power light pulse. The current silicon temperature was determined by measuring the varying dif-

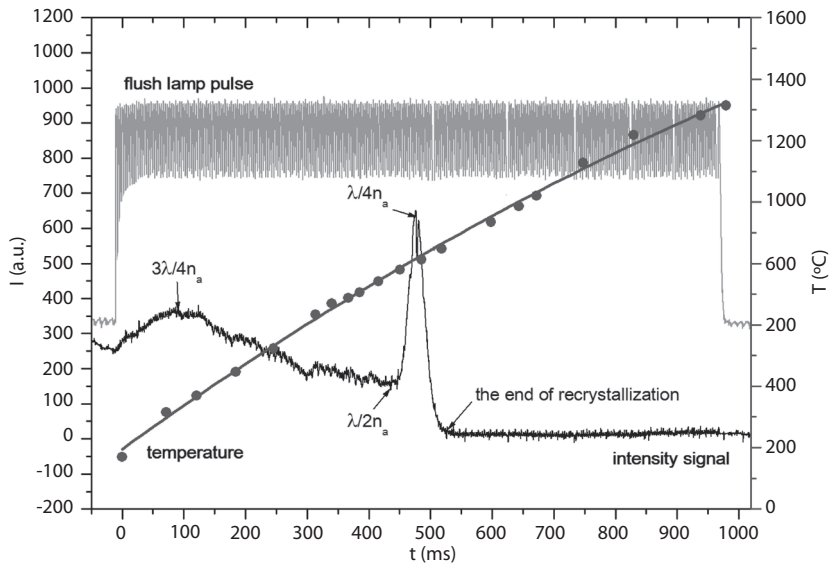


**Fig. 1.** Signal of changes in the intensity of the first diffraction peak from the amplitude grating during irradiation of a sample with laser pulses with a light power density of  $120 \text{ W/cm}^2$  and a duration of 970 ms and the shape of a light pulse. Time dependence of the sample temperature under pulsed light heating.

fraction angle of the probing laser beam. The diffraction angle was varied over time because the period of the diffraction grating increased as a result of the dynamic thermal expansion of the crystal. An initial grating was formed on the surface of the silicon plate with a period of  $d = 4 \mu\text{m}$ . The radiation beam of a He-Ne laser with  $\lambda = 0.6328 \mu\text{m}$  was used as the probing beam; the measured signal was recorded in the pair of symmetric fifth order diffraction maxima.

The optical diffraction method for fast measurement of current temperature and dynamic of recrystallization on the surface of implanted silicon at light pulse irradiation was suggested and realized.

On the sample surface two grating were formed: the amplitude grating with period of  $50 \mu\text{m}$  and the phase grating with period of  $4 \mu\text{m}$ . The phase grating is the temperature sensor of the sample. The amplitude grating for measurement of structural-phase changes is used. Single-crystal silicon KDB-1 (100) orientation and  $400 \mu\text{m}$  thickness were chosen as a semiconductor sample.

The current silicon temperature was determined by measuring the varying of diffraction angle of the probing laser beam. The diffraction angle was varied over time because the period of the diffraction grating increased as a result of the dynamic thermal expansion of the crystal. The measured signal was recorded in the pair of symmetric fifth-order diffraction maxima.

The amplitude grating was formed by implantation with phosphorous ions by photolithography method. As a result of implantation, on the silicon surface amorphous cells with size  $40 \times 40 \mu\text{m}$  enclosed by a net of single-crystal silicon were formed. The recrystallization of amorphous cells during pulse light heating changes the diffraction efficiency this grating. To register the diffraction efficiency the intensity change of first diffraction maximum was recorded.

The radiation beam of a He-Ne laser with  $\lambda = 0.6328 \mu\text{m}$  was used as the probing beam. The light irradiation of silicon samples was performed on a UOL.P-1 setup by flash lamps.

For an example in Fig. 1 the curves of temperature and intensity changes are shown. The signal amplitude disappears at time of 540 ms. On this time the solid-phase recrystallization of the implanted fragments ended.

## Low-Field Spectroscopic Studies of Magnetic Resonance Contrast Agents

*Ya. V. Fattakhov, A. R. Fakhрутdinov, V. N. Anashkin, V. A. Shagalov, K. S. Saikin, M. K. Galyaltdinov, D. D. Gabidullin, N. M. Gafiyatullin, and N. A. Krylatykh*

*Laboratory of the Methods of Medical Physics, Zavoisky Physical-Technical Institute, Russian Academy of Sciences, Kazan 420029, Russian Federation, dinarld@mail.ru*

Nowadays magnetic resonance imaging (MRI) has become one of the most popular human organism diagnostic method. Applying contrasting agents in MRI allows to improve observed objects contrast. In low field tomography, where due to objective reasons low signal to noise ratio and low image definition take place, applying magnetic-resonance contrasting agents (MRCA) is particularly important.

Preliminary reserches made on low-field medical magnetic resonance imaging system “TMR-0.06-KFTI” with 0.06 Tl magnetic field have showed efficiency of applying MRCA for neoplasm detecting in low fields [1]. Water solutions of different contrast agents (used for medical purposes) concentration have been analyzed. According to obtained concentration dependence of nuclear spin-spin and spin-lattice relaxation was made conclusion about contrast agent concentration optimum value in low-field MRI. Relaxation measurements satisfy with obtained on low-field MR imaging system images of analyzed objects in T1-weighted image mode. Reserches were made in room-temperature (24 °C – 296 K) and in closed to human body temperature (37 °C – 310 K).

1. Balakin V.E., Biktimirov E.F., Gilyazutdinov I.A., Zhavoronkov A.E., Salikhov K.M., Sahapova L.R., Fattakhov Ya.V., Khabirov R.A., Khasanov R.Sh., Khafizov R.T., Yusupova L.R.: *Oncosurgery*. 2, 86 (2009)

## EPR, UV, and DFT Study of Spin-Crossover Complexes Fe(III) and Their Photoisomerizable Ligands

L. Gafiyatullin, L. Savostina, L. Mingalieva, T. Ivanova, O. Turanova,  
G. Ivanova, A. Turanov, and I. Ovchinnikov

Zavoisky Physical-Technical Institute, Russian Academy of Sciences, Kazan 420029,  
Russian Federation, sasha\_turanov@rambler.ru

The most perspective objects to create the liquid crystal (LC) systems with photocontrolled magnetic properties are complexes Fe(III) with  $N_2O_3$  five-dentate ligands containing in the sixth position a molecule that changes conformation under the influence of photoirradiation.

In this study are described *cis-trans*-isomerization of 4-styrylpyridine, 4-octyloxy-4'-styrylpyridine (sp),  $H_2$ salten- $OC_{18}H_{37}$  ( $H_2L$ ) and first time synthesized mixed-ligand complex  $[FeL(sp)]BPh_4$  in isotropic solution and in LC solution TI18-23 under irradiation. Phase transitions of substances and mixtures studied by polythermal microscopy. Information on the magnetic properties of the complex was obtained by EPR.

Using density functional theory (DFT and TD-DFT with PBE functional in the basis 6-311G (d, p) by program ORCA) carried out a quantum-chemical calculations *cis*-, *trans*-, and cyclic conformations of the molecules, the energy levels, the electron density distribution, and absorption spectra in UV range, which correlate well with experimental ones.

By UV spectroscopy it was found that *cis* $\leftrightarrow$ *trans* transitions in thin films of styrylpyridine dissolved in LC is much slower than in isotropic solutions. It was shown that when the film surface is bordered by a solid body, the conversion speed is significantly reduced compared to the case of the free film surface up to a complete termination of isomerization.

EPR studies were performed in the X-band at  $T = 5\text{--}300$  K. It was found that the complexes  $[FeL(sp)](BPh_4)$  have thermally induced spin transition in the temperature range 130–300 K. It was shown that photoirradiation leads to the formation of complexes Fe(III) in low-spin state.

## Gradient System Control Unit for MRI System “Tmr-Kfti”

*N. M. Gafiyatullin, Ya. V. Fattakhov, N. A. Krylatykh, and D. D. Gabidullin*

*Zavoisky Physical-Technical Institute, Russian Academy of Sciences, Kazan 420029,  
Russian Federation, niyaz.gafiyatullin@gmail.com*

Control and program studio block for gradient pulses generating are developed for magnetic resonance tomograph “TMR-KFTI”. These properties are required: high linearity and wide dynamic range of pulses, low noise level, ability to form orthogonal magnetic field gradients in arbitrary basis (“virtual gradients” method), flexible supervision and control.

To implement these all properties vector processor was designed. The main component is Field-programmable Gate Array (FPGA), for which program was written to execute all functions of gradient system

Also it is important to obtain all data about adjustment, gradient pulses forms and transformation matrix from control computer. For this computer program support has to be realized as well.

Another important aspect of service backup is ability to distance and credible diagnostics to avoid different emergency conditions. We suppose to implement the troubleshooting by the Internet.

The block-scheme of this device is shown on Fig. 1

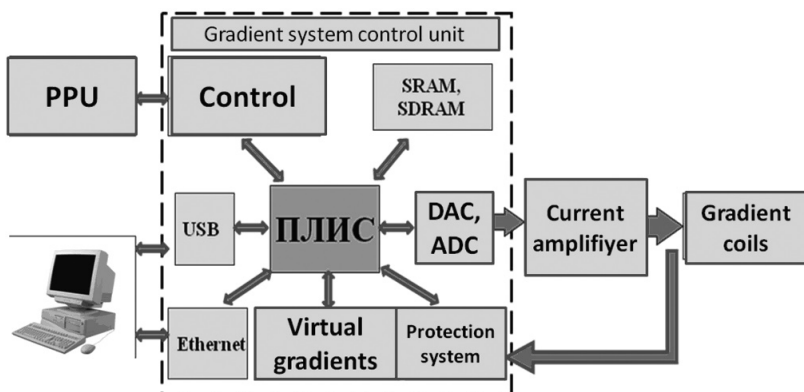


Fig. 1. Block-scheme of gradient system control unit.

## EPR Line Shape of a System of Two Coupled Spins with Difference Rates of Transverse Relaxation

*R. T. Galeev*

*Zavoisky Physical-Technical Institute, Russian Academy of Sciences, Kazan 420029,  
Russian Federation galeev@kfti.knc.ru*

We analyze effect of relaxation processes on EPR line shape of a system of two coupled spins  $S = 1/2$  with the like (nearly like)  $g$ -factors. It is well known that isotropic interaction doesn't lead to a splitting EPR line in this case. But we consider the pair which is nonequivalent in relaxation properties. It is supposed that transverse relaxation times of the spins can be essentially different from each other and longitudinal relaxation times are sufficiently long, so we can neglect by non-adiabatic contribution in transversal relaxation rate. It turned out that the difference in the transversal relaxation rates leads to appearance in the kinetic equation of the coefficients which describe the exchange between one-quantum coherences (transversal cross-relaxation). These coherences are related to the allowed transitions between triplet states and the forbidden transitions between singlet state and triplet states. Possible spectroscopic manifestations of such exchange in EPR spectra have been considered.

This study was supported in part by grant NSh-6267.2010.2.

## The Calculation of Correctional System for the Basic Field of Magnetic Resonance Imaging with a Permanent Magnet

*E. R. Galiakberova*<sup>1</sup>, *R. T. Galeev*<sup>2</sup>, and *A. R. Fakhrutdinov*<sup>2</sup>

<sup>1</sup>*Kazan Federal University, Kazan 420008, Russian Federation*

<sup>2</sup>*Laboratory of the Quantum Dynamics and Informatics, Zavoisky Physical-Technical Institute, Russian Academy of Sciences, Kazan 420029, Russian Federation, galeev@kfti.knc.ru,*

<sup>3</sup>*Laboratory of the Methods of Medical Physics, Zavoisky Physical-Technical Institute, Russian Academy of Sciences, Kazan 420029, Russian Federation, fakhrutdinov@mail.knc.ru*

The main characteristics of the magnetic system (MS) for MRI are the magnetic induction and magnetic field homogeneity in the operating area. So the homogeneity of magnetic field is one of the key parameters affecting the quality of the images in MRI. Therefore developers of MS pay more attention to setting a homogeneous magnetic field.

There are several ways to correct the magnetic field: 1) by the family of coils [1], each operating by its own current; 2) shimming by passive elements (pieces of ferromagnetic material) [2]; 3) shimming by active elements (permanent magnets, such as, Nd-B-Fe) [3], arranged in a specific way in the space around the operating area.

In our research we represent a model of correctional system, based on small permanent magnets (magnetic dipoles). It allows to create a complete set of spherical harmonics of the magnetic field up to fourth order (total of 24 harmonics). The evaluation of the effectiveness of correctional system with using of known commercial magnetic dipoles was made.

1. Weston A.A.: *Rev. Sci. Instrum.*, **32**, 241 (1961)
2. Zhao Wei, Tang Xiao-ying, Hu Guo-jun, Liu Yong: *Proceedings of 19<sup>th</sup> International Workshop on Rare Earth Permanent Magnets & Their Applications*, p. 415–418, 2008.
3. Tang Xin, Hong Li-Ming, Zu Dong-Lin: *Chin. Phys.* **19**, 078702(1-8) (2010)

## Vibrational Spectroscopy and Quantum Chemical Computations as a Tool for Metal Spin State Diagnostics

*T. P. Gryaznova<sup>1</sup>, S. A. Katsyuba<sup>1</sup>, M. Yu. Filatov<sup>2</sup>, I. A. Bezkishko<sup>1</sup>,  
V. A. Milyukov<sup>1</sup>, and O. G. Sinyashin<sup>1</sup>*

<sup>1</sup> *Arbuzov Institute of Organic and Physical Chemistry, Russian Academy of Sciences,  
Kazan 420088, Russian Federation, gryaznovat@iopc.ru*

<sup>2</sup> *Zernike Institute for Advanced Materials, University of Groningen, Groningen, Netherlands*

A dependence of infrared (IR) and Raman spectra of transition metal complexes on spin state (SpSt) of the metal is poorly studied. Present work is aimed at estimation of possibilities of vibrational spectroscopy combined with quantum chemistry for diagnostics of metal SpSt.

Possible stable structures of several mononuclear Ni, Co and Fe complexes with different types of coordination ( $\pi$ ,  $\sigma$ ) with various organic ligands and different SpSts of metals were found by optimization, and the spectra computed for every form were compared with the experimental IR and Raman spectra of the compounds. It is demonstrated that changes in SpSt of the metals influence both geometry and vibrational spectra of the complexes. The main factor influencing IR spectra is the changes of the molecular force field caused by the low-spin / high-spin transition, while the concomitant geometry changes play a minor role. The spectral changes are observed both in low-frequency range, corresponding to metal-ligand vibrations, and in the mid-frequency range, where ligand vibrations are shown to be sensitive to the spin state of all the studied compounds.

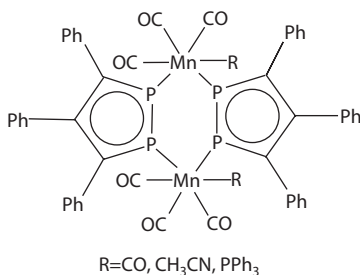


**Fig. 1.** Structure of binuclear Mn complexes under study.

This prompted us to use the carbonyl ligands as a sort of a spectral probe for SpSt diagnostics in binuclear Mn complexes with 1,2-diphosphapentadienide anion (Fig. 1).

Computational analysis demonstrated that CO stretching vibrations are highly sensitive to SpSt and oxidation state of Mn. A comparison of computed and experimental IR and Raman spectra in the corresponding range suggests the dynamical equilibrium of several spin and/or oxidation states of Mn atoms in the complexes.

## Paramagnetic Proteins of Blood as Biomarkers of Malignant Neoplasm Anemia in Urogenital System

*M. I. Ibragimova<sup>1</sup>, A. I. Chushnikov<sup>1</sup>, V. N. Moiseev<sup>2</sup>, V. Yu. Petukhov<sup>1</sup>,  
and E. P. Zheglov<sup>1</sup>*

<sup>1</sup>*Zavoisky Physical-Technical Institute, Russian Academy of Sciences, Kazan 420029,  
Russian Federation, ibragimova@kfti.knc.ru*

<sup>2</sup>*Tatarstan Republic Cancer Hospital, Kazan 420029, Russian Federation*

It is well known that one of the evidence of the malignant neoplasm's occurrence can be anemia. The frequency of anemia occurrence can depend on localization and growth stage of tumor but such correlation is not always observed. In clinical practice for anemia screening the measure of hemoglobin (Hb) level and packed cell volume are usually used. However for anemia diagnostics the determination of transferrin (Tf) concentration and the level of its iron saturation can be more informative. As a rule for Tf measuring turbidimetric methods and nephelometric assay are used. At the same time the unique advantage of EPR is the possibility to detect the integral concentration of  $\text{Fe}^{3+}$  ions bound to Tf molecules ( $\text{Fe}^{3+}$ -Tf) and  $\text{Cu}^{2+}$ -ceruloplasmin ( $\text{Cu}^{2+}$ -Cp) as well. The aim of this work was to study paramagnetic proteins of blood in anemia malignant tumor growth by using EPR-spectroscopy.

Equal quantity of blood was taken into 0.5 ml syringe and then was frozen in liquid nitrogen. EPR spectra were recorded using Varian E-12 spectrometer with frequency of  $\sim 9.38$  GHz at 77 K. As long as the width and the shape of lines are unchanged the quantitative analysis of spectra were performed by measuring peak-to-peak intensity of derivative absorption line for samples with equal mass.

Venous blood samples were investigated in patients with a diagnosis of cancer urinary bladder and kidney on the I–IV tumor stages as well as in two control groups: blood donors and volunteers of adult outpatient department. It is common knowledge that Hb level in blood less than  $\leq 120$  g/l is well-defined indicator of anemia. Independently of tumor stages the  $\sim 30\%$  of investigated patients with cancer and  $\sim 15\%$  of investigated blood donors + volunteers of adult outpatient department fall into this category.

The mean  $\text{Fe}^{3+}$ -Tf concentration and its standard deviation in all groups were closely equal:  $43 \pm 27$  a.u. in patients with cancer,  $41 \pm 25$  a.u. in blood donors and  $40 \pm 17$  a.u. in volunteers of adult outpatient department. At the same time the existence of patients both with extremely low (0 up to 10 a.u.)

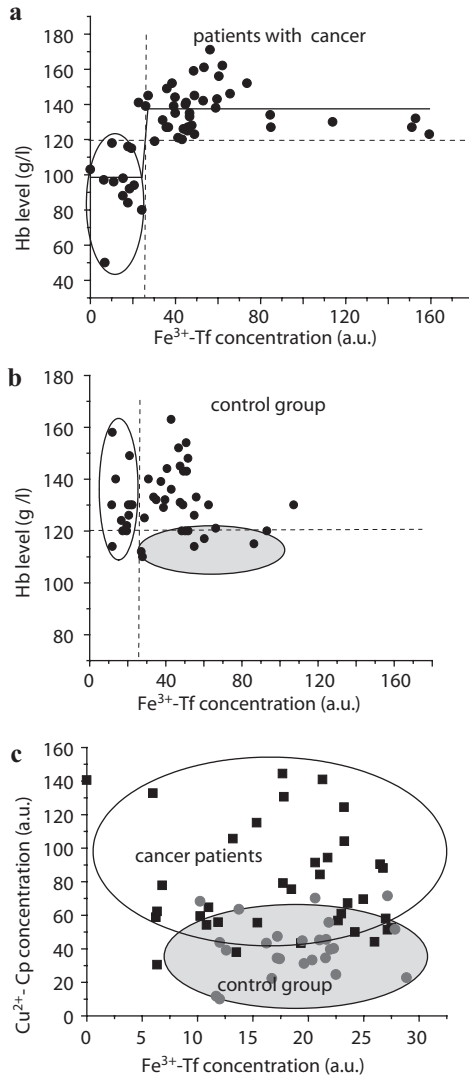


**Fig. 1.** Correlation between Hb level and the concentration of Fe<sup>3+</sup>-Tf molecules in blood: **a** for patients with cancer; straight solid line is the result of piecewise-linear approximation; **b** for control group; **c** relationship between Cu<sup>2+</sup>-Cp and Fe<sup>3+</sup>-Tf concentrations in cancer patients and control group.

and high ( $>120$  a.u.) levels of  $\text{Fe}^{3+}$ -Tf was the distinctive feature of cancer pathology. Independently on the tumor stage such cases were registered for  $\sim 8\%$  и  $\sim 4\%$  patients with cancer respectively.

The study of  $\text{Fe}^{3+}$ -Tf and Hb levels correlation is of obvious practical and fundamental interest. Presented in Fig. (1a, b) the relationship between  $\text{Fe}^{3+}$ -Tf and Hb levels in blood of patients with cancer and control groups illustrates the existing distinctions between cancer pathology and norm. As can be seen from Fig. 1a in cancer patients the  $\text{Fe}^{3+}$ -Tf concentration in the range of 0–25 a.u. was correlated with Hb level in the range of  $\leq 120$  g/l. Piecewise-linear approximation of the data allowed revealing the fact of anemia appearance. At the same time the  $\text{Fe}^{3+}$ -Tf concentration was not correlation with both the growth stage of tumor and the degree of anemia. On the other hand, for volunteers from control group at low  $\text{Fe}^{3+}$ -Tf concentration (marked area for  $\text{Fe}^{3+}$ -Tf  $\leq 25$  a.u.) the normal value of Hb is observed (Fig. 1b). For volunteers with the diagnosis “anemia” the normal value of  $\text{Fe}^{3+}$ -Tf concentration (shaded area) was revealed.

Thus, the low Hb level at low concentration of  $\text{Fe}^{3+}$ -Tf can be the biomarker of cancer.

The relationship between concentrations of serum  $\text{Fe}^{3+}$ -Tf and  $\text{Cu}^{2+}$ -Cp proteins for two groups patients (with urinary bladder + kidney cancer and control group) are presented in Fig. 1c. As can be seen from the figure the concentration of  $\text{Cu}^{2+}$ -Cp is in the norm for 80% volunteers from control groups while it is elevated for more then 80% patients with cancer. It was established the existence of a statistically significant difference between patients with cancer and control group in serum  $\text{Cu}^{2+}$ -Cp value ( $P < 0.0001$ ).

Thereby the high level of  $\text{Cu}^{2+}$ -Cp at the low level  $\text{Fe}^{3+}$ -Tf concentration in patients suffering from anemia (Hb  $\leq 120$  g/l) can be used as other biomarker for diagnostic cancer in urogenital system even at early stages of malignant tumor growth.

## Coherent Transfer of Spin Hyperpolarization in Coupled Spin Systems at Variable Magnetic Field

K. L. Ivanov<sup>1</sup>, S. E. Korchak<sup>2</sup>, A. S. Kiryutin<sup>1</sup>, A. V. Yurkovskaya<sup>1</sup>, T. Köchling<sup>1</sup>,  
and H.-M. Vieth<sup>1</sup>

<sup>1</sup> International Tomography Center SB RAS, Novosibirsk, Russian Federation

<sup>2</sup> Freie Universität Berlin, Berlin D-14195, Germany

Many mechanisms utilized for hyperpolarization of nuclear spins show a strong dependence on the strength of the external magnetic field  $B$ . Usually the field giving optimum polarization efficiency does not coincide with the field that is suited best for detection. Therefore, field-cycling schemes have been devised that allow switching the field strength between two or more levels without sacrificing spectral resolution at detection and are successfully applied to improving hyperpolarization. The cycling has to be sufficiently fast that the loss of polarization by relaxation is not detrimental. At closer inspection, however, the situation becomes more complicated, particularly in multi-spin systems, since strong coupling of spins, i.e.  $\delta\sigma \cdot \gamma B < 2J$ , can be the cause of efficient polarization re-distribution among them. Moreover, the process of field variation itself can change the population of the spin-eigenstates, in particular, when regions are passed where level-crossings occur as they are frequently seen at fields up to several Tesla even for scalar spin-spin coupling  $J$  of only a few Hertz. In such cases also the speed of field-cycling is of importance, because non-adiabatic field change transforms polarization into coherence and vice versa. By incrementing spin evolution times an oscillatory exchange of polarization between spins is observable allowing efficient manipulation of polarization flow.

We have developed theoretical methods, which describe coherence re-distribution of hyperpolarization (most notably, CIDNP and PHIP) among scalar coupled spins at arbitrary magnetic field strength. Theoretical predictions are in very good agreement with the field-cycling experiments done at the FU-Berlin. The field dependence of polarization has been studied in detail; possible applications of the transfer phenomena are discussed.

Acknowledgement. This work was supported by the Russian Foundation for Basic Research (grants No. 09-03-00837, 11-03-00356, 11-03-00296), Program of the Division of Chemistry and Material Science RAS (Project No. 5.1.1).

## Angular Dependence of ESEEM Signal in the Pair Spin Polarized Quartet–Radical

*Yu. E. Kandrashkin*

*Zavoisky Physical-Technical Institute, Russian Academy of Sciences, Kazan 420029,  
Russian Federation, spinalgebra@gmail.com*

Distance determination of the spin labels based on the Electron Spin Echo Envelope Modulation (ESEEM) technique is one of the most powerful methods for extraction the structural information in the biological systems. Typically stable nitroxide radicals are used as spin labels. Several model systems that consist of different paramagnetic centers such as Gd and Cu have been investigated recently. These labels have relatively strong anisotropy of the g-tensors and zero-filed splitting. Here we demonstrate the possibility of extracting of the orientation of the stable radical in the frame of the principal axes of the photoexcited quartet zero-field tensor.

The photoexcited quartet state has non-equilibrium populations of the spin sublevels that are characterized by multiplet polarization. The microwave pump of the transition  $\pm 3/2 \leftrightarrow \pm 1/2$  can form stimulated net polarization [1] that can be observed at the transition  $+1/2 \leftrightarrow -1/2$ . This polarization has strong orientation dependence and can be used for the structure determination in the ESEEM experiments. We will present the pulse sequence for the experiment where ESEEM sequence is applied to the stimulating polarized sublevels  $\pm 1/2$  of the photoexcited quartet state and the radical. The results of the numerical experiment demonstrate that the comparison of the Fourier transform of the ESEEM data with the pattern found for the angular distribution of the intensity of the quartet sublevels' transition  $+1/2 \leftrightarrow -1/2$  has high orientation selectivity.

The work was supported by the grant of Leading Scientific School of the Russian Federation 6267.2010-2.

1. Kandrashkin Yu.E., van der Est A.: Appl. Magn. Reson. **40**, 189–204 (2011)

## Computer Simulation of PELDOR Experiment for Three-Spin Systems

*I. T. Khairuzhdinov and K. M. Salikhov*

*Zavoisky Physical-Technical Institute, Russian Academy of Sciences, Kazan 420029,  
Russian Federation, semak-olic@mail.ru*

Pulse Electron Double Resonance signals depend on the dipole – dipole interaction between paramagnetic centers. This effect can be used for the measuring distances between paramagnetic centers [1].

The methodology of the distance measurements is well elaborated in case of the correlated pairs of paramagnetic centers which are randomly distributed in a sample. However, the spatial design of paramagnetic centers in groups (clusters) can be of importance [2].

Keeping this fact in mind we have performed computer simulating of PELDOR signals for spin triads. The triads assumed to be randomly oriented. The results obtained are compared with those available in literature.

This work is supported by the RFBR grant 09-03-00612-a and the leading school grant NSh-6267 2010-2.

1. Milov A.D., Salikhov K.M., Schirov M.D.: Solid State Physics **23**, 975 (1981)
2. Tsvetkov Y.D., Milov A.D. in: Electron Paramagnetic Resonance: from Fundamental Research to Pioneering Applications @ Zavoisky award (Salikhov K.M., ed.), p. 170–171. AXAS, New Zealand, 2009.

## Determination of the Iron Oxides Nature in Polymeric Nanocomposites by EPR Spectroscopy

*S. S. Khutshishvili, T. I. Vakulskaya, S. A. Korzhova, T. V. Kon'kova,  
A. S. Pozdnyakov, T. G. Ermakova, and G. F. Prozorova*

*A. E. Favorsky Irkutsk Institute of Chemistry of the Russian Academy of Sciences,  
Siberian Branch, Irkutsk 664033, Russian Federation, khutshishvili\_sp@yahoo.com*

Trivalent iron oxides  $\text{Fe}_2\text{O}_3$ ,  $\text{Fe}_3\text{O}_4$ ,  $\text{Fe}_2(\text{SO}_4)_3$  possess superparamagnetic properties and are capable of forming low-dimensional nanoparticles (sizes of order 8 nm). These oxides are widely used in magnetic resonance tomography as contrast substances [1]. Nanocomposites on basis of the water-soluble polymers containing iron oxides can possess a prolonged action and represent perspective usefulness materials in medicine. We have investigated magnetic properties of new obtained nanocomposites containing iron oxides nanoparticles, which are stabilized within polymeric matrix of poly-1-vinyl-1,2,4-triazole. Variation of reaction conditions, in particular, content of polymer, iron(III) sulfate and sodium tetrahydridoborate in the initial reaction media lead to receiving both soluble and insoluble in water nanocomposites, with various iron mass content, %: 3.5 (**1**), 1.0 (**2**), 14.8 (**3**), 20.0 (**4**). According to transmission electron microscopy data for polymeric nanocomposites containing iron oxides its nanoclusters' have mainly sizes of about 3–9 nm (see Fig. 1).

Nanocomposites possess thermal stability up to 200–250 °C and electric conductivity, which amounts to  $10^{-13}$ – $10^{-12}$  S/sm.

In the EPR spectra of nanocomposites **1–4** there are considerable differences, which reveal of occurrence in the samples of various iron oxides types. Water-soluble nanocomposites **1** and **2** give in EPR spectrum very wide signals of about 830 and 450 G, respectively, with different  $g$ -factors. In spectrum of the sample **2** except wide singlet with  $g = 2.017$ , are observed weak lines in the range of  $g = 4.3$  and  $g = 2.68$ . Insoluble nanocomposites **3** and **4** with high iron mass content (14.8 and 20.0%, respectively) also show in EPR spectra extra wide signals, thus nanocomposite **3** gives signal with extension of order 7000 G, where its width between points of the maximum inclination come to 560 G. EPR characteristics of the nanocomposite **4** are similar to the nanocomposite **2**. In result the experimental data evidence of various environments of iron containing clusters in mentioned nanocomposites. Besides, in the nanocomposite **4**, as well as in the nanocomposite **2**, there are weak absorption centers in the area  $g = 4.3$ . Comparison of the obtained magnetic characteristics

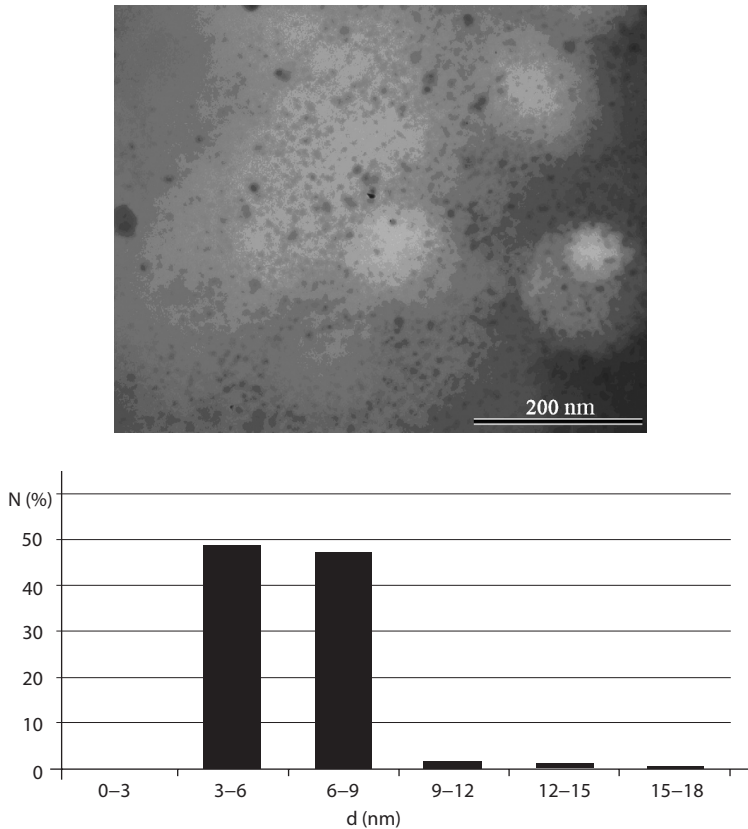


Fig. 1. Electronic microphotography and cluster size distribution of nanocomposite 1.

for nanocomposite **1-4** with corresponding parameters of EPR spectra of iron oxides in various glasses matrixes [2–4] allows to assume, that in the all composites are available superparamagnetic and ferromagnetic oxides of trivalent iron ( $\text{Fe}_2\text{O}_3$  and  $\text{Fe}_3\text{O}_4$ ) in various ratios. The specified iron oxides are organized as nanoclusters in which collective interactions between the electronic spins are shown, that lead to wide signals. Beside the tetrahedral coordinated ions of trivalent iron give characteristic absorption in the area  $g = 4.3$ . Thus the wide signals in the nanocposites **2** and **4** mainly responsible to  $\text{Fe}_3\text{O}_4$ , and mixture of  $\text{Fe}_2\text{O}_3$  and  $\text{Fe}_3\text{O}_4$  in the nanocposites **1** and **3** contain in preference  $\text{Fe}_2\text{O}_3$ .

The work was supported by Foundation for Basic Research (grant 11-03-00022).

1. Shimanovskii N.L., Panov V.O., Semeikin A.V., Sergeev A.I., Akopdzhanov A.G., Bykov I.V., Manvelov E.V., Naumenko V.Yu.: *Experimental'naya i klinicheskaya farmakologiya* **6**, 23 (2010)
2. Gubin S.P., Koshkarev Yu.A., Khomutov G.B., Yurkov G.Yu.: *Uspekhi Khimii* **74**, 539 (2005)
3. Salado J., Insausti M., Gil de Muro I., Lezama L., Rojo T.: *J. Non-Crystalline Solids* **354**, 5207 (2008)
4. Adrelean I., Andronache C., Cimpean C., Pascuta P.: *J. Optoelectronics and Advanced Materials* **8**, 1372 (2006)

## Manifestation of the Compensating Effect for the Self-Diffusion Coefficient of Molecules in Liquid Crystals

*A. B. Konov and K. M. Salikhov*

*Zavoisky Physical-Technical Institute, Russian Academy of Sciences, Kazan 420029, Russian Federation, andrey654@yandex.ru*

It has been found that the activation energy  $E_a$  and the pre-exponential factor  $D_0$  in the Arrhenius temperature dependence  $D(T) = D_0 \exp(-E_a/RT)$  obtained from the temperature dependence of the self-diffusion coefficient of the liquid-crystal molecules in different temperature ranges [1] satisfy a simple relation: the logarithm of the  $D_0$  is linearly dependent on the activation energy  $E_a$ .

It is known that for a series of homotypic chemical reactions an analogous correlation between  $k_0$  and  $E_a$  is observed for the temperature dependence of the rate constant  $k$ . This is the so-called *compensating effect*. By using the theory of monomolecular reactions of the polyatomic molecules for the calculation of the self-diffusion coefficient, the cooperativity degree of the elementary act of the molecular diffusion has been estimated in the studied system at different temperatures (structural states). It has been shown that the temperature variation results in the change of the size of the kinetic unit (the number of atoms directly involved in the elementary diffusion act).

1. Selivanova N.M., Galeeva A.I., Konov A.B., Gnezdilov O.I., Salikhov K.M., Galyametdinov Yu.G.: *Rus. J. Phys. Chem. A* **84**(5), 82 (2010)

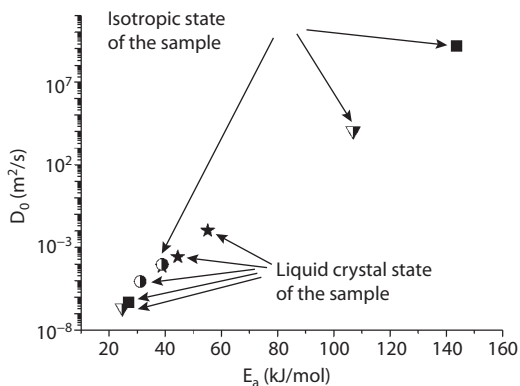


**Fig. 1.**  $D_0$ - $E_a$  dependence in semi-logographic coordinates.

## Improvement of Selective Hole-Burning Technique Using a Fast-Relaxing Paramagnetic Compound

*K. Konov and R. Zaripov*

*Zavoisky Physical-Technical Institute, Russian Academy of Sciences, Kazan 420029,  
Russian Federation, kostyakonov@gmail.com*

At present pulse methods based on the observation of electron spin echo are widely used to determine the distance between paramagnetic species. In particular, they are used in biological researches. In contrast to other techniques, where the modulation due to dipolar interaction is observed at the variation of the interpulse delay, the selective hole-burning method is based on the direct observation of the modulation on electron spin echo (Fig. 1). The main advantage of the selective hole-burning method is that it is a single-frequency experiment. Therefore, this method does not demand much of the equipment.

The main restriction for this method is the significant attenuation of the modulation amplitude as the spin-lattice relaxation times become too long. A nitroxide biradical was studied. The nitroxide biradicals have long

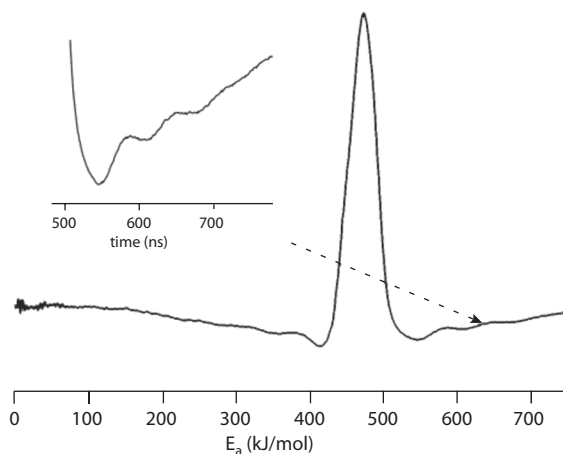


**Fig. 1.** Electron spin echo modulation.

relaxation times and this leads to the decrease in the modulation amplitude. To shorten the relaxation times a fast-relaxing paramagnetic species (a dysprosium complex) was added to the biradical solution. It was shown in this work that the addition of the fast-relaxing paramagnetic species considerably enhances the modulation amplitude and, as a result, enhances the distance determination accuracy.

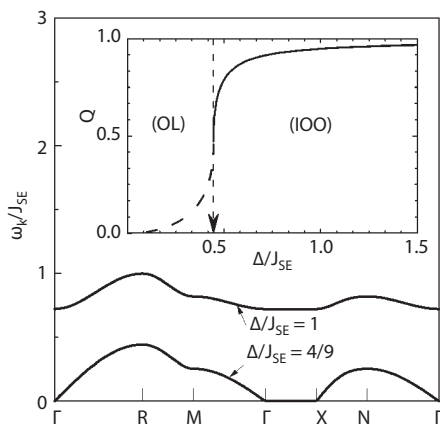
1. Dzuba S.A., Koderu Y., Hara H., Kawamori A.: *Appl. Magn. Reson.* **6**, 391–399 (1994)
2. Hara H., Kawamori A.: *Appl. Magn. Reson.* **13**, 241–257 (1997)

## Competition between the Crystal Field and Superexchange Interactions in the $t_{2g}$ Orbital Mott Insulators

*S. Krivenko*

*Kazan Federal University, Kazan 420008, Russian Federation, s.a.krivenko@mail.ru*

Physics of electronic planar d-orbitals ( $xy$ ,  $xz$ ,  $yz$ ) of cubic  $t_{2g}$  triplet levels of transition metal ions is challenging in pseudocubic perovskite oxides  $RTiO_3$  and  $RVO_3$  ( $R$  is a rare-earth ion) [1]. With a related model of the  $d^1(t_{2g})$ -electron Mott insulator, I have investigated a competition between the two typical interactions, controlling the orbital states: The on-site local crystal field (LCF) tends orbital to order, while the intersite superexchange (SE) introduces their fluctuations. The both interactions coexist in perovskites: The LCF is created by the  $GdFeO_3$ -type structural distortion (GFOD) [2]. In turn, the SE originates from electronic hoppings, allowed by the Pauli principle, between non-orthogonal orbital states of adjacent sites. I have found the dependence of the orbital states on a relation between and the exchange energy  $J_{SE}$  and the energy  $\Delta$  of the triplet level splitting due to the LCF with the  $D_{3d}$  symmetry: The dispersion  $\omega_k$  of the orbital modes and the orbital polarization  $Q$ , calculated in the Born approximation for the spin-orbital SE coupling, are plotted in the Figure. I have established the two regimes of the model: (i) Massive orbital waves in



the state with the induced orbital order (IOO), when the LCF coupling dominates. (ii) The gapless orbital liquid-like (OL) fluctuations, accompanied by the vanishing polarization  $Q$ , when the SE prevails. Accordingly, the present generalized model lets to segregate the regions of applicability of the previous, conflicting theories, based on either the LCF [2] or SE [3] interaction, for the orbital physics of the oxides (see the Inset in the Fig. 1). The present study reveals the crossover between these regimes about  $\Delta \approx J_{SE}/2$ , where both of the approaches [2, 3] become inappropriate.

1. Khaliullin G.: Prog. Theor. Phys. Suppl. **160**, 155 (2005), and references therein.
2. Mochizuki M., Imada M.: Phys. Rev. Lett. **91**, 167203 (2003)
3. Khaliullin G., Maekawa S.: Phys. Rev. Lett. **85**, 3950 (2000)

## Optimization of Device for Measuring of Magnetic Field Inhomogeneity

*N. Krylatykh, A. Fakhrutdinov, and R. Khabipov*

*Laboratory of the Methods of Medical Physics, Zavoisky Physical-Technical Institute,  
Russian Academy of Sciences, Kazan 420029, Russian Federation, npyrkina@yandex.ru*

Magnetic resonance, which has great performance in soft tissue imaging, is very sensitive to magnetic field inhomogeneities. It is important task for Magnetic resonance imaging systems designer to measure the inhomogeneity and create the map of the basic magnetic field. To obtain the field's inhomogeneity data one usually uses single probe device. In this type of devices all measurements are made by single contour, which in turn measures the basic field's strength at different places of the working space sphere. To obtain the finally field's map from the data received by the measuring device amplitudes of the spherical functions are calculated. This technique has a well accuracy of the measurements. There are not some measurement errors because all the measurements are made by single probe. The main shortcoming of this technique is the long period of the measuring experiment. This is especially important if the magnetic field, generated by the electromagnet may have time instability. To reduce the duration of the experiment one has to create a device to automatically measure the field's map.

To create a measuring device, which consists of more than one probe it is necessary to optimize the probes localization on the working space sphere. Generally, it is sufficient for basic field correction to know only the amplitudes of spherical functions, which contribute to the field inhomogeneity. That is why the main task is not a calculating of final field's map and correct calculating of spherical functions amplitudes. According to the theory, the field inside the sphere which surface measures the field on can be divided into spherical functions so that the field will be represented as a contributions's sum of every function.

By the mathematical simulation the efficient of the different probes configuration were checked. The mathematical model takes into account the localization of probes on the working space sphere and allows calculate the coefficients of the reflection for every spherical function. So, the measuring device may be optimized for different sizes of working sphere because of the different number of sensors.

## The Problem of the Nano-Structures Diagnostics for the Needs of Spintronics by Magnetic Resonance Methods

*G. S. Kupriyanova, A. P. Popov, A. Y. Zyubin, A. Orlova, E. Prokhorenko, A. Goykhman, and P. Ershov*

*Physical Department, I. Kant Baltic Federal University, Kaliningrad 236041, Russian Federation, galkupr@yandex.ru*

The research of magnetic tunnel junctions (MTJ), consisting of the ferromagnetic–insulator–ferromagnetic structures, which are the main element of the random access memory of novel generation, is of a very special interest. Several requirements to the materials combination for the MTJ were found, which are the following: a) high conductivity electrons polarization in a ferromagnetic electrode, b) a possibility of an independent magnetization switching in two ferromagnetic electrodes; c) the absence of paramagnetic phase on the interface; d) the thickness of the tunnel insulator layer within 2–3 nm; e) the homogeneity of an insulator; f) the roughness of the insulator within the ranges of monolayer thicknesses; g) the absence of defects [1]. One of the important task is the development of diagnostic complex to predict potential applications possible for the structures formed as functional elements for spintronics.

In this presentation we discuss the problems of the diagnostic method creation based on the ferromagnetic resonance method, which allows to predict the functional properties of the formed structures on the basis of the magnetic state. Some models are proposed to predict a possibility of an independent magnetization switching between ferromagnetic electrodes in MTJ.

As an example, the results of the study of three layer structures for the needs of spintronics such as Ni/SiO<sub>2</sub>/Fe, Ni/SiO<sub>2</sub>/Co and Fe/Fe<sub>3</sub>O<sub>4</sub>/MgO/Fe<sub>3</sub>Si are presented. We demonstrate the opportunities of the ferromagnetic resonance method for the diagnostics of the orientation properties and the crystallographic and magnetic phase state of monolayers and multi-layer structures for the further applications in spintronics

The work was supported by Ministry of Education (Contract 02.740.11.0550).

1. Parkin S.S.P., Kaiser C., Panchula A., Rice P.M., Hughes B., Samat M., Yang S.: Nature Mat. **3**, 862 (2004)

Zeeman-Switched Photon Echo in  $\text{LuLiF}_4:\text{Er}^{3+}$  and  $\text{YLiF}_4:\text{Er}^{3+}$ 

V. N. Lisin and A. M. Shegeda

Zavoisky Physical-Technical Institute, Russian Academy of Sciences, Kazan 420029,  
Russian Federation, vlinin@kfti.knc.ru

We describe and demonstrate a method for performing ultrahigh-resolution optical spectroscopy in the time domain which utilizes modulations in the intensity of the two-pulse photon echo in the presence of a perturbation that splits the optical transition frequencies of two or more subgroups of ions. The method is applied to systems exhibiting the Zeeman effect:  $\text{YLiF}_4:\text{Er}^{3+}$  and  $\text{LuLiF}_4:\text{Er}^{3+}$  (0.025 at.%). The ionic transition frequency is switched by applying a pulsed magnetic field. Zeeman shift of  $\approx 10$  MHz is observed in the pulsed magnetic field of  $\approx 2$  G amplitude and 30 ns duration. A magnetic moment difference between the ground and metastable crystal field components of the  ${}^4\text{F}_{9/2}(\text{I})$  excited state is determined.

The backward two-pulse photon echo is excited by a linearly polarized ( $\pi$ -polarization) tunable dye laser (linewidth  $0.1 \text{ \AA} \approx 6$  GHz, pulse duration 12 ns) operating with a repetition rate of 12 Hz. The operation temperature is 2 K. The propagation directions  $\mathbf{k}$  of the exciting first and second light pulses are

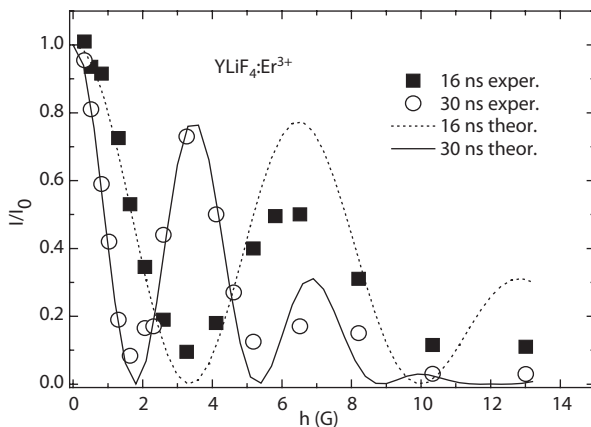


Fig. 1. Zeeman modulation in  $\text{YLiF}_4:\text{Er}^{3+}$ .

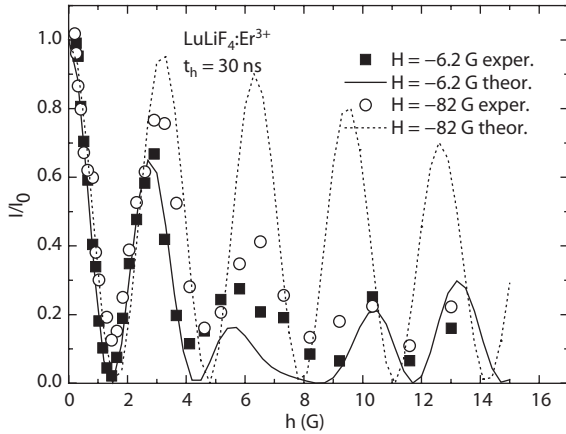


Fig. 2. Zeeman modulation in  $\text{LuLiF}_4:\text{Er}^{3+}$ .

perpendicular to optical axis  $\mathbf{C}$  ( $\mathbf{k} \perp \mathbf{C}$ ). Electrical field of the laser pulses light is directed along the crystal axis ( $\mathbf{E} \parallel \mathbf{C}$ ).

The pulsed magnetic field  $\mathbf{h}$  is obtained through the use of a Helmholtz pair of coils, wound with 6 turns each and having a diameter of  $d = 5.4$  mm ( $\text{LuLiF}_4$ ),  $6.4$  mm ( $\text{YLiF}_4$ ) and a separation of  $1$  mm. The sample is placed within the coils so that the C-axis is parallel to the field produced by the coils ( $\mathbf{h} \parallel \mathbf{C}$ ). In order to observe a contribution of the superhyperfine interaction Er-F, a dc magnetic field  $\mathbf{H}$  is also applied parallel to the C-axis ( $\mathbf{H} \parallel \mathbf{C}$ ). The amplitude  $H$  is as less as larger then a local magnetic field  $H_{\text{loc}}$  ( $H_{\text{loc}} \approx 5$  G), the local field acting at the  $\text{Er}^{3+}$  site. It is studied a behavior of the photon echo intensity and duration versus the magnetic fields amplitudes ( $H \leq 800$  Oe,  $h \leq 32$  G) and magnetic pulse duration ( $12 \leq t_h \leq 30$  ns) and times of switching on.

It is observed that echo intensity is strongly changed if the homogeneous magnetic field pulse is switched on during the echo formation: between the first and second laser pulses or between the second laser and echo pulses. A relative value  $I/I_0$  of the photon echo intensity is an oscillation function of the magnetic field pulse amplitude as you can see in Fig. 1 and Fig. 2. The oscillation period is inversely proportional quantity to the magnetic pulse duration  $t_h$ . There is used local the  $\text{Er}^{3+}$  ion site symmetry and the magnetic dipole-dipole interaction between the  $\text{Er}^{3+}$  electron spin and eight neighboring F nuclear magnetic moments in a theoretical interpretation of the experiment results. The eigenvalues and eigenvectors of the electron-nuclear excitations in the ground and excited states of the  $\text{Er}^{3+}$  ion are obtained with the numerical diagonaliza-

tion of the  $512 \times 512$  matrix ( $2^9 = 512$ ) as in the presence as in the absence of a magnetic field of the pulse. Then a density matrix is calculated. The magnetic field of the pulse is also calculated using the Biot-Savart law.

As you can see in Fig. 1 the  $\text{YLiF}_4:\text{Er}^{3+}$  experimental and theory results are in quantitative agreement if it is used very well known  $g$ -factor values [1] ( $g_{g\perp} = 8.13$ ,  $g_{g\parallel} = 3.14$ ,  $g_{e\perp} < 0.1$ ,  $g_{e\parallel} = 9.84$ ). Here index  $g$  denotes ground and  $e$  indicates excited electron states accordingly. The  $\text{Er}^{3+}$   $g$ -factor values in  $\text{LuLiF}_4$  are  $g_{g\perp} = 8.09$ ,  $g_{g\parallel} = 3.09$  [2]. The  $g_{e\parallel}$  and  $g_{e\perp}$  values are do not known. The best agreement with experiment in high magnetic fields  $H \gg H_{\text{loc}}$  is reached at  $g_{e\parallel} = 10.6$  and  $g_{e\perp} < 0.1$ . In the low magnetic field  $H \approx H_{\text{loc}}$  echo intensity value is depends on superhyperfine interaction and the best agreement with experiment is reached if superhyperfine interaction is halved.

The financial support of the Division of Physical Sciences, Russian Academy of Sciences (programs "Optical Spectroscopy and Frequency Standards") is gratefully acknowledged.

1. Wannemacher R., Boye D., Wang Y.P., Pradhan R., Grill W., Rives J.E., Meltzer R.S.: *J. of Luminescence* **45**, 431 (1990)
2. Abdulsabirov R.Yu., Antipin A.A., Korableva S.L., Rahmatullin R.M., Rosentzweig Yu.K.: *Izv. Vuzov, Physica*, no. 2, 24 (1988)

## CPMG Echo Amplitudes with Arbitrary Refocusing Angle: Explicit Expressions, Asymptotic Behavior, Approximations

*N. N. Lukzen<sup>1</sup>, A. B. Doktorov<sup>2</sup>, and M. V. Petrova<sup>1</sup>*

<sup>1</sup> *International Tomography Center SB RAS, Novosibirsk, Russian Federation, luk@tomo.nsc.ru*

<sup>2</sup> *Institute of Chemical Kinetics and Combustion SB RAS, Novosibirsk, Russian Federation*

Long trains of periodic RF pulses make an integral part of MRI methods. Extensively used multiple echoes can serve as an example of such kind. Earlier we developed a new effective approach for calculation of magnetization evolution under the influence of trains of periodic RF pulses in the framework of the generating functions (GF) formalism [1–2]. Generating function is defined as a function of complex variable  $z$ :  $F(z) = M_1 + M_2z + M_3z^2 + \dots + M_nz^{n-1} + \dots$ . Here,  $M_n$  is, for instance, the  $n$ -th echo amplitude. Generating function comprises complete information about all echo amplitudes at once. In this work Carr-Purcell-Meiboom-Gill pulse sequence with arbitrary excitation and refocusing angles and resonance offset of RF pulses is considered. Exact explicit analytical formula for echo magnetization amplitudes were derived employing earlier obtained generating functions [1–2] for the echo amplitudes. The echo-amplitudes are expressed in terms of Legendre polynomials. The dependence of asymptotic behavior of echoes on RF pulse refocusing angle was studied; analytical approximation for echoes was also obtained. It was shown that at refocusing angle  $\alpha \neq \pi$  the echo amplitudes decay is defined not only by spin-spin relaxation time  $T_2$  as usually but also spin-lattice relaxation time  $T_1$  and the refocusing angle. Accuracy of asymptotics and approximations were tested by comparison with exactly calculated echo amplitudes. The cases of MRI and NMR-loggins are considered.

The work was supported by Foundation for Basic Research (grant 11-03-00296).

1. Lukzen N.N., Petrova M.V., Koptyug I.V., Savelov A.A., Sagdeev R.Z.: *J. Magn. Res.* **196**, 164–169 (2009)
2. Lukzen N.N., Savelov A.A.: *J. Magn. Res.* **185**, 71–76 (2007)

## ESR Study of Ternary Dilute Alloys Cu-Me-Er

*S. Lvov and E. Kukovitsky*

*Zavoisky Physical-Technical Institute, Russian Academy of Sciences, Kazan 420029,  
Russian Federation, lvov@kfti.knc.ru*

Impurity-impurity interaction in metals is important task of solid state chemistry. In case of the diluted alloys experimental studying of such interaction substantially restrains the limited set of experimental methods (PAC, TDPAC, nuclear  $\gamma$ -resonance). For each of these methods the limited circle of studied alloys is peculiar. In particular, methods of the perturbed angular correlation do not allow studying alloys with rare-earth elements. In experiments on Mössbauer effect a problem is reception of suitable sources. We inform here that the ESR method also can be useful for studying impurity-impurity interactions in the diluted metal alloys.

Erbium 3+ ion in copper host gives isotropic spin-resonance signal, characteristic for Kramers doublet  $\Gamma 7$  in cubic crystalline field [1, 2]. Thus, it is interesting to use  $\text{Er}^{3+}$  as a probe of impurity atoms states in copper. We report the ESR measurements in single crystals of ternary dilute alloy  $\text{Cu}_{1-x}\text{Me}_x\text{:Er}^{3+}$  (Me = Ni, Pd, Pt). Concentration of erbium due to its low solubility in copper was evaluated as about  $10^{-2}$  at.%. Experiments were carried out with Varian E-12 ESR spectrometer, X-band, in temperature range 1.7–4.2 K.

The ESR spectrum presents a superposition of signal of  $\text{Er}^{3+}$  in crystalline field of cubic symmetry (isotropic  $g$ -factor) with  $I = 0$ , signals of the hyperfine structure of  $^{167}\text{Er}$  isotope ( $I = 7/2$ , abundance 22%), and also some additional spectra showing angular dependence. Measurements of angular dependences of the additional spectra in these alloys revealed existence of 6 magnetically nonequivalent centers, and its behavior can be explained by spin Hamiltonian with effective spin 1/2 Eq. (1)

$$\mathcal{H} = \beta(g_{xx}H_x\tilde{S}_x + g_{yy}H_y\tilde{S}_y + g_{zz}H_z\tilde{S}_z), \text{ or } \mathcal{H} = \beta(\mathbf{H} \cdot \mathbf{g} \cdot \tilde{\mathbf{S}}), \quad (1)$$

with  $g^2 = l^2g_{xx}^2 + m^2g_{yy}^2 + n^2g_{zz}^2$ .  $l$ ,  $m$  и  $n$  – respective directional cosine,  $g_{xx}$  and  $g_{zz}$  are along  $\langle 110 \rangle$  axes,  $g_{yy}$  – along  $\langle 100 \rangle$ . The values of  $g$ -tensor are shown in Table below.

This points to the fact that cubic crystal field for part of erbium 3+ ions experiences rhombic deformation along axes of second order  $C_2$ . Formation

**Table 1.** Experimental  $g$ -factor values of  $\text{Er}^{3+}$  for Cu-Me-Er single crystals.

Me	$g_{xx}$	$g_{yy}$	$g_{zz}$
Ni	$9.06 \pm 0.05$	$7.10 \pm 0.05$	$3.65 \pm 0.01$
Pd	$9.26 \pm 0.02$	$7.27 \pm 0.02$	$3.558 \pm 0.003$
Pt	$9.61 \pm 0.05$	$7.22 \pm 0.05$	$3.060 \pm 0.015$

of such rhombic centers can be explained by substitution of one of 12 copper ions with Me-impurity ions in nearest neighborhood of  $\text{Er}^{3+}$ . Increase of cubic field distortion is observed in Ni-Pd-Pt row along  $\langle 110 \rangle$  direction and in less extent along  $\langle 100 \rangle$ .

The samples with different Me-impurity concentrations showed an increase of rhombic-centers intensity with increase of Me-concentration. Er-Ni complexes arisen at 0.15–0.25 at.% of Ni. Optimal concentration was 1 at.% Ni to follow complete angular dependence. Meantime, such concentrations were already 0.25 and 0.1 at.% in case of Pd and Pt, respectively. Extracted absorption signals allow concluding that concentration of erbium ions with Me as a neighbor considerably exceeds concentration expected for random distribution of these impurities.

These facts specify in presence of attractive interaction between nickel, palladium and platinum ions and erbium ions in copper host. Binding energy for Er-Ni, Er-Pd and Er-Pt pairs was estimated with use of pairs/(single ions) concentration ratios.

1. Al'tshuler T.S., Zaripov M.M., Kukovitsky E.F., Khaimovich E.P., Kharakhash'yan E.G.: JETP Lett. **20**, no. 6, 187 (1974)
2. L'vov S.G., Kukovitsky E.F., Vagizov F.G.: Hyperfine Int. (C) **1**, 72 (1996)

## Spin Properties of Electron in Two Dimensional Quantum Dot Arrays

*A. Lyubin, A. Zinovieva, and A. Dvurechenkii*

*Institute of Semiconductor Physics RAS, Novosibirsk 630090, Russian Federation,  
forlus@gmail.com*

A dimensionality reduction leads to the appearance of new effects, many of them are governed by symmetry of nanostructures. The low symmetry of nanostructures can lead to appearance of additional spin relaxation mechanisms, which takes place in the arrays of tunnel-coupled quantum dots (QDs) with structure-inversion-asymmetry. At high density of QDs the overlapping between localized states is sufficient for coming in force the most efficient Dya-konov-Perel mechanism of spin relaxation. In this case the spin relaxes during series of random tunneling events (in hopping transport) through precession in the effective magnetic field whose direction can be changed after each tunneling event.

Two types of samples were grown: the QD structure with single shaped QDs (hut-clusters) consisted of vertical stack of four Ge QDs layers. Ge islands have the shape of hut-clusters with the average lateral size  $l = 20$  nm and height  $h = 2$  nm. The density of QDs is  $\sim 10^{11}$  cm $^{-2}$ .

The QD structure with *dome*-clusters contains 6 layers of QDs. The STM of test structure shows the bimodal distribution of QDs (*huts* and *domes*). The density of *dome*-clusters is  $10^9$  cm $^{-2}$ .

The spin echo measurements were carried out at temperature 4.5 K in resonance magnetic field  $H = 3470$  G. A two-pulse Hahn echo experiment ( $\pi/2$ - $\tau$ - $\pi$ - $\tau$ -echo) was used to measure  $T_2$ . In order to observe a longitudinal spin relaxation (corresponding time  $T_1$ ), a different pulse sequence is applied ( $\pi$ - $\tau$ - $\pi/2$ - $T$ - $\pi$ - $T$ -echo).

Both types of structures demonstrate the EPR signals from electrons localized in QD layers. The  $g$ -factor and EPR line width of EPR line depends on the type of the structure. The narrowest EPR lines (width  $\Delta H \sim 0.8$  G) was detected for the first type structures. The principal values of  $g$ -factor are very close to  $g$ -factor values in uniaxially deformed Si.

According to results of two-pulse Hahn echo experiment for both types structures the spin echo behavior can be described by superposition of two exponentially decaying functions. The decay parameters give two times of spin

dephasing: for the first type structure  $T_2(1) \sim 0.9 \mu\text{s}$  and  $T_2(2) \sim 20 \mu\text{s}$ ; for the second type structure  $T_2(1) \sim 0.28 \mu\text{s}$  and  $T_2(2) \sim 3 \mu\text{s}$ .

The analysis of an inversion signal recovery, measured in three-pulse echo experiments, also shows a two characteristic times of spin relaxation for both structures. For the first type structure relaxation is about  $T_1(1) \sim 400 \text{ ns}$  and  $T_1(2) \sim 10 \mu\text{s}$ . For the second structure  $T_1(2) \sim 2 \mu\text{s}$  and  $T_1(1) \sim 20 \mu\text{s}$ .

For interpretation of results the existence of two electron groups with different spin relaxation times is suggested. For the first type structure both groups are formed by electrons in QD layers. These groups located in Si spacers with different width and have the different probability of electron hopping between Ge QDs. In both groups of carriers the special relation between  $T_2$  and  $T_1$ ,  $T_2 \sim 2T_1$ , is observed. The unusual relation  $T_2 > T_1$  confirms that the spin relaxation is caused by the interaction with the effective magnetic field arising due to the structure-inversion-asymmetry. For the second structure the spin echo signal is also formed by two groups of electrons. There are the free electrons in Sb-doped Si layers with isotropic  $g$ -factor = 1.9987 and electrons localized in QD layers ( $g_{zz} = 1.9995$  and  $g_{xx} = g_{yy} = 1.9984$ ). For first group the relation  $T_2 < T_1$  is observed, while for QD electrons the inverse relation ( $T_2 < T_1$ ) is obtained.

## ALD/CVD Synthesis of Magnetic Tunnel Junctions

*R. Mantovan<sup>1</sup>, S. Vangelista<sup>1</sup>, B. Kutrzeba-Kotowska<sup>1</sup>, S. Cocco<sup>1</sup>, A. Lamperti<sup>1</sup>,  
G. Tallarida<sup>1</sup>, D. Mameli<sup>1,2</sup>, and M. Fanciulli<sup>1,3</sup>*

<sup>1</sup>Laboratorio MDM, IMM-CNR, Agrate Brianza 20846, Italy

<sup>2</sup>Dipartimento di Scienze Chimiche, Università di Cagliari, Cittadella Universitaria,  
Cagliari 09042, Italy

<sup>3</sup>Dipartimento di Scienza dei Materiali, Università di Milano Bicocca, Milano, Italy

Magnetic tunnel junctions (MTJs) are core elements in modern magnetic non-volatile memories [1]. MTJs are constituted by two ferromagnetic (FM) electrodes separated by an ultrathin tunnel barrier, and the magnetization of one of the FM layers (the bit element) is free to change under external magnetic field or via spin polarized currents [1]. The synthesis of MTJs with chemical route has been poorly attempted so far [2]. Chemical vapour deposition (CVD) and atomic layer deposition (ALD) methods combine the versatility of depositing a wide range of materials on large area substrates with the relatively low cost,

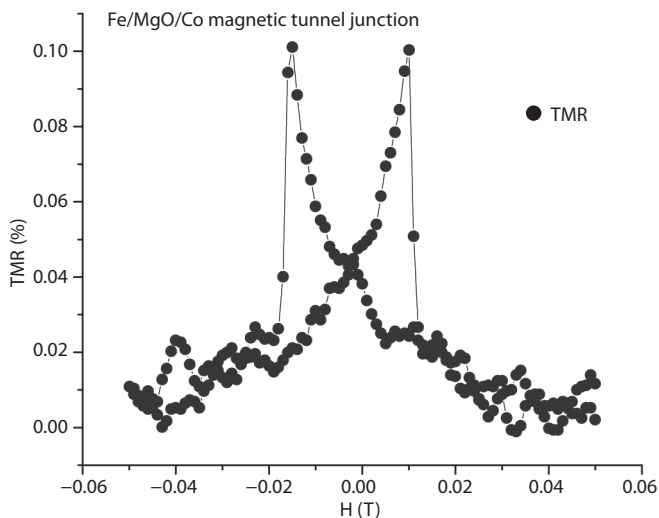


**Fig. 1.** TMR of a Fe/MgO/Co MTJ produced by ALD/CVD.

when compared to more traditional methods such as sputtering, molecular beam epitaxy, and pulsed laser deposition. Moreover, ALD is ideally suitable for the deposition of ultrathin, perfectly stoichiometric and conformal oxides for inclusion into MTJs as tunnel barriers. We developed a combined ALD/CVD, in which we can perform the (full *in situ*) deposition of several FMs and ultrathin MgO. Fig. 1 shows the change in the perpendicular-to-plane resistance of a Fe/MgO/Co stack upon an external magnetic field change (tunnel magnetoresistance, TMR), which has been patterned in a cross-bar geometry by standard photolithography. The non-zero TMR demonstrates the feasibility of the developed ALD/CVD method for the synthesis of functional MTJs. We acknowledge financial support from the Cariplo Foundation in the framework of the SPAM<sup>3</sup> project (code n. 2008.2363).

1. Chappert C., Fert A., Nguyen Van Dau V.: Nat. Mat. **6**, 813 (2007)
2. Bubber R., Mao M., Schneider T., Hegde H., Sin K., Funada S., Shi S.: IEEE Trans. Magn. **38(5)**, 2724 (2002)

## EPR Investigation of Spin-Spin Interactions in [Fe(L)<sub>3</sub>][Cr<sub>2</sub>(OH)(Ac)(nta)<sub>2</sub>] · nH<sub>2</sub>O (L = phen, bpy)

*L. V. Mingalieva<sup>1</sup>, V. K. Voronkova<sup>1</sup>, R. T. Galeev<sup>1</sup>, A. A. Sukhanov<sup>1</sup>,  
V. Chiornea<sup>2</sup>, and Gh. Novitchi<sup>2</sup>*

<sup>1</sup> *Zavoisky Physical-Technical Institute, Russian Academy of Sciences, Kazan 420029,  
Russian Federation, klyuda@yandex.ru*

<sup>2</sup> *Department of Chemistry, Moldova State University, Chisinau MD-2028, Republic of Moldova*

In this paper the results of EPR investigation of two compounds [Fe(phen)<sub>3</sub>][Cr<sub>2</sub>(OH)(Ac)(nta)<sub>2</sub>] · 6.25H<sub>2</sub>O (**I**), [Fe(bpy)<sub>3</sub>][Cr<sub>2</sub>(μ-OH)(μ-Ac)(nta)<sub>2</sub>] · 9H<sub>2</sub>O (**II**) (where bpy – α,α'-dipyridyl; phen – o,o-phenanthroline; Ac<sup>-</sup> – Acetate ion; nta – nitrilotriacetate-ion) are presented. This investigation showed the presence of the anisotropy of the exchange interaction between Cr (III) ions and

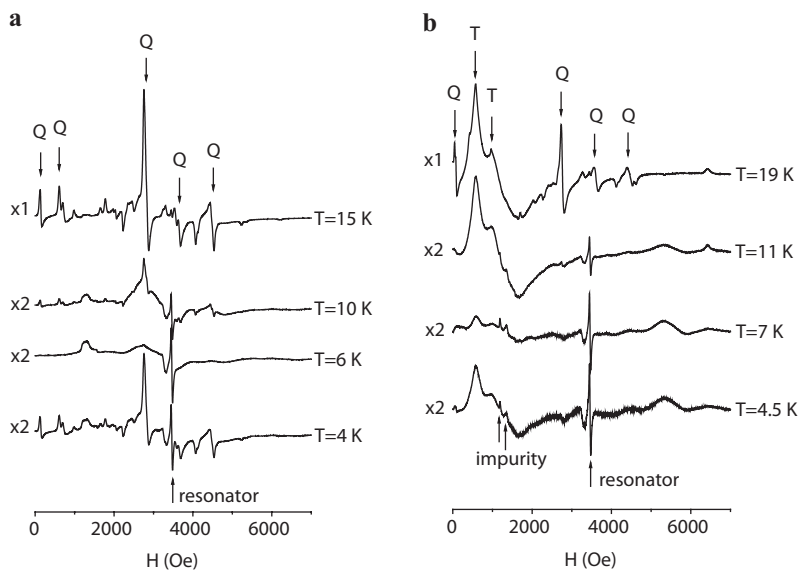


**Fig. 1.** The low-temperature dependence of EPR spectrum of polycrystalline samples (where Q is quintet, T is triplet; relative enhancement of the signal is shown on the left-hand of the spectra) of **I** (a) and of **II** (b) in X-band.

a feature of the temperature dependence of the EPR spectra. The compounds **(I)** and **(II)** are constructed from  $[\text{Cr}_2(\text{OH})(\text{Ac})(\text{nta})_2]^{2-}$  dimers. The distances between the chromium ions in dimers are 3.482 Å for **(I)** and 3.49 Å for **(II)**. The nearest environment of the Cr (III) ion has octahedral coordination [1]. According the magnetic susceptibility data the antiferromagnetic exchange interaction between the Cr (III) ions with  $J = 21.6 \text{ cm}^{-1}$  (**I**) and  $J = 27.2 \text{ cm}^{-1}$  (**II**) leads to the formation of the spin states with  $S = 1, 2, 3$  [1].

EPR investigation of the polycrystalline samples in X-band was carried out on a Bruker EMX/plus spectrometer in the temperature range from 300 to 4 K. An analysis of the temperature dependence of the EPR spectra allowed us to assign transitions to the triplet ( $S = 1$ ), quintet ( $S = 2$ ) and septet ( $S = 3$ ) spin states (Fig. 1).

The spectra for a pair of spins with  $S_{\text{Cr}_1} = S_{\text{Cr}_2} = 3/2$  were simulated in the model taking into account the single-ion anisotropy term  $D_{\text{Cr}}$ , dipole-dipole interaction of spins in the pair, isotropic and anisotropic exchange interactions. Fitting of the experimental and simulated spectra allows us to determine the anisotropic part of the exchange interaction between Cr(III) ions in **I** and **II**.

The investigation shown that the intensity of the EPR spectra decreases when the temperature decrease to 6–7 K in full accordance with magnetic susceptibility data. However at further lowering temperature the intensity of the spectra increases (Fig. 1). The possible reasons for this temperature dependence including the assumption that the values of the exchange interaction decrease with decreasing of temperature are discussed. The change of the exchange interaction may be due to small changes of the angles in the bridging fragments of dimers [2, 3].

This research was partly supported by the grant of the President of the Russian Federation for Support of Leading Scientific Schools nr. NSh-6267.2010.2

1. Ciornea V., Shova S., Novitchi G. *et al.*: Russ. J. Coord. Chem. **35**, 11, 827–833 (2009)
2. Ren Q., Chen Z., Zhang L.: Chem. Phys. Lett. **364**, 485–483 (2002)
3. Moskvina A.S., Bostrem I.Gh.: Solid State Physics **19**, 9, 1616–1626 (1977)

## NMR Evidence for Charge and Orbital Order of Cobalt Ions in $\text{Na}_{2/3}\text{CoO}_2$

*I. R. Mukhamedshin<sup>1</sup>, and H. Alloul<sup>2</sup>*

<sup>1</sup> *Institute of Physics, Kazan Federal University, Kazan 420008, Russian Federation,  
Irek.Mukhamedshin@ksu.ru*

<sup>2</sup> *Laboratoire de Physique des Solides, Université Paris-Sud, Orsay 91405, France*

The cobaltates  $\text{Na}_x\text{CoO}_2$  are layered oxide materials somewhat similar to the cuprates in as much as the charge doping of the  $\text{CoO}_2$  layers is controlled on a large range by variation of the Na content. One significant difference with the cuprates is that the Co of the  $\text{CoO}_2$  plane are ordered on a triangular lattice and not on a square lattice as for the  $\text{CuO}_2$  plane of the cuprates. A rich variety of physical properties ranging from ordered magnetic states, large thermoelectric effect, high Curie-Weiss magnetism and metal insulator transition, superconductivity *etc* have then been observed in the cobaltates. NMR experiments and structural investigations in the cobaltates have given evidence that for  $x > 0.5$  a large interplay occurs between atomic arrangements and electronic properties, as the Na atoms are found to be ordered [1]. In this talk we report a complete set of  $^{59}\text{Co}$  NMR data taken on the  $x = 2/3$  phase of sodium cobaltates  $\text{Na}_x\text{CoO}_2$ , for which we have formerly established the in plane Na ordering and its three dimensional stacking [2]. We resolved all the parameters of the Zeeman and quadrupolar Hamiltonians for all cobalt sites in the unit cell and report the temperature dependencies of the NMR shift and spin lattice relaxation  $T_1$  data for these sites. The moderately complicated atomic structure resumes then in a very simple electronic structure in which the electrons delocalize on the kagomé sublattice of the triangular lattice of Co sites. The observation of a single temperature dependence of the spin susceptibilities indicates that a single band picture applies, and that the magnetic properties are dominated by the static and dynamic electronic properties at the cobalt sites. We evidence that they display a strong in plane electronic anisotropy initially unexpected but which accords perfectly with an orbital ordering along the kagomé sublattice organization.

This work was partially supported by the RFBR (project №10-02-01005-a) and Ministry of Education and Science of the Russian Federation.

1. Alloul H., Mukhamedshin I. R., Collin G., Blanchard N.: EPL **82**, 17002 (2008)
2. Platova T.A., Mukhamedshin I.R. *et al.*: Phys. Rev. B **80**, 224106 (2009)

## Pulsed Reaction Yield Detected EPR of Radical Pairs. Theoretical Treatment

*E. A. Nasibulov<sup>1,2</sup>, K. L. Ivanov<sup>2</sup>, and L. V. Kulik<sup>3</sup>*

<sup>1</sup> *Novosibirsk State University, Novosibirsk 630090, Russian Federation,  
nasibulov@tomo.nsc.ru*

<sup>2</sup> *International Tomography Center SB RAS, Novosibirsk 630090, Russian Federation*

<sup>3</sup> *Institute of Chemical Kinetics and Combustion SB RAS, Novosibirsk 630090,  
Russian Federation*

Optically detected EPR and RYDMR methods for detecting transient radical pairs are particularly useful due to their high sensitivity as compared to the standard EPR techniques. The idea of such methods is monitoring the fraction of singlet radical pairs,  $\rho_{ss}(t)$ , by measuring the reaction yield and affecting it by applying static or oscillating magnetic fields. By means of such techniques one can detect short-lived radicals at room temperature and probe their magnetic interactions. It is possible to indirectly detect the EPR of radical pairs not only by optical methods but using other observables, for instance, detecting magnetic fields induced changes in photo-current.

In this work we investigated theoretically a possibility of extending the potential of the reaction yield detected EPR by applying short pulses of the microwave field. Pulsed methods in standard EPR of radical pairs are nowadays well-developed; however, in the case of RYDMR the observable is not spin magnetization, which is the case for EPR, but  $\rho_{ss}(t)$ . For this reason theoretical treatment is required to fully exploit the potential of the pulsed techniques. We have studied the formation of “spin echo”, i.e., the possibility of refocusing the initial singlet state of the radical pair by applying different pulse sequences. We confirmed the known result of Salikhov and Molin (J. Phys. Chem., **97**, 13259 (1993)) and obtained that  $\rho_{ss}$  can be completely refocused by a single non-selective 180-degree pulse. In addition, we studied the possibility of observing modulations of such  $\rho_{ss}$ -echo caused by inter-radical and intra-radical interactions in the radical pairs. For this purpose somewhat more elaborate pulse sequences are required, which resemble the pulsed ELDOR and ENDOR sequences. Our preliminary results show that  $\rho_{ss}(t)$  observable allows one to probe magnetic interactions in the short-lived radical pairs.

Acknowledgement. This work was supported by the Russian Foundation for Basic Research (grants No. 09-03-00837, 09-03-91006-FWF, 11-03-00356, 11-03-00296).

## Algorithm for Optimizing the Using of Contrast Agents in Low-Field MRI

*I. A. Nurmamyatov*

*Zavoisky Physical-Technical Institute, Russian Academy of Sciences, Kazan 420029, Russian Federation, el-a-nur@yandex.ru*

The issue of quality diagnostic of pathology is not less important than proper and effective treatment, since early diagnostic of the disease increases the effectiveness of treatment.

The method of magnetic resonance imaging allows to detect tumors at early stage of development, and quality of diagnostic can be improved by contrast agents, such as gadolinium salts and chelates, what is strong paramagnet and it effectively reduces the spin relaxation in the surrounding tissues. The problem of MRI contrast is highly relevant today, therefore new contrast agents based on other paramagnets are constantly creating. The optimal dosage of this agents remains to be established. Optimization of the dosage is very important because in the various magnetic fields required contrast is achieved with different concentrations of contrast agents (hereinafter – CA) in the blood. This article submits an algorithm for optimizing the using the CA in low-field MRI.

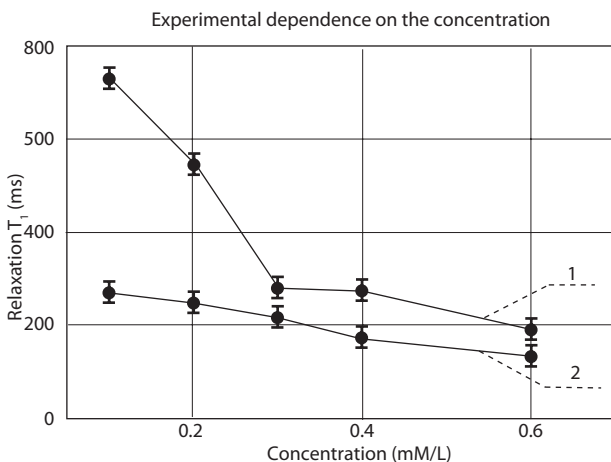


**Fig. 1.** Gadopentetic acid is illustrated with the 1st line and Gadobutrol is illustrated with the 2nd line.

CA based on gadolinium, although conventionally considered to have no contraindications, all the same toxic and not recommended in large doses to patients with disorders of the urinary system. For this group of patients the results of these researches allows to take an MRI diagnostics with a lower risk for the organism. CA effectively decreases  $T_2$  relaxation times, and also with them the useful signal decreases, so the dosage should be adjusted so to take into account three factors: effectiveness of the used CA, quality of the signal and the toxic load on the patient. The proposed algorithm for optimization allows to take into account these three factors.

The optimization algorithm for industrial CA was worked out in the Zavoisky Physical-Technical Institute. In the study  $T_1$  relaxation times of a mixture of distilled water with CA was measured by several methods (Kwasaki-Bene, inversion-recovery, Carr-Purcell) and with different concentrations in the field of 0.06 T. [1] Concentrations has been proposed in 0.6, 0.4, 0.3, 0.2, 0.1 mM/L and this concentrations based on pharmacological description of the industrial CA and clinical trials conducted by manufacturer. The experiment showed that the CA – gadopentetic acid effectively reduces the  $T_1$  relaxation already at 0.3 mM/L concentration (recommended dose of manufacturer is 0.6 mM/L), and CA gadobutrol effectively reduces the  $T_1$  relaxation already at 0.2 mM/L concentration (recommended dose of manufacturer 0.6 mM/L). Based on the results of experiment it is clear that in the field of 0.06 T diagnostic is no less effective with lower concentrations than the manufacturer recommends to use. Also these results of study allow to reduce the dosage of CA while maintaining acceptable diagnostic quality.

On the basis of this algorithm doses of CA can be optimized in other magnetic fields. In addition, measurements carried out on industrial samples also allows us to create an algorithm for optimization of dosages of new CA (as noted above) or dosages of complexes of registered CA with glucose.

1. Bernstein M., King K., Zhou X.: Handbook of MRI Pulse Sequences. Elsevier Academic Press, 2004.

## TR EPR Investigation of Excited State Anthraquinone/TEMPO Radical Complexes

*A. A. Obynochny<sup>1</sup>, A. A. Sukhanov<sup>1</sup>, V. R. Gorelik<sup>2</sup>, and V. F. Tarasov<sup>3</sup>*

<sup>1</sup> *Zavoisky Physical-Technical Institute, Russian Academy of Sciences, Kazan 420029, Russian Federation, aobynoch@mail.ru*

<sup>2</sup> *International Tomography Center SB RAS, Novosibirsk 630090, Russian Federation, vit@tomo.nsc.ru*

<sup>3</sup> *Semenov Institute of Chemical Physics RAS, Moscow 119991, Russian Federation, spinchem@chph.ras.ru*

Multispin systems are of particular interest for the development of multifunctional molecular magnetic materials, particularly those that are switchable between paramagnetic and ferromagnetic states [1], and the construction of molecular devices designed to transform and store light energy [2]. Typically, these systems are comprised of a chromophore bind through a spacer or directly to a paramagnetic unit. There are a few examples in the literature where the chromophore (molecular triplet) and paramagnetic centers are not bonded at all or create very weak complexes in aromatic solvents. One of such an example is the quinones and nitroxide radicals in low temperature toluene glasses [3].

Despite on the apparent simplicity of the latter the TR EPR spectra of their electronically excited states still need interpretation. Indeed, in many cases the TR EPR spectra of polarized nitroxide radicals are almost identical to the

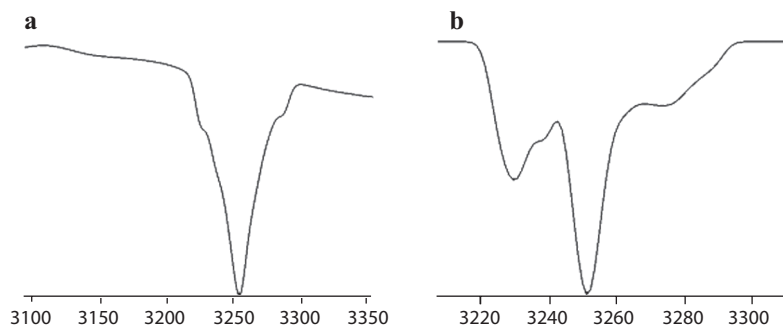


**Fig. 1.** Results of computation of the X-band TR EPR spectra of the system comprised of excited molecular triplet state and nitroxide radical TEMPO.

radicals with the electron spin in Boltzmann equilibrium. The only difference is that the polarized radical is in emissive mode (Fig. 1a). However, in the other systems (for instance anthraquinone/TEMPO) emissive single signal dominates the spectral pattern (Fig. 1a). Both the nature and the way of creation of this signal are still unclear.

In this work, the computational model which has been suggested in [3] is modified with the aim to calculate not only the TR EPR spectra of the nitroxide radicals resulted in dissociation or relaxation of the complex but the TR EPR spectra of the spin quartet and doublet electronically excited states of complexes. Using this model we found out that nitroxide radical can be polarized in emissive mod (as is shown in Fig. 1b) only if the exchange interaction between the excited triplet of chromofore and a radical is comparable with the zero-field-splitting (ZFS) in the triplet. The single emissive signal can be generated only for systems with a weak ZFS, tenfold smaller than that in the triplet state of chromofore. That suggests that nitroxide radical is likely to interact with the sandwich structure comprised of two chromofore molecules. Otherwise, there are chemical processes resulting to this observation.

The work was supported by Foundation for Basic Research (grant 10-03-00791).

1. Teki Y., Tamekuni H., Haruta K., Takeuchi J., Miura Y.: *J. Mater. Chem.* **18**, 381 (2008)
2. Dance Z.E.X., Ahrens M.J., Vega A.M., Ricks A.B., McCamant D.W., Ratner H.A., Wasielewski M.R.: *J. Am. Chem. Soc.* **130**, 830 (2008)
3. Tarasov V.F., Shkrob I.A., Trifunac A.D.: *J. Phys. Chem. A* **106**, 4838 (2002)

## Spin-Crossover Fe(III) Complexes with Light-Sensitive Properties

*I. V. Ovchinnikov, T. A. Ivanova, O. A. Turanova, and G. I. Ivanova*

*Zavoisky Physical-Technical Institute, Russian Academy of Sciences, Kazan 420029,  
Russian Federation*

At present time photomagnetism of monomolecular [1] and cluster [2] system is one of the most attractive and rapidly developing areas of photomagnetism. Particular interest is to study the spin-crossover complexes with  $3d^5$  (Fe III) and  $3d^6$  (Fe II) electronic configuration, spin state of which  $S = 1/2 \leftrightarrow S = 5/2$  or  $S = 0 \leftrightarrow S = 2$  is influenced by temperature and/or photo-irradiation.

In the presented work the spin-transition properties of the synthesized compounds  $[\text{Fe}(\text{salten-R})\text{L}]\text{BPh}_4$ , (L = py, stpy, stpy12, mepepy) and the possibility of changing their spin-state under light irradiation were studied by EPR. Fe(III) ions are coordinated by pentadentate  $\text{N}_3\text{O}_2$  ligands ( $\text{H}_2\text{salten-R}$ , R = H;  $\text{OC}_{18}\text{H}_{37}$ ). The reason in the using of ligand with R =  $\text{OC}_{18}\text{H}_{37}$  is the potential possibility to produce liquid-crystal properties of compound. EPR measurements were performed at X-band at temperatures (5–300) K. The incomplete spin transition from the high ( $S = 5/2$ ) to the low-spin ( $S = 1/2$ ) state in the range (300–130) K is observed in all the powdered compounds. It is manifested in the decrease of the integral intensity of the EPR signal from the high-spin states with decreasing temperature. The thermodynamic parameters of the spin transition:  $T_c = 250$  K; the enthalpy change  $\Delta H = 8.310 \text{ kJ} \cdot \text{K}^{-1} \cdot \text{mol}^{-1}$ , the entropy change  $\Delta S = 33.24 \text{ J} \cdot \text{K}^{-1} \cdot \text{mol}^{-1}$ , and the residual content of high-spin fraction  $r = 0.15$  are determined. The transition parameters do not change (within experimental error) with the insertion of long alkyl substituents and with changing of light-sensitive ligand.

A decrease of the integral intensity of high-spin signal after laser irradiation with  $\lambda = 522 \text{ nm}$  is observed in the EPR spectra of powdered compounds. It is interpreted as the transition (8–13)% of high-spin complexes to low-spin one in accordance to the number of exposed complexes at the used irradiation technique. The signal intensity is restored in about 5 minutes after discontinue irradiation. The effect is observed in very wide temperature interval and demand threshold value of excitation power density. This effect in solid state differs from LIESST (light induced excited-spin-state trapping) phenomenon well known for many spin-crossover Fe complexes. We are going to use the additional investigation methods to understand the features of observed effect.

1. Venkataramani S., Jana U. *et al.*: Science 445 (2011)
2. Ohkoshi S., Imoto K. *et al.*: Nature Chem. DOI: 10.1038/NCHEM,1067 (2011)

## **$^{19}\text{F}$ NMR and Local Fields in Double Rare-Earth Fluoride $\text{LiTbF}_4$**

*I. V. Romanova, A. V. Egorov, S. L. Korableva, and M. S. Tagirov*

*Kazan Federal University, Kazan 420008, Russian Federation, Irina.Choustova@ksu.ru*

Double lithium rare-earth fluorides crystallizing in the tetragonal scheelite ( $\text{CaWO}_4$ ) structure ( $C_{4h}^6$ ) attract much attention as model objects in physics of magnetism.  $\text{LiTbF}_4$  is dipolar Ising-like ferromagnet ( $T_C = 2.89$  K) [1]. Single crystal of  $\text{LiTbF}_4$  was grown using Bridgeman-Stockbarger method. After crystallographic axes definition by using X-ray diffractometer, it was shaped as a sphere to obtain the homogeneous demagnetizing field. The angular dependences of  $^{19}\text{F}$  NMR spectra have been obtained in the external magnetic field oriented in the basis plane of  $\text{LiTbF}_4$  by using homebuilt CW NMR spectrometer with a frequency sweep. Taking into account magnetic dipole-dipole interactions between the rare-earth ions and the fluorine nuclei and introducing, similarly to ref. [2], additional superhyperfine interactions, we have simulated the angular dependence of the  $^{19}\text{F}$  NMR spectrum which is in excellent agreement with the experimental data.

We present a corrected set of transferred hyperfine interaction constants for  $\text{LiTbF}_4$ . Diagonal components of this tensor are similar, but the nondiagonal component is much larger than the corresponding parameters in ref. [2]. The corrected set of crystal field parameters for the  $\text{Tb}^{3+}$  ions in  $\text{LiTbF}_4$  used in our calculations of the local magnetic fields was checked by the analysis of the previously published data [3] on the  $\text{LiTbF}_4$  magnetization in high magnetic fields directed along and normal to the crystal  $c$ -axis.

1. Aminov L.K., Malkin B.Z., Teplov M.A.: Handbook on the Physics and Chemistry of Rare Earths, vol. 22. North-Holland, Amsterdam, 1996.
2. Hansen P.E., NevaldR.: Phys. Rev. B **16**, 146 (1977)
3. Kazei Z.A., Snegirev V.V., Abdulsabirov R.Yu., Korableva S.L. *et al.*: 34 Conference on Low Temperature Physics, Proceedings, part 1, p. 13, 2006.

## EPR and Luminescence of $\text{Li}_2\text{Zn}_2(\text{MoO}_4)_3$ Crystals Doped with Transition Metal Ions

*A. A. Ryadun<sup>1</sup>, V. A. Nadoliny<sup>1</sup>, and A. A. Pavluk<sup>1</sup>*

*Nikolaev Institute of Inorganic Chemistry SB RAS, Novosibirsk 630090, Russian Federation, dosca@yandex.ru*

Scintillation materials attract research interest due to extensive application in medicine, nuclear research, and space programs [1]. One of the most promising scintillation materials is  $\text{Li}_2\text{Zn}_2(\text{MoO}_4)_3$  double molybdate crystals.  $\text{Li}_2\text{Zn}_2(\text{MoO}_4)_3$  began to attract interest because of its possible application in experiments on search for rare events, such as double beta decay or interaction with dark matter particles. In recent years there have appeared some publications about growing and studying properties of  $\text{Li}_2\text{Zn}_2(\text{MoO}_4)_3$  double molybdate crystals. Correctly chosen conditions of  $\text{Li}_2\text{Zn}_2(\text{MoO}_4)_3$  crystal growth allowed us to grow large optically homogeneous and virtually stoichiometric both pure and activated by different transition metal ions (Cu, Cr, Fe, Ti) crystals by the low-gradient Czochralski method (Fig. 1) [2]. The conducted studies of  $\text{Li}_2\text{Zn}_2(\text{MoO}_4)_3$  by EPR spectroscopy allowed us to determine the charge state and lattice location for Cu, Fe, Cr ions. Investigation of luminescence shown that the luminescence with very short lifetimes is observed for pure crystals at room temperature ( $\lambda = 388 \text{ nm}$ ,  $\tau_1 = 2 \text{ ns}$  and  $\tau_2 = 6 \text{ ns}$ ). The

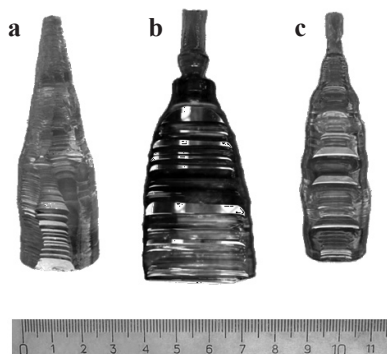


**Fig. 1.** Appearance and the color of the crystals (**a** pure, **b** 0.03%  $\text{Cu}^{2+}$ , **c** 0.01%  $\text{Cr}^{3+}$ ).

luminescence with  $\lambda = 560$  nm and lifetime  $\tau = 100$  ns is observed both for pure and for activated by transition metal ions crystals at 77 K. Besides, the luminescence intensity with  $\lambda = 560$  nm depends on nature and concentration of transition metal ions. It is assumed that low-temperature luminescence is accounted for by cationic vacancies providing charge compensation of transition metals ions.

1. Globus M., Grinyov B., Jong Kyung Kim: Inorganic Scintillators for Modern and Traditional Applications. Institute For Single Crystals, Kharkiv (Ukraine), 2005.
2. Pavlyuk A.A., Vasiliev Ya.V., Kharchenko L.Yu., Kuznetsov F.A.: Proceedings of the Asia Pacific Society for Advanced Materials APSAM-92. Shanghai, 1992.

## EPR Spectra and Quantum Chemistry Calculations of Structure and Magnetic Resonance Parameters of Methylsubstituted Radical Cations

*L. I. Savostina<sup>1</sup>, G. M. Zhidomirov<sup>2</sup>, M. Ya. Mel'nikov<sup>2</sup>, and I. D. Sorokin<sup>2</sup>*

<sup>1</sup> *Zavoisky Physical-Technical Institute, Russian Academy of Sciences, Kazan 420029, Russian Federation, savostina@mail.knc.ru*

<sup>2</sup> *Lomonosov Moscow State University, Moscow 119991, Russian Federation*

Radicals and radical cations are important intermediates, they are able to engage in the photochemistry reactions and influence the direction and efficiency of chemical processes.

The EPR spectra of four-membered rings trimethylene oxide ( $C_3H_6O^+$ -TMO) (Fig. 1a), trimethylene sulfide ( $C_3H_6S^+$ -TMS) (Fig. 1b) and azetidine radical cation ( $C_3H_6NH^+$ ) (Fig. 1c) were measured. Quantum-chemical calculations of geometries and the hyperfine structure of generated paramagnet-

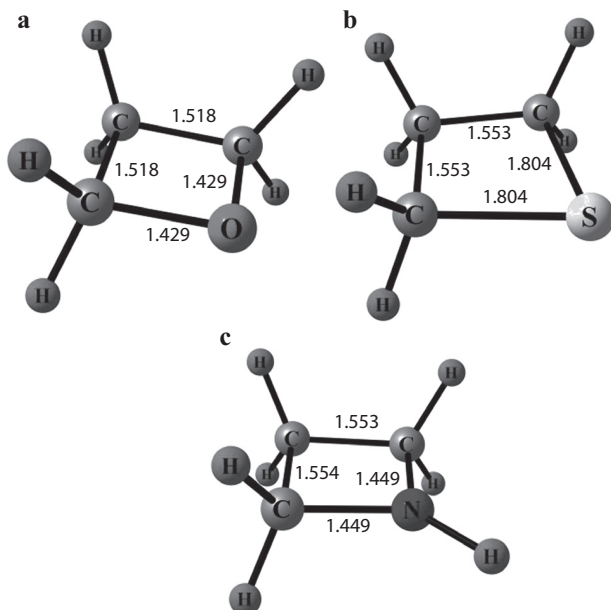


**Fig. 1.** Structure of trimethylene oxide (a), trimethylene sulfide (b) and azetidine (c) radical cation.

**Table 1.** Experimental and calculated values of isotropic HFC constants\* (mT) for the TMO, TMS and azetidine.

	TMO		TMS		Azetidine			N 	⊥	iso
	β-CH <sub>2</sub> (mT)	γ-CH <sub>2</sub> (mT)	β-CH <sub>2</sub> (mT)	γ-CH <sub>2</sub> (mT)	β-CH <sub>2</sub> (mT)	H (NH) (mT)				
Exp. 2. (for azetidine*)	6.5	1.15	3.2	1.2	5.38	2.27	5.45	0.8	2.35	
Calculation in 2. PBE/Λ22 (Priroda)	6.91	1.28	3.45	0.46	–	–	–	–	–	
B3LYP/IGLO-III (PBE/TZVP – for TMS) (ORCA)	6.79	1.26	3.9	1.26	5.81	1.97	4.29	0.02	1.43	
PBE0/cc-pCVTZ (ORCA)	6.58	1.15	3.5	0.2	5.63	2.1	4.26	0.1	1.35	
B3LYP/EPR-III (6-311G** – for TMS) (ORCA)	7.16	1.33	3.4	0.25	6.11	2.15	4.3	0.02	1.44	

\* Data of this paper.

ic species were performed by the functional density theory using the hybrid functional PBE and B3LYP. 6-311G\*\*, TZVP, cc-pCVTZ, EPR-III, IGLO-III basis sets were used for calculation. The calculations were performed with the ORCA program [1].

The geometry of the radical cations and neutral molecules of trimethylene oxide and trimethylene sulfide was found to be planar, while azetidine radical cation also was found to be planar, but NH-group of the neutral molecules of azetidine have angle of 18–20' relative to the plane of the ring.

Hyperfine coupling constants (HFC) were also calculated using the DFT method. It was shown in Table 1 that good agreement calculation data with experimental data was observed for calculation using the hybrid functional PBE0 and cc-pCVTZ basis set.

The financial support of the Foundation for Basic Research (grant 10-03-90743) and Leading Scientific Schools (SC-6267.2010.2) is gratefully acknowledged.

1. Petrenko T., Krylova O., Neese F., Sokolowski M.: *New J. Phys.* **11**, 015001 (2009)
2. Mel'nikov M.Ya., Kalugina A.D., Mel'nikova O.L., Pergushov V.I., Tyurin D.A.: *High Energy Chemistry.* **43**, 303 (2009)

## Investigations of $\text{La}_{1-x}\text{Sr}_x\text{Mn}_{0.925}\text{Zn}_{0.075}\text{O}_3$ ( $x = 0.075; 0.095; 0.115$ ) Ceramics

*K. R. Sharipov<sup>1</sup>, R. M. Eremina<sup>1</sup>, L. V. Mingalieva<sup>1</sup>, I. A. Fayzrahmanov<sup>1</sup>,  
A. G. Badelin<sup>2</sup>, and A. V. Evseeva<sup>2</sup>*

<sup>1</sup> *Zavoisky Physical-Technical Institute, Russian Academy of Sciences, Kazan 420029,  
Russian Federation, shakamr@yandex.ru*

<sup>2</sup> *Astrakhan State University, Astrakhan 414025, Russian Federation, alexey\_badelin@mail.ru*

Materials with colossal magnetoresistance (CMR) have attracted special attention because of the large collection of exotic and fundamental physical and chemical properties [1]. The choice of zinc as a doping element for these materials was stimulated by the fact that a zinc-doped manganites have been found interesting voltage characteristics which contain regions with negative differential resistance of N-type [2]. The compositions of samples of  $\text{La}_{1-x}\text{Sr}_x\text{Mn}_{0.925}\text{Zn}_{0.075}\text{O}_3$  ( $x = 0.075; 0.095; 0.115$ ) were chosen because the total concentration of divalent ions of strontium and zinc ( $x + 0.075$ ) =  $c$  is near

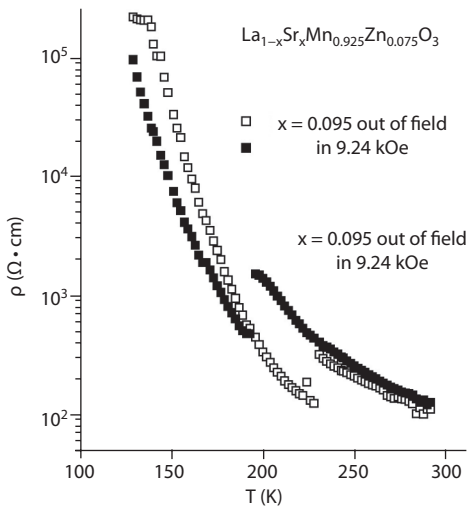


**Fig. 1.** Temperature dependence of resistivity of  $\text{La}_{1-x}\text{Sr}_x\text{Mn}_{0.925}\text{Zn}_{0.075}\text{O}_3$  compound.

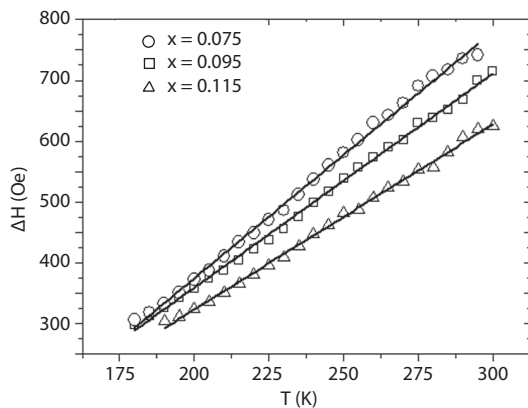


**Fig. 2.** Temperature dependence of the ESR linewidth of  $\text{La}_{1-x}\text{Sr}_x\text{Mn}_{0.925}\text{Zn}_{0.075}\text{O}_3$  ( $x = 0.075$  – circles,  $x = 0.095$  – squares,  $x = 0.115$  – triangles) ceramics.

the boundary “orthorhombic-rhombohedral structure” on both sides of it in the phase diagram of pure lanthanum-strontium manganite  $\text{La}_{1-x}\text{Sr}_x\text{MnO}_3$  [3].

The measurements of conductivity of the  $\text{La}_{1-x}\text{Sr}_x\text{Mn}_{0.925}\text{Zn}_{0.075}\text{O}_3$  ( $x = 0.075$ ;  $0.095$ ;  $0.115$ ) ceramics were carried with a certified X-ray method of crystal structure. It is established that is observed dependence of the resistivity from the magnetic field at  $x = 0.095$  in the temperature range from 190 to 228 K (Fig. 1). We connected this behavior to the Maxwell-Wagner effect [4, 5]. Similar behavior was not observed for samples with  $x = 0.075$ ;  $0.115$ .

EPR spectrum of  $\text{La}_{1-x}\text{Sr}_x\text{Mn}_{0.925}\text{Zn}_{0.075}\text{O}_3$  ( $x = 0.075$ ;  $0.095$ ;  $0.115$ ) contains a single line at  $g \approx 1.978 \pm 0.005$ , due to manganese ions. ESR linewidths were linearly increased with increasing temperature from 180 to 380 K for all samples, the slope decreases with increasing strontium concentration (Fig. 2).

1. Dagotto E., Hotta T., Moreo F.: *Physics Reports* **344**, 1–153 (2001)
2. Karpasyuk V.K., Badelin A.G., Smirnov A.M., Sorokin V.V., Evseeva A., Doyutova E., Shchepetkin A.A.: *Journal of Physics: Conf. Series* **200**, 052026 (2010)
3. Urushibara A., Moritomo Y., Arima T., Asamitsu A., Kido G., Tokura Y.: *Phys. Rev. B* **51**, 14103 (1995)
4. Senis R., Balcells L., Laukhin V., Martinez B., Fontcuberta J., Pinsard L., Revcolevschi A.: *J. Appl. Phys.* **87**, 5609 (2000)
5. Janhavi P. Joshi, Bhat S.V.: *Journal of Magnetic Resonance* **168**, 284 (2004)

## EPR Investigation of the Fe<sup>III</sup>Dy<sup>III</sup> Coordination Clusters

*A. Sukhanov<sup>1</sup>, V. Voronkova<sup>1</sup>, A. Baniodeh<sup>2</sup>, G. Novitchi<sup>2,3</sup>, and A. K. Powell<sup>2</sup>*

<sup>1</sup> *Zavoisky Physical-Technical Institute, Russian Academy of Sciences, Kazan 420029, Russian Federation, ansukhanov@mail.ru*

<sup>2</sup> *Institute of Inorganic Chemistry, Karlsruhe Institute of Technology, University of Karlsruhe, Karlsruhe 76131, Germany*

<sup>3</sup> *Institute of Chemistry, Academy of Sciences of Moldova, Chisinau MD-2028, Moldova*

The design of single-molecule magnets (SMMs) has become a hot area of research due to the potential applications of such compounds in new storage and information-processing technologies [1, 2]. Coordination complexes built up of transition metal and rare-earth ions have recently attracted much attention in the field of molecular magnetism. Indeed, high magnetic anisotropy of many rare-earth ions may hold the key the magnetic anisotropy of mixed clusters to obtain new SMMs [3].

Recently, a new series of compounds built up of similar Fe<sup>III</sup>Dy<sup>III</sup> clusters has been synthesized and studied using Mössbauer spectroscopy [4]. It was shown that ligand substitution in this series of compounds influences the direction of the magnetic anisotropy of Dy ions. We here present a study of these clusters by EPR. The aim of this study is to obtain information about spin-spin interactions and ground and excited spin states in these clusters. The EPR spectra were measured on a Bruker *EMX/plus* spectrometer equipped ER4102ST X-band resonator and a 4116DM dual mode resonator. We carried out measurements of the temperature dependence of EPR spectra of polycrystalline samples from 4 to 290 K. The observed differences of the EPR spectra were analyzed on the basis of the simulated spectra and data obtained by Mössbauer spectroscopy.

1. Caneschi A., Gatteschi D., Sessoli R.: *J. Am. Chem. Soc.* 113 (1991)
2. Affronte M., Troiani F., Ghirri A.: *J. Phys. D* **40**, 2999 (2007)
3. Ishikawa N.: *Struct Bond* **135**, 211 (2010)
4. Mereacre V., Baniodeh A.: *J. Am. Chem. Soc.*, DOI: 10.1021/ja206941e (2011)

## Structure and Magnetic Properties of Chromium Impurity Ions as Studied by Multifrequency EPR

V. Tarasov<sup>1</sup>, D. Akhmetzyanov<sup>1</sup>, A. Konovalov<sup>1</sup>, E. Zhiteitcev<sup>1</sup>, and E. Zharikov<sup>2,3</sup>

<sup>1</sup> *Zavoisky Physical-Technical Institute, Russian Academy of Sciences, Kazan 420029, Russian Federation, phys-tech@kfti.rnc.ru*

<sup>2</sup> *Laser Materials and Technology Research Centre, General Physics Institute of RAS, Moscow, Russian Federation, postmaster@gpi.ru*

<sup>3</sup> *D. I. Mendeleev University of Chemical Technology of Russia, Moscow 125047, Russian Federation, rector@muctr.ru*

Impurity chromium ions in synthetic forsterite are thoroughly studied in connection with the high efficient laser generation of Cr<sup>4+</sup> ion in forsterite. But chromium impurity ions in synthetic forsterite form several types of impurity centers, differing in their charge condition (Cr<sup>2+</sup>, Cr<sup>3+</sup> and Cr<sup>4+</sup>) and localization in the forsterite crystal lattice. Relative concentration of different chromium centers depends of various factors. The aim of report is to present our results in study of structure and magnetic properties of chromium ions in forsterite by means of multifrequency EPR spectroscopy. Measurements were carried out in the frequency region 9-300 GHz on Varian E-12 X-band spectrometer and frequency tunable broad band spectrometer with BWO oscillators as sources of microwave radiation. We studied dependence of relative concentration of various chromium impurity centers on co-doping chromium-forsterite samples by lithium, on concentration of oxygen in atmosphere during the crystal grows, on ionizing irradiation.

It was established that essential part of chromium ions substitute Mg<sup>2+</sup> crystal positions in the form of divalent ions. Trivalent chromium reveal strong tendency to dimer self-organization. As a result, concentration of Cr<sup>3+</sup> dimmers is several order higher than it may be expected under statistical distribution of chromium ions in forsterite crystal lattice. Crystal/melt distribution coefficient for Cr<sup>4+</sup> ions increases noticeably with content of oxygen in the atmosphere during the crystal growth increasing from 0.03 to 0.23 vol. %.

The work was partly supported by Russian Foundation for Basic Research (grant 09-07-97006) and the grant of the President of the Russian Federation NSh-6267.2010.2

## Unambiguous Determination of Spin-Hamiltonian Parameters of Low Symmetry Paramagnetic Centers with $S_{\text{eff}} \geq 2$

*V. A. Ulanov<sup>1,2</sup>, I. M. Safarov<sup>1</sup>, M. M. Zaripov<sup>2</sup>, and G. S. Shakurov<sup>2</sup>*

<sup>1</sup> *Industrial Electronics Department, Kazan State Power Engineering University, Kazan 42066, Russian Federation, ulvlad@inbox.ru*

<sup>2</sup> *Zavoisky Physical-Technical Institute, Russian Academy of Sciences, Kazan 420029, Russian Federation*

At present, electron paramagnetic resonance method has become a widely used powerful experimental tool with applications in many areas of physics, chemistry, biology, and so on. Usually, due to the spin-Hamiltonian approach the experimental results can be represented by spin-Hamiltonian parameters and “effective” electron spin momentum  $S_{\text{eff}}$ . In most cases the investigators use the EPR spectrometers that can be tuned in a narrow frequency band (X- or Q-band). These spectrometers are very good, one by one, in the cases of paramagnetic objects with a non-integer  $S_{\text{eff}} \leq 3/2$ . But sometimes, the paramagnetic object studied by EPR method must be characterized by  $S_{\text{eff}} \geq 2$ . When symmetry of the crystal field acting in position of such a paramagnetic object is rather low the number of spin-Hamiltonian parameters become large. Moreover, in such cases energy levels of the lowest spin multiplet, characterized by  $S_{\text{eff}}$ , are splitted and energy intervals between these levels become greater than electromagnetic quantum in the cavity of an EPR spectrometer. In the latest case an investigator must use high-frequency EPR spectrometer. It must be noted that in the case  $S_{\text{eff}} \geq 2$  a narrow band EPR spectrometer do not allow determining all spin-Hamiltonian parameters; one can find only some non-linear combinations of these parameters [1].

In this work we have examined the problem in the unambiguous determination of spin-Hamiltonian parameters of the paramagnetic centers with  $S_{\text{eff}} \geq 2$  embedded in the ionic crystals. The experimental results on  $\text{Cr}^{2+}$ ,  $\text{Fe}^{3+}$  and  $\text{Ni}^{3+}$ - $\text{Ni}^+$  centers in the fluorite type crystals were considered as examples. It was found that the unambiguous determination of spin-Hamiltonian parameters could be possible only with the wide-band tunable EPR spectrometer.

1. Abragam A., Bleaney B.: Electron Paramagnetic Resonance of Transition Ions. Clarendon, Oxford, 1970.

## Optically Detected ESR of Radical Ion Pairs Induced by Vacuum Ultraviolet

*V. N. Verkhovlyuk and O. A. Anisimov*

*Institute of Chemical Kinetics and Combustion SB RAS, Novosibirsk 630090,  
Russian Federation, v\_ver@kinetics.nsc.ru*

Optically Detected ESR (ODESR) spectroscopy is one of the powerful and informative methods to study mechanisms of chemical reactions, since most of them proceed through radical ion stage. This method was created in 1980<sup>th</sup> in Novosibirsk and allowed to greatly raise (several orders of magnitude in comparison with ordinary ESR) sensitivity of registration of the ESR spectra for short lived organic radical cations and anions in liquid solutions. Investigations using ODESR allowed obtaining much new information about liquid phase reaction with radical ions involved in, but more wide application of the method has been restrained by relatively low spectral resolution (about 0.1 mT) for ODESR signals of radical ions.

Such resolution is limited not by apparatus reasons, but rather by the used method of generation of radical ion pairs (X-rays). In this case every act of energy absorption is accompanied by formation of multiple primary radical ion pairs (radiation track). Most of these pairs are in the neighborhood of another pairs or products of their transformation (often paramagnetic). This leads to spin-spin interaction in the pairs and, hence, to broadening of ESR spectrum lines. To avoid the appearance of dense radiation track one can use photochemical method of pair generation. One such method is vacuum ultraviolet radiation (VUV). Here, the energy of the quantum is slightly more than the ionization potential of the solvent molecule (typical value is about 10 eV for alkanes), and each quantum generates only one radical pair, therefore this generation method is free from appearance of dense tracks and can be very perspective for registration of ODESR spectra. By this moment a working version of set up for observation of ODESR spectra of radical ions under VUV was created. A modification to operating ODESR spectrometer, which allows changing irradiation source from X-ray tube to deuterium lamp Hamamatsu L7293-50 on-the-fly was designed and implemented. The VUV source radiates in the range from 115 to 400 nm (quantum energy from 10.7 to 3 eV). Using interference filter with maximum of transmission at 119 nm (10.4 eV), the first ODESR spectra for liquid non polar solutions under vacuum ultraviolet radiation were obtained.

The work was supported by Foundation for Basic Research (grant 11-03-00550-a).

## Application to the Electron Spins of Pulse Sequences Designed for the Nuclear Spins

*M. Volkov and K. M. Salikhov*

*Zavoisky Physical-Technical Institute, Russian Academy of Sciences, Kazan 420029,  
Russian Federation, mihael-volkov@rambler.ru, salikhov@kfti.knc.ru*

Until now, the world is searching for physical systems, which could become a base element for quantum computation. As qubits can be used, for example, nuclear or electron spins equal to  $1/2$ . Particle with spin  $1/2$  in magnetic field has two energy levels: unexcited and excited. These are referred to as the qubit state  $|0\rangle$  and  $|1\rangle$ , respectively. In the systems of nuclear spins has been realized many quantum algorithms because methods of managing the dynamics of spins and the registration of their states are very well developed in the pulse NMR spectroscopy. In addition, the systems of nuclear spins usually have relatively long relaxation times, which allow us to implement during them a large number of logical operations. But, unfortunately, as a result of these studies it was found that nuclear spins are not suitable for use in quantum computers, because they have sufficiently long durations of execution of single logical operations. This is related to the fact that the constants of interaction of nuclear spins with each other are small and amount to tens or hundreds of hertz. As a result, in case of using nuclear spins as qubits the duration of the single logical operations less than a few milliseconds can not be achieved. At the same time constants of the interaction of electron spins with each other or with nuclear spins amount to tens or hundreds of megahertz, so they have much greater prospects for their use as qubits, rather than nuclear spins. However, pulse sequences, which are designed for use in nuclear-spin quantum logic operations, are carried out reliably, so it would be wise to use that experience in order to implement quantum logic operations on electron spins. Our goal consisted to find out how effective pulse sequences, which are successfully implemented on the nuclear spins, implement quantum logic operations in systems of electron spins.

In order to implement any quantum algorithm, it is enough to be able to implement the two logical gates: NOT and CNOT, because they are universal logical gates, that is, any quantum algorithm can be implemented by them [1]. The logical gate NOT realizes an inversion of the qubit state. The implementation of the logic gate NOT is simple because it affects only on one spin and can be realized by turn of a spin on 180 degree using radiofrequency pulse.

The controlled-NOT gate (called CNOT gate) consists in what if the first qubit (control qubit) is in some defined state (for example, one), then the second qubit will be inverted, but if the first qubit is in another state, then the second qubit will not be changed. To implement the CNOT gate is more complicated because it required the presence of two spins, with the existence of some interaction between them. In this connection the implementation of the logical gate CNOT is particular interest to us.

In this work were performed the calculations of functioning of pulse sequences which were designed for nuclear spins in case of using electron spins as qubits. As a result of these calculations we found out that systems with two electron spins, in which the modulus of the ratio of their interaction constant with each other to the difference of their frequencies is less than one-quarter are promising for the implementation of quantum algorithms on them, because in this case the difference between the states which are obtained after application the pulse sequences realizing the preparation a two spin system in a pseudo pure states and implementation of the quantum logic gate CNOT are small enough.

In addition, we found the consequence of the existence of the hyperfine interaction. For this purpose we have chosen as a two electron spin system a symmetric stable TEMPO biradical. The entire spin ensemble is divided into nine subensembles, which differ from each other in first and second frequencies of the spins. In the first three of these the frequencies of the both spins are equal, but the remaining six subensemble have the different frequencies of spins. During the implementation of the pulse sequences we apply pulses, intended for the first spin at a frequency of one component of the hyperfine structure, and pulses, intended for a second spin on the frequency of the other components of the hyperfine structure.

The results of the calculations showed us that the presence of the hyperfine interaction leads to a shift of the line phases of the second spin, so that we can not unambiguously determine the state of the controlled qubit after the action of the quantum logic gate CNOT. Therefore it is desirable to use unsymmetric biradical instead of the symmetric biradical, such as, for example, BDPA-TEMPO biradical [2], in which it is necessary to replace the nuclei of atoms of nitrogen  $^{14}\text{N}$  by nuclei  $^{15}\text{N}$  having a nuclear spin equal  $\frac{1}{2}$ .

1. Barenco A., Bennett C.H., Cleve R., DiVincenzo D.P., Margolus N., Shor P., Sleator T., Smolin J.A., Weinfurter H.: *Phys. Rev. A* **52**, 3457 (1995)
2. Dane E.L., Maly T., Debelouchina G.T., Griffin R.G., Swager T.M.: *Org. Lett.* **11**, 1871 (2009)

## ESR of P-Containing Substances in Electrochemistry and Biology

*B. G. Yavishev*

*Kazan Branch, International Forum of Scientists and Experts, Kazan, Russian Federation*

In the capacity of coordinated active additives in En-electrolyte were investigated N, O and P-containing substances. Electrochemical researches have shown complexing function of En in the presence of pyrophosphate (Py) is strongly blocked. ESR spectra reflecting processes of a complex formation in (Py+En) electrolyte in a cell and in model solutions had hyperfine structure (HFS) corresponding to both Py and En complexes, i.e., there was a mixture of these complexes. NMR data of these complexes have confirmed existence of both types. However, differences of HFS of Py and En complexes in a mixture and individual solutions and also increasing out of plane  $\pi$ -coupling allow one to consider that in an axial position is coordinated Py in case of En complex of Cu (II) and En in case of Py complex, plane  $\sigma$ -coupling is weakened. The high stability of Py complexes of Cu (II) indicates the formation of understressed ( $6-8^\circ$ ) four-term cycle in which the copper ion coordinates two atoms of O-of P-group. The ligand field has tetragonal symmetry. These circumstances explain formation and existence of Py complexes of Cu(II) at presence coordinated active En. Detected anomalously high activity of P-containing electrolytes with respect to N- and O-containing ones it is represented important at comparison:

- 1) with analysis of the role of P in structures of DNA and RNA – phosphonic acid is the joining bridge between nucleotides, and breakages and the subsequent connections in their threads occur only in these bridges (it causes mutations);
- 2) the role of P in cell energetic at splitting ATP to ADP and AMP in mitochondria.

## Magnetic Resonance of Crystalline Nanoparticles in Nervous Tissue of Snail

*S. V. Yurtaeva*<sup>1</sup>, *V. N. Efimov*<sup>1,3</sup>, *V. S. Iydin*<sup>2</sup>, *Kh. L. Gainutdinov*<sup>4</sup>,  
and *G. G. Jafarova*<sup>4</sup>

<sup>1</sup> *Laboratory of Molecular Radiospectroscopy, Zavoisky Physical-Technical Institute, Russian Academy of Sciences, Kazan 420029, Russian Federation, yurtaeva@mail.knc.ru*

<sup>2</sup> *Laboratory of Spin Physics and Spin Chemistry, Zavoisky Physical-Technical Institute, Russian Academy of Sciences, Kazan 420029, Russian Federation,*

<sup>3</sup> *Institute of Physics of Kazan, Federal University, Kazan 420008, Russian Federation, vefimov.51@mail.ru*

<sup>4</sup> *Laboratory of Biophysics, Zavoisky Physical-Technical Institute, Russian Academy of Sciences, Kazan 420029, Russian Federation, gainutdinov@mail.knc.ru*

Nowadays it is known about the biogenic nanoscaled magnetite crystals, localized in human and animal brain tissues [1]. It is also discussed the hypotheses

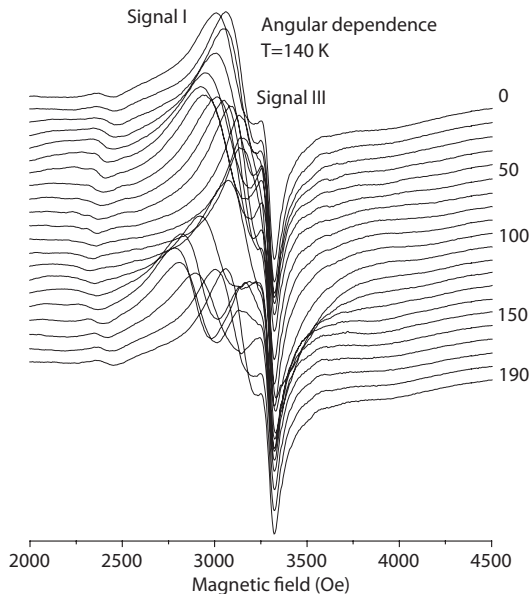


**Fig. 1.** Angular dependence of MR-spectra of nervous tissue of snail with injected iron.

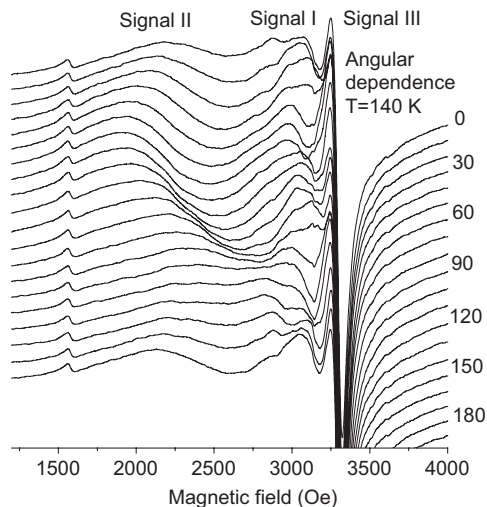


**Fig. 2.** Angular dependence of MR-spectra of nervous tissue of control snail.

that brain magnetite may be a component of the mechanisms of long-term memory [2].

The object of the work was to detect crystal particles in nervous tissue by means of electron magnetic resonance (MR) spectroscopy. As the model biological system we used the nervous system of snail. The hemolymph of snail is the Cu-containing system in which Fe content is low and iron is mainly included in enzymes and may also be accumulated in magnetite nanocrystals.

All the measurements were made on X-band electron paramagnetic resonance (EPR) spectrometer Bruker-EMX. Frozen samples of nerve tissues were investigated: control tissues and nerve tissues with enlarged amount of iron after the injection of iron citrate. The samples were investigated in a wide range of temperatures from room temperature to 4 K using a helium flow cryostat.

By means of MR-spectroscopy ferromagnetic (FMR) signals characterized by the orientation dependence were found in nerve tissue. Signals of three types were detected in MR spectra (Fig.1, 2): two anisotropic FMR signals, corresponding to crystalline particles (called as high field and low field signals I and II accordingly) and EPR signal of  $\text{Cu}^{2+}$  for paramagnetic center of hemo-

cyanin protein which is the main protein in hemolymph of snale (signal III).  $\text{Cu}^{2+}$  signal was isotropic with  $g \approx 2.06$ , it is not discussed in this work.

In this study the angular dependencies (Fig.1, 2) and temperature dependencies of FMR signals I and II were investigated. It was found the existence of two types of crystal particles evidently in isolated form (high field signal I) and in aggregated form (low field signal II).

Temperature behavior of signals I and II was different: in decreasing the temperature the signal I was moving to lower fields but the signal II was still. Both signals are anisotropic with different anisotropic characteristics. That means the magnetic ordering of the particles in nerve tissue along some direction. To identify the signals we investigated also the tissues with enlarged concentration of iron. As a result of injection of additional amount of iron in the system after 24 hours the signal corresponding to isolated particles increased. This fact allows us to suppose that the isolated particles may belong to ferritin nanoparticles with magnetite core. Isolated particles are characterized by the cubic anisotropy (Fig. 1). The similar characteristics were previously detected for magnetite nanoparticles, extracted from insect tissues. Aggregated particles demonstrated the axial anisotropy of resonance field (Fig. 2), and the higher value of anisotropy parameter. The signal of aggregated particles increased within 3 days after a few injections of iron citrate.

The research is supported by grant RFBR № 09-04-97020-p\_Povolzhje\_a.

1. Brik A.B.: Ukr.J. Phys.Opt. **11**, Suppl. 1 S46 (2010)
2. Banachlocha M.A.M., Bokkon I., Banachlocha H.M.: Medical Hypotheses **74**, 254 (2010)

## Magnetic Resonance of Ferritin in Tumor Tissue

S. V. Yurtaeva<sup>1</sup>, V. N. Efimov<sup>1,2</sup>, N. I. Silkin<sup>2</sup>, A. A. Rodionov<sup>2</sup>, M. V. Burmistrov<sup>3</sup>,  
A. V. Panov<sup>3</sup>, and A. A. Moroshek<sup>3</sup>

<sup>1</sup>Laboratory of molecular radiospectroscopy, Zavoisky Physical-Technical Institute, Russian Academy of Sciences, Kazan 420029, Russian Federation, yurtaeva@mail.knc.ru

<sup>2</sup>Kazan Federal University, Kazan 420008, Russian Federation, vefimov.51@mail.ru

<sup>3</sup>Volga Regional Branch of N. N. Blokhin Russian Cancer Scientific Center of RAMS, Kazan, Russian Federation

Ferritin molecules are the unique example of nanoparticles in living nature. They are present in all living creatures from bacteria to mammals and are a universal storage form of iron. Ferritin molecule consists of the protein shell and crystal core inside it. Disregulations in the processes of loading and extraction of iron ions in this molecule can lead to various diseases. Ferritin is of special interest in oncology, because it may be accumulated in some tumors and blood in the case of cancer, but the mechanism of its functioning in tumor is not enough understood. Iron plays an important role in the metabolism of tumor cells. Some studies consider the level of ferritin in blood serum as an indicator of treatment prognosis. The function of ferritin depends on the structure of protein shell and crystal core.

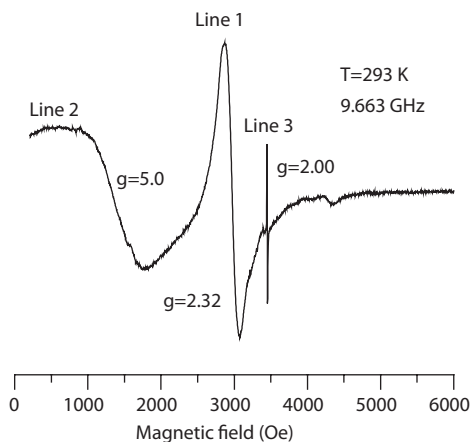


**Fig. 1.** EMR spectrum of tumor after radiation therapy.

One of the methods to detect the magnetic ferritin nanoparticles is the method of electron magnetic resonance (EMR). It is known that for the crystal core of ferritin ferromagnetic resonance (FMR) is observed [1], as the energy is absorbed not by the individual spins of the ions, but by total magnetic moment of the crystal nanoparticle. FMR signals contain the information about the structure, size and magnetic properties of iron-based crystal nanoparticles of ferritin core.

It is known, that in tumors there is the transformation of ferritin shell: synthesis of H-rich ferritins is increased compared to healthy tissues, and such variation of protein shell structure influences the core structure. Consequently, the main objective of this study was to investigate magnetic characteristics and the structure of ferritin crystalline core in tumor by EMR- and to compare the characteristics of spectra of normal and tumor tissues.

Lyophilized samples of malignant human tumors exposed and not exposed to radiation therapy were investigated by means of EMR-spectroscopy. The measurements were taken over the temperature range 4÷280 K at X-band EPR spectrometer Bruker-ESP-300. Three types of lines were detected in samples (Fig. 1): line 1 (linewidth  $\sim 150\text{--}300$  Oe) with  $g \sim 2.1\div 2.4$ , corresponding to the FMR of isolated particles, broad line 2 (linewidth  $\sim 1000$  Oe) with  $g \sim 5$ , corresponding to the FMR of aggregated particles, and a narrow line of free radicals ( $g \approx 2$ ).

FMR signals of isolated iron-based nanoparticles were detected only in the spectra for 25% of the samples despite of the fact of irradiation. The cubic orientational dependence of the signals of isolated particles has been found at the room temperature. To identify the origin of this line temperature dependencies of the resonance spectra were studied. The special features in the temperature dependencies of resonance spectra are observed near the temperature  $\sim 125$  K. They are the jump of line width, achieving the maximum of intensity of magnetic resonance signal and the variation of resonance shift direction with temperature. These features may be character for Verwey phase transition in magnetite. So these particles may be attributed to ferritin protein with the crystal core in the form of magnetite. The obtained characteristics were compared to the resonance characteristics of ferritin in healthy tissues [2]. The temperature dependencies of magnetic resonance characteristics of ferritin in tumors are different from the characteristics of magnetic resonance of ferritin in healthy tissue. The temperature dependencies of magnetic resonance characteristics of ferritin in tumors are different from the characteristics of the magnetic resonance of ferritin in healthy tissue.

In spectra of irradiated tumor tissues low field FMR signals corresponding to aggregates of iron particles were also detected. That may be a manifestation

of enlargement of lysosomes, containing aggregates of ferritin and hemosiderin as a result of radiation therapy. The corresponding FMR signal with  $g \sim 5$  may reflect the destructive effects of irradiation.

This work was partly supported by grant MO № 1.83.11 of the Ministry of Education and Science of Russian Federation.

1. Wainberg E., El-Jaick L.J., Linhares M.P., Esquivel D.M.S.: *J. Magn. Res.* **153**, 69 (2001)
2. Mosiniewicz-Szablewska E., Slawska-Waniewska A., Świątec K., Nedelko N., Galazka-Friedman J., Friedman A.: *Appl. Magn. Res.* **24**, 429 (2003)

## Development of a New Approach to NMR Diagnostics of Malignant Tumors Using the Metal Compounds with Antineoplastic Activity

L. N. Zalyalyutdinova, D. A. Nasybullina, and A. Y. Sabirova

Department of Pharmacology, Kazan State Medical University, Kazan 420012,  
Russian Federation, imanaev@mail.ru

Success in therapy of many diseases, especially oncological, depends directly on well-timed adequate visualization of pathological focus. This problem is successfully solved by magnet resonance imaging (MRI) [1]. In order to improve the quality of image magnet-resonance contrasting agents are studied and used. They contain salts of metals, such as gadolinium, iron, manganese and others. Their disadvantages are multi-factorial. Obviously the most significant of them is absence of organ-specificity. Others include inability to penetrate into the cells, low relaxation, presence of side effects that occur preferably in presence of renal, hepatic and polyorganic failure, as well as development of life-threatening anaphylactic reactions [2–6].

For these reasons development of new approaches to MRI diagnostics of tumors using new compounds, particularly low-toxic amino acid complexes and compositions containing various micronutrients is a matter of great importance. These complexes have high selectivity, high relaxation efficacy and are capable of penetrating through the cytoplasm membrane. The purpose of this study is to develop a new MRI contrast based on low-toxic amino acid complex of lithium, which was synthesized in the laboratory of coordination compounds in Kazan State University (KSU) by A. V. Zakharov, V. G. Shtyrlin *et al.*

We have recently shown that the compound has an antineoplastic activity against transplanted animal tumors, transplanted cell lines of human tumors and tumor cells obtained from cancer patients' biopsies [7]. This and several other compositions of amino acids with metals that have antineoplastic activity, have been patented [8, 9].

Studies were conducted at transplanted solid tumors of experimental animals. In the *ex-vivo* experiments the dynamics of the following parameters was determined: the spin-lattice relaxation time ( $T_1$ ), the spin-spin relaxation time ( $T_2$ ) and diffusion of water molecules coefficient of serum and tumor in the NMR spectrometer "Minispec PC-120", "Bruker", Germany. It was previously shown that the diffusion of water coefficient in plasma of healthy people and

patients with metastatic tumors of various localizations are markedly different. Diffusion of water coefficient in cancer patients is reduced, as compared to healthy volunteers [10]. In animal experiments application of amino acid complex of lithium caused a significant change in the relaxation times and the diffusion of water coefficient in tumors without affecting these parameters in serum.

Thus, a new amino acid complex of lithium may be of great interest for further investigations as a potent low-toxic MRI-contrast.

1. Smith J.R., Brown P.L.: *Phys. Rev. B* **150**, 123 (2004)
2. P.A. Rink: *Magnetic Resonance in Medicine* (Trans. from English by V. E. Sinitsyn), p. 226. GEOTAR, Moscow 2003.
3. Craciunescu O.I., Thrall D.E., Vujaskovic Z., Dewhirst M.W.: *Int J Hyperthermia.* ; 26(7):625-37, 2010.
4. Heidenreich A., Albers P., Classen J., Graefen M., Gschwend J., Kotzerke J., Krege S., Lehmann J., Rohde D., Schmidberger H., Uder M., Zeeb H.; Association of Urologic Oncology of the German Cancer Society. *Urol Int.* 85(1), 1–10 (2010). Epub 2010 Jul 26. Review.
5. Floriani I., Torri V., Rulli E., Garavaglia D., Compagnoni A., Salvolini L., Giovagnoni A.: *J. Magn. Reson. Imaging* 31(1), 19–31 (2010)
6. Bogdanov A. Jr, Mazzanti M.L.: *Semin Oncol.* 38(1), 42–54 (2011)
7. Zalyalyutdinova L.N. *et al.*: Proceedings of the 4<sup>th</sup> International Congress, p. 100–101. Khabarovsk, October 3–7, 2005.
8. The patent № 2114853 C1 RU on 07/10/1998
9. The patent № 2151596 C1 RU on 06/27/2000
10. Vasiliev G.I., Zalyalyutdinova L.N. *et al.*: Structure and dynamics of molecular systems. Abstracts and reports at the X Russian Conference, p. 61. Kazan–Moscow–Yoshkar-Ola–Ufa, Russia, 2003.

## Paramagnetic Centers of Blood Plasma and Their Prognostic Value for Tumor Innidiation

L. N. Zalyalyutdinova<sup>1</sup>, R. G. Yakhin<sup>2</sup>, N. A. Samigullina<sup>2</sup>, and A. Y. Sabirova<sup>1</sup>

<sup>1</sup> Department of Pharmacology, Kazan State Medical University, Kazan 420012, Russian Federation, imanaev@mail.ru

<sup>2</sup> Institute of Ecology and Subsoil Use Problems of the Academy of Sciences of Tatarstan Republic, Kazan 420089, Russian Federation, Samigullinan@mail.ru

Free radical reactions definitely play an important role in the metabolic processes of the human body, both in physiological and pathological conditions in general and in malignancies in particular. Antioxidant system functions to protect the organism from oxidative stress that accompanies most pathological processes. One of the links of this defence is ceruloplasmin/transferrin system and thiol groups of proteins [1, 2]. Ceruloplasmin is a copper-containing glycoprotein of blood plasma that has its amino acid residues bound with 7 atoms of copper, 3 of which are in paramagnetic condition. Ceruloplasmin performs a number of important biological functions in the organism. It up-regulates the stability of cell membranes, takes part in iron metabolism, immunological reactions and ion exchange, has an antioxidant effect and inhibits lipid peroxidation. Ceruloplasmin performs a marked role in the regulation of the ionic state of iron – the oxidation of  $\text{Fe}^{2+}$  to  $\text{Fe}^{3+}$ , which makes it possible for the iron to be put into transferrin molecule without formation of iron toxic side products. Maintaining of normal iron metabolism and transport is a vital function of ceruloplasmin. Transferrin is an iron-transporting plasma protein, consisting of a single polypeptide chain with two centers for the localization of  $\text{Fe}^{3+}$  iron. Transferrin provides cells and tissues with iron and is a link in the chain of synthesis of iron-containing proteins, especially hemoglobin. [3].

Nowadays ceruloplasmin is considered to be a diagnostic oncomarker at various locations of tumors. The increase in blood levels of ceruloplasmin was reported at cancer of breast, head and neck, gastrointestinal tract, prostate, testis, lungs. However, increase in ceruloplasmin is observed at inflammatory processes and trauma as well [4–8]. This indicates that ceruloplasmin as a oncomarker is a nonspecific.

The aim of the study was to examine the content of ceruloplasmin and transferrin of blood plasma of experimental animals with transplanted lymphosarcoma – a tumor that can metastasize.

Samples of blood plasma of healthy rats and tumor-bearing animals were placed in quartz ampoules with a diameter of 4 mm, stored in liquid nitrogen

and their paramagnetic spectra were recorded at a radiospectrometer ER-200 (“Bruker”, Germany) equipped with a computer “Aspect-2000”. Terms of recording the spectra were the following: magnetic field strength was 6500 G, microwave power 16 dB, filter constant 200 ms, amplitude of the magnetic field modulation 5 Gs. A aqueous solution of TEMPO (2,2,6,6-tetramethylpiperidine-1-oxyl) at a concentration of  $2.5 \cdot 10^{-5}$  was used as a EPR spin probe. The results were counted statistically.

At a course of studying of blood plasma of intact (healthy) animals with EPR, the following paramagnetic centers were found:  $g = 4.3$  belonging to  $\text{Fe}^{3+}$ ;  $g = 2.05$ , due to  $\text{Cu}^{2+}$ , and  $g \sim 2.0$ . The same signals were detected at the animals’ blood plasma at day 20, but the intensity of ceruloplasmin and transferrin was significantly higher, than that of healthy rats. Tumor growth was accompanied by a marked significant decrease in plasma transferring, moderate but statistically significant reduction of ceruloplasmin and consequently a substantial increase in ceruloplasmin|transferrin ratio. Morphological examination showed lymph node metastases present at tumor-bearing animals.

The results of the research may indicate that plasma antioxidant defence breaks down at tumor metastasis, whereas the determination of the ceruloplasmin/transferrin ratio may be of reliable prognostic value.

1. Skulachev V.P.: Soros Educational Journal no 3, 4–16 (1996)
2. Vashchenko V.I., Vashchenko T.N.: *Psychofarmakol. Biol. Narcol.* **6**, no. 3. 1254–1269 (2006)
3. Defrere S., Lousse J.C., Gonzalez-Ramos R. *et al.*: *Mol.* no. 33 (10), 632–633 (2006)
4. Gruys E., Toussaint M.: *J. Zhejiang. Univers. Sci. B.* **6(11)** 1045–1056, (2005)
5. DeVita L., Balisteri C.R., Arcolio F. *et al.*: *Immun. Ageing.* **29**, 33 (2006)
6. Sumnaya D.B., Kuchin D.G.: *Neuroimmunology* no. 3, 12–13 (2005)
7. Belaya O.L., Fomina I.G., Bayder L.M. *et al.*: *Clin. Med.* no. 7. 46–50 (2006)
8. Pogoreltsev V.I., Moiseev V.N., Ibragimova M.I. *et al.*: *Klin. lab. diagnostika* no. 4., 17–20 (2010)

## New Aspects of the Nanoscale Distance Measurement Using Pulse EPR

*R. Zaripov<sup>1</sup>, L. Kulik<sup>2</sup>, and K. Salikhov<sup>1</sup>*

<sup>1</sup> *Zavoisky Physical-Technical Institute, Russian Academy of Sciences, Kazan 420029, Russian Federation, zaripov.ruslan@gmail.com*

<sup>2</sup> *Institute of Chemical Kinetics and Combustion of the RAS, Novosibirsk 630090, Russian Federation*

Electron paramagnetic resonance (EPR) techniques are actively used to measure nanoscale distances. Information about the distance between two interacting paramagnetic particles can be obtained from the dipole-dipole interaction value. It is known that the dipole-dipole interaction depends on the distance ( $r$ ) between the interacting particles as  $\sim 1/r^3$ . It is necessary to use different EPR techniques for different distance ranges due to the competition dipole-dipole interaction with hyperfine interaction with magnetic nuclei. For example, continuous-wave EPR based on the analysis of the EPR spectral line shape allows to determine distances of up to 1.5 nm. Pulse EPR techniques is applied to determine distances in the range of 1.5–8 nm. In pulse EPR techniques, information about the dipole-dipole interaction is obtained by the analysis of the frequency and depth of the electron spin echo modulation due to the dipole-dipole interaction. Up to now there are several approaches to the determination of distances in the 1.5–8 nm scale. However, the dipole-dipole interaction is rather weak at such distances between paramagnetic centers and it is some difficult to reveal this effect in EPR experiments at the background of the hyperfine interaction with magnetic nuclei. Therefore the problem to develop the theory and experimental techniques for the determination of distances between paramagnetic centers remains topical.

Each of pulse EPR techniques has its own restrictions in the manifestation of the dipole-dipole interaction due to different reasons. These limitations are associated with both the equipment specifications and effect of the molecular dynamics and paramagnetic spin relaxation. Therefore it is necessary to take into account such factors during the determination of the distance between paramagnetic centers by means of EPR techniques.

In our work the effect paramagnetic relaxation and molecular mobility on the manifestation of the dipole-dipole interaction in pulse experiments on the distance determination was studied in detail. It was established in three-pulse stimulated echo experiments that the increase in the electron spin-echo enve-

lope modulation depth associated with the dipole-dipole interaction is due to the increase in the longitudinal relaxation rate. It was shown that in the case of the four-pulse electron double resonance the random modulation of the dipole-dipole interaction due to molecular mobility can result in the modulation frequency shift.

The work was supported by the RFBR grant № 09-03-00612-a, Russian President grant № 02.120.11.5317-MK and NSh-6267.2010.2.

## Investigation of Millisecond to Second Motions in Proteins Using Exchange NMR-Spectroscopy

T. Zinkevich<sup>1</sup>, K. Saalwachter<sup>2</sup>, D. Reichert<sup>2</sup>, B. Reif<sup>3</sup>, and A. Krushelnitsky<sup>4</sup>

<sup>1</sup> *Zavoisky Physical-Technical Institute, Russian Academy of Sciences, Kazan 420029, Russian Federation, tatyana-vilkova@ya.ru*

<sup>2</sup> *Faculty of Science, University of Halle, Halle 06120, Germany, detlef.reichert@physik.uni-halle.de*

<sup>3</sup> *Technische Universität München, München 80333, Germany, reif@tum.de*

<sup>4</sup> *Kazan Institute of Biochemistry and Biophysics, Russian Academy of Sciences, Kazan 420111, Russian Federation, askn@mail.ru*

Molecular motions in proteins play a crucial role in carrying out their unique biological function. Studying of these motions is an important scientific problem. The range of characteristic times of motions in proteins is from femtoseconds to seconds, and even minutes. The time scale of slow dynamics coincides with one of biologically relevant processes. That's why slow conformational motions are most interesting for the proteins biological function.

In this work we investigate slow motions by the solid-state (SS) <sup>15</sup>N NMR-spectroscopy method. As a test sample we choose 2H, 15N-enriched microcrystalline protein (SH3 domain of alpha-spectrin) with a partial back-exchange of labile protons. Application of perdeuterated microcrystalline proteins with a back substitution of small portion of labile protons [1] has considerably expanded capabilities of the SSNMR spectroscopy to explore internal protein dynamics with a site-specific resolution. There are two most important advantages of dilution of proton system: first, it makes proton line widths narrow which enables proton detection of the high resolution spectra and thus, considerable enhancement of the sensitivity. Second, it makes proton driven spin diffusion between <sup>15</sup>N nuclei negligible. Spin diffusion prevents studying slow internal motions by means of solid state exchange methods: motions that are slower than the spin diffusion are invisible in these experiments. Thus, suppressing spin diffusion due to dilution of the proton system in a protein solves these problems and allows obtaining more certain and reliable information on molecular dynamics.

The slow motions in the ms-s time scale are accessible using solid state MAS exchange experiment. The main concept of the method is: transverse magnetization is created by an initial 90° pulse or cross-polarization step and allowed to evolve during the period  $t_1$  under its characteristic frequency  $\omega_1$ . This frequency arises from the nuclear spin interaction which operates during  $t_1$ . At the end of  $t_1$ , the magnetization is stored along external magnetic field

for a period  $\tau_m$ , the mixing time, during which molecular dynamical process may occur. Finally, the magnetization is returned to the transverse plane, where it again evolves under its characteristic frequency  $\omega_2$ . If molecular motion or spin exchange occurs during  $\tau_m$  (which happens if the correlation time  $\tau_c < \tau_m$ ) then  $\omega_2$  and  $\omega_1$  are different, and this affects the intensity of the signal. Analysis of the resulting spectrum in terms of molecular motions relies on the frequencies  $\omega_1$  and  $\omega_2$  being constant during  $t_1$  and  $t_2$  periods, respectively, i.e., on their being no molecular motion during these periods. It is for this reason that exchange experiments are only suitable for studying slow molecular motions. From the dependencies of resulting signals on the mixing time the correlation time of motion can be determined, also it allows to make conclusions about geometry of the motion. In this experiment the most important feature is that motional models are not required to extract the dynamic information.

In the isolated  $^{15}\text{N}$ - $^1\text{H}$  pair there are four relevant nuclear magnetic interactions: 1)  $^{15}\text{N}$  chemical shift anisotropy (CSA), 2)  $^{15}\text{N}$ - $^1\text{H}$  dipolar coupling 3)  $^{15}\text{N}$  isotropic chemical shift and 4)  $^{15}\text{N}$ - $^1\text{H}$  J-coupling. The former three interactions can be modulated by motions and can be informative for dynamics studies (J-coupling can not). Using different MAS-synchronized pulse schemes, including recoupling and decoupling methods, one may select one of these three useful interactions and cancel the three others. Originally this method (so-called CODEX sequence) used the CSA interaction 2. Deuterated samples allow using other magnetic interactions as well. In this contribution we compare the results of the CODEX experiments utilizing the  $^{15}\text{N}$ - $^1\text{H}$  dipolar 3 and  $^{15}\text{N}$  isotropic chemical shift (i.e. non-recoupled) interactions. The magnitude of  $^{15}\text{N}$ - $^1\text{H}$  dipolar coupling is about 11.5 kHz, and even small amplitude motions with an order parameter (dimensionless quantity used to characterize motional amplitude) 0.9–0.99 modulate the dipolar coupling in the range of hundreds-thousands Hz. In contrast to dipolar coupling, the isotropic chemical shift difference between different subconformations is usually less than 30–40 Hz. It is clear that the larger interaction is more useful for obtaining dynamic information. Thus, the dipolar coupling seems to be more convenient for studying molecular dynamics; however, in some cases the comparative analysis of the dipolar and non-recoupled CODEX data may provide qualitatively new information on the conformational motions. This work is a very indicative example of the advantages of the solid state approaches to studying dynamics since only the solid state experiments allow such a play with different magnetic interactions.

1. Chevelkov *et al.*: *Angew. Chem., Int. Ed.* **45**, 3878 (2006)
2. de Azevedo *et al.*: *J. Am. Chem. Soc.* **121**, 8411 (1999)
3. Krushelnitsky *et al.*: *Am. Chem. Soc.* **131**, 12097 (2009)

## AUTHOR INDEX

Abrosimov, N. V.	32
Adachi, T.	138
Akdoğan, N.	72
Akhmetov, M. M.	148
Akhmetzyanov, D.	221
Aktaş, B.	28
Alakshin, E. M.	85
Alfonsov, A.	124, 151
Altshuler, T. S.	152
Anashkin, V. N.	171
Anisimov, O. A.	223
Antonova, O.	154
Arda, L.	74, 159, 160
Aswartham, S.	124
Atsarkin, V. A.	29
<b>Badelin, A. G.</b>	218
Bagryanskaya, E. G.	30, 81
Bakirov, M.	156
Bales, B.	156
Baniodeh, A.	220
Baranov, P. G.	98
Barbon, A.	35
Barskiy, D. A.	11
Basini, M.	41
Bayazitov, A. A.	158
Behr, G.	129
Belli, M.	32, 88
Bennati, M.	45
Bezkishko, I. A.	125, 143, 176
Bisogni, V.	127
Biziaev, D.	36
Bloshkin, A. A.	75
Blum, C. G. F.	151
Bobrov, A. I.	37
Bombor, D.	151
Bowman, M. K.	34, 90
Braicovich, L.	127
Brodhun, F.	45

Brookes, N. B.	127
Brustolon, M.	35
Büchner, B.	112, 113, 117, 124, 125, 127, 129, 131, 132, 135, 137, 140 143, 144, 151
Bukharaev, A.	36
Burmistrov, M. V.	230
Buzdin, A. I.	55
Cakiroglu, O.	159, 160
Cakiroglu, O.	74
Canevali, C.	41
Carl, P.	56
Castelli, L.	8
Chiornea, V.	204
Christou, G.	131
Chshiev, M.	23
Chuklanov, A.	36
Chushnikov, A. I.	178
Cocco, S.	88, 202
Collauto, A.	35
Deisenhofer, J.	124
Dejneka, A.	107
Demidov, E. S.	37
Demidov, V. V.	29
Deminov, R. G.	121
Denysenkov, V.	45
Dieny, B.	23
Dmitriev, A.	103
Dogan, N.	74, 159, 160
Doktorov, A. B.	197
Domracheva, N. E.	161
Drechsler, S.-L.	113, 117
Dubinskii, A.A.	17
Dvurechenskii, A. V.	3, 75, 200
Dzikovski, B.	39
Dzuba, S. A.	4
Earle, K. A.	76
Efimov, V. N.	227, 230
Egorov, A. V.	213
Eichhoff, U.	77
Eremin, E. V.	64
Eremina, R. M.	164, 218
Erkovan, M.	28

---

Ermakova, T. G.	184
Ermolaeva, O. L.	79
Ershov, P.	193
Evseeva, A. V.	218
Evstigneeva, M.	144
Fakhrutdinov, A. R.	171, 175, 192
Falin, M. L.	166, 167
Fanciulli, M.	32, 41, 88, 202
Farle, M.	114
Farrakhov, B.	169
Fattakhov, Ya. V.	158, 169, 171, 173
Fayzrahmanov, I. A.	218
Fedin, M.	30
Fel'dman, E. B.	42
Ferrari, G.	88
Feussner, I.	45
Fielding, A. J.	45
Filatov, M. Yu.	176
Fittipaldi, M.	8
Flores, M.	17
Fominov, Ya. V.	121
Fraerman, A. A.	46, 79, 105
Freed, J. H.	26, 39
Fujisawa, M.	58
Fuki, M.	47
Gabidullin, D. D.	171, 173
Gainutdinov, Kh. L.	227
Gafiyatullin, L.	172
Gafiyatullin, N. M.	171, 173
Galeev, R. T.	174, 175, 204
Galiakberova, E. R.	175
Galyaltdinov, M. K.	169, 171
Garifullin, I. A.	6, 132
Garif'yanov, N. N.	132
Gatteschi, D.	8
Gavrilova, T. P.	164
Gazizulin, R. R.	85
Geck, J.	127
Gerasimov, K. I.	167
Ghiringhelli, G.	127
Goldfarb, D.	10
Golubov, A. A.	121

Gorelik, V. R.	81, 210
Goryunov, Y. V.	152
Goykhman, A.	193
Gracheva, I. N.	107
Gribkov, B. A.	37, 79, 105
Grishin, Yu.	83
Gromov, I.	84
Gruzdev, M. S.	161
Gryaznova, T. P.	176
Guagliardo, F.	88
Gubaev, A. I.	107
Gumarov, G. G.	148
Gusev, S. N.	37
Gusev, S. A.	79, 105
Hara, H.	56
Hess, C.	129, 135, 151
Hey-Hawkins, E.	125, 143
Hlubek, N.	129
Höfer, P.	56, 77, 84
Ibragimova, M. I.	178
Il'in, A. I.	60
Ise, T.	56
Ivanov, K. L.	207
Ivanova, G. I.	172, 212
Ivanova, T. A.	172, 212
Ivanov, K. L.	181
Iyidin, V. S.	128, 227
Jafarova, G. G.	227
Kamenev, A.	140
Kandrashkin, Yu. E.	128, 182
Karminskaya, T. Yu.	121
Karzanov, V. V.	37
Kataev, V.	115, 124, 125, 131, 132, 143
Kataeva, O. N.	125, 143
Katsyuba, S. A.	176
Kaul, A.	140
Kawamori, A.	53
Khabipov, R.	192
Khairuzhdinov, I. T.	183
Khaliullin, G.	116
Khanipov, T.	36
Khasanov, R.	138

---

Khomskii, D. I.	118
Khramtsova, E. A.	50
Khutshishvili, S. S.	184
Kikuchi, H.	58
Kim, J. S.	124
Kindo, K.	58
Kirichenko, E. N.	128
Kiryutin, A. S.	181
Kitagawa, M.	56
Klauss, H.-H.	135
Klimov, A. Yu.	79, 105
Klingeler, R.	113, 117, 125, 140, 143, 144
Klochkov, A. V.	85
Kobayashi, T.	58
Kobori, Y.	47
Koch, C.	45
Köchling, T.	181
Koike, Y.	138
Kokorin, A. I.	86
Kon'kova, T. V.	184
Konov, K.	188
Konov, A. B.	187
Konovalov, A.	221
Konstantinova, E. A.	86
Konygin, G. N.	148
Koplak, O.	103
Koptyug, I. V.	11
Korableva, S. L.	213
Korchak, S. E.	181
Körner, J.	137
Korzhova, S. A.	184
Kothe, G.	48
Kovtunov, K. V.	11
Kraus, R.	127
Krivenko, S.	190
Krivolapov, D.	143
Krug von Nidda H.-A.	124
Kruppa, A. I.	50
Krupskaya, Y.	125, 131, 143
Krushelnitsky, A.	239
Krylatykh, N. A.	171, 173, 192
Krzyaniak, M.	34

Kugel, K. I.	118
Kukovitsky, E.	198
Kulik, L. V.	207, 237
Kupriyanov, I. N.	96
Kupriyanov, M. Yu.	121
Kupriyanova, G. S.	193
Kusrayev, Yu. G.	13
Kutrzeba-Kotowska, B.	202
Kuzian, R.	113, 117
Kuzmin, V. V.	85
Kuzmova, T.	140
Lamperti, A.	202
Lang, G.	124
Larionov, A. V.	60
Latypov, V. A.	166, 167
Lebedev, D.	36
Leksin, P. V.	132
Leonhardt, A.	137
Leshina, T. V.	50
Lesnikov, V. P.	37
Leti, G.	88
Levchenko, A. V.	152
Levchuk, S. A.	37
Likhtenshtein, G. I.	51
Lin, J.-Y.	144
Link, G.	48
Lin, T.-S.	48
Lipps, F.	124
Lisin, V. N.	194
Loidl, A.	124
Lonnecke, P.	125
Lorenz, W. E. A.	113, 117
Lubitz, W.	15, 17, 83
Luetkens, H.	135
Lukaschek, M.	48
Lukzen, N. N.	94, 197
Lvov, S.	198
Lyubin, A.	200
Maeter, H.	135
Magin, I. M.	50
Malek, J.	113, 117
Mamedov, D. V.	164

---

Mameli, D.	202
Mamin, R. F.	136
Mantovan, R.	202
Maryasov, A. G.	34, 90
Matsuo, A.	58
Mazuoka, H.	30, 53
Mazzeo, G.	88
Medvedeva, L.	144
Mel'nikov, M. Ya.	216
Mel'nikov, A. S.	55
Milyukov, V. A.	125, 143, 176
Milyaev, M. A.	22
Mingalieva, L. V.	172, 204, 218
Mironov, V. L.	79, 105
Möbius, K.	17
Moiseev, V. N.	178
Moiseev, S.	93
Monnay, C.	127
Moretti Sala, M.	127
Morgunov, R.	103
Mori, N.	56
Morita, Y.	56
Moro, F.	131
Moroshek, A. A.	230
Morozova, O. B.	69
Morozov, V. A.	94
Mühl, T.	137
Mukovskii, Ya. M.	164
Nadolinny, V. A.	96, 214
Nakasuji, K.	56
Nakazawa, S.	56
Nalbandyan, V.	144
Nasibulov, E. A.	207
Nasybullina, D. A.	233
Nateprov, A. N.	152
Nedopekin, O. V.	121
Nenashev, A. V.	3
Neu, V.	137
Newton, M. E.	96
Nishida, S.	56
Nishihara, S.	58
Nishimoto, S.	113, 117

Noji, T.	138
Novitchi, Gh	204, 220
Nurgazizov, N.	36
Nurmamyatov, I. A.	208
<b>O</b> bynochny, A. A.	210
Ohba, Y.	53
Ohta, H.	58
Okubo, S.	58
Orlova, A.	193
Ovcharenko, V.	30
Ovchinnikov, I. V.	172, 212
Özdemir, M.	28
<b>P</b> aleari, S.	41
Palyanov, Yu. N.	96
Panov, A. V.	230
Parameswaran, A.	143
Pascua, G.	135
Pavlova, E. D.	37
Pavluk, A. A.	214
Petrenko, O. A.	100
Petrova, M. V.	197
Petukhov, V. Yu.	148, 178
Pievo, R.	45
Podolskii, V. V.	37
Polyakov, N. E.	50
Popov, A. P.	193
Powell, A. K.	59, 220
Pozdnyakov, A. S.	184
Prati, E.	88
Prisner, T. F.	19
Prokhorenko, E.	193
Prozorova, L. A.	100
Prozorova, G. F.	184
Pugach, N. G.	55
Pyataev, A. V.	161
<b>R</b> ahimi, R.	56
Rakhmanov, A. L.	118
Rakhmatullin, R.	83
Rameev, B.	97
Rautskiy, M. V.	64
Reichert, D.	239
Reif, B.	239

---

Reijerse, E.	83
Revcolevski, A.	129, 135
Ribeiro, P.	129
Richter, J.	113, 117
Rodan, S.	151
Rodionov, A. A.	107, 230
Rogov, V. V.	79, 105
Romanova, I. V.	213
Rosner, H.	113
Roth, G.	129
Rotta, D.	41
Ryadun, A. A.	214
Ryazanov, V. V.	20
Rybin, D. S.	148
Ryzhanova, N. V.	23
Saalwachter, K.	239
Sabirova, A. Y.	233, 235
Safarov, I. M.	222
Sagdeev, R. Z.	11
Saikin, K. S.	158, 171
Saint-Martin, R.	129, 135
Sakurai, T.	58
Salakhov, M. Kh.	107
Salakhutdinov, L.	138
Salikhov, K. M.	143, 156, 183, 187, 224, 237
Samigullina, N. A.	235
Sangregorio, C.	8
Sapozhnikov, M. V.	37
Sato, K.	56
Savelieva, O.	144
Savitsky, A.	17, 83
Savostina, L. I.	172, 216
Sboychakov, A. O.	118
Schmalbein, D.	84
Schmidt, O. G.	132
Schmitt, M.	113
Schmitt, T.	127
Schumann, J.	132
Sekretenko, A. V.	60
Shagalov, V. A.	171
Shakirov, I.	36
Shakurov, G. S.	222

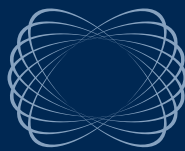
Sharipov, K. R.	218
Shegeda, A. M.	194
Shen, J.-R.	53
Shermadini, Z.	135
Shiomi, D.	56
Silkin, N. I.	230
Simonelli, L.	127
Singh, S.	129
Sinyashin, O. G.	125, 143, 176
Skourski, Y.	117
Skovpin, I. V.	11
Smolyakov, D. A.	64
Soltamova, A. A.	98
Soltamov, V. A.	98
Sorace, L.	8
Sorokin, I. D.	216
Sosin, S. S.	100
Stamatatos, T. C.	131
Strelkov, N. V.	23
Sukhanov, A. A.	204, 210, 220
Synnikov, P. P.	107
Tagirov, L. R.	121
Tagirov, M. S.	61, 85, 213
Takui, T.	56
Talanov, Yu.	138
Talantsev, A.	103
Tallarida, G.	202
Tarassenko, S. A.	63
Tarasov, V. F.	81, 210, 221
Tasiopoulos, A. J.	131
Tayurskii, D. A.	85
Teitel'baum, G.	138
Tipikin, D.	39
Topkaya, R.	28
Toyota, K.	56
Trepakov, V. A.	107
Turanova, O. A.	172, 212
Turanov, A.	172
Tyurin, V. S.	128
Udalov, O. G.	79
Ulanov, V. A.	222
Useinov, A.	139

---

Ustinov, V. V.	22
Vakulskaya, T. I.	184
van den Brink, J.	113, 117, 127
van Slageren, J.	131
Vangelista, S.	202
Vasilchikova, T.	140
Vasiliev, A.	140, 144
Vavilova, E.	143
Vdovichev, S. N.	105
Veber, S. L.	30, 96
Vedyayev, A. V.	23
Vellei, A.	41
Vennam, P. R.	34
Verkhovlyuk, V. N.	223
Vieth, H.-M.	181
Vock, S.	137
Volkonskyi, O.	151
Volkov, N. V.	64
Volkov, M.	224
Volkova, O.	140
Voronkova, V. K.	128, 143, 204, 220
Weidner, J.-U.	48
Weiner, L.	67
Wizent, N.	117
Wolny, F.	137
Wolter, A.	113, 144, 151
Wurmehl, S.	124, 151
Yago, T.	48
Yakhin, R. G.	235
Yakimov, A. I.	75
Yamauchi, S.	25, 30, 53
Yaschuk, Yu. P.	128
Yatsyk, I. V.	164
Yavishev, B. G.	226
Yoshino, T.	56
Yurkovskaya, A. V.	69, 181
Yurtaeva, S. V.	227, 230
Yusupov, R. V.	107
Zahn, R.	124
Zaitsev, S.	103
Zakharova, Yu. A.	81
Zalyalyutdinova, L. N.	233, 235

Zaripov, R.	143, 188, 237
Zaripov, M. M.	222
Zharikov, E.	221
Zheglov, E. P.	148, 178
Zheng, X. G.	58
Zhidomirov, G. M.	216
Zhiteitcev, E.	221
Zhitomirsky, M. E.	100
Zhivonitko, V. V.	11
Zhou, K.	127
Ziatdinov, A. M.	109
Zinkevich, T.	239
Zinovieva, A. F.	3, 200
Zvereva, E.	144
Zvyagin, A. A.	135
Zyubin, A. Y.	193





ФИЗТЕХПРЕСС

[www.kfti.knc.ru](http://www.kfti.knc.ru)